Convex Contact Representations of Planar Graphs

vorgelegt von
M. Sc.
Hendrik Schrezenmaier
ORCID: 0000-0002-1671-9314

der Fakultät II – Mathematik und Naturwissenschaften
der Technischen Universität Berlin
zur Erlangung des akademischen Grades

Doktor der Naturwissenschaften
Dr. rer. nat.

vorgelegte Dissertation

Promotionsausschuss:

Vorsitzender:	Prof. Dr. Jörg Liesen
Gutachter:	Prof. Dr. Stefan Felsner
Gutachter:	Dr. Daniel Gonçalves
Gutachter:	Prof. Dr. Torsten Ueckerdt

Berlin 2021

Abstract

The goal of this dissertation is to study contact representations of plane graphs with convex shapes in the plane, with a special focus on convex polygons.

The classical Circle Packing Theorem by Koebe from 1936 states that each plane graph has a contact representation with disks, i.e., the vertices of the graph are represented by interiorly disjoint disks in the plane such that the edges of the graph correspond to touching disks. A remarkable generalization of this theorem is the Convex Packing Theorem by Schramm. It states that, if we prescribe an individual compact convex prototype for each vertex of a plane graph, there exists a contact representation of this graph in which each vertex is represented by a scaled copy of its prototype. In the case that the prototypes do not have smooth boundaries, the only known proof of this theorem is based on the Brouwer fixed point theorem and does not seem to give any insights into questions like those for the uniqueness or the complexity of the computation of the contact representations.

In this dissertation we study contact representations of plane graphs with so called *similarly-aligned odd K-gons* and *parallel-sided even K-gons* for a fixed K. These classes of polygons generalize equiangular and therefore also regular K-gons for odd and even K, respectively. We describe the combinatorial structure of these contact representations by integral flows of planar graphs with prescribed excesses at the vertices, known as ω-flows. In particular, we obtain a lattice structure on the set of all possible contact structures of a graph. This lattice structure plays a role in an algorithm that is supposed to compute a contact representation of a given graph with individually prescribed similarly-aligned odd K-gons or parallel-sided even K-gons as prototypes for the vertices. Based on a contact structure, the algorithm builds a system of linear equations and solves it. If the solution is non-negative, it encodes the wanted contact representation. In this case the representation is constructed and the algorithm terminates. Otherwise negative variables guide a change of the contact structure and the procedure is restarted with the new contact structure. Similar algorithms have been proposed for contact representations with homothetic triangles and squares. We cannot prove that this procedure terminates. But using the ideas of this approach, we can still prove the existence of the wanted contact representation. With a convergence argument we can then reprove the existence of contact representations of plane graphs with arbitrary individually prescribed compact convex prototypes for the vertices.

Zusammenfassung

In dieser Arbeit beschäftigen wir uns mit Kontaktdarstellungen planarer Graphen mit konvexen Formen in der Ebene, mit besonderem Fokus auf konvexe Polygone.

Ein klassisches Resultat auf diesem Gebiet ist das Kreispackungstheorem von Koebe von 1936, das besagt, dass jeder planare Graph eine Kontaktdarstellung mit Kreisscheiben besitzt, d. h., die Knoten des Graphen werden als Kreisscheiben in der Ebene mit paarweise disjunktem Inneren dargestellt, so dass die Kanten des Graphen den Paaren sich berührender Kreisscheiben entsprechen. Eine bemerkenswerte Verallgemeinerung dieses Theorems ist das Konvexpackungstheorem von Schramm. Dieses besagt, dass, wenn wir für jeden Knoten eines planaren Graphen einen individuellen kompakten konvexen Prototyp vorschreiben, dieser Graph eine Kontaktdarstellung besitzt, in der jeder Knoten durch eine skalierte Kopie seines Prototyps dargestellt wird. Wenn die Ränder der Prototypen nicht glatt sind, beruht der einzige bekannte Beweis dieses Theorems auf dem Fixpunktsatz von Brouwer und scheint keine Erkenntnisse zu liefern, die bei der Beantwortung von Fragen nach der Eindeutigkeit oder der Komplexität der Berechnung der Kontaktdarstellungen helfen.

In dieser Dissertation untersuchen wir Kontaktdarstellungen planarer Graphen mit so genannten *ähnlich ausgerichteten ungeraden K-Ecken* und *parallelseitigen geraden K-Ecken* für ein festes K. Diese Klassen von Polygonen sind Verallgemeinerungen von gleichwinkligen und damit insbesondere regulären K-Ecken für ungerade beziehungsweise gerade K. Wir beschreiben die kombinatorische Struktur dieser Kontaktdarstellungen als ganzzahlige Flüsse von planaren Graphen mit vorgeschriebenen Überschüssen an den Knoten, so genannte ω-Flüsse. Insbesondere erhalten wir eine Verbandsstruktur auf der Menge aller möglichen Kontaktstrukturen eines Graphen. Diese Verbandsstruktur spielt eine Rolle in einem Algorithmus, der eine Kontaktdarstellung eines gegebenen Graphen mit individuell vorgegebenen ähnlich ausgerichteten ungeraden K-Ecken oder parallelseitigen geraden K-Ecken als Prototypen für die Knoten berechnen soll. Basierend auf einer Kontaktstruktur stellt der Algorithmus ein lineares Gleichungssystem auf und löst es. Wenn die Lösung nichtnegativ ist, kodiert sie die gesuchte Kontaktdarstellung. In diesem Fall kann die Kontaktdarstellung konstruiert werden und der Algorithmus terminiert. Andernfalls geben die negativen Variablen einen Hinweis, wie die Kontaktstruktur geändert werden kann, und die Prozedur wird mit der neuen Kontaktstruktur neu gestartet. Ähnliche Algorithmen sind bereits für die Berechnung von Kontaktdarstellungen mit homothetischen Dreiecken und Quadraten vorgeschlagen worden. Wir können nicht beweisen, dass der Algorithmus terminiert. Allerdings können wir die Ideen dieses Algorithmus verwenden, um die Existenz der gesuchten Kontaktdarstellungen zu beweisen. Mit Hilfe eines Konvergenzarguments erhalten wir schließlich einen neuen Beweis für die Existenz von Kontaktdarstellungen planarer Graphen mit beliebigen individuell vorgeschriebenen kompakten konvexen Prototypen für die Knoten.

Acknowledgements

This dissertation is the result of my research that was conducted in the *Arbeitsgruppe Diskrete Mathematik* at Technische Universität Berlin under the supervision of Stefan Felsner. I would like to thank

- Stefan Felsner for arousing my interest in discrete mathematics already in an early phase of my studies and finally introducing me to the area of contact representations and giving me the opportunity to join his group as part of the research project *Graphs with Geometric Representations*. I appreciate his open door policy and the freedom he gave me to find and follow my own research interests.
- all my former colleagues Veit, Linda, Manfred, Raphael, and Felix for the nice atmosphere and interesting discussions. Especially, I would like to thank Manfred for being a great person to share my office with, for introducing me to SageMath, and for implementing a first version of the K-gon contact representation program and Raphael for sharing my interest into contact representations.
- the COGA-group for the great time, the board game nights, and all the table football matches.
- Raphael, Manfred, and Felix for proof-reading this thesis.
- Daniel Gonçalves and Torsten Ueckerdt for their interest to read this thesis and for being part of my committee.

Table of Contents

1 Introduction **1**
- 1.1 Overview of the literature . . . 1
- 1.2 Our contribution . . . 6
- 1.3 Outline . . . 6

2 Preliminaries **8**
- 2.1 Graphs . . . 8
- 2.2 Polygons . . . 10
- 2.3 α-orientations and ω-flows . . . 10

3 The combinatorial structure of polygon contact representations **13**
- 3.1 Triangle, rectangle, and primal-dual triangle contact representations . 13
  - 3.1.1 Homothetic triangle contact representations . . . 13
  - 3.1.2 Rectangle contact representations . . . 15
  - 3.1.3 Homothetic primal-dual triangle contact representations . . . 18
- 3.2 Similarly-aligned odd K-gon contact representations . . . 21
  - 3.2.1 K-color forests . . . 24
  - 3.2.2 Bijection to K-contact structures . . . 28
  - 3.2.3 The distributive lattice . . . 36
- 3.3 Parallel-sided even K-gon contact representations . . . 38
  - 3.3.1 K-color forests . . . 40
  - 3.3.2 Bijection to K-contact structures . . . 42
  - 3.3.3 The distributive lattice . . . 60

4 Systems of linear equations **63**
- 4.1 Equations for triangle and rectangle contact representations . . . 64
  - 4.1.1 Equations for triangle contact representations . . . 64
  - 4.1.2 Equations for square contact representations . . . 66
  - 4.1.3 Parametrization of the equations . . . 69
- 4.2 Gluing polygons together . . . 70
- 4.3 Handling pseudotriangles . . . 75
- 4.4 Equations for similarly-aligned odd K-gon contact representations . . 88
- 4.5 Equations for parallel-sided even K-gon contact representations . . . 98

4.6 Properties of the solutions . . . 105
4.6.1 Solutions with negative variables . . . 105
4.6.2 Solutions without negative variables . . . 115
4.6.3 How flipping the K-contact structure changes the solution . . . 122
4.7 Drawings from solutions with negative variables . . . 128

5 Existence of convex contact representations **132**
5.1 Overview of known results . . . 132
5.2 New proof for K-gon contact representations . . . 133
5.3 Derived proof for general convex shapes . . . 142

6 Algorithms **145**
6.1 A fast heuristic . . . 145
6.1.1 Implementations . . . 146
6.1.2 Bounding the worst case number of iterations . . . 148
6.2 A slow heuristic . . . 150

7 Conclusion **152**

Bibliography **157**

A Overview of structures associated with contact representations **163**

B Visualizations of the heuristic **171**

Chapter 1

Introduction

There are many ways to visualize a graph. The most simple kind of such geometric representations are *node-link diagrams* where the vertices of the graph are represented by points and the edges are represented by curves connecting the two endpoints. Another class of geometric representations of graphs are *intersection representations*. Here the vertices are represented by geometric objects and the edges by intersections of the two objects corresponding to the incident vertices. In this work, we want to focus on *contact representations* which are intersection representations where the geometric objects are allowed to touch but not to overlap according to some specified notion. For a general survey on the connections of geometry and graph theory see the survey by Lovász [Lov19] which contains many beautiful and unexpected examples.

1.1 Overview of the literature

There is a large body of work about contact representations of graphs. In this section we will give a brief overview of this literature. Some of the results mentioned in this section will be explained in more detail in the later chapters.

Circles. One of the earliest results concerning contact representations is Koebe's Circle Packing Theorem [Koe36] from 1936. It states that all planar graphs can be represented by touching disks. See Fig. 1.1 for an example of such a representation.

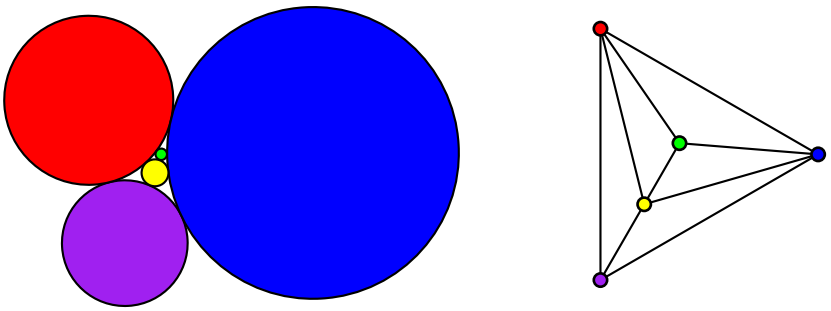

Figure 1.1: A touching disks representation of a five-vertex planar graph.

Since this theorem had been forgotten for quite a while and has been rediscovered by Thurston [Thu79b, ch. 13] in the late 1970s as a consequence of the work of Andreev [And70a; And70b], it is also known as the Koebe-Andreev-Thurston theorem.

If the graph is 3-connected, there exist disk contact representations of the graph itself and of its planar dual that are intersecting in a special manner, known as *primal-dual disk representation*. This stronger version of the theorem has been proven by Pulleyblank and Rote (unpublished, see [FR19]) and by Brightwell and Scheinerman [BS93], see also [FR19] for a simple and elegant elementary proof.

Segments. Contact representations with line segments are quite well understood: We know that each planar bipartite graph has a contact representation with interiorly disjoint horizontal and vertical line segments [BNZ91; FOP94]. Further, each triangle-free planar graph has a contact representation with line segments with only three different slopes [CCD+02]. Using a technique similar to one that we will use in this thesis, Gonçalves [Gon19] proved a slightly stronger version of this theorem for Eulerian triangulations. If we allow arbitrarily many different slopes, the subgraphs of planar Laman graphs are exactly the planar graphs admitting a contact representation with line segments (Thomassen (unpublished manuscript), see [Fel13]).

The special case of contact representations of maximal planar bipartite graphs, i.e., planar quadrangulations, with interiorly disjoint horizontal and vertical line segments is already studied in a seminal paper by Brooks, Smith, Stone, and Tutte from 1940 [BSST40]. In this case, the contact representation induces a rectangulation of a rectangle, i.e., a dissection of a rectangle into smaller rectangles, also known as a *floorplan*, see Figs. 1.2a and 1.2b. By considering an electrical flow in the visibility graph of the horizontal segments with unit capacity on each edge, Brooks et al. are able to obtain a squaring of a rectangle, i.e., a dissection of a rectangle into squares, whose segment contact graph is the same as the segment contact graph of a given rectangulation of a rectangle. The same result is achieved by Felsner [Fel13] with a different approach. This is the first example of an approach that plays a central role in this thesis. It begins with an encoding of the combinatorial structure of the

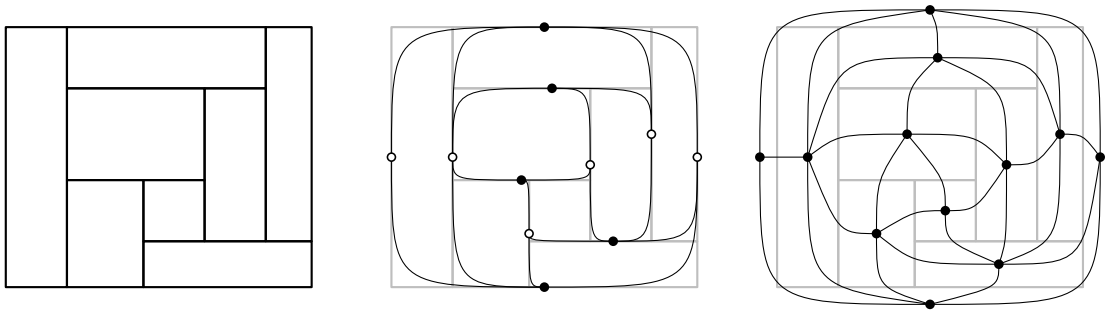

(a) A rectangulation of a rectangle. (b) The corresponding segment contact graph. (c) The corresponding rectangle contact graph.

Figure 1.2: Different contact graphs associated with a rectangulation of a rectangle.

segment contact representation in the form of a *separating decomposition*. This is a 2-orientation of the segment contact graph, i.e., an orientation in which each vertex, except the vertices corresponding to the top and bottom segment, has exactly two outgoing edges, together with a certain coloring of the edges. This combinatorial data encodes the basic geometric relationships of the floorplan. From this data, a system of linear equations is extracted that is supposed to compute the wanted squaring. The variables represent the side lengths of the squares. This system can be shown to be uniquely solvable. If the solution is non-negative, the squaring can be constructed from the side lengths given by the solution. Otherwise, the negative variables can be used as indicators how to change the separating decomposition so that the solution of the new system of equations is non-negative and thus provides all the necessary information to construct a squaring.

Rectangles and squares. A rectangulation of a rectangle can not only be interpreted as a contact system of horizontal and vertical segments but also as contact system of axis-aligned rectangles. For the resulting contact graph, it is helpful and common practice to interpret the four sides of the enclosing rectangle as the vertices of the outer face, see Fig. 1.2c. In this work, we refer to these contact representations as *rectangle contact representations*. In the literature, they are also known as *rectangular duals*. Exactly the inner triangulations of a 4-cycle without chords in the outer 4-cycle and without separating 3-cycles admit such a rectangle contact representation [Ung53; KK85]. Rectangle contact representations can be computed in linear time by the following approach: First compute a combinatorial structure and then use this structure for the construction of the contact representation. This approach was first taken by He [He93] who calls this combinatorial structure *regular edge labeling*. Here we use the name *transversal structure* which goes back to [Fus07; Fus09]. Also in the case of rectangle contact representations, the question has been studied whether it is possible to prescribe the aspect ratios of the rectangles, e.g., representing all vertices by squares. Based on the concept of *extremal length*, Schramm [Sch93] proves the existence of rectangle contact representations with prescribed aspect ratios for each vertex for graphs without separating 4-cycles. Schramm also shows that the contact representation is unique up to scaling. Lovász [Lov19] reproves this result using *antiblocking convex corner polytopes*. For computing rectangle contact representations, the most practical approach is similar to the approach of Felsner [Fel13] for computing squarings as segment contact representations. This time we use a transversal structure as the combinatorial data to set up a system of linear equations. The variables are the lengths of the contacts of two rectangles. It can be proven that the system has a unique solution. If the solution is non-negative, the wanted contact representation can be constructed from the lengths given by the solution. Otherwise, the negative variables can guide a change of the transversal structure. This step is iterated until the solution is non-negative. The drawback of this method is that it has not been proven that this iterative procedure actually stops. But in practical experiments it always terminated. The approach is described in [Fel13], for more details see [Ruc11], and for an implementation see [Pic11]. The author of this thesis

was able to use this strategy (setting up a system of linear equations and changing the transversal structure for improvements) to reprove the existence of rectangle contact representations with prescribed aspect ratios, i.e., Schramm's result, in his master thesis [Sch16].

Triangles. In by now classical work, de Fraysseix et al. [FOR94] show that every planar triangulation has a contact representation with triangles. They use *Schnyder woods* (Schnyder [Sch90a] himself calls them *realizers*) or, more precisely, the corresponding concept of *canonical orderings* as an encoding of the combinatorial structure of the contact representation, guiding a successive placement of the triangles. The construction can be adapted in such a way that all triangles are isosceles and have a horizontal basis and all contacts are between a corner of a triangle and the interior of a side of another triangle, see Fig. 1.3a. Gonçalves et al. [GLP12] show that each 4-connected planar triangulation has a contact representation with equilateral triangles with a horizontal basis. Their proof is an application of the Convex Packing Theorem by Schramm [Sch07]. The most practical approach for computing equilateral triangle contact representations is again based on solving systems of linear equations. This time, we use a Schnyder wood as combinatorial data to set up this system. The variables of the system represent the side lengths of the dual triangles corresponding to the faces of the triangulation. As in the previous cases, it can be shown that the system is uniquely solvable. If the solution is non-negative, the contact representation can be constructed from the side lengths given by the solution. If there are negative variables, they can be used to guide a change of the Schnyder wood. This step is iterated until the solution of the system of equations is non-negative. As for the analogous procedure for the computation of squarings, while it has been observed in all practical examples, it has not been proven that the iteration actually stops. This approach is sketched in [Fel09]. For more

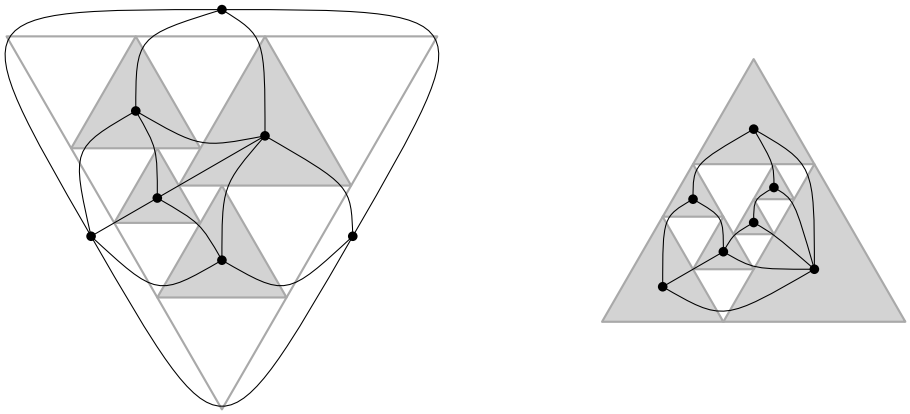

(a) A triangle contact representation.

(b) A primal-dual triangle contact representation.

Figure 1.3: Examples of triangle contact representations with equilateral triangles.

details including an implementation and statistical data on the number of iterations see [Ruc11]. Also in the case of triangle contact representations, the author of this thesis was able to use this strategy of setting up a system of linear equations and changing the Schnyder wood for improvements to reprove the existence of equilateral triangle contact representations, i.e., the result by Gonçalves et al., in his master thesis [Sch16], see also [Sch17].

Another nice result from [GLP12] is that every 3-connected planar graph has a *primal-dual triangle contact representation*, i.e., there exists a dissection of a triangle into smaller triangles such that the side-side contact graph is bipartite and the corner-side contact graphs of the two classes of the bipartition represent the primal and the dual graph, see Fig. 1.3b. In the proof, *generalized Schnyder woods*, which are introduced by Felsner [Fel01], are used as an encoding of the combinatorial structure of the primal-dual triangle contact representation, guiding the construction of this contact representation.

General convex shapes. We mentioned above that the proof of the existence of equilateral triangle contact representations in [GLP12] is an application of the Convex Packing Theorem by Schramm [Sch07], a strong theorem based on his Monster Packing Theorem. It allows to prescribe an individual convex prototype for each vertex of a plane triangulation and guarantees the existence of a contact representation of this triangulation in which each vertex is represented by a scaled copy of its own prototype. In general, it can happen that some of the prototypes are scaled down to a single point but not if the prototypes have smooth boundaries. The drawback of this approach is that the proof of the Monster Packing Theorem uses Brouwer's fixed-point theorem and therefore does not lead to an efficient way to compute the contact representations. Schramm [Sch91] gives an alternative proof of the Convex Packing Theorem for the case in which the boundaries of the prototypes are smooth. This time, the proof is more elementary and also proves the uniqueness of the contact representation if the outer vertices of the given triangulation are represented by the three sides of a given triangle.

Shapes in 3-space. Although we focus on contact representations in the plane in this thesis, we want to mention, for completeness, that there is also literature about contact representations in 3-space. Thomassen [Tho86] showed that each planar graph has a contact representation with axis-aligned boxes in 3-space, see also [BEF+12] for an alternative proof using Schnyder woods. Felsner and Francis [FF11] improved this by showing that planar graphs have contact representations with axis-aligned cubes. But, in contrast to Thomassen, they cannot guaranty that the cube contacts are proper, i.e., that the intersection has non-zero area. The question whether each planar graph has a proper contact representation with cubes has then been studied in [BEF+12; AKK16]. They present partial results, but leave the general question open. Another generalization of Thomassen's result was proved in [AEK+15] by showing that each planar graph has a primal-dual contact representation with boxes.

Also contact representations of 2-dimensional shapes in 3-space have been studied.

In [ERS+19] it was shown that each planar graph has a contact representation with convex polygons in 3-space. In [FKU20] this result was strengthened for 3-colorable planar graphs by showing that those graphs have a contact representation with axis-aligned rectangles in 3-space.

1.2 Our contribution

Our main goal is to develop a theory of convex contact representations that is independent of Schramm's Monster Packing Theorem. The reason for this aim is that the approach with the Monster Packing Theorem seems not to allow answering two central questions: Can a contact representation be computed efficiently? And is a contact representation unique under certain constraints? Thereby, we will mainly focus on the discrete case that the prototypes are convex polygons since this case is not covered by the proof of the Convex Packing Theorem in [Sch91].

The base for this theory will be an approach using systems of linear equations similar to the ones mentioned in the last section for computing contact representations with squares and equilateral triangles. Since these systems of equations are based on combinatorial objects describing the combinatorial structure of a contact representation, we will first study the combinatorial structure of contact representations with regular K-gons for a fixed K. In fact, we will not only consider regular K-gons as prototypes but a more general class of K-gons that also includes equiangular K-gons. With these combinatorial structures at hand, we will introduce systems of equations for the computation of contact representations with this class of K-gons. We will show that these systems of equations are suitable to be used for the procedure which is based on solving the system of equations belonging to a given combinatorial structure, then changing this structure based on the signs of the variables in the solution, and repeating these steps until the solution is non-negative and the contact representation can be constructed from this solution. We will discuss the performance of the resulting procedure by proving lower bounds on the worst case number of iterations and comparing these to statistical data from practical experiments.

Further, we will prove the existence of contact representations with prototypes from the considered class of K-gons along the lines of the approach taken by the author of this thesis in [Sch16; Sch17]. Thereby, we will simplify the proofs in [Sch16; Sch17] by superseding the technical geometric part of these original proofs. Finally, using a convergence argument, we will reprove a variant of Schramm's Convex Packing Theorem that is weaker than the original Convex Packing Theorem only in the point that it is less flexible concerning the representation of the outer face of the graph.

1.3 Outline

This thesis is structured as follows: In Chapter 2, we introduce some basic notions that are used throughout this thesis and recall some theory on orientations of graphs

with prescribed out-degrees. In Chapter 3, we recall transversal structures, Schnyder woods, and generalized Schnyder woods as the combinatorial structures of rectangle contact representations, triangle contact representations, and primal-dual triangle contact representations. After that, we will study the combinatorial structures of similarly-aligned odd K-gon contact representations and parallel-sided even K-gon contact representations as generalizations of contact representations with regular K-gons for odd and even K, respectively. Then, in Chapter 4, we will describe systems of linear equations that are based on the combinatorial structures from Chapter 3 and are supposed to compute a contact representation inducing these contact structures. Further, we will prove its unique solvability and some structural results on the solution. In Chapter 5, we will use these systems of equations to prove the existence of similarly-aligned odd K-gon and parallel-sided even K-gon contact representations. Afterwards, we will reprove a slightly weaker version of Schramm's Convex Packing Theorem using these results. Then, in Chapter 6, we will develop two algorithmic approaches for the computation of similarly-aligned odd K-gon and parallel-sided even K-gon contact representations that are also based on the systems of linear equations from Chapter 4. The first one performs well in practice and the second one is inspired by the proof of the existence of the contact representations in Chapter 5. But both algorithms lack a proof of termination. For the first algorithm, we will prove lower bounds to the worst case running time and compare these to the performance observed in practical experiments. Finally, in Chapter 7, we complete this thesis by stating open questions and future directions of research.

In Appendix A, there is an overview of the structures associated with contact representations that are defined in Chapter 3. This is meant to be an easy to find place to look up these structures when reading the thesis. In Appendix B, there are some beautiful illustrations of the first algorithmic approach from Chapter 6.

Chapter 2

Preliminaries

In this chapter we will introduce some basic notations that we will use throughout the thesis. In Section 2.1 we will focus on notations concerning graphs and in Section 2.2 we will focus on notations concerning polygons. Further, in Section 2.3, we will recall some results concerning orientations of graphs with prescribed out-degrees and flows with prescribed excesses.

2.1 Graphs

All graphs considered in this thesis are connected and finite. They can be simple graphs or multigraphs and they can be directed or undirected. If nothing else is said (or is clear from the context), we assume that all graphs are simple and undirected. In general, we denote an edge between the vertices v and w as vw or wv and do not distinguish between these two notations. If we want to specify the orientation of the edge (in a directed graph), we denote the edge as (v, w), if it is oriented from v to w, and as (w, v) if it is oriented from w to v. For a directed graph, the number of incoming edges of a vertex v is called the *in-degree* of v, denoted by $\deg^-(v)$, and the number of outgoing edges of v is called the *out-degree* of v, denoted by $\deg^+(v)$. For graph-theoretic terms not defined here we refer to [Die17].

Plane graphs. A *plane* graph is a graph together with a fixed combinatorial crossing-free embedding to the plane: this means that for each vertex of the graph the clockwise order of its incident edges is fixed. In particular, with the *embedding* of a plane graph we always mean a combinatorial embedding and not a fixed drawing in the plane. A *plane triangulation* is a plane graph all of whose faces have degree three. An *inner triangulation of a K-cycle* is a plane graph with an unbounded face of degree K and all bounded faces of degree three. Further, in this thesis we always require the K-cycle of the unbounded face to be an induced cycle, i.e., not to have any chords. We denote the unbounded face of a graph as the *outer face*. Further, we call the vertices and edges that are incident to the outer face *outer vertices* and *outer edges*, respectively. The remaining vertices, edges, and faces are denoted by *inner vertices*, *inner edges*, and *inner faces*.

Counting edges and faces. By Euler's formula, an inner triangulation of a K-cycle with n vertices (including the K vertices of the outer face) has exactly $3n - K - 3$ edges and $2n - K - 1$ faces.

Medial graph. The *medial graph* of a plane graph G has a vertex for each edge of G and an edge between two vertices for each face of G in which their corresponding edges occur consecutively. Since the crossing-free embedding of G induces a crossing-free embedding of the medial graph of G (see Fig. 2.1), the medial graph is also considered as a plane graph.

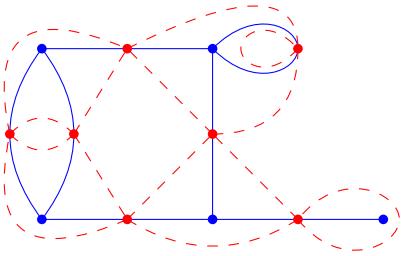

Figure 2.1: A plane graph in blue and its medial graph in red.

Angular graphs. The *angular graph* of a plane graph G is the plane bipartite graph whose two vertex classes are the vertices of G and the faces of G. The vertices corresponding to the faces of G are placed into the face of G they correspond to. The angular graph has, for each vertex v of G and for each pair of consecutive incident edges of v, an edge leaving v between these two edges and going to the unique face-vertex that is reachable without intersecting any edge or vertex of G. If we remove the vertex corresponding to the outer face of G from the angular graph, the embedding of the remaining graph is unique. Figure 2.2 shows an example.

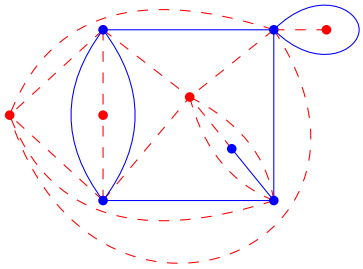

Figure 2.2: A plane graph in blue and its angular graph in red (including the blue vertices).

Maximal plane graphs. In most cases, we only consider contact representations of inner triangulations of K-cycles in this thesis. Note that statements about the existence or the computational complexity of the calculation of certain contact representations for inner triangulations of a K-cycle usually carry over to all plane

graphs since each plane graph is an induced subgraph of an inner triangulation of a K-cycle of size $O(n + K)$ where n is the number of vertices of the original graph, see, e.g., [GIP18].

2.2 Polygons

In this work, a *polygon* is a closed polygonal chain, i.e., it has no holes. We use the convention that a polygon has *sides* and *corners*, in contrast to a graph that has *edges* and *vertices*. A polygon is *simple* if it has distinct corners, the interiors of the sides are disjoint, and the sides do not pass through corners. A polygon is *weakly simple* if, for each $\varepsilon > 0$, the corners can be perturbed within a distance of ε such that the resulting polygon is simple. In this work, all polygons are weakly simple. The sum of the interior angles of a weakly simple k-gon is $(k-2)\pi$ and its area is $\frac{1}{2}\sum_{i=0}^{k-1}(x_{i+1}y_i - x_i y_{i+1})$ where $(x_0, y_0), \ldots, (x_{k-1}, y_{k-1})$ are the coordinates of its corners in clockwise order and indices are to be understood modulo k.

We call a corner of a polygon *convex*, if the inner angle at this corner is at most π, and we call it *concave* if it is at least π. A polygon with only convex corners is called a *convex polygon* and a polygon with exactly three convex corners is called a *pseudotriangle*. Two polygons are called *(positive) homothetic* if they can be transformed into each other by translation and scaling (with a positive factor).

Now let $x_0, \ldots, x_{k-1} \in \mathbb{R}^2$ be the coordinates of the corners of a polygon in clockwise order. Then the *slope* of the side between the corners x_i and x_{i+1} is defined as the equivalence class of the vector $x_{i+1} - x_i$ under the equivalence relation where $y \sim z$ if and only if there is an $\beta > 0$ such that $y = \beta z$. We call two sides of slopes s and s' *parallel*, if $s = s'$, and *antiparallel* if $s = -s'$.

2.3 α-orientations and ω-flows

α-orientations. An *α-orientation* is an orientation of a graph with prescribed numbers of incoming and outgoing edges for each vertex, given by a function α.

Definition 2.1 (α-orientation)**.** Let G be a graph and let $\alpha : V(G) \to \mathbb{N}$ be a mapping. Then an *α-orientation* of G is an orientation X of the edges of G such that $\deg^+_X(v) = \alpha(v)$ for all $v \in V(G)$.

Felsner [Fel04] shows that the following condition, which is obviously necessary for the existence of an α-orientation, is also sufficient.

Theorem 2.2 (Felsner [Fel04])**.** *Let $G = (V, E)$ be a graph and let $\alpha : V \to \mathbb{N}$. Then there exists an α-orientation of G if and only if $\sum_{v \in V} \alpha(v) = |E|$ and $\sum_{v \in A} \alpha(v) \leq |E_{\text{inc}}(A)|$ for every $A \subset V$, where $E_{\text{inc}}(A)$ denotes the set of edges incident to a vertex in A.*

The set of all α-orientations of a plane graph carries the structure of a distributive lattice. Below we refer to [Fel04] for this result, but as noted in [FO01] it has already

been proved in the PhD thesis of Ossona de Mendez [Oss94]. To be able to describe the cover relation of this distributive lattice, we need some more definitions.

Definition 2.3 (Chordal path)**.** A *chordal path* of a simple cycle C in a directed plane graph is a directed path consisting of edges in the interior of C whose first and last vertex are vertices of C. These two vertices are allowed to coincide.

Definition 2.4 (Essential cycle (α-orientation))**.** A simple cycle C of G is an *essential cycle* if there exists an α-orientation of G in which C is a directed cycle and has no chordal path.

Definition 2.5 (Flip (α-orientation))**.** A *flip* is the reorientation of an essential cycle from counterclockwise to clockwise.

This flip operation exactly describes the cover relation in the distributive lattice.

Theorem 2.6 (Felsner [Fel04])**.** *The following relation on the set of all α-orientations of a plane graph G is the cover relation of a distributive lattice: An α-orientation X' of G covers an α-orientation X of G if X' can be obtained from X by a flip.*

ω-flows. The concept of α-orientations can be generalized to the setting of integral flows on graphs.

Definition 2.7 (Excess)**.** Let D be a directed graph and let $f : E(D) \to \mathbb{Z}$ be a flow on G. Then the *excess* of a vertex $v \in V(D)$ is defined as $\text{excess}(v) := \sum_{e \in E^-(v)} f(e) - \sum_{e \in E^+(v)} f(e)$.

Definition 2.8 (ω-flow)**.** Let D be a directed graph, and let $c_l, c_u : E(D) \to \mathbb{Z}$ and $\omega : V(D) \to \mathbb{Z}$ be mappings. Then a flow f on D is called an (ω, c_l, c_u)-*flow* (or for short ω-*flow*) if $c_l(e) \leq f(e) \leq c_u(e)$ for all $e \in E(D)$ and $\text{excess}(v) = \omega(v)$ for all $v \in V(D)$.

This is indeed a generalization of α-orientations: Given a graph G and a mapping $\alpha : V(G) \to \mathbb{N}$, let D be an arbitrary orientation of G, let $c_l = \mathbf{0}$, let $c_u = \mathbf{1}$, and let $\omega(v) = \alpha(v) - \deg_D^+(v)$ for all $v \in V(G)$. Then an α-orientation X of G can be mapped bijectively to an ω-flow f of D by setting $f(e) = 0$, if e has the same orientation in X and D, and $f(e) = 1$ if e has different orientations in X and D.

Also the set of all ω-flows of a directed plane graph carries the structure of a distributive lattice. Again, we need some definitions to be able to describe the cover relation of this distributive lattice.

Definition 2.9 (Residual graph)**.** For an (ω, c_l, c_u)-flow f of a directed plane graph D, the *residual graph* D_f is the following reorientation of D: an arc $e = (v, w)$ of D is oriented from v to w in D_f if $f(e) < c_u(e)$, and it is oriented from w to v in D_f if $f(e) > c_l(e)$. Note that in D_f an edge can have no orientation, one orientation, or two orientations.

Definition 2.10 (Essential cycle (ω-flow))**.** A simple cycle C in the underlying undirected graph of D is an *essential cycle* if there exists an ω-flow f such that C is a directed cycle in D_f and C has no chordal path in D_f.

Definition 2.11 (Flip (ω-flow))**.** Let C be an essential cycle and let C_{cw} be the clockwise orientation of C. *Flipping* C in a flow of D means increasing the flow value of an arc (v, w) by 1 if $(v, w) \in C_{\text{cw}}$, and decreasing the flow value of an arc (v, w) by 1 if $(w, v) \in C_{\text{cw}}$.

Again, this flip operation exactly describes the cover relation of the distributive lattice.

Theorem 2.12 (Felsner, Knauer [FK09])**.** *The following relation on the set of all ω-flows of a directed plane graph D is the cover relation of a distributive lattice: an ω-flow f' of D covers an ω-flow f of D if f' can be obtained from f by a flip.*

Chapter 3

The combinatorial structure of polygon contact representations

In this chapter we will study the combinatorial structure of contact representations of plane graphs with different classes of convex polygons. In Section 3.1 we will summarize the known results about the combinatorial structures of contact representations with triangles and rectangles. In the rest of this chapter we will finish the characterization of the combinatorial structure of contact representation with regular polygons by considering a generalization of the class of regular K-gons for odd K in Section 3.2 and a generalization of the class of regular K-gons for even K in Section 3.3.

3.1 Triangle, rectangle, and primal-dual triangle contact representations

In this section we give an overview over the results concerning the combinatorial structure of convex polygon contact representations that have been known before the start of the work on this thesis.

3.1.1 Homothetic triangle contact representations

In the introduction we mentioned that the combinatorial structure of triangle contact representations of a plane triangulation can be described by a Schnyder wood. Here we are only interested in the special case of *homothetic triangle contact representations*, i.e., triangle contact representations of a plane triangulation where the triangles are pairwise positive homothetic.

Definition 3.1 (Schnyder wood)**.** A *Schnyder wood* of an inner triangulation G of the 3-cycle b_0, b_1, b_2 is an orientation and coloring of the inner edges of G in the colors $0, 1, 2$ such that the following conditions are satisfied:

(SW1) All edges incident to b_i are oriented towards b_i and colored in the color i.

(SW2) Each inner vertex has in clockwise order exactly one outgoing edge of color 0, one outgoing edge of color 1, and one outgoing edge of color 2, and in the interval between two outgoing edges there are only incoming edges in the third color.

Figure 3.1 gives an illustration of Definition 3.1.

(a) The outer vertex condition (SW1). (b) The inner vertex condition (SW2).

Figure 3.1: The two local conditions of a Schnyder wood.

Now we will sketch how a homothetic triangle contact representation of a graph G induces a Schnyder wood of G. Since homothetic triangle contact representations are a special case of the contact representations studied in Section 3.2, a detailed description will follow in that section. Let T be one of the triangles of the contact representation. We color the corners of T in clockwise order in the colors 0, 1, and 2. Since each of the triangles is homothetic to T, each triangle corner c naturally corresponds to one of the corners c' of T. Then we assign the color of c' also to c. We assume that exactly one corner is involved in each contact of two triangles. We orient the corresponding edge of the contact graph from the triangle contributing the corner to the contact to triangle contributing a side to the contact and color it in the color of the corner involved in the contact, see Fig. 3.2.

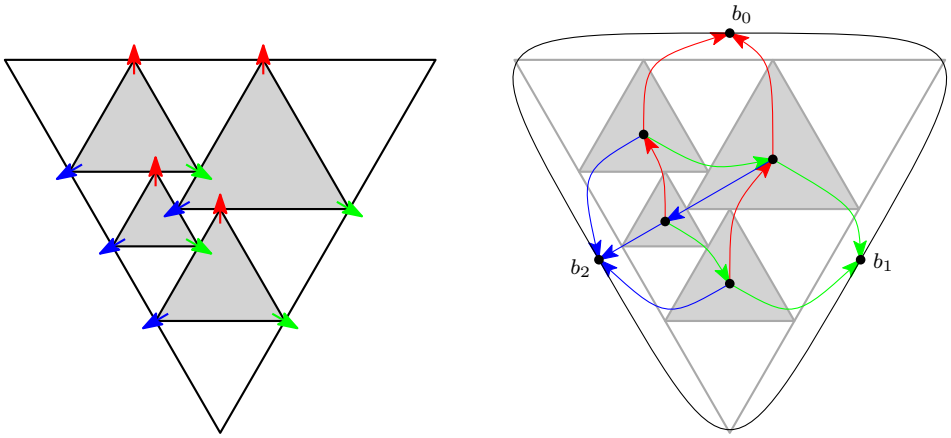

Figure 3.2: The induced Schnyder wood of a homothetic triangle contact representation. The triangles corresponding to the three outer vertices are not completely drawn. Red edges correspond to a top corner, green edge to a lower right corner, and blue edges to a lower left corner of a triangle.

Schnyder [Sch90a] introduced Schnyder woods as *realizers* for the purpose of embedding planar graphs on small grids. In this work he shows that each plane triangulation admits a Schnyder wood.

Theorem 3.2 (Schnyder [Sch90a])**.** *The inner edges of each plane triangulation can be oriented and colored in such a way that the result is a Schnyder wood.*

Schnyder woods are in bijection to certain α-orientations. Indeed, the colors of the edges of a Schnyder wood can be recovered from the edge orientations [FO01]. Therefore, Schnyder woods are in bijection to orientations of the inner edges of the underlying triangulation in which each inner vertex has exactly three outgoing edges. This implies the following theorem.

Theorem 3.3 (Ossona de Mendez [Oss94])**.** *The set of the Schnyder woods of a fixed graph carries the structure of a distributive lattice.*

The flip operation describing the cover relation in this lattice is the reorientation of a 3-cycle from counterclockwise to clockwise and an appropriate adjustment of the colors of the edges. Figure 3.3 shows the effect of such a flip on the triangle contact representation.

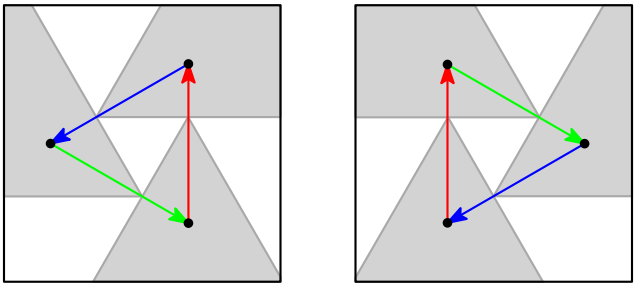

Figure 3.3: Geometric effect of a flip of the induced Schnyder wood on the triangle contact representation.

3.1.2 Rectangle contact representations

We also mentioned in the introduction that transversal structures describe the combinatorial structure of rectangle contact representations of inner triangulations without separating 3-cycles.

Definition 3.4 (Transversal structure)**.** Given an inner triangulation G of the 4-cycle v_N, v_E, v_S, v_W without separating 3-cycles, a *transversal structure* of G is an orientation and coloring of the inner edges of G in the colors red and blue such that the following conditions are satisfied:

(TS1) All inner edges incident to v_N, v_E, v_S, and v_W are incoming red, incoming blue, outgoing red, and outgoing blue edges, respectively.

(TS2) In clockwise order around each inner vertex of G, its incident edges form: a non-empty interval of outgoing red edges, a non-empty interval of outgoing blue edges, a non-empty interval of incoming red edges, and a non-empty interval of incoming blue edges.

Figure 3.4 gives an illustration of Definition 3.4.

(a) The outer vertex condition (TS1). (b) The inner vertex condition (TS2).

Figure 3.4: The two local conditions of a transversal structure.

A rectangle contact representation of a graph G induces a transversal structure of G in the following way: If two neighboring rectangles share a horizontal segment, the corresponding edge is colored red and oriented from the vertex corresponding to the lower rectangle to the vertex corresponding to the upper rectangle. If two neighboring rectangles share a vertical segment, the corresponding edge is colored blue and oriented from the vertex corresponding to the left rectangle to the vertex corresponding to the right rectangle, see Fig. 3.5. In [He93] it is shown that each inner triangulation of a 4-cycle without separating triangles has a rectangle contact representation. More precisely, the following two theorems are shown.

Theorem 3.5 (He [He93])**.** *Each inner triangulation of a 4-cycle without separating triangles admits a transversal structure.*

Theorem 3.6 (He [He93])**.** *For each transversal structure T of G, there exists a rectangle contact representation of G inducing T.*

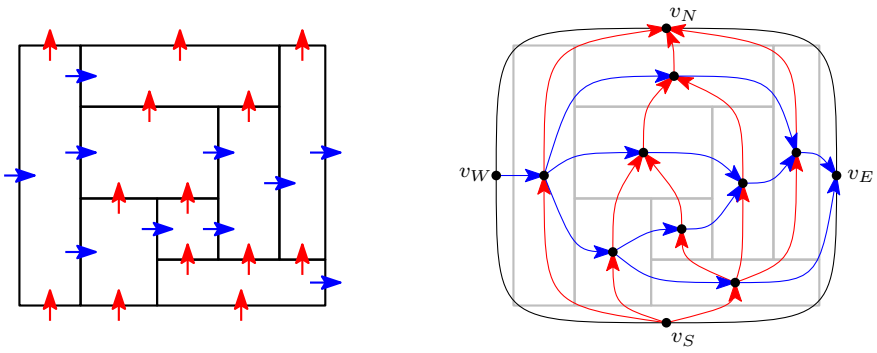

Figure 3.5: The induced transversal structure of a rectangle contact representation. Red edges correspond to a pair of rectangles sharing a horizontal segment, blue edges correspond to a pair of rectangles sharing a vertical segment.

A deeper combinatorial study of transversal structures can be found in the PhD thesis of Fusy [Fus07], see also [Fus09]. There it is shown that the transversal structures of a fixed graph G are in bijection to α-orientations of the medial graph of G which leads to the following theorem.

Theorem 3.7 (Fusy [Fus07; Fus09])**.** *The set of the transversal structures of a fixed graph carries the structure of a distributive lattice.*

The flip operations describing the cover relation in this lattice can be be described as follows: Let C be a 4-cycle in the contact graph G with two red edges and two blue edges such that the vertex of C with an outgoing blue and an outgoing red edge on C has an outgoing red edge pointing into the interior of C or the vertex of C with an outgoing blue and an incoming red edge on C has an outgoing blue edge pointing into the interior of C. Then a flip is a change of the colors of all edges strictly inside C and an appropriate adjustment of the orientations of these edges (the orientations of the edges of a transversal structure are in general forced by the coloring). Figure 3.6 shows the effect of such a flip on the rectangle contact representation.

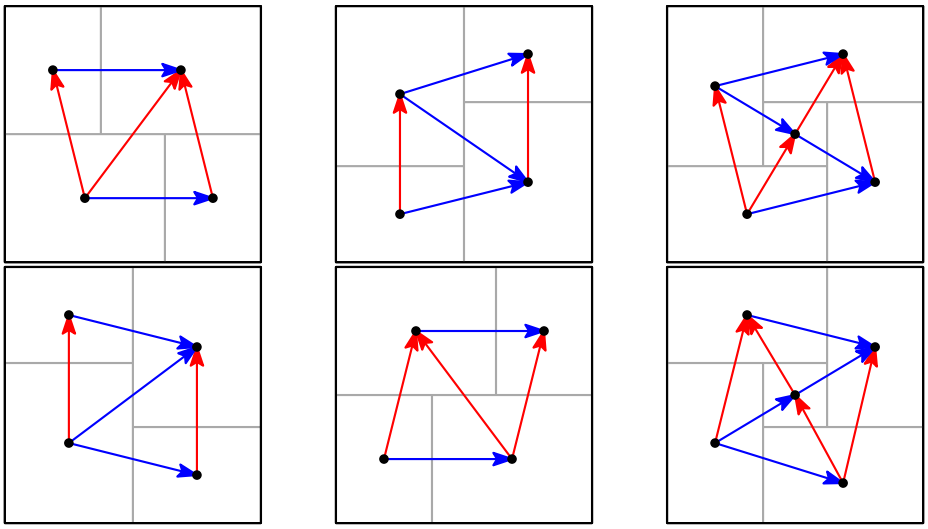

Figure 3.6: The geometric effect of a flip of the induced transversal structure on the rectangle contact representation. Three examples are shown (top-bottom pairs belong together). All the remaining cases are of the third type with more vertices inside the 4-cycle.

Like for Schnyder woods, the distributive lattice of transversal structures is implied by a bijection between transversal structures and certain α-orientations. We set $\alpha_{4,1}(v) = 4$ for each inner vertex of G, $\alpha_{4,1}(f) = 1$ for each inner face of G, $\alpha_{4,1}(v) = 0$ for $v \in \{v_W, v_E\}$, and $\alpha_{4,1}(v) = 2$ for $v \in \{v_S, v_N\}$. Then, according to [Fus07; Fus09], the transversal structures of G are in bijection to the $\alpha_{4,1}$-orientations of the angular graph $\widetilde{G}$ of G without the vertex corresponding to the outer face of G.

Also without constructing a transversal structure as an intermediate step, it can easily be seen that each rectangle contact representation $\mathcal{C}$ of G induces an $\alpha_{4,1}$-orientation of $\widetilde{G}$. The face-vertices of $\widetilde{G}$ correspond to the touching points of segments in $\mathcal{C}$ and the inner vertex-vertices correspond to the rectangles of $\mathcal{C}$. We obtain an $\alpha_{4,1}$-orientation of $\widetilde{G}$ by orienting the four incident edges of each inner vertex-vertex v that are going to the corners of the rectangle corresponding to v as outgoing for v. See Fig. 3.7 for an example.

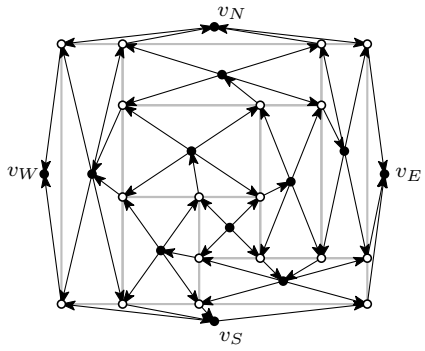

Figure 3.7: The induced $\alpha_{4,1}$-orientation of a rectangle contact representation. The black vertices are the vertex-vertices and the white vertices the face-vertices of $\widetilde{G}$.

3.1.3 Homothetic primal-dual triangle contact representations

The combinatorial structure of a primal-dual triangle contact representation of a 3-connected plane graph can be described as a generalized Schnyder wood, as we mentioned in the introduction. Here, we are only interested in homothetic primal-dual triangle contact representations, i.e., the vertices of the graph are represented by equilateral triangles with a horizontal side at the bottom and the faces of the graph are represented by equilateral triangles with a horizontal side at the top. Generalized Schnyder woods are introduced in [Fel01]. The following definition is from [Fel03].

Definition 3.8 (Generalized Schnyder wood)**.** Let G be a 3-connected plane graph with three designated vertices b_0, b_1, b_2 in this clockwise order on the outer face. The suspension G^σ is obtained from G by attaching half-edges that reach into the outer face at the vertices b_0, b_1, b_2. Then a *generalized Schnyder wood* of G is an orientation and coloring of the edges of G^σ in the colors $0, 1, 2$ satisfying the following conditions:

(gSW1) Each edge is oriented in one or in two opposite directions. Each direction of an edge is colored and, if the edge has two directions, these two directions have different colors.

(gSW2) For $i = 0, 1, 2$, the half-edge at b_i is outgoing at b_i and has color i.

(gSW3) Each inner vertex has in clockwise order exactly one outgoing edge of color 0, one outgoing edge of color 1 and one outgoing edge of color 2. Each incoming edge of color i is in the clockwise sector from the outgoing edge of color $i+1$ to the outgoing edge of color $i-1$ (with indices understood modulo 3).

(gSW4) The boundary of an inner face is not a directed monochromatic cycle.

The way a homothetic primal-dual triangle contact representation of G induces a generalized Schnyder wood of G^σ is similar to the way a homothetic triangle contact representation of a triangulation induces a Schnyder wood of this triangulation. Indeed, if G is a triangulation we obtain the procedure from Section 3.1.1 as a special case. As for homothetic triangle contact representations, we can associate the corners of the primal triangles with the colors 0, 1, and 2. Let us assume that the intersection of each triple of primal triangles is empty. Then in a contact point of two primal triangles there is either exactly one corner of a primal triangle involved or exactly two corners are involved. We orient each edge as outgoing from each vertex whose corresponding primal triangle contributes a corner c to the contact and color this direction in the color of c, see Fig. 3.8a. If there are three primal triangles sharing a common point, this can be treated as a degenerate version of the case that only two corners are involved in each contact.

Felsner [Fel01], who introduces generalized Schnyder woods, also proves their existence.

Theorem 3.9 (Felsner [Fel01])**.** *Each 3-connected plane graph admits a generalized Schnyder wood.*

Like Schnyder woods and transversal structures, also the generalized Schnyder woods of a graph G are in bijection to α-orientations of a graph $\widetilde{G}$ which is defined as follows [Fel04]: The graph $\widetilde{G}$ has a vertex for each vertex of G, a vertex for

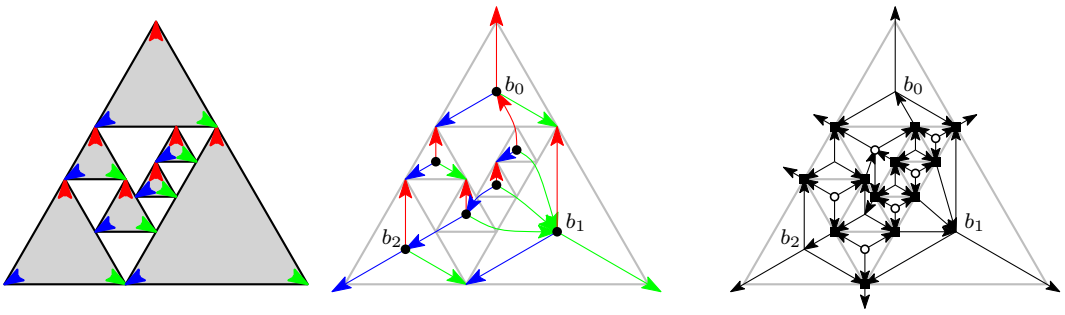

(a) The induced generalized Schnyder wood. Red edges correspond to a top corner, green edges to a lower right corner, and blue edges to a lower left corner of a triangle.

(b) The corresponding α-orientation of $\widetilde{G}$.

Figure 3.8: The induced generalized Schnyder wood of a homothetic primal-dual triangle contact representation and the corresponding α-orientation of $\widetilde{G}$.

each face of G, and a vertex for each edge of G. For each vertex-edge and face-edge incidence in G, there is an edge in $\widetilde{G}$ between the corresponding vertices. Additionally, for $i = 0, 1, 2$, there is an edge between b_i and the vertex corresponding to the outer face of G. Then the generalized Schnyder woods of G are in bijection to $\alpha_{3,1}$-orientations of $\widetilde{G}$ with $\alpha_{3,1}(v) = 3$ for each vertex v corresponding to a vertex or an inner face of G, $\alpha_{3,1}(v) = 1$ for each vertex v corresponding to an edge of G, and $\alpha_{3,1}(v) = 0$ for the vertex v corresponding to the outer face of G.

We can also directly see that a homothetic primal-dual triangle contact representation of G induces an $\alpha_{3,1}$-orientation of $\widetilde{G}$. The edge-vertices of $\widetilde{G}$ correspond to the corners of the triangles in the contact representation. We give each vertex-vertex and face-vertex outgoing edges to the three edge-vertices corresponding to the three corners of the corresponding triangle. The remaining edges are oriented as outgoing for the incident edge-vertex, see Fig. 3.8b.

The bijection between generalized Schnyder woods and $\alpha_{3,1}$-orientations of $\widetilde{G}$ also implies to following theorem.

Theorem 3.10 (Felsner [Fel04])**.** *The set of the generalized Schnyder woods of a fixed graph carries the structure of a distributive lattice.*

The flip operation cannot be described as easily as in the previous cases. Felsner [Fel04] shows that the essential cycles in the $\alpha_{3,1}$-orientations of $\widetilde{G}$ can have lengths 4, 6, 8, 10, and 12. Figure 3.9 shows the effects of some examples of flips corresponding to essential cycles of lengths 4, 6, and 8 on the contact representation.

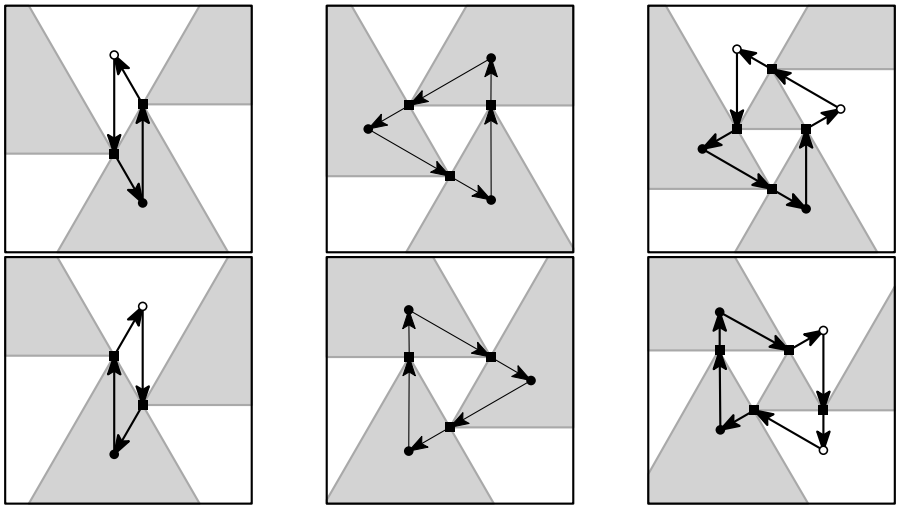

Figure 3.9: The geometric effect of a flip of the induced $\alpha_{3,1}$-orientation of $\widetilde{G}$ on the primal-dual triangle contact representation. Three examples are shown (top-bottom pairs belong together) that are corresponding to essential cycles of lengths 4, 6, and 8.

3.2 Similarly-aligned odd K-gon contact representations

In this section we will study the combinatorial structure of so-called *similarly-aligned odd K-gon contact representations*. This class of contact representations is a generalization of the class of contact representations with equiangular K-gons for a fixed odd K which again is a generalization of contact representations with regular K-gons for a fixed odd K. A K-gon is *equiangular*, if all its inner corner angles are equal, and it is *regular* if it is equiangular and all its side lengths are equal. If we talk about regular or equiangular K-gon contact representations, we always assume that all K-gons have the same alignment, i.e., all K-gons have a horizontal side at the bottom. The study of regular pentagon contact representations has been initiated in the bachelor thesis of Steiner [Ste16] and has been continued in [FSS18b] and its conference version [FSS17]. The followup paper [FSS18a] studies equiangular K-gon contact representations for arbitrary fixed odd K. The important progress is the generalization of the parameter K. The step from regular to equiangular is marginal since the combinatorial properties of contact representations with regular pentagons that are exploited in [FSS17; FSS18b] are exactly those derived from the fact that regular pentagons are equiangular pentagons. The purpose for the generalization from equiangular to similarly-aligned K-gons in this work is to make the results applicable to a broader class of contact representations in a later chapter. Again, the combinatorial properties of these contact representations that we will exploit in this work are exactly those properties that are exploited in [FSS18a] for equiangular K-gon contact representations. Therefore, in this section it suffices if the reader has only the special case of equiangular (see Fig. 3.10a for an example) or even only regular K-gons (see Fig. 3.10b for an example) in mind.

Let us now give a definition of similarly-aligned odd K-gon contact representations. For two convex polygons A and B, we say that the corner c of A *can touch* the side s of B if there are translates A' of A and B' of B such that the interiors of A' and B' are disjoint and the corner c' of A' corresponding to the corner c of A is contained in the relative interior of the side s' of B' corresponding to the side s of B.

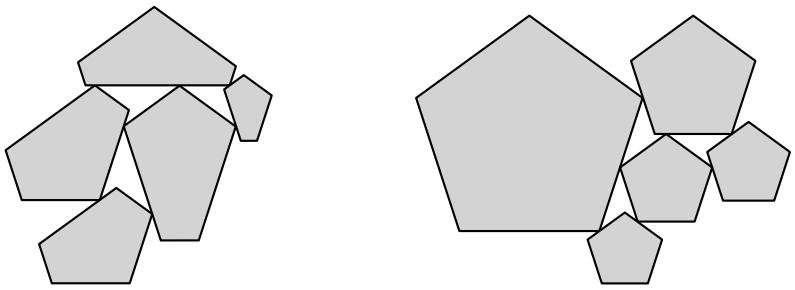

(a) An equiangular pentagon contact representation.

(b) A regular pentagon contact representation.

Figure 3.10: Two pentagon contact representations of the same graph.

In particular, c' is not allowed to be at an endpoint of s'. If additionally $A' \cap B' = c'$, we say that c can touch s *properly*.

Note that, for a fixed side s of B, there are exactly two possible cases. In the first case there is exactly one corner c of A that can touch s and then c can touch s properly. In the second case there are exactly two corners c and c' of A that can touch s and then c and c' are consecutive corners of A, the side of A between c and c' is antiparallel to s, and neither c nor c' can touch s properly.

Let G be a graph and let $K \geq 3$ be an odd number. For each vertex v of G, let P_v be a convex K-gon whose sides are labeled cyclically in clockwise order with $0, \ldots, K-1$ and whose corners are labeled with the label of the opposite side, i.e., the corner between the sides i and $i+1$ has label $i + \frac{K+1}{2}$. Here (and in the rest of this work) these labels are to be understood modulo K, i.e., labels i and $i + zK$ are the same for all $i, z \in \mathbb{Z}$. We denote the side and corner of P_v which are labeled with i by $\text{side}_i(P_v)$ and $\text{corner}_i(P_v)$, respectively. The polygons P_v, $v \in V(G)$, are called *(properly) similarly-aligned odd K-gons* if, for each ordered pair (v, w) of adjacent vertices in G and for each label $i \in \{0, \ldots, K-1\}$, $\text{corner}_i(P_v)$ can touch $\text{side}_i(P_w)$ (properly).

Theorem 3.11. *If G has a contact representation $\mathcal{C}$ with similarly-aligned odd K-gons, then G is a planar graph.*

Proof. First we show that for each edge vw of G there is a label i such that $\text{corner}_i(P_v)$ touches $\text{side}_i(P_w)$ or $\text{corner}_i(P_w)$ touches $\text{side}_i(P_v)$ in $\mathcal{C}$. Assume that $\text{corner}_i(P_v)$ touches $\text{side}_j(P_w)$ for some $j \neq i$. Then also $\text{corner}_j(P_v)$ can touch $\text{side}_j(P_w)$. Thus $\text{corner}_i(P_v)$ and $\text{corner}_j(P_v)$ have to be consecutive corners of P_v and the side between these two corners has to be antiparallel to $\text{side}_j(P_w)$. Therefore, we have $|i-j| = 1$ and due to symmetry we can assume that $j = i+1$. Thus $\text{corner}_{i+1}(P_v)$ touches $\text{side}_{i+1}(P_w)$ or $\text{corner}_{i+\frac{K+1}{2}}(P_w)$ touches $\text{side}_{i+\frac{K+1}{2}}(P_v)$ in $\mathcal{C}$, see Fig. 3.11.

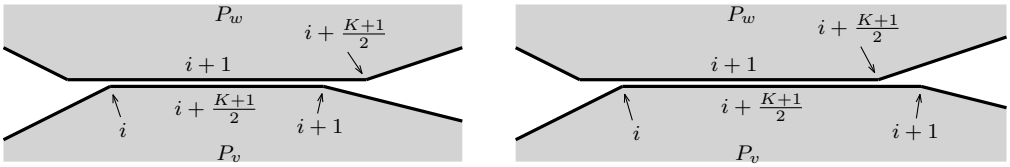

Figure 3.11: If $\text{side}_{i+1}(P_w)$ and $\text{side}_{i+\frac{K+1}{2}}(P_v)$ are antiparallel and $\text{corner}_i(P_v)$ touches $\text{side}_{i+1}(P_w)$, then $\text{corner}_{i+1}(P_v)$ touches $\text{side}_{i+1}(P_w)$ or $\text{corner}_{i+\frac{K+1}{2}}(P_w)$ touches $\text{side}_{i+\frac{K+1}{2}}(P_v)$.

Now let p be a point in $\mathcal{C}$ where two or more corners touch. Let i and j be the labels of two corners involved in this touching. Then $j \in \{i + \frac{K-1}{2}, i + \frac{K+1}{2}\}$ since these are the labels of the endpoints of a side with label i. In particular, we have $i \neq j$. Therefore, there are at most three corners involved in the touching at p. If there are three corners involved, we further have $i + \frac{K+1}{2} \in \{(i + \frac{K-1}{2}) + \frac{K-1}{2}, (i + \frac{K-1}{2}) + \frac{K+1}{2}\}$. The former implies $K = 3$, the latter would imply $K = 1$, in contradiction to $K \geq 3$.

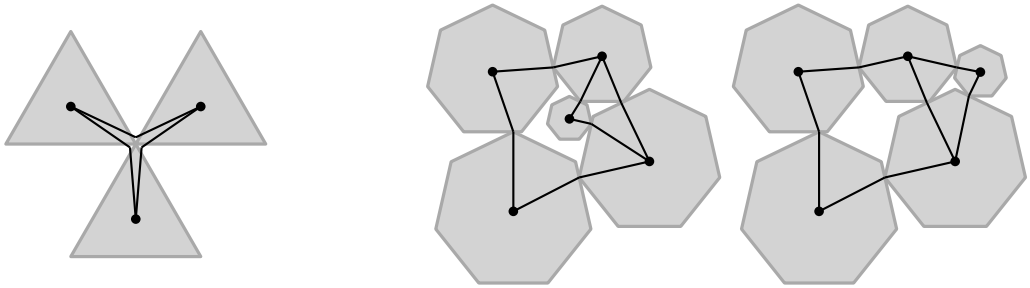

(a) Perturbed edge drawings in the induced embedding of a 3-cycle represented by three triangles with a common touching point.

(b) Two contact representations with regular 7-gons of the same graph G but with different induced embeddings of G.

Figure 3.12: The crossing-free drawing of G induced by its similarly-aligned odd K-gon contact representation.

We obtain a crossing-free drawing of G in the following way: We place each vertex v into the interior of P_v. Let vw be an edge of G represented in $\mathcal{C}$ by a touching of $\text{corner}_i(P_v)$ and $\text{side}_i(P_w)$. Then we draw vw by connecting v and w straight-line to $\text{corner}_i(P_v)$. If there are exactly two corners meeting in a point, we just drew the corresponding edge of G twice in exactly the same way. If there are three corners meeting in a point p, we have to perturb the three bends of the drawings of the three corresponding edges of G a bit to get rid of the crossing at p, see Fig. 3.12a. □

We call the crossing-free embedding of G obtained from a contact representation $\mathcal{C}$ as described in the proof of Theorem 3.11 the embedding *induced* by $\mathcal{C}$. See Fig. 3.12b for an example of two contact representations of the same graph inducing different embeddings of this graph. A point in $\mathcal{C}$ where two or three corners touch in one point is called an *exceptional touching*.

From now on, we will only consider plane graphs G and with a contact representation of G we will mean a contact representation inducing the given embedding of G. Moreover, we will restrict the class of considered graphs G to the class of inner triangulations of a K-cycle where the outer vertices play a special role: Let G be an inner triangulation of the K-cycle $a_0, \ldots, a_{K-1}$ (in clockwise order) for some odd $K \geq 3$. As before, the inner vertices v of G are represented by a convex K-gon P_v.

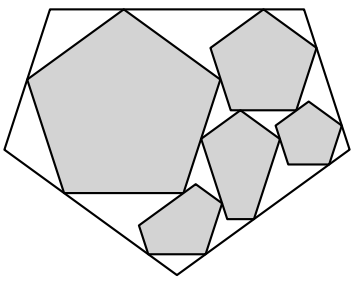

Figure 3.13: An equiangular pentagon contact representation.

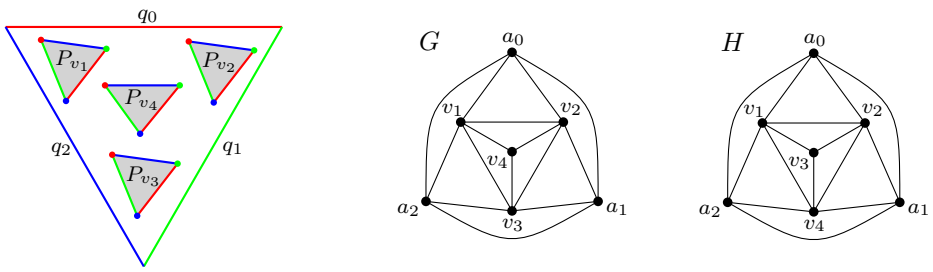

Figure 3.14: For the graph G, the polygons shown on the left side are similarly-aligned. The corresponding labeling of the sides and corners is indicated by the colors red (0), green (1), and blue (2). For the graph H, these polygons are not similarly-aligned because the side q_1 can only be touched by the upper right corner of P_{v_4} and the side q_2 can only be touched by the upper left corner of P_{v_4}, contradicting the clockwise order of the labels of the corners of P_{v_4}.

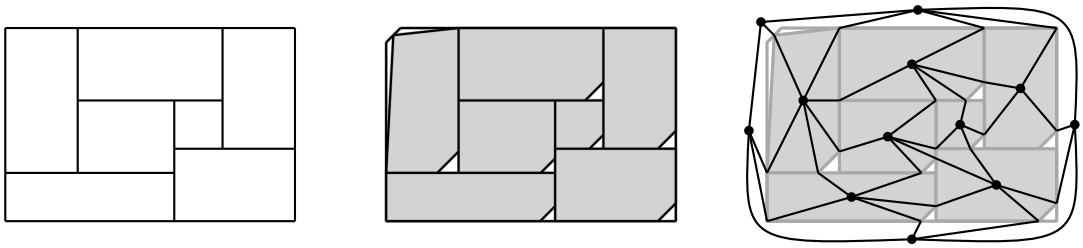

Figure 3.15: A rectangle contact representation (left) can be transformed into a non-properly similarly-aligned pentagon contact representation (middle) by clipping off the lower right corner of each rectangle. Additionally, the rectangle in the top left corner has to be perturbed since otherwise the upper left side of the outer pentagon would vanish. The left figure shows the induced embedding of the underlying graph.

But the outer vertices $a_0, \dots, a_{K-1}$ of G are represented by the sides $q_0, \dots, q_{K-1}$ (in clockwise order), respectively, of an additional convex K-gon Q. The polygons P_v are similarly-aligned odd K-gons. For the polygon Q, a similar property is fulfilled: If v is an inner vertex adjacent to the outer vertex a_i, then $\text{corner}_i(P_v)$ can touch the side q_i of the complement of Q. See Fig. 3.13 for a simple example we will use throughout this section to illustrate all concepts, see Fig. 3.14 for a more sophisticated example, and see Fig. 3.15 for an example of a non-properly similarly-aligned odd K-gon contact representation.

3.2.1 K-color forests

We will now introduce a combinatorial object that generalizes Schnyder woods in such a way that allows us to describe the combinatorial structure of similarly-aligned odd K-gon contact representations also for $K > 3$. Remember that Schnyder woods describe the combinatorial structure in the case $K = 3$, see Section 3.1.1.

For the rest of this section let $K \geq 3$ be a fixed odd number and let G be an inner triangulation of the K-cycle $a_0, \dots, a_{K-1}$ (in clockwise order).

Definition 3.12 (K-color forest (odd))**.** A *K-color forest* of G is an orientation and coloring of the inner edges of G in the colors $0, \dots, K-1$ with the following properties:

(F1) For $i = 0, \dots, K-1$, all inner edges incident to a_i are oriented towards a_i and colored in the color i.

(F2) For each inner vertex v, the incoming edges of v build K (possibly empty) blocks B_i, $i = 0, \dots, K-1$, of edges of color i and the clockwise order of these blocks is $B_0, \dots, B_{K-1}$. Moreover, v has at most one outgoing edge of color i and such an edge has to be located between the blocks $B_{i+\frac{K-1}{2}}$ and $B_{i+\frac{K+1}{2}}$.

Figure 3.16 gives an illustration of Definition 3.12.

(a) The outer vertex condition (F1). (b) The inner vertex condition (F2).

Figure 3.16: The two local conditions of a K-color forest shown for the example $K = 5$. Note that each inner vertex has at most one outgoing edge but arbitrarily many incoming edges of each color.

The following theorem shows the key correspondence between K-color forests and similarly-aligned odd K-gon contact representations.

Theorem 3.13. *Every similarly-aligned odd K-gon contact representation $\mathcal{S}$ induces a K-color forest on its contact graph G.*

Proof. First assume that $\mathcal{S}$ has no exceptional touchings, i.e., all touchings involve a polygon corner and the interior of a polygon side. Let e be an inner edge of G. If both incident vertices of e are inner vertices, e is realized in $\mathcal{S}$ by a touching of a corner of a K-gon P_v and a side of a K-gon P_w which have the same label i. Then we orient e from v to w and color it in color i. If an outer vertex a_i is incident to e (since G has no chords, e is incident to at most one outer vertex), e is realized in $\mathcal{S}$ by a touching of the corner with label i of a K-gon P_v and the side q_i of the K-gon Q. Then we orient e from v to a_i and color it in color i. It follows from the definition of the labeling of the corners and sides of the K-gons and from the fact that each corner of a K-gon can be involved in at most one contact that this yields a K-color forest. See Fig. 3.17 for an example.

Now let p be an exceptional touching in $\mathcal{S}$. From Theorem 3.11 we know that in p either two corners with labels i and j with $j \in \{i + \frac{K-1}{2}, i + \frac{K+1}{2}\}$ touch or exactly three corners with labels 0, 1, and 2 touch and $K = 3$. If there are only two corners involved in the touching, let these be $\text{corner}_i(P_v)$ and $\text{corner}_j(P_w)$. Then

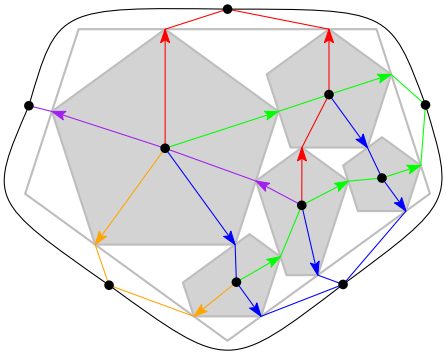

Figure 3.17: The 5-color forest induced by the contact representation of Fig. 3.13.

we either orient the edge vw from v to w and color it in color i, or we orient it from w to v and color it in color j, see Fig. 3.18a. Since in the first case there will not be an outgoing edge of w with color j and in the second case there will not be an outgoing edge of v of color i, the properties of a K-color forest are locally fulfilled. If there are three corners involved in the touching, let these be $\text{corner}_0(P_u)$, $\text{corner}_1(P_v)$, and $\text{corner}_2(P_w)$. Then we either orient the edges of the triangle uvw as $(u,v),(v,w),(w,u)$ and color them in the colors $0,1,2$, respectively, or we orient the edges as $(u,w),(w,v),(v,u)$ and color them in the colors $0,2,1$, respectively. In either case, the properties of a 3-color forest (or equivalently Schnyder wood) are fulfilled, see Fig. 3.18b. □

(a) The two possibilities to orient and color an edge of G corresponding to an exceptional touching of exactly two corners.

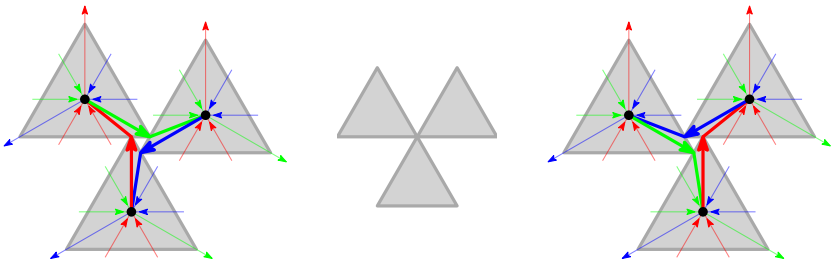

(b) The two possibilities to orient and color the three edges of G corresponding to an exceptional touching of three corners.

Figure 3.18: Situations in which the induced K-color forest is not unique. In both cases it is shown how the coloring can be interpreted as a resolution of the exceptional touching.

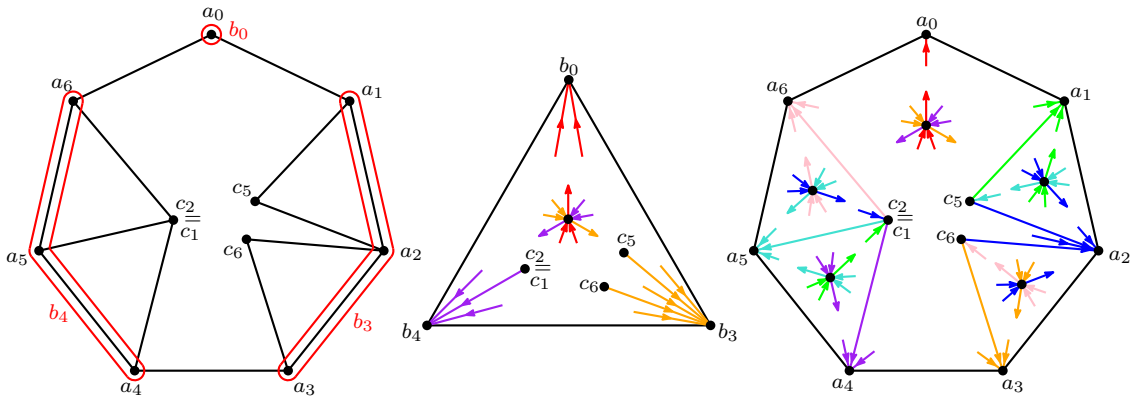

Figure 3.19: Construction of a 7-color forest of an inner triangulation G of the 7-cycle $a_0, \dots, a_6$ by contracting edges (left), using the existence of a Schnyder wood for the triangulation obtained from that (middle), and finally, after undoing the contractions, using the existence of Schnyder woods for subtriangulations of G (right).

As already mentioned, in the case $K = 3$, a K-color forest of G is the same as a Schnyder wood of G. Remember (Theorem 3.2) that for every plane triangulation G there exists a Schnyder wood of G. We use this result to proof the existence of a K-color forest of G also for all $K \geq 5$. We want to mention that this is not the proof strategy that is used in [FSS18a]. There the proof technique from [FO01] for the existence of Schnyder woods is mimicked. Here we just apply this result which leads to a shorter and more elegant proof. This proof strategy is also used in [FSS18b].

Theorem 3.14. *Let G be an inner triangulation of the K-cycle $a_0, \dots, a_{K-1}$. Then there exists a K-color forest of G.*

Proof. The following construction is illustrated in Fig. 3.19 for the case $K = 7$. We contract the edges $a_1a_2, a_2a_3, \dots, a_{\frac{K-3}{2}}a_{\frac{K-1}{2}}$ to a vertex $b_{\frac{K-1}{2}}$ and the edges $a_{K-1}a_{K-2}, a_{K-2}a_{K-3}, \dots, a_{\frac{K+3}{2}}a_{\frac{K+1}{2}}$ to a vertex $b_{\frac{K+1}{2}}$. Thereby, for $i = 1, \dots, \frac{K-3}{2}$, the maximal triangle $a_ia_{i+1}c_{i+\frac{K+1}{2}}$ incident to the edge a_ia_{i+1} is contracted to the edge $c_{i+\frac{K+1}{2}}b_{\frac{K-1}{2}}$ and, for $i = \frac{K+1}{2}, \dots, K-2$, the maximal triangle $a_ia_{i+1}c_{i+\frac{K+1}{2}}$ incident to the edge a_ia_{i+1} is contracted to the edge $c_{i+\frac{K+1}{2}}b_{\frac{K+1}{2}}$. In particular, the vertices inside these triangles are removed. Further let $b_0 := a_0$. This results in an inner triangulation T of the triangle $b_0, b_{\frac{K-1}{2}}, b_{\frac{K+1}{2}}$. Due to Theorem 3.2 there exists a Schnyder Wood S of T (we use the colors $0, \frac{K-1}{2}, \frac{K+1}{2}$ instead of $0, 1, 2$).

We take the colors and orientations of all inner edges not inside one of the triangles $a_ia_{i+1}c_{i+\frac{K+1}{2}}$ from T to G. Then we change the colors of all edges incident to an outer vertex a_i from $\frac{K-1}{2}$ or $\frac{K+1}{2}$ to i. Now, for each $i \in \{1, \dots, K-2\} \setminus \{\frac{K-1}{2}\}$, to determine the colors of the edges inside the triangle $a_ia_{i+1}c_{i+\frac{K+1}{2}}$, we construct another Schnyder wood inside this triangle where a_i has incoming edges in color i, a_{i+1} has incoming edges in color $i+1$, and $c_{i+\frac{K+1}{2}}$ has incoming edges in color $i + \frac{K+1}{2}$.

It is clear that this coloring of G fulfills property (F1) of a K-color forest. It remains to show that also property (F2) is fulfilled. For the vertices inside one of the

separating triangles $a_i a_{i+1} c_{i+\frac{K+1}{2}}$ this is clear since the Schnyder wood property (SW2) for the respective subset of colors implies (F2). For the same reason a vertex v with $v \neq c_i$ for all i fulfills (F2). Let us now see what changes if $v = c_i$ for some i. If $v = c_i = c_{i+1} = \cdots = c_j$ with $1 \leq i \leq j \leq \frac{K-3}{2}$ and $v \neq c_{i-1}, c_{j+1}$, then the outgoing edge of color $\frac{K+1}{2}$ is in clockwise order replaced by an outgoing edge of color $i + \frac{K-1}{2}$, arbitrarily many incoming edges of color i, an outgoing edge of color $i + 1 + \frac{K-1}{2}$, arbitrarily many incoming edges of color $i+1$, and so on, and finally an outgoing edge of color $j + \frac{K+1}{2}$. Since the preceding block of incident edges is the block of incoming edges of color 0 and the succeeding block of incident edges is the block of incoming edges of color $\frac{K-1}{2}$, this does not violate (F2). Analogously, the replacement of the outgoing edge of color $\frac{K-1}{2}$ in the case that $v = c_i$ for some $i \in \{\frac{K+1}{2}, \ldots, K-2\}$ does not violate (F2). Hence, the constructed coloring and orientation of G is indeed a K-color forest. □

3.2.2 Bijection to K-contact structures

Remember (Theorem 3.3) that the set of Schnyder woods of a graph carries the structure of a distributive lattice since Schnyder woods are in bijection to 3-orientations. Our goal for the remaining part of the section is to achieve a similar result for K-color forests by establishing a bijection to certain ω-flows.

In a K-color forest every inner vertex has at most K outgoing edges. The following lemma allows us to add edges to artificial vertices of constant in-degree so that the out-degree of every inner vertex becomes exactly K. The statement of the lemma corresponds to the geometric fact that in a contact representation of an inner triangulation G of a K-cycle with similarly-aligned odd K-gons the area between three K-gons corresponding to an inner face of G that is not incident to an outer edge of G is a pseudotriangle with $\frac{K+3}{2}$ corners, i.e., a polygon with exactly $\frac{K-3}{2}$ concave corners and 3 convex corners.

We say that in an angle between two consecutive incident edges of a vertex v of a K-color forest an outgoing edge of color i is *missing* if we could add an outgoing edge of color i in this angle without violating property (F1) or (F2) at v. The number of outgoing edges missing in this angle is then the number of colors i such that an outgoing edge of color i is missing in this angle.

Lemma 3.15. *Let G be endowed with a K-color forest and let f be a face of G that is not incident to an outer edge of G. Then in the three inner angles of f there are exactly $\frac{K-3}{2}$ outgoing edges missing in total.*

Proof. Let v be an inner vertex of G and let e_1 and e_2 be two consecutive edges in the counterclockwise cyclic order of incident edges of v. Let i and j be the colors of e_1 and e_2, respectively. Then in the angle at v from e_1 to e_2 in counterclockwise direction the number of missing outgoing edges modulo K is

- **i)** $i - j$ if both edges are incoming at v,
- **ii)** $i - j - 1$ if both edges are outgoing at v,
- **iii)** $i - j + \frac{K-1}{2}$ if one of the edges is incoming at v and the other one outgoing at v.

Now let f be a face of G that is not incident to an outer edge of G. Let i, j, and k be the colors of the three edges of f in clockwise order. Then the number of outgoing edges missing in the three inner angles of f modulo K is

i) $(i-j+\frac{K-1}{2})+(j-k+\frac{K-1}{2})+(k-i+\frac{K-1}{2})=\frac{3K-3}{2}\equiv\frac{K-3}{2} \pmod K$, if the orientation of the three edges of f is cyclic, and

ii) $(i-j+\alpha)+(j-k+\beta)+(k-i+\gamma)=\alpha+\beta+\gamma$ with $\{\alpha,\beta,\gamma\}=\{0,-1,\frac{K-1}{2}\}$ and therefore $\alpha+\beta+\gamma=\frac{K-3}{2}$, if the orientation of the three edges of f is acyclic.

Thus the number of outgoing edges missing in these three angles is at least $\frac{K-3}{2}$.

Let n_v be the number of inner vertices of G, let n_e be the number of inner edges of G, and let n_f be the number of faces of G that are not incident to an outer edge of G. Then, due to Euler's formula, $n_e+K=3(n_v+K)-K-3$, which implies $n_e=3(n_v-1)+K$, and $n_f+K+1=2(n_v+K)-K-1$, which implies $n_f=2(n_v-1)$. Therefore, the total number of missing outgoing edges in all angles of all inner vertices is $Kn_v-n_e=(K-3)(n_v-1)=\frac{K-3}{2}n_f$. Hence, the number of missing outgoing edges in the three inner angles of each face that is not incident to an outer edge of G is exactly $\frac{K-3}{2}$. □

Definition 3.16 (Stack extension (odd))**.** The *stack extension* $G^\star$ of G is the extension of G that contains an extra vertex in every face that is not incident to an outer edge. These new vertices are connected to all three vertices of the respective face. We call the new vertices *stack vertices* and the vertices of G *normal vertices*. Analogously, we call the new edges *stack edges* and the edges of G *normal edges*.

Note that the stack extension of G is the sum of G and the angular graph of G without the vertex corresponding to the outer face of G.

Definition 3.17 (K-contact structure (odd))**.** A *K-contact structure* of G is an orientation of the inner edges of $G^\star$ together with a weight function $w : E_{\text{inner}}(G^\star) \to \mathbb{N}$ on the inner edges of $G^\star$ such that

(S1) $w(e)=1$ for each normal edge e,

(S2) each stack edge is oriented towards its incident stack vertex,

(S3) the out-flow of each normal vertex u is K, i.e., $\sum_{e\in E^+(u)} w(e)=K$,

(S4) the in-flow of each stack vertex v is $\frac{K-3}{2}$, i.e., $\sum_{e\in E^-(v)} w(e)=\frac{K-3}{2}$.

For each K-color forest F of G we obtain a corresponding K-contact structure S in the following way: the orientation of the normal edges is inherited from F and the weight of the stack edge $e=uv$ in S is defined as the number of missing outgoing edges (see Lemma 3.15) of u in the angle corresponding to e. Later we will see that this mapping from the K-color forests of G to the K-contact structures of G is bijective.

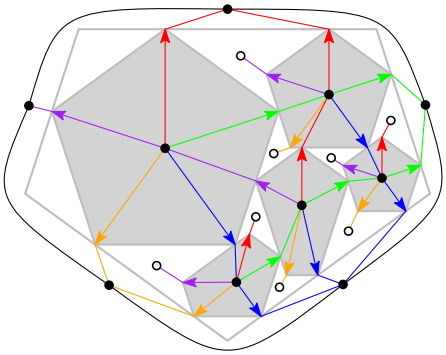

Figure 3.20: The 5-proper coloring of $G^\star_+(S)$ for the K-contact structure S induced by the contact representation of Fig. 3.13. This is an extension of the 5-color forest induced by this contact representation, see Fig. 3.17.

Definition 3.18. Let S be a K-contact structure on G. Then we can associate with S a modified version of $G^\star$ where each inner edge e is replaced by $w(e)$ parallel edges (if $w(e) = 0$, the edge e is deleted) and all edges are oriented as in S. We denote this graph by $G^\star_+(S)$. In statements about the graph $G^\star_+(S)$ for all K-contact structures S we simply write $G^\star_+$.

Definition 3.19 (K-proper coloring (odd))**.** A *K-proper coloring* of $G^\star_+$ is a coloring of the inner edges of $G^\star_+$ in the colors $0, \dots, K-1$ such that the following properties are fulfilled:

(C1) For $i = 0, \dots, K-1$, all edges incident to the outer vertex a_i have color i.

(C2) Each inner normal vertex has exactly one outgoing edge in each color and the clockwise order of the colors is $0, \dots, K-1$.

(C3) Incoming edges of a normal vertex, which are located between the outgoing edges of colors i and $i+1$ in clockwise order, have color $i + \frac{K+1}{2}$.

Figure 3.20 shows an example of a K-proper coloring. Note that the properties of a K-proper coloring are exactly the properties of a K-color forest applied to the normal vertices of $G^\star_+$.

Observation 3.20. *Let F be a K-color forest of G and let S be the corresponding K-contact structure of F. Then the coloring of the inner edges of F can be extended to a K-proper coloring of $G^\star_+(S)$.*

The following fact will later be useful.

Lemma 3.21. *Let $G^\star_+$ be endowed with a K-proper coloring. Then each stack vertex has at most one incoming edge of each color.*

Proof. Let u be a stack vertex and let v and w be two consecutive neighbors of u in the clockwise order of the neighbors of u. Suppose that there are edges from v and

from w to u with the same color c. Let q and r be maximal such that there are edges of colors $c-q,\dots,c$ from v to u and there are edges of colors $c,\dots,c+r$ from w to u. Since u has exactly $\frac{K-3}{2}$ incoming edges, we have $q+r+2\leq\frac{K-3}{2}$. Assume that the edge vw is oriented from v to w (the other case is symmetric). Then the color of (v,w) is $c-q-1=c+r+\frac{K+1}{2}$. Therefore, $q+r+2=\frac{K-1}{2}$, a contradiction. □

Remember that Lemma 3.15 corresponds to the geometric fact that in a contact representation of G the similarly-aligned odd K-gons corresponding to a 3-cycle of G enclose a pseudotriangle, i.e., a polygon with exactly 3 convex corners, with $\frac{K-3}{2}$ concave corners. Now we generalize this lemma to cycles of arbitrary length in G. This generalization corresponds to the geometric fact that the similarly-aligned odd K-gons corresponding to an ℓ-cycle of G enclose a polygon with exactly ℓ convex corners and $\frac{K-1}{2}\ell-K$ concave corners.

Lemma 3.22. *Let C be a simple cycle of length ℓ in G. Then, if we view C as a cycle on the normal vertices of $G^\star_+$, there are exactly $\frac{K-1}{2}\ell-K$ edges pointing from C into the interior of C, i.e., edges with their start vertex on C and with both incident faces in the interior of C.*

Proof. First we view C as a cycle in G. Let k be the number of vertices strictly inside C. Since G is an inner triangulation of a K-cycle, by Euler's formula, there are exactly $2k+\ell-2$ faces and $3k+\ell-3$ edges strictly inside C.

Now we view C as a cycle in $G^\star_+$. In addition to the $3k+\ell-3$ normal edges, there are $\frac{K-3}{2}$ stack edges in each face. Hence, the number of edges strictly inside C is $(3k+\ell-3)+\frac{K-3}{2}(2k+\ell-2)$. At each normal vertex we see K starting edges. Therefore, there are Kk edges starting at a vertex strictly inside C. Taking the difference, we find that there are $\frac{K-1}{2}\ell-K$ edges pointing from a vertex on C into the interior of C. □

Given a K-color forest of G, we denote by T_i the set of oriented edges of color i, and by T_i^{-1} we denote the set T_i with all edges reversed.

Lemma 3.23. *For each i, the orientation*

$$T:=\sum_{j=i-\frac{K-1}{2}}^{i}T_j+\sum_{j=i+1}^{i+\frac{K-1}{2}}T_j^{-1}$$

of the inner edges of G is acyclic.

Proof. Assume there is a simple oriented cycle C of length ℓ in T. Because of the symmetry of the definition of a K-color forest, it suffices to consider the case that C is oriented clockwise.

We define the auxiliary function $\pi:\{0,\dots,K-1\}\to\mathbb{N}$ as follows: for $j=0,\dots,\frac{K-1}{2}$, we set $\pi(i-j)=j$ and, for $j=1,\dots,\frac{K-1}{2}$, we set $\pi(i+j)=j-1$. Let e be an edge of color c ending at a vertex v and e' an edge of color c' starting at v in the orientation T. From Fig. 3.21 we can read off the following: In the

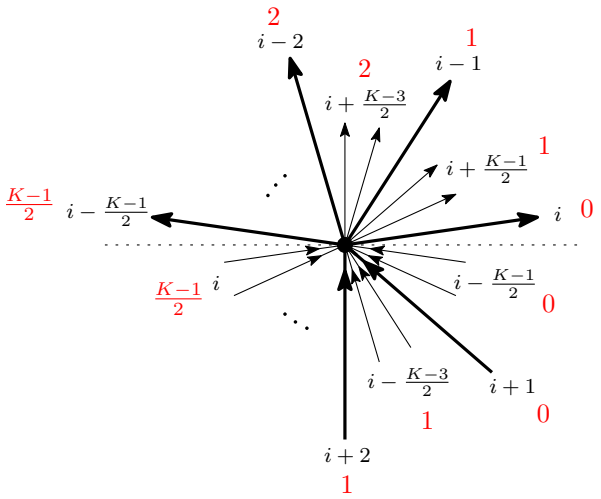

Figure 3.21: The possible incident edges of an inner vertex v in T. For an incoming edge of color c below the dotted line, the red value is $\frac{K-1}{2} - \pi(c)$ and counts the number of thick edges in the counterclockwise angle from this edge to the dotted line. For an outgoing edge of color c' above the dotted line, the red value is $\pi(c')$ and counts the number of thick edges in the clockwise angle from this edge to the dotted line. The thick edges are exactly those that are outgoing at v in $G^\star_+$.

counterclockwise angle of v between e and the dotted line, there are $\frac{K-1}{2} - \pi(c)$ edges which are outgoing in $G^\star_+$. In the clockwise angle of v between e' and the dotted line, there are $\pi(c')$ outgoing edges. Hence, there are exactly $\pi(c') + (\frac{K-1}{2} - \pi(c))$ edges pointing away from v in the counterclockwise angle of v between e and e' in $G^\star_+$.

Now let $e_0, \dots, e_{\ell-1}$ be the edges of the cycle C and let c_j be the color of the edge e_j for $j = 0, \dots, \ell - 1$. Then the number of edges pointing from C into the interior of C in $G^\star_+$ is

$$\sum_{j=0}^{\ell-1} \left(\pi(c_{j+1}) - \pi(c_j) + \frac{K-1}{2} \right) = \frac{K-1}{2}\ell$$

with indices taken modulo ℓ. This is in contradiction to Lemma 3.22 and, therefore, completes the proof. □

In the following lemma, edge colors refer to the K-proper coloring of $G^\star_+(S)$ for a fixed K-contact structure S. For a stack edge e, we say that e has color c if there is an edge parallel to e in $G^\star_+(S)$ that has color c.

Lemma 3.24. *Let P be a walk in $G^\star$ starting with a normal vertex such that all edges on P leaving a normal vertex have the same color c and the edges on P leaving a stack vertex are always the first incident edge of this stack vertex in clockwise order after the edge reaching it. Then P is a path.*

Proof. Let F be the K-color forest corresponding to S and, for $i = 0, \dots, K-1$, let T_i be the set of oriented edges of color i in F. We will now construct a walk P'

in $T := \sum_{i=c-\frac{K-1}{2}}^{c} T_i + \sum_{i=c+1}^{c+\frac{K-1}{2}} T_i^{-1}$ with the property that, if P has a subcycle, then also P' has a subcycle.

Let u, v, w be three consecutive vertices in P where u, w are normal vertices and v is a stack vertex. Due to Lemma 3.15, there are at most $\frac{K-5}{2}$ edges in $G^\star_+(S)$ parallel to the edge (u, v) of color c. Therefore, the edge uw is in $G^\star_+(S)$ either oriented from u to w and has one of the colors $c - \frac{K-3}{2}, \dots, c-1$ or it is oriented from w to u and has one of the colors $c+1, \dots, c+\frac{K-3}{2}$. Thus in both cases the edge (u, w) is in T and we can define P' as the walk obtained from P by skipping all stack vertices.

Now suppose that P has a subcycle. Then the first repeated vertex in P has to be a normal vertex since each stack vertex has only one incoming edge of color c due to Lemma 3.21. Therefore, also P' has a subcycle, in contradiction to Lemma 3.23. □

Now we want to describe K-contact structures as (ω, c_l, c_u)-flows for particular functions ω, c_l, and c_u (remember the introduction to ω-flows in Section 2.3). Let D be a fixed orientation of $G^\star$ without the edges of the outer face, in which each stack edge is oriented towards its incident stack vertex and each normal edge has an arbitrary fixed orientation. We define mappings $\omega_K : V(D) \to \mathbb{Z}$ and $c_l, c_u : E(D) \to \mathbb{Z}$ as follows: If v is a normal vertex, we set $\omega_K(v) = \deg^-_D(v) - K$ and, if v is a stack vertex, we set $\omega_K(v) = \frac{K-3}{2}$. If e is a normal edge, we set $c_l(e) = 0$ and $c_u(e) = 1$ and, if e is a stack edge, we set $c_l(e) = 0$ and $c_u(e) = \frac{K-3}{2}$. Then the following describes a bijective mapping from a K-contact structure S to an (ω_K, c_l, c_u)-flow f. We set

$$f(e) = \begin{cases} 0 & \text{if } e \text{ is a normal edge and has different orientations in } S \text{ and } D, \\ 1 & \text{if } e \text{ is a normal edge and has the same orientation in } S \text{ and } D, \\ w(e) & \text{if } e \text{ is a stack edge,} \end{cases}$$

and call f the *induced ω_K-flow* of S.

Lemma 3.25. *Let S be a K-contact structure of G such that $G^\star_+(S)$ has a K-proper coloring. Further, let S' be a K-contact structure of G such that the ω_K-flow induced by S' can be obtained from the ω_K-flow induced by S by augmenting the flow on a simple cycle C by one unit. Then also $G^\star_+(S')$ has a K-proper coloring.*

Proof. The graph $G^\star_+(S')$ is obtained from $G^\star_+(S)$ in the following way: Let uv be a stack edge on C with normal vertex u and stack vertex v. If it is oriented from u to v on C, then there is one more edge from u to v in $G^\star_+(S')$ than in $G^\star_+(S)$. If it is oriented from v to u on C, then there is one less edge from u to v in $G^\star_+(S')$ than in $G^\star_+(S)$. Further, for each normal edge e on C, e has different orientations in $G^\star_+(S')$ and in $G^\star_+(S)$.

If we consider C as a cycle in $G^\star$, each edge of $G^\star$ is either outside of C, inside of C, or on C. We translate this notion to the edges of $G^\star_+$. We say that an edge of $G^\star_+$ is outside of C, inside of C, or on C if the corresponding edge of e in $G^\star$ is outside of C, inside of C, or on C, respectively.

We will now give a detailed description of the procedure to obtain a K-proper coloring of $G^\star_+(S')$ from a K-proper coloring of $G^\star_+(S)$. The idea is the following:

If C is oriented clockwise (the case that C is oriented counterclockwise is symmetric), each normal vertex v on C loses an outgoing edge on C in counterclockwise direction and gains an outgoing edge on C in clockwise direction. Therefore, all outgoing edges of v inside of C pass on their colors to the next outgoing edge of v in counterclockwise direction in the cyclic order of incident edges of v. To retain a K-proper coloring, also the outgoing edges of normal vertices inside of C have to pass on their colors in that manner. This process of passing on the colors is equivalent to increasing the colors of all edges inside of C by one.

More formally, we do the following: We do not change the colors of the edges outside of C. Now we distinguish whether C is oriented clockwise or counterclockwise.

i) First, let C be oriented clockwise (see Fig. 3.22 for an illustration of this case). Then we increase the colors of all edges inside of C by one. For a stack edge on C that is oriented from the stack vertex v to the normal vertex u in C, we delete the leftmost edge from u to v and do not change the colors of the other edges from u to v. For a stack edge on C that is oriented from the normal vertex v to the stack vertex w in C, we add a new edge e from v to w to the right of the other edges from v to w. The color of e is the color of the first outgoing edge of v in $G^\star_+(S)$ in the clockwise order of the incident edges of v inside of C (including the edge (v, u) on C). We do not change the colors of

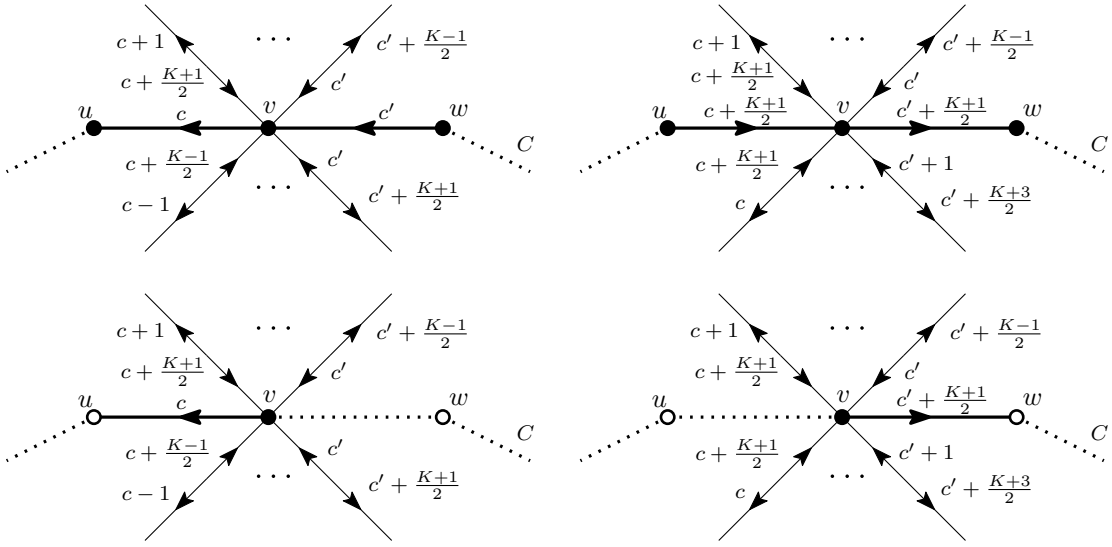

Figure 3.22: The local changes of the K-proper coloring around a normal vertex v on a cycle C on which the ω_K-flow is increased. The upper row shows the case of two incident normal vertices on C, the lower row the case of two incident stack vertices on C. The edges drawn above (below) C are the incident edges of v outside (inside) of C that are closest to C in the cyclic order of incident edges of v. For these edges the colors for both possible orientations are shown. In the lower figures, the edge (v, u) is the leftmost edge from v to u and the edge (v, w) is the rightmost edge from v to w. Further, in these figures, the edges shown above C might be incident to u or w but not the edges below C.

the other edges from v to w. For a normal edge on C, we add $\frac{K+1}{2}$ to its color from $G^\star_+(S)$.

ii) Now let C be oriented counterclockwise. Then we decrease the colors of all edges inside of C by one. For a stack edge on C that is oriented from the stack vertex v to the normal vertex u in C, we delete the rightmost edge from u to v and do not change the colors of the other edges from u to v. For a stack edge on C that is oriented from the normal vertex v to the stack vertex w in C, we add a new edge e from v to w to the left of the other edges from v to w. The color of e is the color of the first outgoing edge of v in $G^\star_+(S)$ in the counterclockwise order of the incident edges of v inside of C (including the edge (v, u) on C). We do not change the colors of the other edges from v to w. For a normal edge on C, we add $\frac{K-1}{2}$ to its color from $G^\star_+(S)$.

For the vertices not on C the local properties of a K-proper coloring are still fulfilled after this change since the incident edges have not changed and either the colors have not changed, or all colors are decreased by one, or all colors are increased by one. It only remains to check the colors of the edges incident to a normal vertex on C. Also for such a vertex v, for the same reason as before, the colors of two consecutive incident edges in the cyclic order of incident edges fulfill the properties of a K-proper coloring if both edges are inside of C or both edges are outside of C. The remaining case that one of the two edges is on C is verified in Fig. 3.22 for the case that C is oriented clockwise. Note that the two cases shown in this figure can be seen as all four possible cases (incoming and outgoing normal and stack edge) since, in each of the four subfigures, the part to the left of v is independent to the part to the right of v. The case that C is oriented counterclockwise is symmetric. □

Theorem 3.26. *For each K-contact structure S of G, the graph $G^\star_+(S)$ has a unique K-proper coloring.*

Proof. We begin with the proof of the existence of a K-proper coloring. Due to Theorem 3.14, there exists a K-color forest F_0 of G. Let S_0 be the K-contact structure induced by F_0. Then S_0 has a K-proper coloring by Observation 3.20. Since in the difference of two ω_K-flows the excess of all vertices is 0, the ω_K-flow corresponding to S can be obtained from the ω_K-flow corresponding to S_0 by iteratively augmenting it on a simple cycle. Hence, it follows from Lemma 3.25 that S has a K-proper coloring.

Now we show the uniqueness of the K-proper coloring. Because of properties (C2) and (C3), the knowledge of the color of an edge incident to an inner normal vertex v implies the knowledge of the colors of all edges incident to v. Due to property (C1), the colors of the edges incident to the outer vertices are fixed. Since G is connected, this implies that the colors of all inner edges are fixed. □

Corollary 3.27. *The mapping from a K-color forest of G to the induced K-contact structure is a bijective mapping from the set of the K-color forests of G to the set of the K-contact structures of G.*

3.2.3 The distributive lattice

Since K-contact structures are in bijection to ω_K-flows, the set of all K-contact structures of G carries the structure of a distributive lattice. We want to figure out the cover relation in this distributive lattice.

Definition 3.28 (Flip (odd K-contact structure))**.** Let S be a K-contact structure of G. If $K = 3$, we call the reorientation of a triangle in S (consisting of normal edges) from counterclockwise to clockwise a *flip* in S. If $K \geq 5$, let (u, v) be a normal edge in S and let w be the stack vertex such that the face uvw lies on the left side of (u, v). Then we call the reorientation of (u, v) combined with decreasing the weight of vw by one and increasing the weight of uw by one a *flip* in S.

Theorem 3.29. *The flip operation is the cover relation of a distributive lattice on the set of all K-contact structures of a graph G.*

Proof. Let C be an essential cycle in $G^\star$. Then there exists an ω_K-flow f such that C is an oriented cycle in the residual graph D_f and has no chordal path in D_f. We can assume that D is the orientation of $G^\star$ given by the K-contact structure S corresponding to f. Further, let $G^\star_+ := G^\star_+(S)$.

Claim 1. *There is no edge pointing from a normal vertex on C into the interior of C in D and there is no edge in the interior of C that is incident to a stack vertex on C.*

Proof. Let v be a vertex on C and let $e = vw$ be an incident edge inside of C. If e is a normal edge oriented from v to w in D, let c be the color of e in the K-proper coloring of $G^\star_+$. If v is a normal vertex and w is a stack vertex, let c be the color of one of the edges from v to w in the K-proper coloring of $G^\star_+$. If v is a stack vertex, let c be the color of one of the edges from w to v in $G^\star_+$ where w is the neighbor of v following v on C. Let P be the walk that starts with the edge e and continues at each normal vertex with the outgoing edge of color c and at each stack vertex with the first incident edge in clockwise order after the incoming edge. From Lemma 3.24 we deduce that, if this walk cycles, then it begins with a stack vertex and this stack vertex is the first repeated vertex. Hence, P reaches C before or at the moment of its first vertex repetition. Let P' be the subpath of P from the beginning to the point when it reaches C first.

Note that P only uses the following types of edges:

- **i)** normal edges in their orientation in D, which is opposite to the orientation in D_f,
- **ii)** edges from a normal vertex u to a stack vertex v only if there is an edge from u to v in $G^\star_+$, whence (v, u) is an edge of D_f,
- **iii)** edges from a stack vertex u to a normal vertex v only if u has an incoming edge in $G^\star_+$ that does not come from u (if u is the start vertex of P, we can choose the edge from the successor of u on C to u and otherwise the incoming edge of u in P), whence again (v, u) is an edge of D_f.

Therefore, the reversed path $\overline{P'}$ of P' is a chordal path of C in D_f, in contradiction to the assumption that C is an essential cycle. △

Claim 2. *If $K = 3$, the cycle C has length 3 and only consists of normal vertices. If $K \geq 5$, the cycle C contains at least one stack vertex.*

Proof. Assume that C contains only normal vertices. Then, according to Lemma 3.22, there are exactly $\frac{K-1}{2}\ell(C) - K$ edges pointing from a vertex on C into the interior of C. Thus, due to Claim 1, we have $\frac{K-1}{2}\ell(C) - K = 0$ and therefore $\ell(C) = \frac{2K}{K-1}$. Since K and $K-1$ are relative prime for all $K \geq 3$, the only solution of this equation is $\ell(C) = K = 3$.

Further, if $K = 3$, the cycle C only consists of normal vertices as in an ω_3-flow the capacities for stack edges e are $c_l(e) = c_u(e) = 0$ whence stack edges have no orientation in D_f. △

For the case $K = 3$, Claim 2 already finishes the proof. In the case $K \geq 5$, we still need to show that C is a facial cycle. So, let $K \geq 5$ and let v be a stack vertex on C that exists due to Claim 2. Let w_1 and w_2 be the predecessor and the successor of v on C, respectively. Let $u \neq w_1, w_2$ be the third neighbor of v in $G^\star$. Then, due to Claim 1, the edge vu is outside of C. Now, unless C is a facial cycle, the edge w_1w_2 is an inner chord of C. In either orientation the edge forms a chordal path, in contradiction to the assumption that C is an essential cycle. □

Figure 3.23 shows the effect of a flip of the K-contact structure on the contact representation in the case $K \geq 5$. For an illustration of the case $K = 3$ see Fig. 3.3 on Page 15.

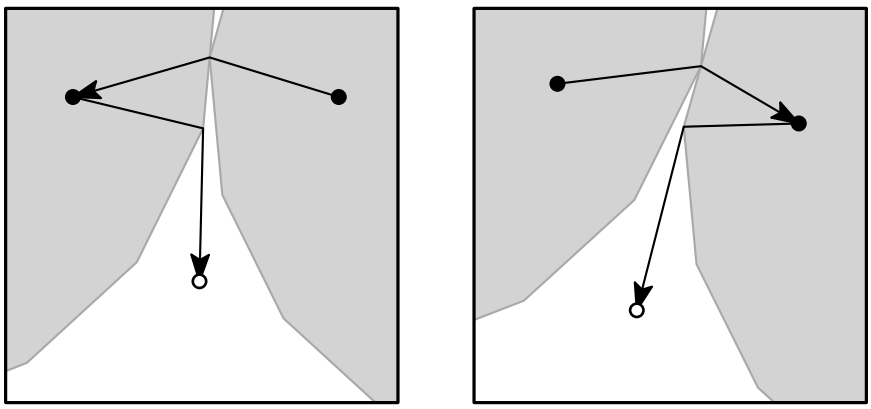

Figure 3.23: The geometric effect of a flip of the induced K-contact structure on the similarly-aligned odd K-gon contact representation in the case $K \geq 5$.

3.3 Parallel-sided even K-gon contact representations

In the last section we studied contact representations with similarly-aligned odd K-gons as a generalization of contact representations with regular K-gons for odd $K \geq 3$. In this section we will complete the study of contact representations with regular K-gons by considering *parallel-sided even K-gon contact representations* as a generalization of contact representations with equiangular, and therefore also regular, K-gons for even $K \geq 6$. The structure of this section is similar to the structure of the previous section. But the proofs in the later part of this section are quite different from those in Section 3.2.

Let us start with the definition of similarly-aligned odd K-gon contact representations. Let G be a graph and let $K \geq 6$ be an even number. For each vertex v of G, let P_v be a convex K-gon whose sides are labeled cyclically in clockwise order with $0, \ldots, K-1$. We denote the side of P_v which is labeled with i by $\text{side}_i(P_v)$. Further, we denote the corner of P_v between $\text{side}_i(P_v)$ and $\text{side}_{i+1}(P_v)$ by $\text{corner}_i(P_v)$. The polygons P_v, $v \in V(G)$, are called *parallel-sided even K-gons* if, for each vertex v of G and for each label i, $\text{side}_i(P_v)$ and $\text{side}_{i+\frac{K}{2}}(P_v)$ are antiparallel and, for each pair v, w of vertices and each label i, $\text{side}_i(P_v)$ and $\text{side}_i(P_w)$ are parallel. As in the last section, it suffices if the reader has the special case of equiangular (see Fig. 3.24a for an example) or even only regular K-gons (see Fig. 3.24b for an example) in mind.

One might wonder why we exclude the case $K = 4$ from our studies in this section. The reason is that the structural results from this section do not hold for parallelograms. But the known results for contact representations with rectangles we summarized in Section 3.1.2 also apply to contact representations with parallelograms since rectangle contact representations can be transformed into contact representations with parallelograms of equal alignment by a shear mapping. Hence, the combinatorial structure of contact representations with parallelograms is well-understood.

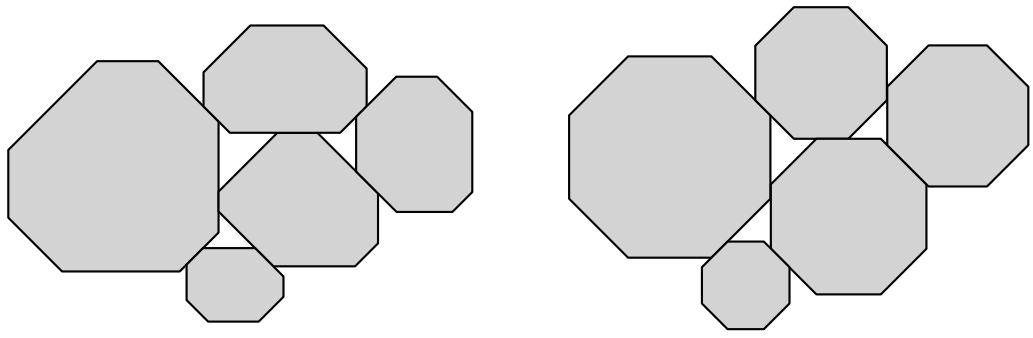

(a) An equiangular octagon contact representation.

(b) A regular octagon contact representation.

Figure 3.24: Two octagon contact representations of the same graph.

Theorem 3.30. *If G has a contact representation $\mathcal{C}$ with parallel-sided even K-gons, then G is a planar graph.*

Proof. First, we argue that for each edge vw of G a corner of P_v touches P_w or a corner of P_w touches P_v. If the intersection of P_v and P_w is a single point, this is clear. Otherwise, the intersection is a line segment and both endpoints of this line segment are corners of P_v or P_w.

Now let p be a point in $\mathcal{C}$ where two or more corners touch. Let i and j be the labels of two corners involved in this touching. Then $j \in \{i+\frac{K}{2}-1, i+\frac{K}{2}, i+\frac{K}{2}+1\}$. In particular, we have $i \neq j$. Therefore, there are at most four corners involved in the touching at p. If there are four corners involved, we further have $i+\frac{K}{2}-1 \in \{(i+\frac{K}{2})+\frac{K}{2}-1, (i+\frac{K}{2})+\frac{K}{2}, (i+\frac{K}{2})+\frac{K}{2}+1\}$. The first one implies $K=0$, the second one $K=2$, and the third one $K=4$, all in contradiction to $K \geq 6$. Similarly, we can show that, if there are three corners involved, we have $K=6$ and the labels of the three corners are either $0,2,4$ or $1,3,5$.

We obtain a crossing-free drawing of G in the following way: We place each vertex v into the interior of P_v. For each edge vw of G, we choose a point p in the intersection of P_v and P_w and connect v and w straight line to p. If we choose the same point p for different edges, then $K=6$ and there are three corners meeting in p. But then, for any two labels i,j of the labels of the three corners in p, we have $i \neq i+\frac{K}{2}$. Hence, none of the pairwise contacts of the three involved hexagons is a single-point contact. Therefore, we can change the choice of the point p for each of the three contacts to a point in the interior of the segment in which the two hexagons intersect. □

Note that moving the bend point p of the drawing of an edge vw inside the interior of the segment in which P_v and P_w intersect does not change the combinatorial embedding of G obtained from $\mathcal{C}$. Therefore, we can refer to this drawing as the drawing of G *induced* by $\mathcal{C}$. A point in $\mathcal{C}$ where two or three corners touch in one point is called an *exceptional touching*.

From now on, we will only consider plane graphs G and with a contact representation of G we will mean a contact representation inducing the given embedding of G. Moreover, we will restrict the class of considered graphs G to the class of inner trian-

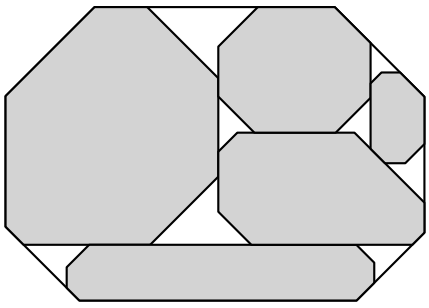

Figure 3.25: An equiangular octagon contact representation.

gulations of a K-cycle where the outer vertices play a special role: Let G be an inner triangulation of the K-cycle $a_0, \dots, a_{K-1}$ (in clockwise order) for some even $K \geq 6$. As before, the inner vertices v of G are represented by a convex K-gon P_v. But the outer vertices $a_0, \dots, a_{K-1}$ of G are represented by the sides $q_0, \dots, q_{K-1}$ (in clockwise order), respectively, of an additional convex K-gon Q. The polygons P_v are parallel-sided even K-gons. For the polygon Q, a similar property is fulfilled: For $i = 0, \dots, K-1$, the side q_i is antiparallel to $\text{side}_i(P_v)$ for all inner vertices v of G. See Fig. 3.25 for an example that we will use throughout this section to illustrate all concepts.

3.3.1 K-color forests

The K-color forests for odd K are generalizations of Schnyder woods. Thus one might think that, since transversal structures describe the combinatorial structure of contact representations with parallel-sided 4-gons (see Section 3.1.2), a generalization of transversal structures to more than two colors describes the combinatorial structure of contact representations with parallel-sided even K-gons. The example in Fig. 3.26 shows that with such a generalization we are not able to fully describe the combinatorial structure of these contact representations. Therefore, we choose an approach similar to that one in the last section.

For the rest of this section, let $K \geq 6$ be a fixed even number and let G be an inner triangulation of the K-cycle $a_0, \dots, a_{K-1}$ (in clockwise order).

We define the graph $2G$ to be the plane graph obtained from G by replacing each inner edge (except one inner edge incident to each outer vertex) by two parallel edges forming a face of degree two. For an outer vertex a_i of G, let $e_0, e_1, e_2, \dots$ be the clockwise order of incident edges of a_i in G with outer edges e_0 and e_1. Then e_2 is the edge incident to a_i which is not replaced by two parallel edges in $2G$.

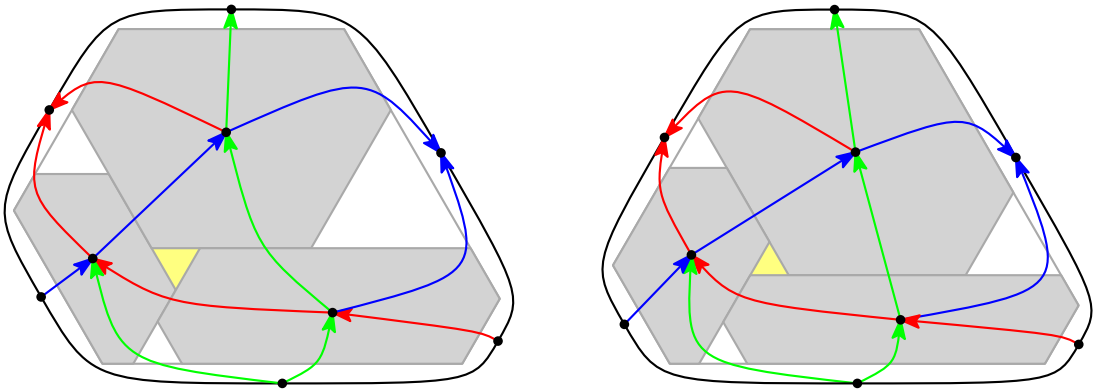

Figure 3.26: Two contact representations with equiangular hexagons of the same graph that induce the same generalized transversal structure. Nevertheless, the combinatorial structures of these two representations can be further distinguished (see the highlighted triangle in the middle).

(a) The outer vertex condition (F1). (b) The inner vertex condition (F2).

Figure 3.27: The local conditions of a K-color forest shown for the example $K = 6$.

Definition 3.31 (K-color forest (even))**.** A *K-color forest* of G is an orientation and coloring of the inner edges of $2G$ in the colors $0, \dots, K-1$ with the following properties:

(F1) For $i = 0, \dots, K-1$, all edges incident to a_i are oriented towards a_i and colored in the color i or $i+1$.

(F2) For each inner vertex v, the incoming edges of v build K (possibly empty) blocks B_i, $i = 0, \dots, K-1$, of edges of colors i and $i+1$, and the clockwise order of these blocks is $B_0, \dots, B_{K-1}$. Moreover, v has at most one outgoing edge of color i and such an edge has to be located between the blocks $B_{i+\frac{K}{2}-1}$ and $B_{i+\frac{K}{2}}$.

Figure 3.27 gives an illustration of Definition 3.31.

Theorem 3.32. *Every parallel-sided even K-gon contact representation $\mathcal{S}$ of G induces a K-color forest on $2G$.*

Proof. First assume that $\mathcal{S}$ has no exceptional touchings (see Fig. 3.28 for an example of this case). Then all touchings are line segments with positive length. Let e be an inner edge of G. If both incident vertices of e are inner vertices, e is realized in $\mathcal{S}$ by an intersection of two K-gons P_v and P_w in a line segment l. Both endpoints of l are corners of P_v or P_w. For each corner of P_u with $u \in \{v, w\}$ of label i at an endpoint of l one of the two copies of e in $2G$ is oriented as outgoing for u and colored in color i. The order of the two copies of e in the cyclic orders of incident edges of v and w corresponds to the order of the two endpoints of l. If an inner vertex v is incident to the outer vertex a_i but not to a_{i+1}, the two copies of the edge va_i are oriented towards a_i and colored in color the colors i and $i+1$ in this order in the clockwise order of incident edges of v. If v is incident to the outer vertices a_i and a_{i+1}, then the single copy of the edge va_i is oriented towards a_i and colored in color i. It follows from the definition of the labeling of the corners and sides of the K-gons and from the fact that each corner of a K-gon can be involved in at most one contact that this yields a K-color forest.

Now let p be a an exceptional touching in $\mathcal{S}$. From the proof of Theorem 3.30 we know that in p either two corners with labels i and $i + \frac{K}{2}$ touch or exactly three corners with labels $0, 2, 4$ or $1, 3, 5$ touch and $K = 6$. If there are only two corners

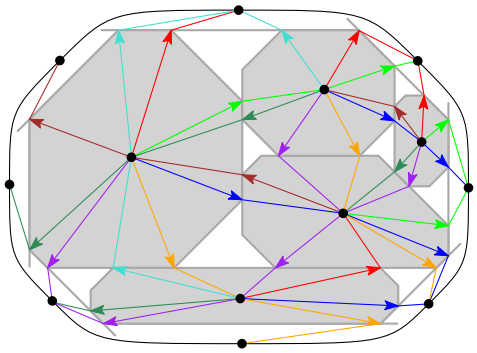

Figure 3.28: The 8-color forest induced by the contact representation of Fig. 3.25.

involved in the touching, let these be $\text{corner}_i(P_v)$ and $\text{corner}_{i+\frac{K}{2}}(P_w)$. Then we orient one of the two copies of the edge vw from v to w and color it in color i, and orient the other copy of the edge vw from w to v and color it in color $i + \frac{K}{2}$. The order of the two copies is chosen arbitrarily. Then, obviously, the properties of a K-color forest are locally fulfilled. If there are three corners involved in the touching, let these be $\text{corner}_0(P_u)$, $\text{corner}_2(P_v)$, and $\text{corner}_4(P_w)$ (the case of the colors $1, 3, 5$ is symmetric). Then the pairwise intersections of P_u, P_v, and P_w are line segments of positive lengths. We will only explain how to treat the copies of the edges uv, vw, and wu corresponding to the exceptional touching. The other copies are treated as explained above (or according to another exceptional touching). We either orient these copies of the edges of the triangle uvw as $(u, v), (v, w), (w, u)$ and color them in the colors $0, 2, 4$, respectively, or we orient the edges as $(u, w), (w, v), (v, u)$ and color them in the colors $0, 4, 2$, respectively. In either case, the properties of a 6-color forest are fulfilled. □

3.3.2 Bijection to K-contact structures

In the previous section we proved the existence of a K-color forest directly by a construction using Schnyder woods. In this section we will first establish a bijection from K-color forest to certain *K-contact structures* and prove the existence of a K-contact structure. This strategy is similar to the strategy used in [FSS18b] for $K = 5$.

We start with proving a lemma that allows us to add edges to artificial vertices of constant in-degree in a K-color forest such that afterwards each inner vertex has exactly K outgoing edges. The statement corresponds to the geometric fact that in a contact representation of an inner triangulation G of a K-cycle with parallel-sided even K-gons the area between three K-gons corresponding to an inner face of G that is not incident to an outer edge of G is a pseudotriangle with $\frac{K}{2}$ corners, i.e., a polygon with exactly $\frac{K-6}{2}$ concave corners and 3 convex corners.

Remember (Page 28) the notion of *missing outgoing edges* in a K-color forest for odd K. Here we will use the analogous notion for K-color forests with even K.

Lemma 3.33. *Let G be endowed with a K-color forest and let f be a face of G that is not incident to an outer edge of G. Then in the three inner angles of f there are exactly $\frac{K-6}{2}$ outgoing edges missing in total.*

Proof. Let v be an inner vertex of G and let e_1, e_2 be two consecutive edges in the counterclockwise cyclic order of incident edges of v. Let i and j be the colors of e_1 and e_2, respectively. Then in the angle of v between e_1 and e_2 the number of missing outgoing edges modulo K is

- **i)** $i - j - 1 + \delta$ with $0 \leq \delta \leq 2$ if both edges are incoming at v,
- **ii)** $i - j - 1$ if both edges are outgoing at v,
- **iii)** $i - j + \frac{K}{2} - 1 + \delta$ with $0 \leq \delta \leq 1$ if one of the edges is incoming at v and the other one outgoing at v.

Now let f be a face of G that is not incident to an outer edge of G. Let i, j and k be the colors of the three edges of f in clockwise order. Then the number of outgoing edges missing in the three inner angles of f modulo K is

- **i)** $(i-j+\frac{K}{2}-1+\delta_1)+(j-k+\frac{K}{2}-1+\delta_2)+(k-i+\frac{K}{2}-1+\delta_3) = \frac{3K-6}{2}+(\delta_1+\delta_2+\delta_3) \equiv \frac{K-6}{2} + (\delta_1 + \delta_2 + \delta_3) \pmod K$ with $0 \leq \delta_1 + \delta_2 + \delta_3 \leq 3$, if the orientation of the three edges of f is cyclic,
- **ii)** $(i - j + \alpha) + (j - k + \beta) + (k - i + \gamma) = \alpha + \beta + \gamma$ with $\{\alpha, \beta, \gamma\} = \{-1 + \delta_1, -1, \frac{K}{2} - 1 + \delta_2\}$ and $0 \leq \delta_1 + \delta_2 \leq 3$, and therefore $\alpha + \beta + \gamma = \frac{K-6}{2} + (\delta_1 + \delta_2)$ with $0 \leq \delta_1 + \delta_2 \leq 3$, if the orientation of the three edges of f is acyclic.

Thus the number of outgoing edges missing in these three angles is at least $\frac{K-6}{2}$.

As in the proof of Lemma 3.15, if n_v denotes the number of inner vertices of G, n_e denotes the number of inner edges of G, and n_f denotes the number of faces of G that are not incident to an outer edge of G, we have $n_e = 3(n_v - 1) + K$ and $n_f = 2(n_v - 1)$. Therefore, the total number of missing outgoing edges in all angles of all inner vertices is $Kn_v - (2n_e - K) = (K - 6)(n_v - 1) = \frac{K-6}{2} n_f$. Hence, the number of missing outgoing edges in the three inner angles of each face that is not incident to an outer edge of G is exactly $\frac{K-6}{2}$. □

Definition 3.34 (Stack extension (even))**.** The *stack extension* $2G^\star$ of $2G$ is the extension of $2G$ with an extra vertex in every triangular face of $2G$ that is not incident to an outer edge. These new vertices are connected to all three vertices of the respective face. We call the new vertices *stack vertices* and the vertices of $2G$ *normal vertices*. Analogously, we call the new edges *stack edges* and the edges of $2G$ *normal edges*.

Definition 3.35 (K-contact structure (even))**.** A *K-contact structure* of G is an orientation of the inner edges of $2G^\star$ together with a weight function $w : E_{\text{inner}}(G^\star) \to \mathbb{N}$ on the inner edges of $2G^\star$ such that

(S1) $w(e) = 1$ for each normal edge e,

(S2) each stack edge is oriented towards its incident stack vertex,

(S3) the out-flow of each normal vertex u is K, i.e., $\sum_{e \in E^+(u)} w(e) = K$,

(S4) the in-flow of each stack vertex v is $\frac{K-6}{2}$, i.e., $\sum_{e \in E^-(v)} w(e) = \frac{K-6}{2}$.

Similar to the graph $G^\star_+(S)$ associated with a K-contact structure S for odd K in the last section, we will now introduce the graph $2G^\star_+(S)$ associated with a K-contact structure S for even K. Additionally, we will define the graph $2G^\star_{++}(S)$ that is an extension of $2G^\star_+(S)$ with edges from stack vertices to normal vertices.

Definition 3.36. Let S be a K-contact structure of G. Then we can associate with S a modified version of $2G^\star$ where each stack edge e is replaced by $w(e)$ parallel edges (if $w(e) = 0$, the edge e is deleted) and all edges are oriented as in S. We denote this graph by $2G^\star_+(S)$. Further, let $2G^\star_{++}(S)$ be the modified version of $2G^\star$ where each stack edge $e = vw$ with normal vertex v and stack vertex w is replaced by $w(e) + 2$ parallel edges where the two outer edges are oriented from w to v and the remaining edges are oriented from w to v. Normal edges are oriented as in S. In statements about the graph $2G^\star_+(S)$ or the graph $2G^\star_{++}(S)$ for all K-contact structures S, we simply write $2G^\star_+$ or $2G^\star_{++}$, respectively.

Remember that Lemma 3.33 corresponds to the geometric fact that in a contact representation of G the parallel-sided even K-gons corresponding to a 3-cycle of G enclose a pseudotriangle, i.e., a polygon with exactly 3 convex corners, with $\frac{K-6}{2}$ concave corners. Now we generalize this lemma to cycles of arbitrary length in G. This generalization corresponds to the geometric fact that the parallel-sided even K-gons corresponding to an ℓ-cycle of G enclose a polygon with exactly ℓ convex corners and $\frac{K-2}{2}\ell - K$ concave corners.

Lemma 3.37. *Let C be a simple cycle of length ℓ in G. Then, if we view C as a cycle on the normal vertices of $2G^\star_+$ without edges in the interior of C which are parallel to edges of C, there are exactly $\frac{K-2}{2}\ell - K$ edges pointing from C into the interior of C, i.e., edges with their start vertex on C and with both incident faces in the interior of C.*

Proof. First we view C as a cycle in G. Let k be the number of vertices strictly inside C. Since G is an inner triangulation of a K-cycle, by Euler's formula, there are exactly $2k + \ell - 2$ faces and $3k + \ell - 3$ edges strictly inside C.

Now we view C as a cycle in $2G^\star_+$. In addition to the $2(3k + \ell - 3)$ normal edges, there are $\frac{K-6}{2}$ stack edges in each face, hence, the number of edges strictly inside C is $2(3k + \ell - 3) + \frac{K-6}{2}(2k + \ell - 2)$. At each normal vertex we see K starting edges. Therefore, there are Kk edges starting at a vertex strictly inside C. Taking the difference, we find that there are $\frac{K-2}{2}\ell - K$ edges pointing from a vertex on C into the interior of C. □

Now we want to prove that there exists a K-contact structure of G by verifying the sufficient conditions for the existence of an α-orientation we presented in Section 2.3. For these calculations we need bounds on the number of incident edges and faces of a set of vertices in a triangulation, which we will prove in the following lemma. For a plane graph H and a subset X of the vertices of H, we denote the set of edges of H incident to a vertex of X by $E_{\text{inc}}(H, X)$ and the set of faces of H incident to a vertex of X by $F_{\text{inc}}(H, X)$.

Lemma 3.38. *Let T be a plane triangulation and let X be a subset of the vertices of T with $1 \leq |X| \leq |V(T)| - 3$. Then*

$$|E_{\text{inc}}(T, A)| \geq 3|X| \ , \quad |F_{\text{inc}}(T, A)| \geq 2|X| + 1 \ .$$

Proof. Let $\overline{X} := V(T) \setminus X$. Then $E_{\text{inc}}(X) = E(T) \setminus E(T[\overline{X}])$. Since T is a triangulation, we have $|E(T)| = 3|V(T)| - 6$. As $T[\overline{X}]$ is a simple plane graph, we also have $|E(T[\overline{X}])| \leq 3(|V(T)| - |X|) - 6$. Putting this together, we obtain the inequality $|E_{\text{inc}}(X)| \geq 3|X|$.

The faces of T contained in $F(T) \setminus F_{\text{inc}}(X)$ are also faces of $T[\overline{X}]$. But at least one face of $T[\overline{X}]$ is not a face of T since it has a vertex of X in its interior. Thus we have $|F_{\text{inc}}(X)| \geq |F(T)| - (|F(T[\overline{X}])| - 1)$. As T is a triangulation, $|F(T)| = 2|V(T)| - 4$. As $T[\overline{X}]$ is planar, $|F(T[\overline{X}])| \leq 2(|V(T)| - |X|) - 4$. Putting this together, we get $|F_{\text{inc}}(X)| \geq 2|X| + 1$. □

Theorem 3.39. *Let G be an inner triangulation of a K-cycle. Then there exists a K-contact structure of G.*

Proof. Let H be the graph obtained from $2G^\star$ by replacing each stack edge by $\frac{K-6}{2}$ parallel edges. We will show that there exists an orientation of the inner edges of H such that each normal vertex has out-degree K and each stack vertex has in-degree $\frac{K-6}{2}$. Then we obtain a K-contact structure of G by giving each normal edge the orientation from H and by setting the weight of each stack edge $e = uv$ with normal vertex u and stack vertex v to the number of edges in H oriented from u to v.

Note that, instead of requiring the in-degree of a stack vertex v to be $\frac{K-6}{2}$, we can require its out-degree to be $\deg(v) - \frac{K-6}{2} = K - 6$. From Theorem 2.2 we take the following sufficient condition for the existence of the orientation we seek for: if for each set W of k normal inner vertices and l stack vertices of H the inequality $|E_{\text{inc}}(H, W)| \geq kK + l(K - 6)$ holds and equality holds if W contains all normal inner vertices and all stack vertices of H, then such an orientation of H exists.

Let X be a set of k inner normal vertices of H and let Y be a set of l stack vertices of H. Let $N^{\text{sta}}(H, X)$ be the neighbors of X that are stack vertices and let $E^{\text{nor}}_{\text{inc}}(H, X)$ be the incident edges of X that are normal edges. If a stack vertex v is a neighbor of a vertex from X, then at least $\frac{K-6}{2}$ incident edges of v are contained in $E_{\text{inc}}(H, X)$. On the other hand, if we reserve $\frac{K-6}{2}$ of the $\frac{3(K-6)}{2}$ incident edges of a stack vertex v for counting them as incident edges of X, there are at least $K - 6$ of them left to be counted as incident edges of Y if $v \in Y$. Therefore, it suffices to show $|E^{\text{nor}}_{\text{inc}}(H, X)| + |N^{\text{sta}}(H, X)|\frac{K-6}{2} \geq kK$ which implies $|E_{\text{inc}}(H, X \cup Y)| \geq kK + l(K - 6)$.

Note that the vertices in X are also vertices of G. A *bad separating triangle* in G is a separating triangle consisting of two outer vertices and one inner vertex. Let $T_0, \ldots, T_{r-1}$ be the maximal bad separating triangles of G and let G' and H' be the graphs obtained from G and H, respectively, by removing all vertices inside the triangles $T_0, \ldots, T_{r-1}$. Let $X' := V(G') \cap X$ and, for $i = 0, \ldots, r - 1$, let X_i be the

vertices of X strictly inside the triangle T_i. Further, we set $k' := |X'|$ and $k_i := |X_i|$ for $i = 0, \dots, r-1$.

To be able to apply Lemma 3.38, we now contract $K-3$ of the K outer edges of G'. Since G' has no bad separating triangles, these contractions produce parallel edges with empty interior. We only keep one of these two parallel edges. We call a contraction of an outer edge an X'-contraction if the unique inner face incident to the contracted edge is incident to a vertex of X'. We always prefer X'-contractions to other contractions. Let G'' be the triangulation obtained from the contractions, let s be the number of contractions that were X'-contractions, and let t be the number of faces of G'' which are incident to two outer vertices and one vertex from X'. Then $t \leq 3$ and, if $s < K-3$, then $t = 0$ since we preferred X'-contractions to other contractions.

By Lemma 3.38 we have $|E_{\text{inc}}(G'', X')| \geq 3k'$ and $|F_{\text{inc}}(G'', X')| \geq 2k'+1$. Since we reduced the number of incident edges and the number of incident faces by 1 with each X'-contraction, we thus have $|E_{\text{inc}}(G', X')| \geq 3k' + s$ and $|F_{\text{inc}}(G', X')| \geq 2k' + 1 + s$.

It follows that $|E^{\text{nor}}_{\text{inc}}(H', X')| = 2|E_{\text{inc}}(G', X')| - (s+t) \geq 6k' + s - t$ and $|N^{\text{sta}}(H', X')| = |F_{\text{inc}}(G', X')| - (s+t) \geq 2k'+1-t$. If $t = 0$, this gives $|E^{\text{nor}}_{\text{inc}}(H', X')| + |N^{\text{sta}}(H', X')|\frac{K-6}{2} \geq 6k' + 2k'\frac{K-6}{2} = Kk'$ and, if $t > 0$, this gives $|E^{\text{nor}}_{\text{inc}}(H', X')| + |N^{\text{sta}}(H', X')|\frac{K-6}{2} \geq (6k' + K - 6) + (2k' - 2)\frac{K-6}{2} = Kk'$.

Now we consider the vertices X_i in the interior of the triangle T_i. According to Lemma 3.38 we have $|E_{\text{inc}}(T_i, X_i)| \geq 3k_i$ and $|F_{\text{inc}}(T_i, X_i)| \geq 2k_i + 1$. We have $|E^{\text{nor}}_{\text{inc}}(H, X_i)| \geq 2|E_{\text{inc}}(T_i, X_i)| \geq 6k_i$ and, since only one inner face of T_i is incident to two outer vertices of G, $|N^{\text{sta}}(H, X_i)| = |F_{\text{inc}}(T_i, X_i)| - 1 \geq 2k_i$. Therefore, $|E^{\text{nor}}_{\text{inc}}(H, X_i)| + |N^{\text{sta}}(H, X_i)|\frac{K-6}{2} \geq 6k_i + 2k_i\frac{K-6}{2} = Kk_i$. Hence, we have

$$
\begin{aligned}
&\left|E^{\text{nor}}_{\text{inc}}(H, X)\right| + \left|N^{\text{sta}}(H, X)\right| \tfrac{K-6}{2} \\
&= \left(\left|E^{\text{nor}}_{\text{inc}}(H', X')\right| + \sum_{i=1}^{r} \left|E^{\text{nor}}_{\text{inc}}(H, X_i)\right|\right) + \left(\left|N^{\text{sta}}(H', X')\right| + \sum_{i=1}^{r} \left|N^{\text{sta}}(H, X_i)\right|\right) \tfrac{K-6}{2} \\
&= \left(\left|E^{\text{nor}}_{\text{inc}}('H, X')\right| + \left|N^{\text{sta}}(H', X')\right| \tfrac{K-6}{2}\right) + \sum_{i=1}^{k} \left(\left|E^{\text{nor}}_{\text{inc}}(H, X_i)\right| + \left|N^{\text{sta}}(H, X_i)\right| \tfrac{K-6}{2}\right) \\
&\geq k'K + \sum_{i=1}^{r} k_i K \\
&= \left(k' + \sum_{i=1}^{r} k_i\right) K = kK \quad .
\end{aligned}
$$

This completes the proof of $|E_{\text{inc}}(H, W)| \geq kK + l(K-6)$.

If G has n vertices, then it has $n-K$ inner vertices and $2n-K-2$ inner faces. Hence, the number of stack vertices in $2G^\star$ is $2(n-K-1)$. It remains to verify that $|E_{\text{inc}}(H, V_{\text{inner}}(H))| = (n-K)K + 2(n-K-1)(K-6)$. Each stack vertex is incident to 3 stack edges in $2G^\star$, this yields $3\frac{K-6}{2}2(n-K-1)$ edges of H. In addition there are $2(3n-2K-3) - K$ normal edges which are incident to inner vertices in $2G$ and thus also in H. Since $3(K-6)(n-K-1) + 2(3n-2K-3) - K = (n-K)K + 2(n-K-1)(K-6)$, this completes the proof. □

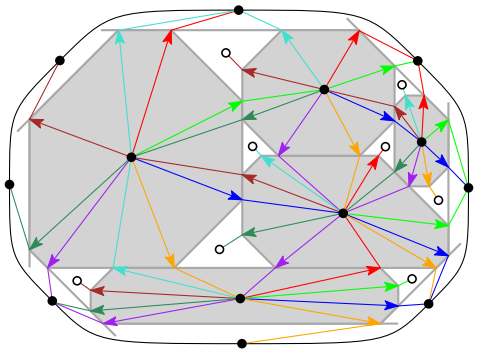

Figure 3.29: The 8-proper coloring of $2G^\star_+(S)$ for the K-contact structure S induced by the contact representation of Fig. 3.25. This is an extension of the 8-color forest induced by this contact representation, see Fig. 3.28.

Definition 3.40 (K-proper coloring (even))**.** A *K-proper coloring* of $2G^\star_+$ is a coloring of the inner edges of $2G^\star_+$ in the colors $0, \ldots, K-1$ such that the following properties are fulfilled:

(C1) Let $i \in \{0, \ldots, K-1\}$ and let $e_0, \ldots, e_{r-1}$ be the edges incident to the outer vertex a_i in clockwise order with outer edges e_0 and e_1. Then $c(e_2) = i, c(e_3) = i+1, c(e_4) = i, c(e_5) = i+1, \ldots, c(e_{r-1}) = i$.

(C2) Each inner normal vertex has exactly one outgoing edge in each color and the clockwise order of the colors is $0, \ldots, K-1$.

(C3) Let $e_0, e_1, \ldots$ be the incoming edges of an inner normal vertex which are located between the outgoing edges of colors i and $i+1$, in clockwise order. Then,

- **i)** if e_0 and e_1 are parallel edges, we require $c(e_0) = i + \frac{K}{2} + 1, c(e_1) = i + \frac{K}{2}$, $c(e_2) = i + \frac{K}{2} + 1, c(e_3) = i + \frac{K}{2}, \ldots$ and,
- **ii)** if e_0 and e_1 are non-parallel edges, we require $c(e_0) = i + \frac{K}{2}, c(e_1) = i + \frac{K}{2} + 1$, $c(e_2) = i + \frac{K}{2}, c(e_3) = i + \frac{K}{2} + 1, \ldots$

Figure 3.29 gives an illustration of Definition 3.40.

Note that the subgraph induced by the normal vertices of $2G^\star_+$ endowed with a K-proper coloring is a K-color forest of G.

Our next goal is to prove that $2G^\star_+$ has a unique K-proper coloring. For this proof we assign values to all angles between consecutive incident edges of the vertices in $2G^\star_{++}$ except those angles in the outer face. We will see that these angle values fulfill properties similar to those of the angles in a crossing-free straight line drawing of $2G^\star_{++}$.

The following definition of these angle values is visualized in Fig. 3.30. We denote the value of the angle at a vertex v between its incident edges e_1 and e_2 that are consecutive in the cyclic order of incident edges of v by $\measuredangle e_1 v e_2$. The definition of these values will be symmetric. Therefore, we do not distinguish between clockwise and counterclockwise angles. Let v be a normal vertex and let e_1 and e_2 be two

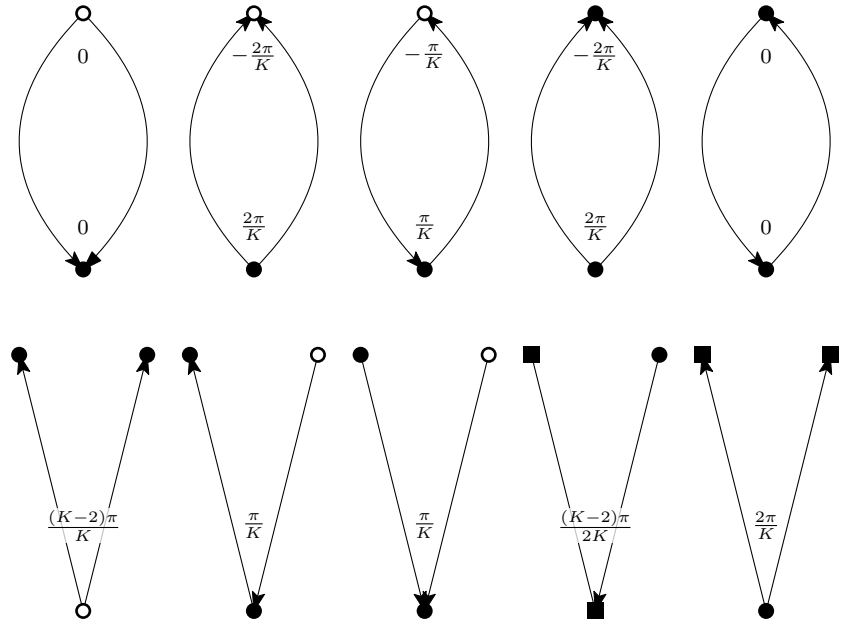

Figure 3.30: Definition of the angle values of $2G^{\star}_{++}$. White vertices are stack vertices, black circles are arbitrary normal vertices, and black squares are outer normal vertices.

parallel edges connecting v to a stack vertex. Then we set $\measuredangle e_1ve_2 := 0$ if e_1 and e_2 are incoming at v, $\measuredangle e_1ve_2 := \frac{2\pi}{K}$ if e_1 and e_2 are outgoing at v, and $\measuredangle e_1ve_2 := \frac{\pi}{K}$ if one of e_1 and e_2 is incoming at v and the other one outgoing at v. Now let v be a normal vertex and let e_1 and e_2 be two parallel edges connecting v to a normal vertex. Then we set $\measuredangle e_1ve_2 := -\frac{2\pi}{K}$ if e_1 and e_2 are incoming at v, $\measuredangle e_1ve_2 := \frac{2\pi}{K}$ if e_1 and e_2 are outgoing at v, and $\measuredangle e_1ve_2 := 0$ if one of e_1 and e_2 is incoming at v and the other one outgoing at v. Next let w be a stack vertex and let e_1 and e_2 be two parallel edges connecting w to a normal vertex. Then we set $\measuredangle e_1we_2 := 0$ if e_1 and e_2 are outgoing at w, $\measuredangle e_1we_2 := -\frac{2\pi}{K}$ if e_1 and e_2 are incoming at w, and $\measuredangle e_1we_2 := -\frac{\pi}{K}$ if one of e_1 and e_2 is incoming at w and the other one outgoing at w. Now let w be a stack vertex and let e_1 and e_2 be two non-parallel outgoing edges connecting w to normal vertices. Then we set $\measuredangle e_1we_2 := \frac{(K-2)\pi}{K}$. Finally, let v be a normal vertex, let e_1 be an edge connecting v to a normal vertex, and let e_2 be an incoming edge connecting v to a stack vertex. Then we set $\measuredangle e_1ve_2 := \frac{\pi}{K}$. This covers all cases not concerning the outer vertices of $2G^{\star}_{++}$. Now let v be an outer normal vertex, let e_1 be an incoming normal edge, and let e_2 be an edge connecting v to another outer vertex. Then we set $\measuredangle e_1ve_2 := \frac{(k-2)\pi}{2K}$. Finally, let v be an inner normal vertex and let e_1 and e_2 be outgoing edges of v connecting it to outer vertices. Then we set $\measuredangle e_1ve_2 := \frac{2\pi}{K}$.

The value of the angle between two non-consecutive incident edges of a vertex of $2G^{\star}_{++}$ is defined as the sum of the values of its partial angles between consecutive incident edges. The following lemmas show some basic properties of these angle values.

Lemma 3.41. *The value of the angle at an inner normal vertex between an incoming stack edge and an outgoing edge without another outgoing edge in between is* $\frac{\pi}{K}$.

Proof. We first prove the following claim.

Claim 1. *The value of the angle at an inner normal vertex between two incoming stack edges without an outgoing edge in between is* 0.

Proof. Let v be an inner normal vertex and let e and e' be two incoming stack edges of v without an outgoing edge of v in between. We prove the statement for the case that there is no incoming stack edge between e and e'. Then the general statement follows by induction on the number of incoming stack edges between e and e'.

We distinguish two cases. If e and e' are neighboring incoming stack edges of v, the angle in between has value 0 by definition. Otherwise, there are exactly two parallel incoming normal edges in between e and e'. The angle between these two normal edges has value $-\frac{2\pi}{K}$ by definition and the two angles between e and e', respectively, and the incoming normal edge have value $\frac{\pi}{K}$ by definition. Therefore, the value of the angle between e and e' is $2\frac{\pi}{K} - \frac{2\pi}{K} = 0$. △

Now let v be an inner normal vertex, let e be an incoming stack edge of v, and let e' be an outgoing edge of v such that there is no outgoing edge of v between e and e'. Let e'' be the incoming stack edge of v that lies between e and e' (including e) such that there are no further incoming stack edges of v between e'' and e'. Then, due to Claim 1, the value of the angles of v between e and e'' is 0. If e'' and e' are parallel edges or e' is a neighboring normal edge of e'', the angle at v between e'' and e' has value $\frac{\pi}{K}$ by definition. Otherwise, e' is a normal edge and between e'' and e' there is an incoming normal edge e''' of v that is parallel to e'. Then the angle between e'' and e''' has value $\frac{\pi}{K}$ by definition and the angle between e''' and e' has value 0 by definition. Hence, in each case the value of the angle between e'' and e' is $\frac{\pi}{K}$ and thus also the value of the angle between e and e' is $\frac{\pi}{K}$. □

Lemma 3.42. *The value of any angle of a stack vertex v between two non-parallel edges is positive.*

Proof. The value of the angle of v between two consecutive non-parallel edges is $\frac{(K-2)\pi}{K}$. The value of the angle of v between two consecutive parallel edges e and e' is $-\frac{\pi}{K}$ multiplied with the number of edges in $\{e, e'\}$ that are incoming at v. Since v has exactly $\frac{K-6}{2}$ incoming edges, the value of an angle of v between two non-parallel edges is at least $\frac{(K-2)\pi}{K} - 2\frac{K-6}{2}\frac{\pi}{K} = \frac{4\pi}{K} > 0$. □

Lemma 3.43. *The value of the angle of an inner normal vertex v between two outgoing edges e and e' without another outgoing edge in between is* $\frac{2\pi}{K}$.

Proof. If e and e' are parallel edges, the angle at v between e and e' has value $\frac{2\pi}{K}$ by definition. If e and e' are consecutive incident edges ending in outer vertices, the angle at v between e and e' has value $\frac{2\pi}{K}$ by definition, too. Otherwise, there is an incoming stack edge e'' of v between e and e'. Then, due to Lemma 3.41, the two angles between e and e'' and between e'' and e' both have value $\frac{\pi}{K}$ whence the angle between e and e' has value $\frac{2\pi}{K}$. □

Lemma 3.44. *The value of an angle of an inner normal vertex v between an incoming and an outgoing edge is non-negative.*

Proof. By Lemma 3.43 the value of an angle of v between two outgoing edges is at least $\frac{2\pi}{K} > 0$. Therefore, it suffices to consider angles of v between an incoming and an outgoing edge without an outgoing edge in between. An angle of v between two incoming edges with exactly three more incoming edges in between has value 0 (such an angle decomposes into an angle between two consecutive parallel incoming normal edges of value $-\frac{2\pi}{K}$, an angle between two consecutive parallel incoming stack edges of value 0, and two angles between an incoming normal edge and a consecutive incoming stack edge of value $\frac{\pi}{K}$). Therefore, it suffices to consider angles of v between an incoming and an outgoing edge without outgoing edges in between and with at most three incoming edges in between. Suppose that such an angle has a negative value. Then this angle α decomposes into an angle between two consecutive parallel incoming normal edges of value $-\frac{2\pi}{K}$, at least one angle between an incoming normal edge and a consecutive incoming stack edge of value $\frac{\pi}{K}$, and

- **i)** an angle between an incoming stack edge and a consecutive parallel outgoing stack edge of value $\frac{\pi}{K}$, or
- **ii)** an angle between two consecutive parallel incoming stack edges of value 0 and an angle between an incoming stack edge and a consecutive outgoing normal edge of value $\frac{\pi}{K}$.

In both cases the sum of these values is already 0. In the second case we have already reached the three incoming edges in between. In the first case we can only add an angle between an incoming normal edge and a consecutive incoming stack edge of value $\frac{\pi}{2} > 0$. Thus, α has a non-negative value. □

The next two lemmas show that these artificial angle values behave similar to the angles in a crossing-free straight-line drawing of G.

Lemma 3.45. *The value of the complete angle of an inner vertex v is 2π.*

Proof. If v is a normal vertex, the statement immediately follows from Lemma 3.43 because a normal vertex has exactly K outgoing edges in $2G^{\star}_{++}$. Now let v be a stack vertex. Then the complete angle of v has exactly three subangles between two consecutive non-parallel outgoing edges each of which has value $\frac{(K-2)\pi}{K}$. The rest of the complete angle of v decomposes into angles between consecutive parallel edges. The value of these angles is $-\frac{2\pi}{K}$ per incident incoming edge. Since v has exactly $\frac{K-6}{2}$ incoming edges, the values of these angles sum up to $\frac{K-6}{2}(-\frac{2\pi}{K}) = -\frac{(K-6)\pi}{K}$. Thus the value of the complete angle of v is $3\frac{(K-2)\pi}{K} - \frac{(K-6)\pi}{K} = 2\pi$. □

Lemma 3.46. *The sum of the values of the inner angles of a simple cycle of length ℓ is $(\ell - 2)\pi$.*

Proof. We first give a proof for the case that the cycle is a facial cycle. Then we will deduce the general case from this special case.

Claim 1. *The sum of the angles in an inner triangular face f of $2G^\star_{++}$ is π.*

Proof. If the incident vertices of f are two normal vertices and one stack vertex, the angle at the stack vertex has value $\frac{(K-2)\pi}{K}$ and the other two angles have value $\frac{\pi}{K}$. Otherwise f is incident to two outer normal vertices and one inner normal vertex. Then the angle at the inner vertex has value $\frac{2\pi}{K}$ and the other two angles have value $\frac{(K-2)\pi}{2K}$. In each of these cases the sum of the values of the three angles is π. △

Claim 2. *The sum of the angles in a face f between two parallel edges in $2G^\star_{++}$ is 0.*

Proof. Let us first consider the case that f is incident to a normal vertex v and a stack vertex w. If both edges of f are outgoing at w, both angles have value 0. If both edges of f are outgoing at v, the angle at v has value $\frac{2\pi}{K}$ and the angle at w has value $-\frac{2\pi}{K}$. If the two edges of f have opposite orientations, the angle at v has value $\frac{\pi}{K}$ and the angle at w has value $-\frac{\pi}{K}$. Now let both vertices of f be normal vertices. If the two edges of f have opposite orientations, both angles have value 0. If both edges of f have the same orientation and are oriented from v to w, the angle at v has value $\frac{2\pi}{K}$ and the angle at w has value $-\frac{2\pi}{K}$. In each of these cases the sum of the values of the two angles is 0. △

Now let C be a simple cycle of length ℓ in $2G^\star_{++}$ with k vertices in its interior. Then, due to Euler's formula, the number of triangular faces inside C is $\ell - 2 + 2k$. Additionally, there can be arbitrarily many faces of degree 2 inside C. Thus, due to Claims 1 and 2, the sum of all angles inside C is $(\ell - 2 + 2k)\pi$. Since, due to Lemma 3.45, the sum of the angles of the vertices inside C is $k \cdot 2\pi$, the sum of the inner angles of the cycle C is $(\ell - 2 + 2k)\pi - 2k\pi = (\ell - 2)\pi$. □

The idea. Remember that our goal is to find a K-proper coloring of $2G^\star_+$. The idea of the construction of the colors is as follows: We start with an inner edge e of $2G^\star_{++}$ and follow a properly defined path that at some point reaches one of the outer vertices. Then the label of this outer vertex will be the color of e. This approach is similar to the proof of the bijection of Schnyder Woods and 3-orientations in [FO01]. In the definition of these paths we aim at continuing with the outgoing edge on the opposite side of a vertex. This is motivated by the following geometric idea: If we are already given an equiangular contact representation, such paths keep a constant slope and therefore run into an outer segment with corresponding slope. If we run into a stack vertex, there is no unique opposite edge. Therefore, the path of e is not unique, but we can associate a unique color with e by showing that all properly defined paths starting with e end in the same outer vertex.

Definition 3.47 (Color preserving walk)**.** The set $\mathcal{P}$ of *color preserving walks* is the set of walks P in $2G^\star_{++}$ that start with an outgoing inner edge of a normal vertex and fulfill the following local properties at an outgoing inner edge $e = uv$ of a normal vertex v in P:

(P1) If v is an outer vertex, i.e., $v = a_i$ for some i, then P ends at v with e being its last edge.

(P2) If v is an inner normal vertex, let e' be the opposite outgoing edge of e at v, i.e., both angles at v between the edges e and e' have value π. Then P is continued with the edge e' after e. See Fig. 3.31a for a visualization.

(P3) If v is a stack vertex, let v_1 and v_2 be the two vertices of G which follow u in the clockwise traversal of the facial cycle of G corresponding to v. Let e_1 be one of the two edges from v to v_1 and let e_2 be one of the two edges from v to v_2 (it does not matter which one we choose). Let β_1 be the value of the clockwise angle of u between e and e_1 and let β_2 be the value of the counterclockwise angle of u between e and e_2. Further, let e_1' and e_2' be the outgoing edges of v_1 and v_2, respectively, such that the clockwise angle of v_1 between e_1 and e_1' has value $2\pi - \beta_1$ and the counterclockwise angle of v_2 between e_2 and e_2' has value $2\pi - \beta_2$. It might be that one of the edges e_1' and e_2' is not well-defined, but at least one of them is. Then P must be continued with either e_1, e_1' or with e_2, e_2' after e. See Fig. 3.31b for a visualization.

For an edge e, we denote by $\mathcal{P}(e)$ the set of color preserving walks starting with e.

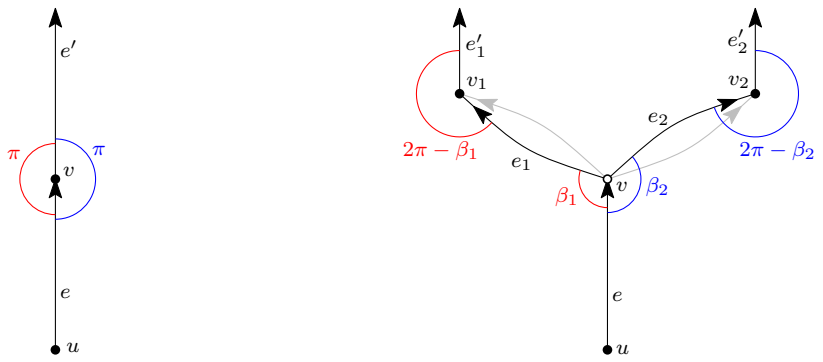

(a) If v is a normal vertex, the successor e' is unique.

(b) If v is a stack vertex, there are two possible continuations e_1e_1' and e_2e_2'. Also the edges e_1 and e_2 are not unique, but e_1' and e_2' are independent from the choice of e_1 and e_2 (compare Lemma 3.48).

Figure 3.31: Construction of the successors of an edge $e = uv$ with normal vertex u in a color preserving walk.

It is not clear that continuing edges as required in Definition 3.47 always exist. In the following lemma we will show that they do exist.

Lemma 3.48. *Let $e = uv$ be an outgoing edge of an inner normal vertex u in $2G^\star_{++}$. Then the set $\mathcal{P}(e)$ of color preserving walks starting with e is not empty.*

Proof. We distinguish three cases concerning the type of the vertex v.

i) If v is an outer normal vertex, there is nothing to show.

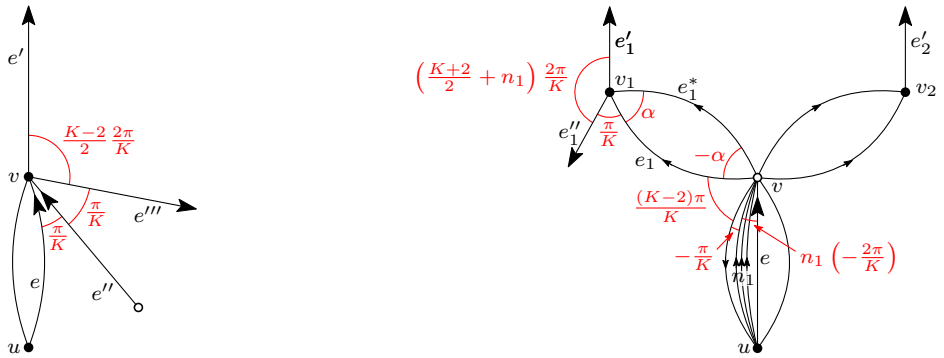

(a) A normal edge $e = (u, v)$, the consecutive stack edge e'', and the next and $\frac{K}{2}$th next outgoing edges e''' and e' of v. Then the angle between e and e' has value π.

(b) A stack edge $e = (u, v)$ with n_1 parallel edges to its left, e''_1 being the first and e'_1 the $(\frac{K+4}{2} + n_1)$th outgoing edge of v_1 after e_1 in clockwise order. Then the values of the angles at v between e and e_1 and at v_1 between e_1 and e'_1 add up to 2π.

Figure 3.32: Constructions showing that color preserving walks are well-defined.

ii) Let v be an inner normal vertex. This case is illustrated in Fig. 3.32a. Then one of the two neighboring edges of e in the cyclic order of incident edges of v is an incoming stack edge. We denote this edge by e''. Let e''' and e' be the first and the $\frac{K}{2}$th outgoing edge of v after e in the direction of e'', respectively. Then the angle between e and e'' has value $\frac{\pi}{K}$ by definition, the angle between e'' and e''' has value $\frac{\pi}{K}$ due to Lemma 3.41, and the angle between e''' and e' has value $\frac{K-2}{2}\frac{2\pi}{K}$ due to Lemma 3.43. Therefore, the angle between e and e' has value $2\frac{\pi}{K} + \frac{K-2}{2}\frac{2\pi}{K} = \pi$. Since, due to Lemma 3.43, the value of the angle between any two outgoing edges of v is at least $\frac{2\pi}{K} > 0$, the edge e' is the unique outgoing edge of v with this property.

iii) Now let v be a stack vertex. This case is illustrated in Fig. 3.32b. Let v_1 and v_2 be the two vertices of G which follow u in the clockwise traversal of the facial cycle of G corresponding to v. Let e_1 and e_1^* be the first and the second edge from v to v_1 in the clockwise cyclic order of v after the edge e, respectively. Let n_1 be the number of edges from u to v between e and e_1 in the clockwise cyclic order of v. Further, let e'_1 be the $\left(\frac{K+4}{2} + n_1\right)$th outgoing edge of v_1 after e_1 in the clockwise cyclic order of v_1. Then the clockwise angle at v between e and e_1 has value $n_1(-\frac{2\pi}{K}) - \frac{\pi}{K} + \frac{(K-2)\pi}{K} = \frac{(K-3-2n_1)\pi}{K}$. If v_1 is not an outer vertex, the clockwise angle of v_1 between e_1 and e'_1 has, due to Lemmas 3.41 and 3.43, value $\frac{\pi}{K} + (\frac{K+2}{2} + n_1)\frac{2\pi}{K} = \frac{(K+3+2n_1)\pi}{K}$. Thus the sum of the values of the clockwise angle of v between e and e_1 and the value of the clockwise angle of v_1 between e_1 and e'_1 is 2π, as required. Since the sum of the value of the clockwise angle of v between e_1 and e_1^* and the value of the clockwise angle of v_1 between e_1^* and e_1 is 0, also the sum of the value of the clockwise angle of v between e and e_1^* and the value of the clockwise angle of v_1 between e_1^* and e'_1 is 2π. Since, due to Lemma 3.43, the value of the angle

between any two outgoing edges of v_1 is at least $\frac{2\pi}{K} > 0$, the edge e_1 is the unique valid outgoing edge of v_1. Because of symmetry we can analogously find a unique valid outgoing edge e_2' of v_2 if v_2 is not an outer vertex. Since stack vertices are by definition adjacent to at most one outer vertex, at least one of the edges e_1' and e_2' is well-defined.

Since in all three cases the set $\mathcal{P}(e)$ is non-empty, this finishes the proof. □

At the moment it is not clear that color preserving walks are finite. If they are finite, they have to end in an outer vertex. But we have to prove that they do not contain subcycles.

If P is a walk with a designated start vertex, then at an inner vertex v between the edges e_i and e_{i+1} of P we can distinguish angles between consecutive incident edges of v on the left side of P and on the right side of P. We define $\text{l-angle}_P(e_i, e_{i+1})$ and $\text{r-angle}_P(e_i, e_{i+1})$ to be the values of those angles on the left and right side of P, respectively. If the path P is clear from the context, we omit the subscript P.

Lemma 3.49. *Let $P = v_0, e_0, v_1, e_1, \ldots, e_k, v_{k+1}$ be a finite subwalk of a color preserving walk with normal vertices v_0 and v_k. Then $\sum_{i=0}^{k-1} \text{l-angle}(e_i, e_{i+1}) = \sum_{i=0}^{k-1} \text{r-angle}(e_i, e_{i+1}) = k\pi$.*

Proof. If $k = 0$, the statement is trivial. Let $k \geq 1$. We distinguish two cases concerning the vertex v_{k-1}.

i) If v_{k-1} is a normal vertex, we have, by Definition 3.47, $\text{l-angle}(e_{k-1}, e_k) = \pi$ or $\text{r-angle}(e_{k-1}, e_k) = \pi$. According to Lemma 3.45, we have $\text{l-angle}(e_{k-1}, e_k) + \text{r-angle}(e_{k-1}, e_k) = 2\pi$ and thus $\text{l-angle}(e_{k-1}, e_k) = \text{r-angle}(e_{k-1}, e_k) = \pi$. Then the statement follows by induction on k.

ii) If v_{k-1} is a stack vertex, we have $k \geq 2$ since v_0 is a normal vertex. Then v_{k-2} is a normal vertex and it follows from Definition 3.47 that $\text{l-angle}(e_{k-2}, e_{k-1}) + \text{l-angle}(e_{k-1}, e_k) = 2\pi$ or $\text{r-angle}(e_{k-2}, e_{k-1}) + \text{r-angle}(e_{k-1}, e_k) = 2\pi$. Therefore, we obtain by Lemma 3.45, as before, that $\sum_{i=k-2}^{k-1} \text{l-angle}(e_i, e_{i+1}) = \sum_{i=k-2}^{k-1} \text{r-angle}(e_i, e_{i+1}) = 2\pi$ and the statement follows by induction on k.

Hence, in both cases the statement of the lemma is true. □

Lemma 3.50. *The color preserving walks $P \in \mathcal{P}(e)$ are paths, i.e., there are no vertex repetitions in P.*

Proof. Suppose that there exists a color preserving path P with a vertex repetition. Let $C = v_0, e_0, v_1, \ldots, v_{\ell-1}, e_{\ell-1}, v_0$ be a minimal subcycle of P. Note that the preceding edge of e_0 in P (if there is one) does not have to be $e_{\ell-1}$ and that the succeeding edge of $e_{\ell-1}$ in P does not have to be e_0.

Claim 1. *The length of C is not two, i.e., $\ell \neq 2$.*

Proof. Suppose that $\ell = 2$. We distinguish three cases concerning the vertices v_0 and v_1.

i) If v_0 and v_1 are normal vertices, the angle at v_1 between e_0 and e_1 inside C has value 0 by definition, in contradiction to Lemma 3.49 which states that it is π.

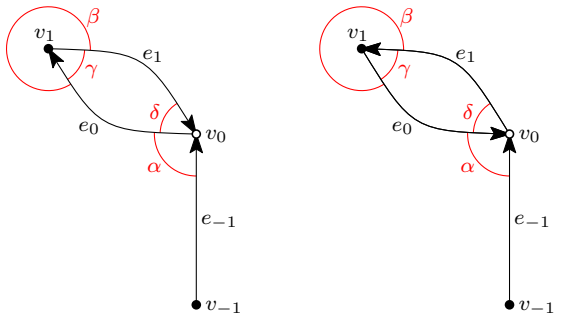

Figure 3.33: A hypothetical subcycle of a color preserving walk of length 2, on the left side clockwise oriented and on the right side counterclockwise oriented. As shown in Lemma 3.50, such a cycle cannot exist.

ii) If v_0 is a stack vertex and v_1 is a normal vertex, e_0 has a preceding edge $e_{-1} = v_{-1}v_0$ in P. Because of symmetry, we can assume that v_1 is the vertex following v_{-1} in the clockwise traversal of the face of G corresponding to v_0. Let α be the value of the clockwise angle at v_0 between e_{-1} and e_0, let β be the value of the clockwise angle at v_1 between e_0 and e_1, let γ be the value of the clockwise angle at v_1 between e_1 and e_0, and let δ be the value of the clockwise angle at v_0 between e_0 and e_1, see Fig. 3.33. Then by Lemma 3.45 we have $\beta + \gamma = 2\pi$ and by Lemma 3.46 we have $\gamma + \delta = 0$. If C is oriented clockwise, we further have $\alpha + \beta = 2\pi$ by Definition 3.47 which implies $\alpha + \delta = 0$, in contradiction to Lemma 3.42. If C is oriented counterclockwise, we have $\alpha + \delta + \gamma = 2\pi$ which implies $\alpha = 2\pi$, in contradiction to Lemma 3.42.

iii) If v_0 is a normal vertex and v_1 a stack vertex, it immediately follows from Definition 3.47 that the successor of e_0 in P is not an edge from v_1 to v_0.

Hence, in all three cases, the assumption that $\ell = 2$ leads to a contradiction. △

Because of Claim 1 it follows from Lemmas 3.42 and 3.44 that the values of all inner angles of C are non-negative. Now we distinguish two cases concerning the vertex $v_{\ell-1}$.

i) If $v_{\ell-1}$ is a normal vertex, the sum of the values of the inner angles of C at the vertices $v_1, \ldots, v_{\ell-1}$ is $(\ell - 1)\pi$ by Lemma 3.49. Since the value of the inner angle of C at v_0 is non-negative, this is a contradiction to Lemma 3.46.

ii) If $v_{\ell-1}$ is a stack vertex, $v_{\ell-2}$ is a normal vertex and therefore the sum of the values of the inner angles of C at the vertices $v_1, \ldots, v_{\ell-2}$ is $(\ell - 2)\pi$ by Lemma 3.49. Since the value of the inner angle of C at v_0 is non-negative and the value of the inner angle of C at $v_{\ell-1}$ is positive due to Lemma 3.42, this is again a contradiction to Lemma 3.46.

Hence, the assumption at the beginning of the proof that $\ell = 2$ is false. □

The following two lemmas are crucial for finding a unique color associated to all color preserving paths in $\mathcal{P}(e)$ for a fixed edge e.

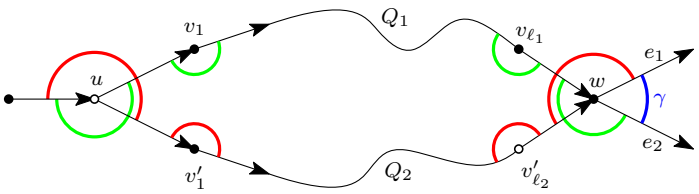

Figure 3.34: Two color preserving paths that coincide up to the stack vertex u, then go in different directions, meet again at the normal vertex w, and therefore form a cycle C. The green angles are the angles on the right of Q_1 and the red angles are the angles on the left of Q_2. If we add the values of the green angles and the values of the red angles, we overcount the values of the inner angles of C by 2π at u and by $2\pi - \gamma$ at w.

Lemma 3.51. *Let $P_1, P_2 \in \mathcal{P}(e)$ be two color preserving paths starting with the same edge e. Then P_1 and P_2 end with the same edge, or they end in the same outer vertex a_i with an odd number of incoming edges between P_1 and P_2 at a_i, or they end in consecutive outer vertices a_i and a_{i+1} with an odd number of incoming edges at a_i and an even number of incoming edges at a_{i+1} between P_1 and P_2.*

Proof. Assume that P_1 and P_2 coincide up to a vertex u, then P_1 goes to the left and P_2 to the right, and at a vertex w they meet again, i.e., w is contained in P_1 and P_2 and the paths P_1 and P_2 have no common vertex in-between u and w. Note that u has to be a stack vertex. Let $Q_1 = u, v_1, v_2, \dots, v_{\ell_1}, w$ and $Q_2 = u, v'_1, v'_2, \dots, v'_{\ell_2}, w$ be the subpaths of P_1 and P_2, respectively, starting at v and ending at w and let C be the cycle of length $\ell_1 + \ell_2 + 2$ obtained by adding Q_1 and Q_2. Then we have $\text{r-angle}_{P_1}(u) + \text{r-angle}_{P_1}(v_1) = 2\pi$ and $\text{l-angle}_{P_2}(u) + \text{l-angle}_{P_2}(v'_1) = 2\pi$. Note that $\text{r-angle}_{P_1}(u) + \text{l-angle}_{P_2}(u)$ is the value of the complete angle at u plus the value of the inner angle of C at u. If w is a stack vertex, v_{ℓ_1} and v'_{ℓ_2} are normal vertices and therefore $\sum_{i=2}^{\ell_1} \text{r-angle}_{P_1}(v_i) = (\ell_1 - 1)\pi$ and $\sum_{i=2}^{\ell_2} \text{l-angle}_{P_2}(v'_i) = (\ell_2 - 1)\pi$. Let β be the inner angle of C at w. Then the sum of the inner angles of C is $2\pi + (\ell_1 - 1)\pi + (\ell_2 - 1)\pi + \beta = (\ell_1 + \ell_2)\pi + \beta$. Due to Lemma 3.46 the sum of the inner angles of C is $(\ell_1 + \ell_2)\pi$. Thus $\beta = 0$. Since the angle between two non-parallel incident edges of a stack vertex is positive due to Lemma 3.42, the assumption that w is a stack vertex is wrong. Therefore, w is an inner normal vertex. Let e_1 and e_2 be the outgoing edges of w that are part of P_1 and P_2, respectively. Let γ be the angle of w between e_1 and e_2, see Fig. 3.34. We have $\sum_{i=2}^{\ell_1} \text{r-angle}_{P_1}(v_i) + \text{r-angle}_{P_1}(w) = \ell_1\pi$ and $\sum_{i=2}^{\ell_2} \text{l-angle}_{P_2}(v'_i) + \text{l-angle}_{P_2}(w) = \ell_2\pi$. Note that $\text{r-angle}_{P_1}(w) + \text{l-angle}_{P_2}(w) + \gamma$ is the value of the complete angle at u plus the value of the inner angle of C at w. Thus the sum of the inner angles of C is $2\pi + \ell_1\pi + \ell_2\pi + \gamma - 2\pi = (\ell_1 + \ell_2)\pi + \gamma$. Therefore $\gamma = 0$ and, due to Lemma 3.43, $e_1 = e_2$. Hence, P_1 and P_2 continue with the same edge at w.

Now let u be the last common vertex of P_1 and P_2. Because of the above observation, u has to be a stack vertex. Assume that P_1 goes to the left and P_2 goes to the right. Let $Q_1 = u, v_1, v_2, \dots, v_{\ell_1}, a_i$ and $Q_2 = u, v'_1, v'_2, \dots, v'_{\ell_2}, a_j$ be the subpaths of P_1 and P_2, respectively, starting at u. Let us first consider the case

that $i < j$, i.e., P_1 and P_2 end in different outer vertices. Let $Q_3 = a_i, a_{i+1}, \dots, a_j$ be a path of outer vertices connecting a_i and a_j. Let C be the cycle of length $\ell_1+\ell_2+2+j-i$ obtained by adding Q_1, Q_2, and Q_3. Further, let k_1 and k_2 be the number of incoming edges at a_i and a_j inside C, respectively. The values of the inner angles of C at u, $v_1, \dots, v_{\ell_1}$, and $v'_1, \dots, v'_{\ell_2}$ are as before. The value of the inner angle of C at a_i is $\frac{(K-2)\pi}{2K}+(k_1 \bmod 2)\frac{2\pi}{K}$, the value of the inner angle of C at a_j is $\frac{(K-2)\pi}{2K}-(k_1 \bmod 2)\frac{2\pi}{K}$, and the value at the inner angles of C at $a_{i+1}, \dots, a_{j-1}$ is $\frac{(K-2)\pi}{K}$. Therefore, the sum of the values of the inner angles of C is $2\pi + (\ell_1 - 1)\pi + (\ell_2 - 1)\pi + (j - i)\frac{(K-2)\pi}{2K} + ((k_1 \bmod 2) - (k_2 \bmod 2))\frac{2\pi}{K} = (\ell_1 + \ell_2 + (j - i)\frac{(K-2)}{K} + ((k_1 \bmod 2) - (k_2 \bmod 2))\frac{2}{K})\pi$. Since, because of Lemma 3.46, the sum of the values of the inner angles of C is $(\ell_1 + \ell_2 + (j - i))\pi$, this implies that $j - i = 1$, that k_1 is odd, and that k_2 is even.

Let us now consider the case that $i = j$, i.e., P_1 and P_2 end in the same outer vertex, but that P_1 and P_2 end with different edges. Let C be the cycle of length $\ell_1 + \ell_2 + 2$ obtained by adding Q_1 and Q_2. Further, let k be the number of incoming edges of a_i between P_1 and P_2. The values of the inner angles of C at u, $v_1, \dots, v_{\ell_1}$, and $v'_1, \dots, v'_{\ell_2}$ are as before. The value of the inner angle of C at a_i is $\pm(1 - (k \bmod 2))\frac{2\pi}{K}$. Therefore, the sum of the values of the inner angles of C is $2\pi + (\ell_1 - 1)\pi + (\ell_2 - 1)\pi \pm (1 - (k \bmod 2))\frac{2\pi}{K} = (\ell_1 + \ell_2)\pi \pm (1 - (k \bmod 2))\frac{2\pi}{K}$. Since, due to Lemma 3.46, the sum of the values of the inner angles of C is $(\ell_1 + \ell_2)\pi$, this implies that k is odd. □

Lemma 3.52. *Let u be a normal vertex and let $e_1 = uv_1, e_2 = uv_2$ be two different outgoing edges of u. Further, let $P_1 \in \mathcal{P}(e_1)$ and $P_2 \in \mathcal{P}(e_2)$ be two color preserving paths starting with these edges. Then P_1 and P_2 do not cross. Further, if P_1 and P_2 end in the same outer vertex a_i, the number of incoming edges of a_i between P_1 and P_2 is even and, if they end in consecutive outer vertices a_i and a_{i+1}, the number of incoming edges at a_i between P_1 and P_2 is even or the number of incoming edges of a_{i+1} between P_1 and P_2 is odd.*

Proof. Assume that P_1 and P_2 have a common vertex different than v and let w be the first such vertex. Let $Q_1 = u, v_1, v_2, \dots, v_{\ell_1}, w$ and $Q_2 = u, v'_1, v'_2, \dots, v'_{\ell_2}, w$ be the subpaths of P_1 and P_2, respectively, that start at u and end at w. Further, let C be the cycle of length $\ell_1 + \ell_2 + 2$ obtained by adding Q_1 and Q_2. If w is a stack vertex or an outer normal vertex, then v_{ℓ_1} and v'_{ℓ_2} are normal vertices and we have $\sum_{i=1}^{\ell_1} \text{r-angle}_{P_1}(v_i) = \ell_1\pi$ and $\sum_{i=1}^{\ell_2} \text{l-angle}_{P_2}(v'_i) = \ell_2\pi$. Due to Lemma 3.43 the value of the angle at u between e_1 and e_2 inside C is at least $\frac{2\pi}{K} > 0$. We denote this value by α. Further, due to Lemma 3.42 the value of the angle at w between the incoming edges $v_{\ell_1}w$ and $v_{\ell_2}w$ inside C is positive. Thus, the sum of the inner angles of C is bigger than $(\ell_1 + \ell_2)\pi$, in contradiction to Lemma 3.46. Therefore, the assumption that w is a stack vertex or an outer normal vertex is wrong and w is an inner normal vertex. Let e'_1 and e'_2 be the outgoing edges of w that are part of P_1 and P_2, respectively. Then we have $\sum_{i=1}^{\ell_1} \text{r-angle}_{P_1}(v_i) + \text{r-angle}_{P_1}(w) = (\ell_1 + 1)\pi$ and $\sum_{i=1}^{\ell_2} \text{l-angle}_{P_2}(v'_i) + \text{l-angle}_{P_2}(w) = (\ell_2 + 1)\pi$. We denote the value of the angle at w between e'_1 and e'_2 outside C by β. Note that, if P_1 and P_2 cross at w, then $\text{r-angle}_{P_1}(w) + \text{l-angle}_{P_2}(w) + \beta$ is the value of the complete angle at w plus the

value of the inner angle of C at w. Therefore, in this case the sum of the values of the inner angles of C is $(\ell_1+1)\pi+(\ell_2+1)\pi+\alpha+\beta-2\pi=(\ell_1+\ell_2)\pi+\alpha+\beta$, in contradiction to Lemma 3.46. Therefore, P_1 and P_2 do not cross at w. Then $\text{r-angle}_{P_1}(w)+\text{l-angle}_{P_2}(w)-\beta$ is the value of the complete angle at w plus the value of the inner angle of C at w, and the sum of the values of the inner angles of C is $(\ell_1+\ell_2)\pi+\alpha-\beta$. Due to Lemma 3.46 this implies $\alpha=\beta$. Therefore, we can inductively repeat the argument for the subpaths of P_1 and P_2 starting at w. Hence, P_1 and P_2 do not cross.

Now let w be the last common vertex of P_1 and P_2. Assume that P_1 goes to the left and P_2 goes to the right. Let $Q_1=w,v_1,v_2,\dots,v_{\ell_1},a_i$ and $Q_2=w,v'_1,v'_2,\dots,v'_{\ell_2},a_j$ be the subpaths of P_1 and P_2, respectively, starting at w. Let us first consider the case that $i=j$, i.e., P_1 and P_2 end in the same outer vertex. Let C be the cycle of length $\ell_1+\ell_2+2$ obtained by adding Q_1 and Q_2. Further, let k be the number of incoming edges at a_i inside C. Then we have $\sum_{i=1}^{\ell_1}\text{r-angle}_{Q_1}(v_i)=\ell_1\pi$ and $\sum_{i=1}^{\ell_2}\text{l-angle}_{Q_2}(v'_i)=\ell_2\pi$. Due to Lemma 3.43 the value of the inner angle of C at w is at least $\frac{2\pi}{K}$. The value of the inner angle of C at a_i is $\pm(1-(k \bmod 2))\frac{2\pi}{K}$. Therefore, the sum of the values of the inner angles of C is at least $(\ell_1+\ell_2)\pi+(k \bmod 2)\frac{2\pi}{K}$. Since, due to Lemma 3.46, this sum is $(\ell_1+\ell_2)\pi$, it follows that k is even.

Now let us assume that $j=i+1$, i.e., P_1 and P_2 end in consecutive outer vertices. Let C be the cycle of length $\ell_1+\ell_2+3$ obtained by adding Q_1 and Q_2 and the outer edge a_ia_{i+1}. Further, let k_1 and k_2 be the number of incoming edges at a_i and a_{i+1} inside C, respectively. Then we have $\sum_{i=1}^{\ell_1}\text{r-angle}_{Q_1}(v_i)=\ell_1\pi$ and $\sum_{i=1}^{\ell_2}\text{l-angle}_{Q_2}(v'_i)=\ell_2\pi$. Due to Lemma 3.43 the value of the inner angle of C at w is at least $\frac{2\pi}{K}$. The value of the inner angle of C at a_i is $\frac{(K-2)\pi}{2K}+(k_1 \bmod 2)\frac{2\pi}{K}$ and the value of the inner angle of C at a_{i+1} is $\frac{(K-2)\pi}{2K}-(k_2 \bmod 2)\frac{2\pi}{K}$. Therefore, the sum of the values of the inner angles of C is at least $(\ell_1+\ell_2+1)\pi+((k_1 \bmod 2)-(k_2 \bmod 2))\frac{2\pi}{K}$. Since, due to Lemma 3.46, this sum is $(\ell_1+\ell_2+1)\pi$, it follows that k_1 is even or k_2 is odd. □

Now we have all the tools at hand we need to prove the existence and uniqueness of a K-proper coloring of $2G^\star_+$.

Theorem 3.53. *The graph $2G^\star_+$ has a unique K-proper coloring.*

Proof. We begin with the proof of the existence of a K-proper coloring. Let P be a color preserving path. Let e' be the last edge of P and let a_i be the end vertex of e'. If e' is the kth incoming edge of a_i in the clockwise order of the incoming edges of a_i between the edges a_ia_{i+1} and a_ia_{i-1}, we assign to P the color i, if k is odd, and the color $i+1$ if k is even. Now let e be an inner edge of $2G^\star_+$. Then e is an inner edge of $2G^\star_{++}$ starting at a normal vertex and we color e in the color assigned to the color preserving paths in $\mathcal{P}(e)$. Due to Lemmas 3.50 and 3.51 this coloring is well-defined. It immediately follows from property (P1) of Definition 3.47 that property (C1) is fulfilled.

Claim 1. *The coloring fulfills property (C2).*

Proof. Let v be an inner normal vertex. Then, due to Lemma 3.52, the outgoing edges of v have pairwise different colors. Let e_1 and e_2 be two consecutive outgoing edges of v in the clockwise order of outgoing edges of v. Let $P_1 \in \mathcal{P}(e_1)$ and $P_2 \in \mathcal{P}(e_2)$ be color preserving paths starting with e_1 and e_2, respectively. Let i be the color of e_1 and suppose that the color of e_2 is not $i+1$. Further, let P be a color preserving path starting at v with assigned color $i+1$. We distinguish three cases.

- **i)** If P ends in a_i, then also P_1 ends in a_i and thus, due to Lemma 3.52, its assigned color is $i-1 \neq i+1$, a contradiction.
- **ii)** If P ends in a_{i+1} and P_2 also ends in a_{i+1}, then, due to Lemma 3.52, the color assigned to P_2 is $i+2 \neq i+1$, a contradiction.
- **iii)** If P ends in a_{i+1} and P_2 does not end in a_{i+1}, then P and P_2 cross, in contradiction to Lemma 3.52.

Therefore, property (C2) is fulfilled. △

Claim 2. *The coloring fulfills property (C3).*

Proof. Let v be an inner normal vertex and let e and e' be two consecutive outgoing edges of v in the clockwise order of outgoing edges of v. Further, let $e_0, e_1, \dots$ be the incoming normal edges of v between e and e' in clockwise order. We distinguish two cases concerning the edges e and e_0.

- **i)** If e and e_0 are parallel edges, the value of the angle at v between e and e_0 is 0. Then the color of e_0 is the color of the outgoing edge e'' of v opposite to e, i.e., the value of the angle at v between e and e'' is π. Due to Lemma 3.43 this is the outgoing edge of color $i + \frac{K}{2}$.
- **ii)** If e and e_0 are not parallel, the value of the angle at v between e and e_0 is $\frac{2\pi}{K}$. Then the color of e_0 is the color of the outgoing edge e''' of v such that the value of the counterclockwise angle at v between e and e''' is $\pi - \frac{2\pi}{K}$. Due to Lemma 3.43 this is the outgoing edge of color $i + \frac{K}{2} + 1$.

Hence, the color of e_0 fulfills property (C3) in both cases. That also the colors of the edges $e_1, e_2, \dots$ fulfill this property, follows from the fact that the value of the angle at a normal vertex between two parallel incoming normal edges is $-\frac{2\pi}{K}$ and the value of the angle at a normal vertex between two consecutive, non-parallel incoming normal edges without an outgoing edge in-between is $\frac{2\pi}{K}$. △

Due to Claims 1 and 2 the given coloring also fulfills the remaining two properties of a K-proper coloring and, hence, is a K-proper coloring.

Now we show the uniqueness of the K-proper coloring. Because of properties (C2) and (C3) the knowledge of the color of an edge incident to an inner normal vertex v implies the knowledge of the colors of all edges incident to v. Due to property (C1), the colors of the edges incident to the outer vertices are fixed. Since G and thus also $2G^\star_+$ is connected, this implies that the colors of all inner edges are fixed. □

Corollary 3.54. *The mapping from a K-color forest of G to the induced K-contact structure is a bijective mapping from the set of K-color forests of G to the set of K-contact structures of G.*

3.3.3 The distributive lattice

We want to conclude this chapter by proving that also the set of K-color forests for even K carries the structure of a distributive lattice.

Similar as for odd K in the last section, we can describe K-contact structures for even K as ω-flows. Therefore, let D be a fixed orientation of $2G^\star$ without the edges of the outer face in which each stack edge is oriented towards its incident stack vertex and each normal edge has an arbitrary fixed orientation. Let $\omega_K : V(D) \to \mathbb{Z}$ and $c_l, c_u : E(D) \to \mathbb{Z}$ be defined as follows: If v is a normal vertex, we set $\omega_K(v) = \deg_D^-(v) - K$ and, if v is a stack vertex, we set $\omega_K(v) = \frac{K-6}{2}$. If e is a normal edge, we set $c_l(e) = 0$ and $c_u(v) = 1$ and, if e is a stack edge, we set $c_l(e) = 0$ and $c_u(e) = \frac{K-6}{2}$. Then the following describes a bijective mapping from a K-contact structure S to an (ω_K, c_l, c_u)-flow f of D. We set

$$f(e) = \begin{cases} 0 & \text{if } e \text{ is a normal edge and has different orientations in } S \text{ and } D, \\ 1 & \text{if } e \text{ is a normal edge and has the same orientation in } S \text{ and } D, \\ w(e) & \text{if } e \text{ is a stack edge.} \end{cases}$$

and call f the *induced ω_K-flow* of S.

Since the set of all ω-flows of a graph carries the structure of a distributive lattice (Theorem 2.12), we immediately obtain a distributive lattice on the set of all K-contact structures of a graph G. We want to figure out the cover relation in this distributive lattice.

Definition 3.55 (Flip (even K-contact structure))**.** Let S be a K-contact structure of G. We call the reorientation of a digon in S, i.e., a face of degree two consisting of normal edges, from counterclockwise to clockwise a *digon flip* in S. If $K = 6$, we call the reorientation of a triangle in S (consisting of normal edges) from counterclockwise to clockwise a *triangle flip* in S. If $K \geq 8$, let (u, v) be a normal edge in S and let w be the stack vertex such that the face uvw lies on the left side of (u, v). Then we call the reorientation of (u, v) combined with decreasing the weight of vw by one and increasing the weight of uw by one a *triangle flip* in S. A *flip* in S is either a digon flip or a triangle flip in S.

Theorem 3.56. *The flip operation is the cover relation of a distributive lattice on the set of all K-contact structures of a graph G.*

Proof. Let C be an essential cycle in $2G^\star$. Then there exists an ω_K-flow f such that C is an oriented cycle in the residual graph D_f and has no chordal path in D_f. We can assume that D is the orientation of $2G^\star$ given by the K-contact structure S corresponding to f. Further, let $2G^\star_+ := 2G^\star_+(S)$.

Claim 1. *There is no edge pointing from C into the interior of C in D.*

Proof. Suppose there is an edge $e = (v, w)$ pointing from C into the interior of C. We distinguish two cases concerning the vertex v.

i) If v is a normal vertex, let P be a color preserving walk starting with e. Due to Lemma 3.50 the walk P is a path ending in an outer vertex. Hence, P starts with a chordal path P' of C in D.

ii) If v is a stack vertex, let P be an arbitrary color preserving walk starting with an edge (w, u) with $u \neq v$. Then the walk $e + P$ is a walk ending in an outer vertex whose only repeated vertex can be the start vertex v. Hence, also in this case $e + P$ starts with a chordal path P' of C in D.

Therefore, the reversed path $\overline{P'}$ of P' is a chordal path in D_f (compare the proof of Theorem 3.29), in contradiction to the assumption that C is an essential cycle. △

Claim 2. *If $K = 6$, the cycle C has length 2 or it has length 3 and only consists of normal vertices. If $K \geq 8$, the cycle C has length 2 or it contains at least one stack vertex.*

Proof. Assume that the length of C is at least 3. Further, assume that C contains only normal vertices. Since C is an essential cycle, there are no edges in the interior of C which are parallel to an edge of C. Then, according to Lemma 3.37, there are exactly $\frac{K-2}{2}\ell(C) - K$ edges pointing from a vertex on C into the interior of C. Thus, due to Claim 1, we have $\frac{K-2}{2}\ell(C) - K = 0$ and therefore $\ell(C) = \frac{2\frac{K}{2}}{\frac{K}{2}-1}$. Since $\frac{K}{2}$ and $\frac{K}{2} - 1$ are relative prime for all $K \geq 6$, the only solution of this equation is $\ell(C) = \frac{K}{2} = 3$.

Further, if $K = 6$, the cycle C only consists of normal vertices as in an ω_6-flow the capacities for stack edges e are $c_l(e) = c_u(e) = 0$ whence there are no stack edges in $2G_f^\star$. △

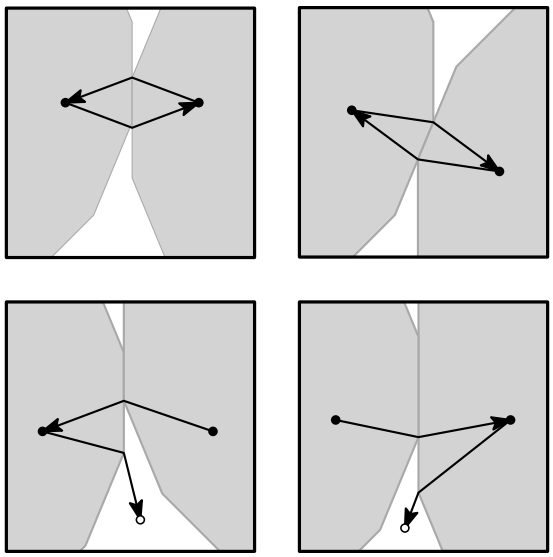

Figure 3.35: The geometric effect of a flip of the induced K-contact structure on the parallel-sided even K-gon contact representation. The first row shows a digon flip, the second row a triangle flip.

Now let $K \geq 8$ and let v be a stack vertex on C. Let w_1 and w_2 be the predecessor and the successor of v on C, respectively. Let $u \neq w_1, w_2$ be the third neighbor of v in $2G^\star$. Then, due to Claim 1, the edge (v, u) is pointing to the outside of C. Now, unless C is a facial cycle, the edge w_1w_2 is an inner chord of C. In either orientation the edge forms a chordal path, hence, C is not an essential cycle. □

Figure 3.35 shows the effect of a flip of the K-contact structure on the contact representation.

Chapter 4

Systems of linear equations

In this chapter we study the following computational problem: We are given an inner triangulation G of the K-cycle $a_0, \dots, a_{K-1}$, a K-contact structure S of G, for each inner vertex v of G a convex polygon P_v, and for the cycle $a_0, \dots, a_{K-1}$ a K-gon Q as prototypes such that the P_v and Q are similarly-aligned odd K-gons, if K is odd, and parallel-sided even K-gons if K is even. Then we want to decide whether G has a similarly-aligned odd K-gon or parallel-sided even K-gon contact representation $\mathcal{C}$, respectively, with the following properties: $\mathcal{C}$ induces the K-contact structure S, in $\mathcal{C}$ each inner vertex v of G is represented by a homothetic copy of its prototype P_v, and the cycle $a_0, \dots, a_{K-1}$ is represented by a K-gon whose sides have the same slopes as Q. We will see that this problem can be solved via a system of linear equations that is supposed to compute the side lengths of the polygons in this contact representation. If all side lengths given by the solution of this system are non-negative, the wanted contact representation exists, otherwise it does not exist. We will see that, especially in the latter case, the solution of the system has many useful properties.

In Section 4.1, we will recall similar, known systems of equations for the computation of contact representations with triangles and rectangles. The knowledge of these systems of equations will help understanding the remaining sections of this chapter. In Section 4.2, we prove a lemma that is crucial for the approach of computing a contact representation by solving a system of linear equations since it states that a non-negative solution of such a system of equations allows us to construct the wanted contact representation. In Section 4.3, we will study equations that enable us to handle the pseudotriangles that appear in contact representations with convex polygons between these convex polygons. Then we will apply these results to come up with systems of linear equations for similarly-aligned odd K-gon contact representations and parallel-sided even K-gon contact representations in Sections 4.4 and 4.5, respectively. Afterwards, in Section 4.6, we will study structural properties of the solutions of these systems of equations. Finally, in Section 4.7, we will see that, if some side lengths given by the solution of the system of equations are negative, the solution still induces a drawing of non-overlapping K-gons representing the vertices of G that is not a contact representation of G anymore.

4.1 Equations for triangle and rectangle contact representations

In this section we will recall the systems of linear equations for the computation of triangle and rectangle contact representations that have been studied before the start of the work on this thesis.

4.1.1 Equations for triangle contact representations

Let G be an inner triangulation of the 3-cycle a_0, a_1, a_2. Remember that in an equilateral triangle contact representation of G each inner vertex of G is represented by an equilateral triangle with a horizontal side at the bottom. The inner faces of G are also represented by equilateral triangles but with a horizontal side at the top (see Fig. 1.3a on Page 4). We will describe a system $\mathcal{A}_S$ of linear equations, depending on a Schnyder wood S of G, for the computation of the sizes of the triangles in an equilateral triangle contact representation of G that induces the Schnyder wood S if such a contact representation exists.

The system $\mathcal{A}_S$ has a variable x_v for each inner vertex v of G and a variable x_f for each inner face f of G. Each variable represents the side length of the triangle representing the corresponding vertex or face, respectively, in the contact representation.

Every inner vertex v induces three equations, one for each color of the Schnyder wood. For $i = 0, 1, 2$, let $F_i(v)$ be the set of incident faces of v that are located in the clockwise sector between the outgoing edges of v of colors $i + 1$ and $i - 1$. Then the equation corresponding to vertex v and color i is

$$x_v = \sum_{f \in F_i(v)} x_f \ .$$

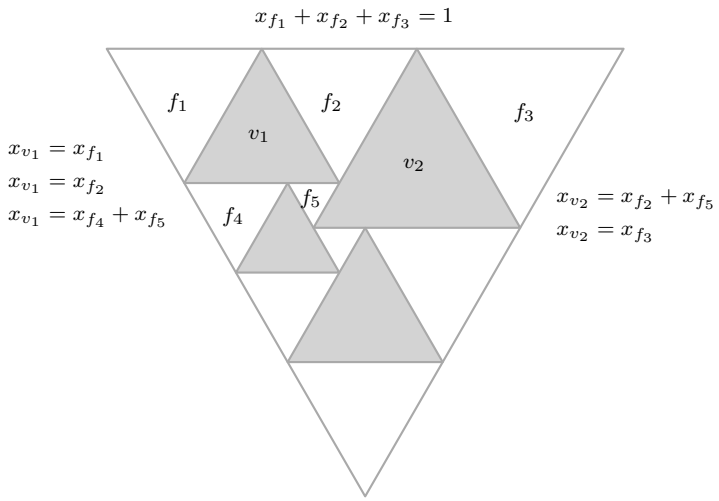

Figure 4.1: Examples for the different kinds of equations for the computation of equilateral triangle contact representations.

The system $\mathcal{A}_S$ has one more equation that concerns the incident faces of the outer vertex a_0. Let $F(a_0)$ be the set of incident inner faces of a_0. Then this last equation is

$$\sum_{f \in F(a_0)} x_f = 1 \ .$$

Figure 4.1 visualizes the different kinds of equations.

This system of equations has first been described in [Fel09] and then further studied in [Ruc11]. They show that the system is uniquely solvable.

Theorem 4.1 (Felsner [Fel09], Rucker [Ruc11]). *The system $\mathcal{A}_S$ is uniquely solvable.*

It is clear that an equilateral triangle contact representation of G with induced Schnyder wood S induces a non-negative solution of $\mathcal{A}_S$ with $x_v > 0$ for all inner vertices v of G and $x_f \geq 0$ for all inner faces f of G. If the graph G is 4-connected or we allow some but not all triangles to collapse to a single point in a triangle contact representation of G (see Fig. 4.2), also the converse holds (in the latter case we might have $x_v = 0$ for some vertices v). This can be proved via a simple application of the theory that we develop in Section 4.2 as we will see in the end of Section 4.4.

Theorem 4.2 (Felsner [Fel09]). *The solution of $\mathcal{A}_S$ is non-negative if and only if G has an equilateral triangle contact representation inducing the Schnyder wood S.*

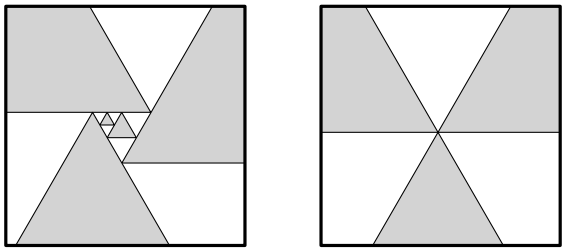

Figure 4.2: If the three triangles corresponding to a separating 3-cycle of G touch in a common point, all triangles corresponding to the vertices inside this 3-cycle are degenerate to a single point.

Surprisingly, if the solution is not non-negative, it still induces a drawing which is no longer a contact representation of G. We will generalize this result to arbitrary similarly-aligned odd K-gon contact representations and parallel-sided even K-gon contact representations in Section 4.7.

Theorem 4.3 (Felsner (unpublished), Rucker [Ruc11]). *If the solution of $\mathcal{A}_S$ has negative entries, it induces a dissection of an equilateral triangle into equilateral triangles, that is not a contact representation of G. The triangles of the dissection still correspond to the vertices and inner faces of G. Vertices v with $x_v > 0$ and faces f with $x_f < 0$ are represented by triangles with a horizontal side at the bottom, vertices v with $x_v < 0$ and faces f with $x_f > 0$ are represented by triangles with a horizontal side at the top.*

Further, the solution of $\mathcal{A}_S$ has the following structural property.

Theorem 4.4 (Felsner [Fel09], Rucker [Ruc11]). *If the solution of $\mathcal{A}_S$ has negative entries, then the edges of G between faces f and f' with $x_f \geq 0$ and $x_{f'} < 0$ can be decomposed into cycles that are directed cycles in the Schnyder wood S.*

This property implies that changing the orientation of the edges between negative and non-negative faces results in a new Schnyder wood of G. This kind of property will play a key role in an algorithmic approach for the computation of contact representations that we will study in Chapter 6. A similar statement has been proved by the author of this thesis for the case of a non-negative solution.

Theorem 4.5 (Schrezenmaier [Sch16; Sch17]). *If the solution of $\mathcal{A}_S$ is non-negative, then the edges of G between faces f and f' with $x_f > 0$ and $x_{f'} = 0$ can be decomposed into 3-cycles that are directed cycles in the Schnyder wood S.*

Further, reorienting such an oriented 3-cycle C in the Schnyder wood S (these are exactly the essential cycles, remember Definition 2.4 and Theorem 3.3) induces a change of the signs of the variables corresponding to the faces and vertices inside C. This kind of property will play a key role in another algorithmic approach we will study in Chapter 6 and in Chapter 5.

Theorem 4.6 (Schrezenmaier [Sch16; Sch17]). *Let S and S' be Schnyder woods of G that are related by a flip of the essential cycle C, i.e., S and S' are a covering pair in the distributive lattice of Schnyder woods of G. Let $\mathbf{x}$ and $\mathbf{x}'$ be the solutions of the systems $\mathcal{A}_S$ and $\mathcal{A}_{S'}$, respectively. Then, for each face f inside C, we have $x_f = x'_f = 0$ or $x_f x'_f < 0$ and, for each vertex v inside C, we have $x_v = x'_v = 0$ or $x_v x'_v < 0$.*

We will prove analogous results to Theorems 4.4 to 4.6 for similarly-aligned odd K-gon and parallel-sided even K-gon contact representations in Section 4.6.

4.1.2 Equations for square contact representations

Now let G be an inner triangulation of the 4-cycle v_N, v_E, v_S, v_W without separating 3-cycles. A *square contact representation* of G is a rectangle contact representation of G in which each inner vertex of G is represented by a square. We will describe a system $\mathcal{A}_T$ of linear equations, depending on a transversal structure T of G, which computes the sizes of the squares in a square contact representation of G that induces the transversal structure T if such a contact representation exists.

The *skeleton graph* of a rectangle contact representation is the plane graph whose vertices are the touching points of the line segments of the contact representation and whose edges are the connected components of the contact representation without the vertices. Note that the edges of the skeleton graph of a rectangle contact representation of G correspond to the inner edges of G, see Fig. 3.5 on Page 16.

The system $\mathcal{A}_T$ has a variable x_v for each inner vertex v of G and a variable x_e for each edge e of G that is not incident to the outer face. Each variable x_v represents

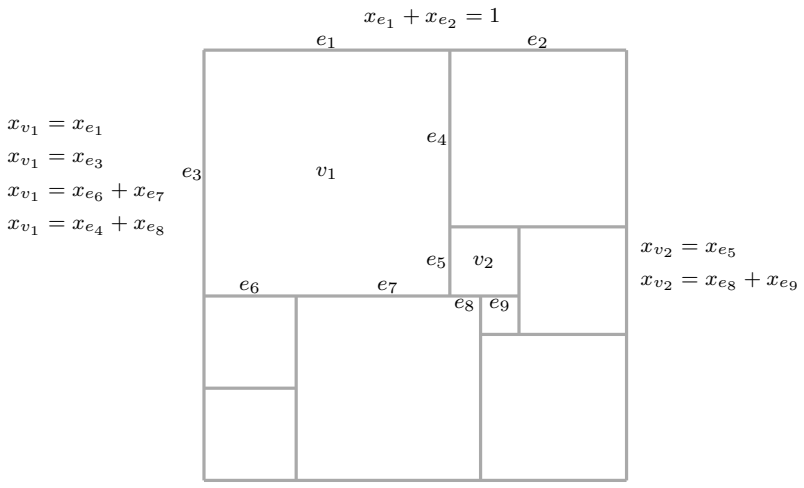

Figure 4.3: Examples for the different kinds of equations for the computation of square contact representations.

the side length of the square representing v and each variable x_e represents the length of the line segment of the contact representation corresponding to e.

Every inner vertex v of G induces four equations. Let $E_{\mathrm{r}}^{-}(v)$ be the set of incoming red, $E_{\mathrm{b}}^{-}(v)$ the set of incoming blue, $E_{\mathrm{r}}^{+}(v)$ be the set of outgoing red, and $E_{\mathrm{b}}^{+}(v)$ the set of outgoing blue edges of v in the transversal structure T. Then these four equations are

$$x_v = \sum_{e \in E_i^{\alpha}(v)} x_e \ , \quad i = \mathrm{r}, \mathrm{b}, \ \ \alpha = -, + \ .$$

The system $\mathcal{A}_T$ has one more equation that concerns the incident edges of the outer vertex v_N. This last equation is

$$\sum_{e \in E_{\mathrm{r}}^{-}(v_N)} x_e = 1 \ .$$

Figure 4.3 visualizes the different kinds of equations.

This system has been described in [Fel13] and then further studied in [Ruc11]. They show that the system is uniquely solvable.

Theorem 4.7 (Felsner [Fel13], Rucker [Ruc11])**.** *The system $\mathcal{A}_T$ is uniquely solvable.*

As in the case of equilateral triangle contact representations, it is clear that a square contact representation of G with induced transversal structure T induces a non-negative solution of $\mathcal{A}_T$. If the graph G has no separating 4-cycles or we allow squares to collapse to a single point in a square contact representation of G (see Fig. 4.4) and, if for four squares touching in a common point we count the contact of one pair of opposite squares but not of the other one, then also the converse holds. Again, this can be proved via a simple application of the theory that we develop in Section 4.2.

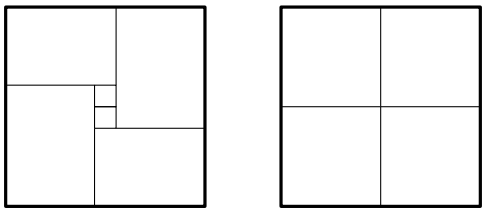

Figure 4.4: If the four squares corresponding to a separating 4-cycle of G touch in a common point, all squares corresponding to the vertices inside this 4-cycle are degenerate to a single point.

Theorem 4.8 (Felsner [Fel13], Rucker [Ruc11]). *The solution of $\mathcal{A}_T$ is non-negative if and only if G has a square contact representation inducing the transversal structure T.*

Also for the remaining results cited in Section 4.1.1, there are analogous results for square contact representation. The first one we want to mention says that, if the solution of $\mathcal{A}_T$ is not non-negative, it still induces a drawing which is no longer a contact representation of G.

Theorem 4.9 (Seibert [Sei15]). *If the solution of $\mathcal{A}_T$ has negative entries, it induces a dissection of a rectangle into squares, each representing an inner vertex of G, that is not a contact representation of G.*

To be able to state results about structural properties of the solution of $\mathcal{A}_T$, we want to recall the bijection between transversal structures and $\alpha_{4,1}$-orientations of the angular graph $\widetilde{G}$ of G mentioned in the end of Section 3.1.2. Note that the inner faces of $\widetilde{G}$ correspond to the edges of the skeleton graph of the wanted square contact representation, see Fig. 3.7 on Page 18. If f is an inner face of $\widetilde{G}$ and e the corresponding edge of the skeleton graph, we thus can set $x_f := x_e$.

Theorem 4.10 (Felsner [Fel13], Rucker [Ruc11]). *If the solution of $\mathcal{A}_T$ has negative entries, then the edges of $\widetilde{G}$ between faces f and f' with $x_f \geq 0$ and $x_{f'} < 0$ can be decomposed into cycles that are oriented cycles in the $\alpha_{4,1}$-orientation corresponding to T.*

Again, there is a similar result for the case of non-negative solutions.

Theorem 4.11 (Schrezenmaier [Sch16]). *If the solution of $\mathcal{A}_T$ is non-negative, the edges of $\widetilde{G}$ between faces f and f' with $x_f > 0$ and $x_{f'} = 0$ can be decomposed into essential cycles that are directed cycles in the $\alpha_{4,1}$-orientation corresponding to T.*

As for triangle contact representations, a flip of the transversal structure induces sign changes for all variables corresponding to vertices and edges inside the essential cycle that is reoriented.

Theorem 4.12 (Schrezenmaier [Sch16]). *Let T and T' be transversal structures of G that are related by a flip of an essential cycle C in the $\alpha_{4,1}$-orientations corresponding to T and T', i.e., T and T' are a covering pair in the distributive lattice of transversal structures of G. Let $\mathbf{x}$ and $\mathbf{x}'$ be the solutions of the systems $\mathcal{A}_T$ and $\mathcal{A}_{T'}$, respectively. Then, for each edge e of G corresponding to a face inside C, we have $x_e = x'_e = 0$ or $x_e x'_e < 0$ and, for each vertex v inside C, we have $x_v = x'_v = 0$ or $x_v x'_v < 0$.*

4.1.3 Parametrization of the equations

In the last two subsections we have seen systems of linear equations for the computation of two quite restricted classes of contact representations: contact representations with homothetic equilateral triangles and contact representations with axis-aligned, and thus also homothetic, squares. These systems of equations can be slightly modified to compute more general classes of contact representations with individually prescribed prototypes for each vertex of the given graph.

Rectangles. A natural way to generalize the problem of finding a square contact representation of a given graph is the problem of finding a rectangle contact representation of a given graph with a prescribed aspect ratio, i.e., the ratio of the height and the width of the rectangle, for each vertex. Then the problem of finding a square contact representation is the special case of prescribing an aspect ratio of 1 for each vertex.

In this more general setting, we can follow the same approach as described in Section 4.1.2. The only thing that changes is that in the equations some coefficients change from 1 to the aspect ratio that is assigned to a vertex. More precisely, let r_v be the aspect ratio assigned to the inner vertex v of G. If the variable x_v corresponds to the width of the rectangle corresponding to v, then the height of this rectangle is $r_v x_v$. Thus the four equations corresponding to this vertex are

$$x_v = \sum_{e \in E_{\mathrm{r}}^{\alpha}(v)} x_e \ , \quad \alpha = -, + \ ,$$
$$r_v x_v = \sum_{e \in E_{\mathrm{b}}^{\alpha}(v)} x_e \ , \quad \alpha = -, + \ .$$

This variant of the system of equations has been studied in [Sch16]. Most of the results listed in Section 4.1.2 have analogous results in this more general case. For more details on this, we refer to [Sch16].

Triangles. Asking for a contact representation with homothetic equilateral triangles is equivalent to asking for a contact representation with right, isosceles triangles

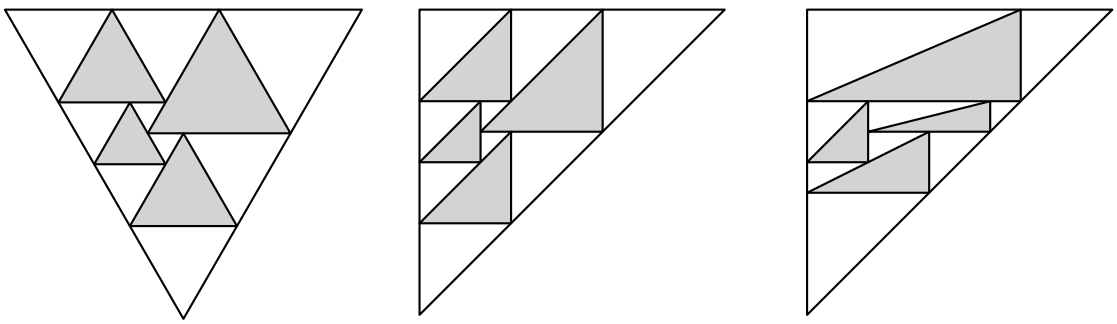

Figure 4.5: A contact representation with equilateral triangles, the equivalent contact representation with right, isosceles triangles, and a contact representation of the same graph with right triangles of different aspect ratios.

with a horizontal side at the bottom and a vertical side at the right. See Fig. 4.5 for an example. This point of view leads to a natural generalization of the problem of finding a homothetic triangle contact representation of a given graph. We can ask for a contact representation with right triangles with a horizontal side at the bottom and a vertical side at the right with an individually prescribed aspect ratio, i.e., the ratio of the vertical and the horizontal side of the triangle, for each vertex.

This variant has been studied in [Sch16; Sch17]. Again, we can follow the same approach as in the simpler variant that is described in Section 4.1.1 and only have to change some coefficients in the equations from 1 to an aspect ratio that is assigned to a vertex. Also in this case, there are analogous results for most of the results listed in Section 4.1.1. For a precise description of the system of equations and the corresponding results, we refer to [Sch16; Sch17].

4.2 Gluing polygons together

The following lemma shows that, if we are given a crossing-free drawing of each inner face of a plane graph and these face drawings fit together at their boundaries, these face drawings can be put together to a crossing-free drawing of the entire graph. This will enable us to obtain a contact representation from a solution of a system of linear equations that ensure that the scaling factors of the prototypes locally fit together. A similar method was used in [BS93] to obtain a primal-dual circle representation from circle radii which are locally fitting together. Our proof of this lemma first appeared in [FSS18b] and then in a slightly generalized version in [FR19].

Lemma 4.13. *Let H be a 2-connected plane graph. For every inner face f of H with incident vertices $v_0, \dots, v_{\deg(f)-1}$ in clockwise order, let P_f be a simple polygon in the plane with corners $p_{f,v_0}, \dots, p_{f,v_{\deg(f)-1}}$ in clockwise order and with interior angle $\beta_{f,v}$ at corner $p_{f,v}$ such that*

(i) for every inner vertex v of H with incident faces $f_0, \dots, f_{\deg(v)-1}$

$$\sum_{i=0}^{\deg(v)-1} \beta_{f_i,v} = 2\pi \ ,$$

(ii) for every outer vertex v of H with incident inner faces $f_0, \dots, f_{\deg(v)-2}$

$$\sum_{i=0}^{\deg(v)-2} \beta_{f_i,v} \leq \pi \ ,$$

(iii) for every inner edge vw of H with incident faces f_1, f_2

$$\|p_{f_1,v} - p_{f_1,w}\| = \|p_{f_2,v} - p_{f_2,w}\| \ .$$

Then there exists a crossing-free straight line drawing of H in which the drawing of every inner face f can be obtained from P_f by translation and rotation.

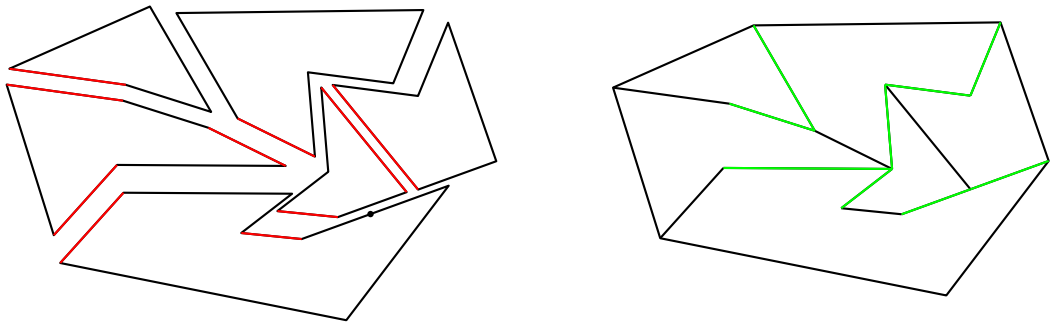

(a) The given face polygons P_f with selected pairs of sides in red that correspond to a spanning tree S of H^*.

(b) The result of gluing the polygons together along the edges of S with the forest $\overline{S}$ marked in green.

Figure 4.6: Obtaining a drawing of a plane graph from the drawings of its faces.

Proof. Let H^* be the dual graph of H without the vertex corresponding to the outer face of H. Further, let S be a spanning tree of H^*. Then we can glue together the polygons P_f of all inner faces f of H along the edges of S. After fixing the position of one of the polygons, this determines a well-defined position for every polygon, see Fig. 4.6. From now on, we denote by $p_{f,v}$ the position of the corner of P_f corresponding to v in this embedding.

For the edges vw of S (considered as a subset of the edges of H), we already know that $p_{f_1,v} = p_{f_2,v}$ and $p_{f_1,w} = p_{f_2,w}$ where f_1, f_2 are the two incident faces of vw (we say that at the edge vw the polygons are *touching in the right way*). For the edges of the complement $\overline{S}$ of S, we need to show this. Note that $\overline{S}$ is a forest in H. Further, each connected component of this forest is incident to at most one outer vertex of H since otherwise the respective component would separate H^*, in contradiction to the connectedness of S. Let v be a leaf of this forest that is an inner vertex of H and let e be the edge of $\overline{S}$ incident to v. Then, for all incident edges $e' \neq e$ of v, we already know that the polygons are touching in the right way at e'. But then also at e the polygons are touching in the right way because condition (i) is fulfilled for v. Since the set of edges we still need to check always remains a forest with each component incident to at most one outer vertex, we can iterate this process until all inner edges of H are checked. Therefore, the positioning of the polygons P_f as defined above determines a well-defined position for the vertices of H. We denote the coordinates of the position p_v of the vertex v by (x_v, y_v).

Claim 1. *The drawing of the outer face of H is a simple polygon.*

Proof. See Fig. 4.7 for two examples of self-intersections of the outer face that we have to exclude. Let k be the number of outer vertices of H and let γ be the sum of the inner angles at the outer vertices. Then we obtain by double counting the sum of all inner angles

$$\sum_{f \text{ inner face of } H} (\deg(f) - 2)\pi = \gamma + \sum_{v \text{ inner vertex of } H} 2\pi$$

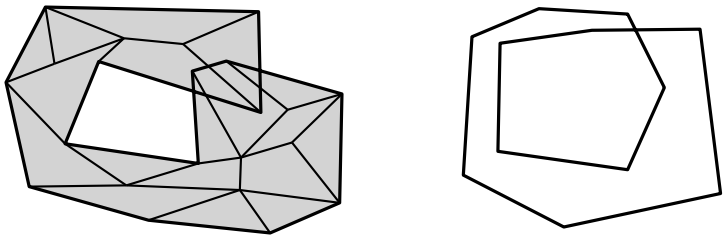

Figure 4.7: Two scenarios of a self-intersecting drawing of the outer face that cannot happen if all conditions of Lemma 4.13 are fulfilled.

and therefore, using Euler's formula,

$$\gamma = (2|E| - k)\pi - 2(|F| - 1)\pi - (|V| - k)2\pi = (k - 2)\pi \ .$$

Together with condition (ii) this implies that the drawing of the outer face is a convex simple polygon. △

Claim 2. *The drawing is crossing-free.*

Proof. Due to Claim 1 the outer face is drawn as a simple polygon. We denote this polygon by P_{f_o}. Since, for each inner face f, each side of the polygon P_f is contained in the boundary of the polygon P_{f_o} or in the boundary of the polygon $P_{f'}$ for some inner face $f' \neq f$, the polygon P_{f_o} is completely covered by the polygons P_f of the inner faces f of H. To prove that the drawing is crossing-free, we need to show that no two polygons P_{f_1} and P_{f_2}, where f_1 and f_2 are inner faces, are overlapping. We will do this by showing that the area of P_{f_o} is equal to the sum of the areas of the polygons P_f of all inner faces f of H. For an inner face f with incident vertices $v_0, \dots, v_{l-1}$ in clockwise order, the area of P_f is

$$\operatorname{area}(P_f) = \frac{1}{2} \sum_{i=0}^{l-1} \left(x_{v_{i+1}} y_{v_i} - x_{v_i} y_{v_{i+1}} \right)$$

where indices are to be understood modulo l. For each inner edge vw of H, there is exactly one inner face of H that has the directed edge (v, w) in its clockwise traversal and there is exactly one inner face that has (w, v) in its clockwise traversal. For each edge (v, w) in the clockwise traversal of the outer face, there is exactly one inner face that has (v, w) in its clockwise traversal and there is no inner face that has (w, v) in its clockwise traversal. Let $w_0, \dots, w_{k-1}$ be the vertices of the outer face in clockwise order. Then

$$\operatorname{area}(P_{f_o}) = \frac{1}{2} \sum_{i=0}^{k-1} \left(x_{w_{i+1}} y_{w_i} - x_{w_i} y_{w_{i+1}} \right) = \sum_{f \text{ inner face of } H} \operatorname{area}(P_f)$$

since all other summands in the latter sum cancel out. △

By Claim 2 the drawing we constructed is crossing free. Because of the construction of the drawing, it is a drawing of H and the drawing of each inner face f is obtained from P_f by translation and rotation. This completes the proof. □

In [FR19] the authors give another beautiful, geometric proof of this lemma that is by induction on the number of inner vertices of H. In this proof, first, all polygons are triangulated. Then, in the induction step, all triangles incident to a fixed inner vertex are glued together to a singe polygon which is then retriangulated (without the inner vertex) which reduces the number of inner vertices by one.

Note that, if we replace condition (iii) in Lemma 4.13 by the stronger condition

(iii*) for every inner edge vw of H with incident faces f_1, f_2

$$p_{f_1,v} - p_{f_1,w} = p_{f_2,v} - p_{f_2,w} \ ,$$

then we obtain a crossing-free straight line drawing of H in which the drawing of every inner face f can be obtained from P_f only by translation (and no rotation).

Allowing degenerate face polygons. Let us now study the case that we require the face polygons P_f only to be weakly simple instead of simple. Then we can again obtain a drawing of H where each face is drawn as the prescribed polygon. The following lemma shows which properties are still fulfilled by this drawing in this weaker setting.

Lemma 4.14. *If the conditions of Lemma 4.13 are fulfilled with the exception that the polygons P_f only have to be weakly simple, then there exists a straight line drawing of H in which the drawings of the edges do not cross, i.e., their intersection is not exactly one point that is in the relative interiors of the drawings of both edges, the drawing of the outer face is a weakly simple convex polygon P_{f_0}, the drawing of the entire graph H is inside P_{f_o}, and the drawing of every inner face f can be obtained from P_f by translation and rotation.*

Proof. The vertex positions in the drawing can be defined exactly as in the proof of Lemma 4.13.

Let C be a simple cycle in H. Then the drawing of C is a polygon P_C that might not be weakly simple. Nevertheless, at a corner p_v of P_C, we can distinguish between the inner and outer angle of P_C at p_v by saying that the inner angle corresponds to the polygons P_f of the incident faces f of v that are inside of C in H. With this notion we can generalize the statement of Claim 1 in the proof of Lemma 4.13.

Claim 1. *Let C be a simple cycle of length ℓ in H. Then the sum of the inner angles of P_C is $(\ell - 2)\pi$.*

Proof. The proof is analogous to the proof of Claim 1 in the proof of Lemma 4.13. △

From Claim 1 it follows as in the proof of Lemma 4.13 that the drawing of the outer face is a weakly simple convex polygon P_{f_o}. That P_{f_o} is completely covered by the polygons P_f of the inner faces f of H, is not as obvious as it was in Lemma 4.13.

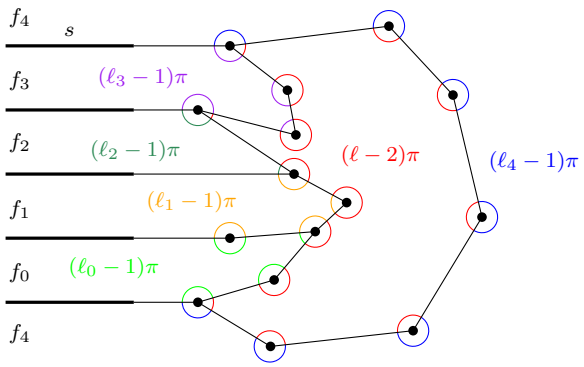

Figure 4.8: The constellation of the proof of Claim 2 in the proof of Lemma 4.14. A cycle $C^* = f_0, \ldots, f_4$ in H^* such that all edges of C^* go through an edge of H which is drawn parallel to s (in the proof of Claim 2 all these drawings contain s, but that does not make any difference for the inner angle sums). The shown value for the sum of the inner angles of the part of P_{f_4} that is inside C^* is not the correct value for the actual drawing but the value that is assumed in the proof of Claim 2. Moreover, here in the figure all polygons are simple, but again it does not make any difference for the angle sums if they are only weakly simple.

Claim 2. *The polygon P_{f_o} is completely covered by the polygons P_f of the inner faces f of H.*

Proof. Suppose that a subpolygon P_{free} of P_{f_o} is not covered. Let s be a subsegment of a side of P_{free} such that, for every inner face f of H, the segment s is either entirely contained in the boundary of P_f, or the intersection of s and the boundary of P_f is a single point, or s and the boundary of P_f are disjoint. Then, because of the construction of the drawing, there has to be a cycle $C^* = f_0, \ldots, f_{r-1}$ in H^* that is only crossing edges of H whose drawings contain the segment s and that is entering and leaving each face f_i through edges whose drawings are antiparallel sides of P_{f_i}. We assume that C^* is oriented clockwise. The other case is symmetric. See Fig. 4.8 for an illustration of this situation. For each face f_i, $i = 0, \ldots, r-1$, the cycle C^* divides the incident vertices of f_i into a part inside C^* and a part outside C^*. Let $v_0^{(i)}, \ldots, v_{\ell_i-1}^{(i)}$ be the counterclockwise traversal of the part inside C^*. The sum of the inner angles of P_{f_i} at the corners $p_{v_j^{(i)}}$, $j = 0, \ldots, \ell_i - 1$, is $(\ell_i - 1)\pi$ since P_{f_i} is a weakly simple polygon and P_{f_i} is entered and left through antiparallel sides by C^*. Further, the sum of the inner angles of the polygonal drawing of the cycle $v_0^{(0)}, \ldots, v_{\ell_0-1}^{(0)} = v_0^{(1)}, \ldots, v_{\ell_1-1}^{(1)} = v_0^{(2)}, \ldots, v_{\ell_{r-1}-1}^{(r-1)} = v_0^{(0)}$ of length $\ell := \sum_{i=0}^{r-1}(\ell_i - 1)$ is $(\ell-2)\pi$ by Claim 1. Then we have

$$\ell \cdot 2\pi = (\ell-2)\pi + \sum_{i=0}^{r-1}(\ell_i - 1)\pi = (\ell-1)2\pi \ .$$

Hence, the assumption that P_{f_o} is not completely covered is false. △

Now we can easily conclude that the entire drawing is inside P_{f_o}.

Claim 3. *The entire drawing of H is inside P_{f_o}.*

Proof. Suppose that a part of the drawing is outside P_{f_o}. Then there is a vertex v of H whose drawing p_v is outside P_{f_o} since P_{f_o} is convex. But then there is an incident face f of v with $\text{area}(P_f \cap P_{f_o}) < \text{area}(P_f)$, i.e., a part of P_f with positive area is outside P_{f_o}. This is a contradiction to Claim 2 and the fact that $\text{area}(P_{f_o}) = \sum_{f \text{ inner face of } H} \text{area}(P_f)$ which can be shown as in the proof of Lemma 4.13. △

It remains to show that the drawings of the edges of H do not cross. Due to Claim 3 the drawings of the edges of the outer face do not cross the drawings of any edge of H. Since, due to Claim 2, there are no holes between the drawings of the inner faces of H, a crossing of the drawings of two inner edges of H would imply the drawings of two inner faces to overlap such that their intersection has positive area, in contradiction to $\text{area}(P_{f_o}) = \sum_{f \text{ inner face of } H} \text{area}(P_f)$, or would imply the drawing of an inner face to overlap itself, in contradiction to the condition that the given face drawings are weakly simple polygons. Hence, also this statement of the lemma is fulfilled. □

Note that also in Lemma 4.14 condition (iii) can be replaced by the stronger condition (iii*), resulting in a drawing in which the drawing of each inner face f can be obtained from P_f only by translation.

4.3 Handling pseudotriangles

The main ingredient that is still missing, if we want to find systems of linear equations for the computation of similarly-aligned odd K-gon contact representations and parallel-sided even K-gon contact representations that are similar to those of Section 4.1, is a way to handle the pseudotriangles that occur in these contact representations between the convex polygons. Therefore, in this section, we will construct a system of linear equations that ensures some variables to be the side lengths of a pseudotriangle with given slopes of the sides.

Remember that by the slope of a side of a polygon we mean the direction vector of this side in clockwise direction around the polygon. We denote the angle on the right side between a side of slope s and a side of slope s' by $\alpha_r(s, s')$. We say that $s_0, \ldots, s_{n-1}$ is a *slope sequence of a pseudotriangle* if the following two properties are fulfilled (here and in the rest of this section, index arithmetic is done modulo n):

- **i)** there are indices $A < B < C$ such that the angle $\alpha_i := \alpha_r(s_i, s_{i+1})$ is in the range $0 \leq \alpha_i \leq \pi$, if $i \in \{A, B, C\}$, and in the range $\pi \leq \alpha_i \leq 2\pi$ if $i \notin \{A, B, C\}$,
- **ii)** these angles fulfill $\sum_{i=0}^{n-1} \alpha_i = (n-2)\pi$.

It is clear that the sequence $s_0, \ldots, s_{n-1}$ fulfills these properties if it is the sequence of slopes of a pseudotriangle in clockwise order. In this section, we will always assume that $s_0, \ldots, s_{n-1}$ is a slope sequence of a pseudotriangle. If P is a polygon whose sequence of slopes in clockwise order is $s_0, \ldots, s_{n-1}$, we say that P *realizes* $s_0, \ldots, s_{n-1}$. Note that a polygon realizing a slope sequence of a pseudotriangle is a pseudotriangle.

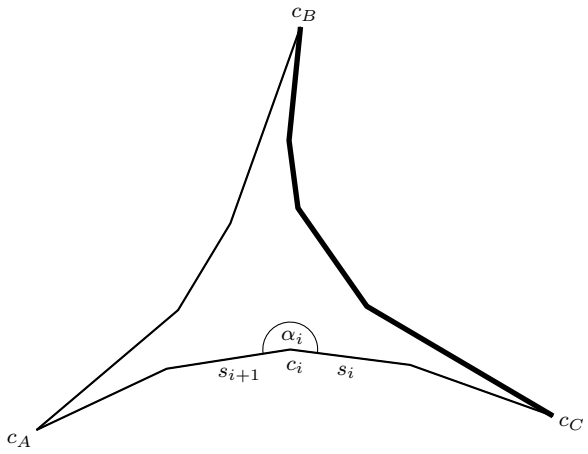

Figure 4.9: A pseudotriangle with one of its three concave arcs highlighted.

Let P be a polygon realizing $s_0, \ldots, s_{n-1}$. If we denote the corner of P between the sides of slopes s_i and s_{i+1} by c_i, then c_A, c_B, c_C are the three convex corners of P in clockwise order. For $(i, j) \in \{(A, B), (B, C), (C, A + n)\}$ we call the union of the sides of slopes $s_{i+1}, \ldots, s_j$ a *concave arc* of P. See Fig. 4.9 for an example.

The following lemmas show modifications that can be applied to a slope sequence of a pseudotriangle such that it remains a slope sequence of a pseudotriangle.

Lemma 4.15. *If $s_0, \ldots, s_{n-1}$ is a slope sequence of a pseudotriangle, then also $-s_0, \ldots, -s_{n-1}$ is a slope sequence of a pseudotriangle.*

Proof. This immediately follows from the fact that $\alpha_r(s, s') = \alpha_r(-s, -s')$ for arbitrary slopes s and s'. □

Lemma 4.16. *If $s_0, \ldots, s_{n-1}$ is a slope sequence of a pseudotriangle and s_i is not the only slope of its concave arc, i.e., not both $i - 1, i \in \{A, B, C\}$, then also $s_0, \ldots, s_{i-1}, s_{i+1}, \ldots, s_{n-1}$ is a slope sequence of a pseudotriangle.*

Proof. We have $\alpha_r(s_{i-1}, s_{i+1}) = \alpha_r(s_{i-1}, s_i) + \alpha_r(s_i, s_{i+1}) - \pi$. Therefore,

$$\alpha_r(s_{i-1}, s_{i+1}) + \sum_{j=i+1}^{i-2+n} \alpha_r(s_j, s_{j+1}) = \sum_{j=0}^{n-1} \alpha_r(s_j, s_{j+1}) - \pi = (n-3)\pi \ .$$

Now we distinguish two cases.

- **i)** If s_i is the first or the last slope of its concave arc, i.e., one of $i-1, i \in \{A, B, C\}$, then $\sum_{j=i+1}^{i-2+n} \geq (n-4)\pi$ and thus $\alpha_r(s_{i-1}, s_{i+1}) \leq \pi$. Further, since s_i is not the only slope of its concave arc, we also have $\alpha_r(s_{i-1}, s_i) \geq \pi$ or $\alpha_r(s_i, s_{i+1}) \geq \pi$ and, therefore, $\alpha_r(s_{i-1}, s_{i+1}) \geq 0$.
- **ii)** If s_i is not the first or the last slope of its concave arc, i.e., $i - 1, i \notin \{A, B, C\}$, then $\sum_{j=i+1}^{i-2+n} \geq (n-3)\pi$ and thus $\alpha_r(s_{i-1}, s_{i+1}) \leq 2\pi$. Further, we then have $\alpha_r(s_{i-1}, s_i) \geq \pi$ and $\alpha_r(s_i, s_{i+1}) \geq \pi$ and, therefore, $\alpha_r(s_{i-1}, s_{i+1}) \geq \pi$.

Therefore, in both cases $s_0, \ldots, s_{i-1}, s_{i+1}, \ldots, s_{n-1}$ is a slope sequence of a pseudotriangle. □

Lemma 4.17. *Let $s_0, \dots, s_{n-1}$ be a slope sequence of a pseudotriangle. If s_i is the first but not the only slope of its concave arc, i.e., $i-1 \in \{A,B,C\}$ and $i \notin \{A,B,C\}$, or s_i is the last but not the only slope of its concave arc, i.e., $i \in \{A,B,C\}$ and $i-1 \notin \{A,B,C\}$, then also $s_0, \dots, s_{i-1}, -s_i, s_{i+1}, \dots, s_{n-1}$ is a slope sequence of a pseudotriangle.*

Proof. We assume that s_i is the first slope of its concave arc. The other case is analogous. Then $0 \le \alpha_{\mathrm{r}}(s_{i-1}, s_i) \le \pi$ and $\pi \le \alpha_{\mathrm{r}}(s_i, s_{i+1}) \le 2\pi$. Since $\alpha_{\mathrm{r}}(s_{i-1}, -s_i) = \pi + \alpha_{\mathrm{r}}(s_{i-1}, s_i)$, we thus have $\pi \le \alpha_{\mathrm{r}}(s_{i-1}, -s_i) \le 2\pi$. Further, since $\alpha_{\mathrm{r}}(-s_i, s_{i+1}) = \alpha_{\mathrm{r}}(s_i, s_{i+1}) - \pi$, we also have $0 \le \alpha_{\mathrm{r}}(-s_i, s_{i+1}) \le \pi$. Finally, $\alpha_{\mathrm{r}}(s_{i-1}, -s_i) + \alpha_{\mathrm{r}}(-s_i, s_{i+1}) = \alpha_{\mathrm{r}}(s_{i-1}, s_i) + \alpha_{\mathrm{r}}(s_i, s_{i+1})$ implies that, if we set $s'_i := -s_i$ and $s'_j := s_j$ for $j \in \{0, \dots, n-1\} \setminus \{i\}$, we have $\sum_{j=0}^{n-1} \alpha_{\mathrm{r}}(s'_j, s'_{j+1}) = \sum_{j=0}^{n-1} \alpha_{\mathrm{r}}(s_j, s_{j+1}) = (n-2)\pi$ whence $s'_0, \dots, s'_{n-1}$ is a slope sequence of a pseudotriangle. □

Cutting a pseudotriangle into triangles. The system of linear equations will be based on a tiling of the pseudotriangle into triangles. If we are given an actual pseudotriangle P realizing the given sequence $s_0, \dots, s_{n-1}$ of slopes, we can extend one of the sides ending at a concave corner p of P into the interior of P until it hits the boundary of P in a point p'. Let us assume that p' is not a corner of P. This divides P into two pseudotriangles whose total number of concave corners is one less than the number of concave corners of P. Then we can continue this process recursively in the two subpseudotriangles until we end up with a tiling of P into triangles. See Fig. 4.10 (first row).

Since we are only given the sequence $s_0, \dots, s_{n-1}$ of slopes of the pseudotriangle, we will construct such a tiling in a more abstract way. We start with an arrangement P of oriented pseudosegments $l_0, \dots, l_{n-1}$ which together form the clockwise traversal

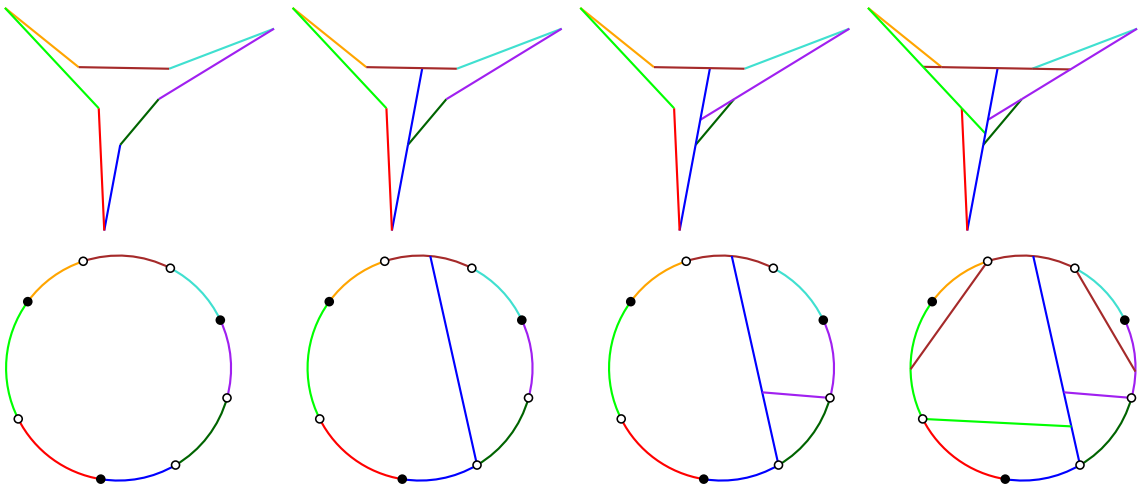

Figure 4.10: Construction of a tiling of a pseudotriangle into triangles. In the first row the construction is shown for the case that we are given an actual pseudotriangle. In the second row it is shown for the case that we are only given the order of convex (black vertices) and concave (white vertices) corners of the pseudotriangle.

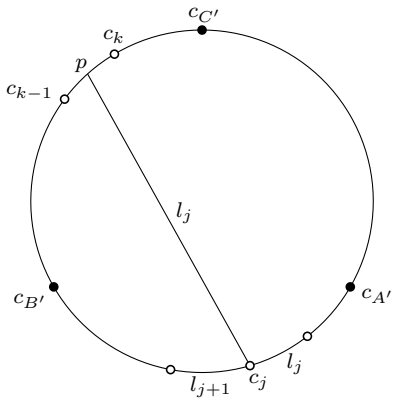

(a) The pseudotriangle P that is cut. The pseudosegment l_j is extended through the interior of P to a point p on the pseudosegment l_k between the corners c_{k-1} and c_k.

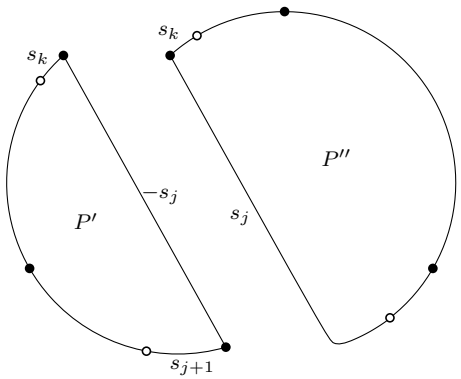

(b) The two pseudotriangles P' and P'' the pseudotriangle P is cut into. Some of the slopes corresponding to the clockwise traversals of P' and P'' are shown where s_i is the slope connected to the pseudosegment l_i.

Figure 4.11: A step in the cutting process of an abstract pseudotriangle. The convex corners of the pseudotriangles are marked as black disks and some of their concave corners are marked as white disks.

of a simple n-gon, i.e., a set of interiorly disjoint curves in the plane without self-intersections such that the endpoint of l_i is the start point of l_{i+1} for all i and the region bounded by $\cup_{i=0}^{n-1} l_i$ is to the right side of each of the l_i. Another way to think of this initial configuration is a closed curve without self-intersections that is divided into n parts. The intersection point of the pseudosegments l_i and l_{i+1} is denoted by c_i. The pseudosegment l_i is supposed to correspond to the side of slope s_i. Since $s_0, \dots, s_{n-1}$ is a slope sequence of a pseudotriangle, this correspondence declares exactly three corners c_A, c_B, c_C as convex corners. Now we choose a concave corner c_j with $j \notin \{A, B, C\}$ and a point p to connect it to. This point p has to be contained in exactly one of the pseudosegments, denoted by l_k, and has to be part of one of the two concave arcs of P not containing c_j. Let $c_{A'}$ and $c_{B'}$ be the convex corners we reach first if we start at c_j and go in counterclockwise and clockwise direction, respectively. Let $c_{C'} \neq c_{A'}, c_{B'}$ be the third convex corner of P. If l_k is part of the concave arc between $p_{A'}$ and $p_{C'}$, we extend the pseudosegment l_{j+1} from c_j through the interior of P to the point p without intersecting any other pseudosegments. If l_k is part of the concave arc between $p_{B'}$ and $p_{C'}$, we extend l_j in the same way. Assume that the latter is the case (the other case is symmetric). Figure 4.11a shows a visualization of this situation. The extension of the pseudosegment l_j divides P into two smaller parts: a part P' which is bounded by connected parts of the pseudosegments $l_{j+1}, \dots, l_k, \overline{l_j}$ in clockwise order, where $\overline{l_j}$ denotes the reverted pseudosegment l_j, and a part P'' which is bounded by connected parts of the pseudosegments $l_k, \dots, l_j$ in clockwise order, see Fig. 4.11b. Now we iterate this procedure in the parts P' and P''. Repeated application of Lemmas 4.16 and 4.17 shows that $s_{j+1}, \dots, s_k, -s_j$ and $s_k, \dots, s_j$ are slope sequences of a pseudotriangle and thus the iteration in P' and P'' is well-defined.

Since in each iteration the total number of concave corners is decreased by one, the procedure terminates with an abstract tiling of a pseudotriangle with slopes $s_0, \dots, s_{n-1}$ into triangles. The *skeleton graph* G_{skel} of this tiling is the plane graph whose vertices are the intersection points of the pseudosegments and whose edges are the connected components of the union of all pseudosegments without the intersection points.

The system of equations. Let x_i be the length of the side of slope s_i in a pseudotriangle with slope sequence $s_0, \dots, s_{n-1}$. Then these length variables fulfill the equation

$$\sum_{i=0}^{n-1} x_i s_i = 0 \tag{4.1}$$

since the boundary of the pseudotriangle is a closed curve. The following lemma shows that also the converse is true.

Lemma 4.18. *Let s_i, $i = 0, \dots, n-1$, be a slope sequence of a pseudotriangle. Then, if x_i, $i = 0, \dots, n-1$, is a non-negative solution of (4.1), there exists a pseudotriangle with sides of slopes s_i and lengths x_i, $i = 0, \dots, n-1$, in clockwise order.*

Proof. It is clear that there is a unique polygon P with sides of slopes s_i and lengths x_i, $i = 0, \dots, n-1$, in this cyclic order. We have to show that P is weakly simple, i.e., that P has no proper self-intersections.

Claim 1. *Two sides of the same concave arc of P have no proper intersection.*

Proof. Let $s_{A'+1}, s_{A'+2}, \dots, s_{B'}$ be the slopes of a concave arc of P. We set $\alpha'_i := \alpha_i - \pi$ for $i = A'+1, \dots, B'-1$. If $\sum_{i=A'+1}^{B'-1} \alpha'_i \le \pi$, then, for $i = A'+1, \dots, B'-1$, all corners $c_{i+1}, \dots, c_{B'}$ are on the left of the side of slope s_i and, hence, the concave arc has no proper self-intersections. If $\sum_{i=A'+1}^{B'-1} \alpha'_i > \pi$, then $\sum_{i=0}^{n-1} \alpha_i > (n-3)\pi + \pi = (n-2)\pi$ since P has only three convex corners. This is a contradiction to the condition that $s_0, \dots, s_{n-1}$ is a slope sequence of a pseudotriangle. △

Claim 2. *Two sides of two consecutive concave arcs of P have no proper intersection.*

Proof. In the situation of the proof of Claim 1, we now also take the angle $\alpha_{A'}$ into consideration. Assume that $\alpha_{A'} + \sum_{i=A'+1}^{B'-1} \alpha'_i \le \pi$. Then all corners $c_{A'+1}, \dots, c_{B'}$ are on the left of the side $c'_A c_{A'-1}$ (of slope $-s_{A'}$) of P. Due to Claim 1, all corners $c_{C'+1}, \dots, c_{A'-1}$ are on the right of the side $c_{A'} c_{A'-1}$. Hence, in this case there are no proper intersections of the concave arcs $c_{C'}, \dots, c_{A'}$ and $c_{A'}, \dots, c_{B'}$. If $\alpha_{A'} + \sum_{i=A'+1}^{B'-1} \alpha'_i > \pi$, we obtain a contradiction to the condition that $s_0, \dots, s_{n-1}$ is a slope sequence of a pseudotriangle, as in the proof of Claim 1. △

Since any two sides of P are either on the same or on consecutive concave arcs of P, Claims 1 and 2 imply that P has no proper self-intersections. □

Finally, we want to show that each slope sequence of a pseudotriangle is indeed the sequence of slopes of pseudotriangle with positive side lengths.

Lemma 4.19. *Let $s_0, \dots, s_{n-1}$ be a slope sequence of a pseudotriangle. Then there are $x_i > 0$, $i = 0, \dots, n-1$, with $\sum_{i=0}^{n-1} x_i s_i = 0$.*

Proof. We start with the solution $x_i = 0$ for $i = 0, \dots, n-1$ that fulfills the equation $\sum_{i=0}^{n-1} x_i s_i = 0$ but not $x_i > 0$ for $i = 0, \dots, n-1$. Now we will increase the values of the x_i in an iterative process, maintaining the invariant that $\sum_{i=0}^{n-1} x_i s_i = 0$.

Due to Lemma 4.16, if $s_{i_0}, s_{i_1}, s_{i_2}$ are slopes from the three different concave arcs, then they form a slope sequence of a pseudotriangle. Therefore, there exists a triangle T whose sides have these slopes. Let $\tilde{x}_{i_0}, \tilde{x}_{i_1}, \tilde{x}_{i_2} > 0$ be the lengths of the sides of T with slopes $s_{i_0}, s_{i_1}, s_{i_2}$, respectively. Then $\tilde{x}_{i_0} s_{i_0} + \tilde{x}_{i_1} s_{i_1} + \tilde{x}_{i_2} s_{i_2} = 0$ and we can increase $x_{i_0}, x_{i_1}, x_{i_2}$ by $\tilde{x}_{i_0}, \tilde{x}_{i_1}, \tilde{x}_{i_2}$, respectively. By repeating this for different triplets i_0, i_1, i_2 such that every $i \in \{0, \dots, n-1\}$ is contained in at least one of them, we finally obtain a solution of $\sum_{i=0}^{n-1} x_i s_i = 0$ with $x_i > 0$ for all $i = 0, \dots, n-1$. □

Now we will formulate another system of linear equations that is based on a tiling of the pseudotriangle into triangles and that turns out to be equivalent to (4.1). The idea is the following: For a triangle with given slopes we know the ratio of its three side lengths. Therefore, one variable per subtriangle determines all three side lengths of this subtriangle. Then the purpose of the equations is to make the side lengths of all these subtriangles fit together.

Let P be an abstract pseudotriangle with slope sequence $s_0, \dots, s_{n-1}$ with a fixed abstract tiling into triangles. Let T be a subtriangle of this tiling and let r_0, r_1, r_2 be the slopes assigned to its sides in clockwise order. Since r_0, r_1, r_2 is a slope sequence of a pseudotriangle, there exists a geometric triangle T' with slopes r_0, r_1, r_2 in clockwise order. For $i = 0, 1, 2$, we denote by $\ell_i > 0$ the length of the side of T' of slope r_i. Note that triangles whose sides have the same slopes are homothetic. If also the clockwise order of the slopes is the same, they are positive homothetic. Thus we can obtain T' from T by scaling it with a unique factor $y_T > 0$ and translating it. For each edge e of the skeleton graph of the given tiling, let z_e be a variable representing the length of this edge. For $i = 0, 1, 2$, let E_i be the set of edges of the skeleton graph the side of T with slope s_i is divided into. Then $y_T \ell_i = \sum_{e \in E_i} z_e$. If we denote $-y_T$ by $\overline{y_T}$, we obtain the equations

$$\ell_i(T)\overline{y_T} + \sum_{e \in E_i(T)} z_e = 0 \ , \quad T \text{ subtriangle}, \ i \in \{0, 1, 2\} \ . \tag{4.2}$$

It remains to express the variables x_j in terms of the z_e. For the pseudosegment corresponding to the slope s_j, let E_j be the set of edges of the outer face of the skeleton graph that are part of this pseudosegment. Then $x_j = \sum_{e \in E_j} z_e$. If we denote $-x_j$ by $\overline{x_j}$, we obtain the equations

$$x_j + \overline{x_j} = 0 \ , \quad j \in \{0, \dots, n-1\} \ , \tag{4.3}$$

$$\overline{x_j} + \sum_{e \in E_j} z_e = 0 \ , \quad j \in \{0, \dots, n-1\} \ . \tag{4.4}$$

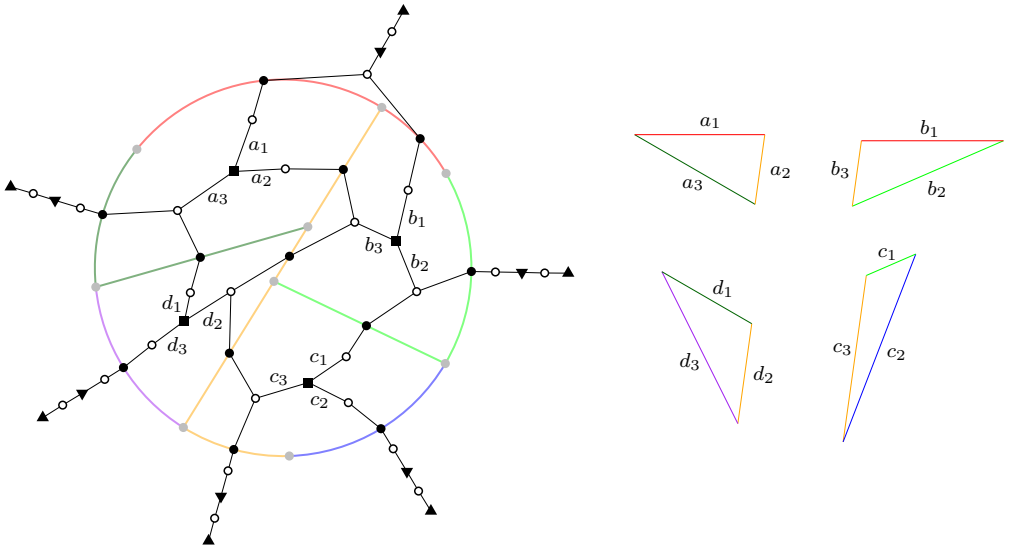

Figure 4.12: The incidence graph of the system of equations for a tiled pseudotriangle. Black vertices are variables-vertices, white vertices are equation-vertices. Black squares correspond to variables of the type $\overline{y_T}$, black circles correspond to variables of the type z_e, black triangles pointing up correspond to variables of the type x_j, and black triangles pointing down correspond to variables of the type $\overline{x_j}$. The labels of the edges are the coefficients of the variables in the equations. The coefficients of the unlabeled edges are 1.

The variable-equation incidence graph of the system of linear equations (4.2)–(4.4) has the following canonical crossing-free drawing (see Fig. 4.12): We start with a crossing-free drawing of the plane graph G_{skel}. The variable-vertices corresponding to the variables z_e are placed on the corresponding edge e of G_{skel}. In each inner face f of G_{skel} we place a star with three leaves. Let T be the subtriangle the face f corresponds to. Then the central vertex of the star is the variable-vertex corresponding to $\overline{y_T}$ and the three leaves of the star are in clockwise order the equation-vertices corresponding to the equations $\ell_i(T)\overline{y_T} + \sum_{e\in E_i(T)} z_e = 0$ for $i = 0, 1, 2$. Note that the remaining adjacent variable-vertices of these three equation-vertices are on the boundary of the face f and can be connected to them inside this face without producing crossings since we have chosen the clockwise order of the three equation-vertices appropriately. Further, we place the equation-vertices corresponding to the equations $\overline{x_j} + \sum_{e\in E_j} z_e = 0$ for $j = 0, \dots, n-1$ in the outer face of G_{skel} and connect them to their adjacent vertices on the edges of the outer face of G_{skel} without producing crossings. We do this in such a way that afterwards all these equation-vertices are incident to the outer face of the drawing of the incidence graph. Finally, we attach a path of length three to each of these equation-vertices in the outer face of the incidence graph. The three vertices of this path are a variable-vertex corresponding to a variable $\overline{x_j}$, an equation-vertex corresponding to an equation $x_j + \overline{x_j} = 0$, and a variable-vertex corresponding to a variable x_j. The following lemma collects some properties of this drawing.

Lemma 4.20. *The variable-equation incidence graph of the system of equations (4.2)–(4.4) has a crossing-free drawing such that the following four properties hold:*

(i) All inner faces are simple cycles of length 10.

(ii) Each of the variable-vertices $x_0, \dots, x_{n-1}$ appears exactly once in the clockwise traversal of the outer face and they appear in this order.

(iii) The walk on the outer face from x_i to x_{i+1} is a simple path of length 14 if s_i and s_{i+1} are the slopes of sides of the same concave arc of P.

(iv) The walk on the outer face from x_i to x_{i+1} is a simple path of length 12 if s_i and s_{i+1} are the slopes of sides of different concave arcs of P.

Proof. Let H be the variable-equation incidence graph of the system of equations (4.2)–(4.4) with its canonical embedding. That the variable-vertices $x_0, \dots, x_{n-1}$ appear exactly once in the traversal of the outer face of H immediately follows from the construction of the drawing. That they appear in the correct order, follows from the correct order of the pseudosegments on the outer face of G_{skel}.

Note that each vertex v of G_{skel} either corresponds to an inner face of H or to a walk on the outer face of H between two vertices x_i and x_{i+1}. Each vertex v of G_{skel} is the endpoint of either one or two peudosegments. If it is the endpoint of only one pseudosegment and the incident edge of v corresponding to this pseudosegment is not part of the outer face of G_{skel}, then v corresponds to an inner face of H. If v is the endpoint of only one pseudosegment and the incident edge of v corresponding to this pseudosegment is part of the outer face of G_{skel}, then v corresponds to a walk on the outer face of H between two vertices x_i and x_{i+1} such that s_i and s_{i+1} are the slopes of sides of the same concave arc of P. And if v is the endpoint of two pseudosegments, then it corresponds to a walk on the outer face of H between two vertices x_i and x_{i+1} such that s_i and s_{i+1} are the slopes of sides of different concave arcs of P. With these observations the counts given in the statement of the lemma can easily be verified. □

In the following we will show that equation (4.1) is equivalent to the system of equations (4.2)–(4.4).

Lemma 4.21. *Each solution of the equations (4.2)–(4.4) fulfills the equation (4.1). Each solution of (4.1) can be extended to a solution of (4.2)–(4.4).*

Proof. We will prove both directions by induction on the number of triangles the pseudotriangle is decomposed into.

If there is only one triangle, both directions are clear. So let us assume that the pseudotriangle P is decomposed into at least two triangles. We will use the same notations for the first cut of P as earlier in this section when we described the cutting of P, compare Fig. 4.11. We also assume that l_k is part of the concave arc between $p_{B'}$ and $p_{C'}$. The case that l_k is part of the concave arc between $p_{C'}$ and $p_{A'}$ is symmetric.

Let G'_{skel} and G''_{skel} be the skeleton graphs of P' and P'', respectively. For a pseudosegment l and two vertices v and w on l in G_{skel}, we denote by $E_{l[v,w]}$ the set of edges of G_{skel} belonging to the part of l between v and w. If $|E_{l[v,w]}| = 1$, we also use the notation $e_{l[v,w]}$. For the edges of G'_{skel} and G''_{skel}, we use the analogous notations $E'_{l[v,w]}, e'_{l[v,w]}$ and $E''_{l[v,w]}, e''_{l[v,w]}$, respectively.

In the following, we consider the system of equations (4.2)–(4.4) for the entire pseudotriangle P but also the systems for the two subpseudotriangles P' and P''. We denote these systems of linear equations by $\mathcal{A}_P$, $\mathcal{A}_{P'}$, and $\mathcal{A}_{P''}$, respectively. Analogously, we denote equation (4.1) for P, P', and P'' by $\mathcal{B}_P$, $\mathcal{B}_{P'}$, and $\mathcal{B}_{P''}$, respectively. In this proof, for $i = 0, \dots, n-1$, we denote the variables x_i by x_{l_i}. Apart from that, we use the same names for the variables of $\mathcal{A}_P$ and $\mathcal{B}_P$ as before. The names of the variables of $\mathcal{A}_{P'}, \mathcal{B}_{P'}$ and $\mathcal{A}_{P''}, \mathcal{B}_{P''}$ are primed versions of the variable names for $\mathcal{A}_P, \mathcal{B}_P$, i.e., x'_l, y'_T, z'_e and x''_l, y''_T, z''_e, respectively.

Now let us assume that we have a solution of $\mathcal{A}_P$. We will assign values to the variables of $\mathcal{A}_{P'}$ that fulfill the equations of $\mathcal{A}_{P'}$. For all edges $e'_{l_j[v,w]}$ of G'_{skel} on the pseudosegment l_j, we set $z'_{e'_{l_j[v,w]}} := \sum_{e \in E_{l_j[v,w]}} z_e$. Further, we set $x'_{\overline{l_j}} := -\sum_{e \in E_{l_j[c_j,p]}} z_e$ and $\overline{x}'_{\overline{l_j}} := -x'_{\overline{l_j}}$. Finally, we set $x'_{l_k} := \sum_{e \in E_{l_k[c_{k-1},p]}}$ and $\overline{x}'_{l_k} := -x'_{l_k}$ and take the values of all other variables of $\mathcal{A}_{P'}$ from the solution of $\mathcal{A}_P$, i.e., we set $x' := x$ for all variables x' of $\mathcal{A}_{P'}$ not explicitly mentioned. By construction, this is a solution of $\mathcal{A}_{P'}$. Therefore, by induction we have

$$\sum_{i=j+1}^{k-1} x_{l_i} s_i + \left(\sum_{e \in E_{l_k[c_{k-1},p]}} z_e \right) s_k - \left(\sum_{e \in E_{l_j[c_j,p]}} z_e \right) s_j = \sum_{i=j+1}^{k} x'_{l_i} s_i + x'_{\overline{l_j}}(-s_j) = 0 \ .$$

Similarly, for P'', we obtain by induction

$$\sum_{i=k+1}^{j-1} x_{l_i} s_i + \left(\sum_{e \in E_{l_j[c_{j-1},c_j]}} z_e + \sum_{e \in E_{l_j[c_j,p]}} z_e \right) s_j + \left(\sum_{e \in E_{l_k[p,c_k]}} \right) z_e s_k = 0 \ .$$

By adding these two equations, we obtain

$$\sum_{i \in \{0,\dots,n-1\} \setminus \{j,k\}} x_{l_i} s_i + \left(\sum_{e \in E_{l_k[c_{k-1},c_k]}} z_e \right) s_k + \left(\sum_{e \in E_{l_j[c_{j-1},c_j]}} z_e \right) s_l = 0 \ ,$$

which is equivalent to $\mathcal{B}_P$ since $\sum_{e \in E_{l_k[c_{k-1},c_k]}} z_e = x_{l_k}$ and $\sum_{e \in E_{l_j[c_{j-1},c_j]}} z_e = x_{l_j}$ by $\mathcal{A}_P$.

Now assume that we have a solution of $\mathcal{B}_P$.

Claim 1. *There are $x'_{\overline{l_j}}, x'_{l_k} \in \mathbb{R}$ such that $\sum_{i=j+1}^{k-1} x_{l_i} s_i + x'_{l_k} s_k - x'_{\overline{l_j}} s_j = 0$.*

Proof. If s_j and s_k are linearly independent in $\mathbb{R}^2$, this is clear. So we assume that s_j and s_k are parallel or antiparallel and distinguish these two cases.

i) Let $s_j = s_k$. Then

$$\pi = \alpha_{\mathrm{r}}(s_j, s_k) = \sum_{i=j}^{k-1} \alpha_{\mathrm{r}}(s_i, s_{i+1}) - (k-j-1)\pi$$

and, therefore,

$$\sum_{i=k}^{j-1+n} \alpha_{\mathrm{r}}(s_i, s_{i+1}) = (n-2)\pi - \sum_{i=j}^{k-1} \alpha_{\mathrm{r}}(s_i, s_{i+1}) = ((j-1+n)-(k-1)-2)\pi \ .$$

Since $\sum_{i=k}^{j-1+n} \alpha_{\mathrm{r}}(s_i, s_{i+1})$ attains this value only if two of the angles $\alpha_{\mathrm{r}}(s_i, s_{i+1})$, $i = k, \dots, j-1+n$, are 0 and the remaining angles are π, this implies that $\sum_{i=k+1}^{j-1+n} x_{l_i} s_i$, s_j, and s_k are pairwise linearly dependent. Hence, also $\sum_{i=j+1}^{k-1} x_{l_i} s_i = -\sum_{i=k}^{j+n} x_{l_i} s_i$, s_j, and s_k are pairwise linearly dependent.

ii) Let $s_j = -s_k$. Then

$$0 = \alpha_{\mathrm{r}}(s_j, s_k) = \sum_{i=j}^{k-1} \alpha_{\mathrm{r}}(s_i, s_{i+1}) - (k-j-1)\pi \ .$$

Since $\sum_{i=j}^{k-1} \alpha_{\mathrm{r}}(s_i, s_{i+1}) = (k-j-1)\pi$ is only possible if one of the angles $\alpha_{\mathrm{r}}(s_i, s_{i+1})$, $i = j, \dots, k-1$, is 0 and the remaining angles are π, this implies that $\sum_{i=j+1}^{k-1} x_{l_i} s_i$, s_j, and s_k are pairwise linearly dependent.

Hence, in both cases we can set $x'_{\overline{l_j}} := 0$ and choose x'_{l_k} appropriately. △

Taking the values $x'_{\overline{l_j}}, x'_{l_k}$ from Claim 1, it follows from $\mathcal{B}_P$ that $\sum_{i=k+1}^{j-1} x_{l_i} s_i + (x_{l_k} - x'_{l_k}) s_k + (x_{l_j} - x'_{\overline{l_j}}) s_j = 0$. Thus we obtain a solution of $\mathcal{B}_{P'}$ by setting $x'_{l_i} := x_{l_i}$ for $i = j+1, \dots, k-1$ and a solution of $\mathcal{B}_{P''}$ by setting $x''_{l_j} := x_{l_j} + x'_{\overline{l_j}}$, $x''_{l_k} := x_{l_k} - x'_{l_k}$, and $x''_{l_i} := x_{l_i}$ for $i = k+1, \dots, j-1$. By induction, these solutions can be extended to solutions of $\mathcal{A}_{P'}$ and $\mathcal{A}_{P''}$, respectively.

Let $p = v_0, v_1, \dots, v_m = c_l$ be the path in G_{skel} on the pseudosegment l_j from p to c_l. Note that p is a vertex of G'_{skel} and G''_{skel} and that, for $i = 1, \dots, m$, the vertex v_i is a vertex of exactly one of the graphs G'_{skel} and G''_{skel}. For $i = 1, \dots, m$, if v_i is a vertex of G'_{skel}, we set

$$z_{e_{l_j[v_{i-1}, v_i]}} := \sum_{e \in E'_{l_j[c_l, v_i]}} z'_e - \sum_{e \in E_{l_j[c_l, v_{i-1}]}} z_e$$

and, if v_i is a vertex of G''_{skel}, we set

$$z_{e_{l_j[v_{i-1}, v_i]}} := \sum_{e \in E''_{l_j[c_l, v_i]}} z''_e - \sum_{e \in E_{l_j[c_l, v_{i-1}]}} z_e \ .$$

All other variables of $\mathcal{A}_P$ are variables of exactly one of the systems $\mathcal{A}_{P'}$ and $\mathcal{A}_{P''}$. By taking their values from the solutions of these systems, we obtain a solution of $\mathcal{A}_P$ that extends the given solution of $\mathcal{B}_P$. □

In the following we will prove that the variable-equation incidence graph H of the system of equations (4.2)–(4.4) has a matching in which all equation-vertices are matched. Further, we can choose to some extent which of the variable-vertices are matched. For two different indices $i_1, i_2 \in \{0, \dots, n-1\}$, we call a perfect matching of $H[V(H) \setminus \{ x_i \colon i \in \{0, \dots, n-1\} \setminus \{i_1, i_2\} \}]$ an $\{x_{i_1}, x_{i_2}\}$-*perfect matching* of H.

Lemma 4.22. *Let $i_1, i_2 \in \{0, \dots, n-1\}$ with $i_1 \neq i_2$. Then there exists an $\{x_{i_1}, x_{i_2}\}$-perfect matching of H.*

Proof. First of all, we remove all variable-vertices of the form x_i and their incident equation-vertices from H. We call this new graph the *reduced variable-equation incidence graph* and denote it by $\widetilde{H}$. Note that the existence of an $\{x_{i_1}, x_{i_2}\}$-perfect matching of H is equivalent to the existence of a perfect matching of $\widetilde{H}[V(\widetilde{H}) \setminus \{ \overline{x_i} \colon i \in \{0, \dots, n-1\} \setminus \{i_1, i_2\} \}]$. We call such a matching an $\{\overline{x_{i_1}}, \overline{x_{i_2}}\}$-perfect matching of $\widetilde{H}$.

The proof will be by induction on the number of triangles the pseudotriangle P is decomposed into. If P is a triangle, the existence of the wanted matching is clear, see Fig. 4.13.

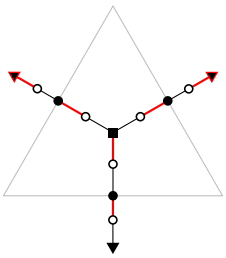

Figure 4.13: A maximum matching of the reduced variable-equation incidence graph $\widetilde{H}$ of the system of equations (4.2)–(4.4) in the trivial case $n = 3$. Two of the variables $\overline{x_i}$ are marked with a red boundary and all vertices except the unmarked variable of the type $\overline{x_i}$ are matched.

Now let us assume that the pseudotriangle P is decomposed into at least two triangles. As in the proof of Lemma 4.21, we will use the same notations for the first cut of P as earlier in this section, when we described the cutting of P (compare Fig. 4.11), and we assume that l_k is part of the concave arc between $p_{B'}$ and $p_{C'}$. The case that l_k is part of the concave arc between $p_{C'}$ and $p_{A'}$ is symmetric.

Let H' and H'' be the reduced variable-equation incidence graphs of the systems of linear equations corresponding to P' and P'', respectively. We choose indices i'_1, i'_2, i''_1, i''_2 such that $i'_1 \neq i'_2$, $i''_1 \neq i''_2$, and $\{i'_1, i'_2, i''_1, i''_2\} = \{i_1, i_2, j, k\}$ as an equality of multisets. By induction there exists an $\{\overline{x_{i'_1}}, \overline{x_{i'_2}}\}$-perfect matching M' of H' and an $\{\overline{x_{i''_1}}, \overline{x_{i''_2}}\}$-perfect matching M'' of H''. We will construct an $\{\overline{x_{i_1}}, \overline{x_{i_2}}\}$-perfect matching M of $\widetilde{H}$ from M' and M''. Figure 4.14 illustrates this construction.

We add all edges of M' and M'' to M that are not incident to $\overline{x_j}$, to $\overline{x_k}$, or to z_e for an $e \in E_{l_j}$. Let u_j and u_k denote the equation-vertices incident to $\overline{x_j}$ and $\overline{x_k}$, respectively. Note that all vertices, except u_k, that are incident to an edge that is currently in M are either vertices of H' or vertices of H''. We distinguish two cases.

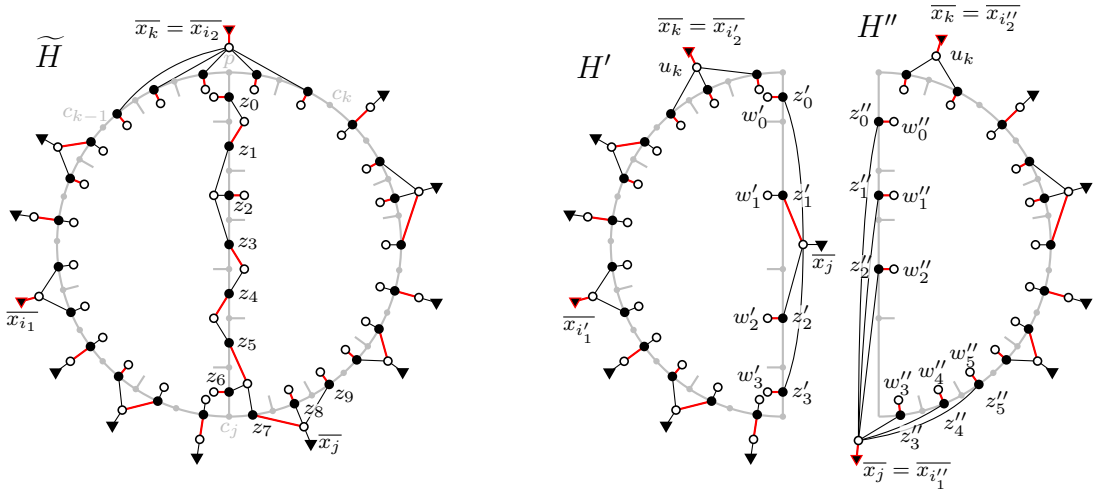

Figure 4.14: The construction of an $\{\overline{x_{i_1}}, \overline{x_{i_2}}\}$-perfect matching of $\widetilde{H}$ from an $\{\overline{x_{i'_1}}, \overline{x_{i'_2}}\}$-perfect matching of H' and an $\{\overline{x_{i''_1}}, \overline{x_{i''_2}}\}$-perfect matching of H''.

i) If $k \in \{i_1, i_2\}$, then $k \in \{i'_1, i'_2\}$ and $k \in \{i''_1, i''_2\}$. Thus $\overline{x_k}$ is matched with its incident equation-vertex u_k in M' and M''. Hence, we can add the edge $\overline{x_k}u_k$ to M and M is currently a matching of $\widetilde{H}$.

ii) If $k \notin \{i_1, i_2\}$, then either $k \in \{i'_1, i'_2\}$ or $k \in \{i''_1, i''_2\}$. In this case, we do not add $\overline{x_k}u_k$ to M and, hence, also in this case, M is currently a matching of $\widetilde{H}$.

The only vertices that still need to be matched to make M an $\{\overline{x_{i_1}}, \overline{x_{i_2}}\}$-perfect matching of $\widetilde{H}$ are the variable-vertices z_e with $e \in E_{l_j}$, some of their incident equation-vertices, and the vertex $\overline{x_j}$ if $\overline{x_j} \in \{i_1, i_2\}$. We denote the variable-vertices z_e with $e \in E_{l_j[p,c_j]}$ in the order from p to c_j by $z_0, \dots, z_{q-1}$ and the variable-vertices z_e with $e \in E_{l_j[c_j,c_{j-1}]}$ in the order from c_j to c_{j-1} by $z_q, \dots, z_{m-1}$. Similarly, in H' we denote the variable-vertices z'_e with $e \in E'_{l_j[p,c_j]}$ in the order from p to c_j by $z'_0, \dots, z'_{m'-1}$ and in H'' we denote the variable-vertices z''_e with $e \in E''_{l_j[p,c_{j-1}]}$ in the order from p to c_{j-1} by $z''_0, \dots, z''_{m''-1}$. Further, let q'' be the index such that $z''_{q''} = z''_e$ for the edge e of G''_{skel} containing the point c_j. For $i = 0, \dots, m' - 1$, we denote the adjacent equation-vertex of z'_i that is not adjacent to $\overline{x_j}$ by w'_i and, for $i = 0, \dots, m'' - 1$, we denote the adjacent equation-vertex of z''_i that is not adjacent to $\overline{x_j}$ by w''_i. We distinguish two cases.

i) If $j \in \{i_1, i_2\}$, then $j \in \{i'_1, i'_2\}$ and $j \in \{i''_1, i''_2\}$ (Fig. 4.15a shows this case). Therefore, M' contains all edges $z'_i w'_i$, $i = 0, \dots, m' - 1$, and M'' contains all edges $z''_i w''_i$, $i = 0, \dots, m'' - 1$. Then, for $i = 0, \dots, m' - 1$, we add the edge $w'_i z_r$ to M with r chosen maximal such that there is an edge $w'_i z_r$ in $\widetilde{H}$. Further, for $i = 0, \dots, m'' - 1$, we add the edge $w''_i z_s$ to M with s chosen maximal such that there is an edge $w''_i z_s$ in $\widetilde{H}$. Finally, we add the edge between x_j and its incident equation-vertex to M.

ii) If $j \notin \{i_1, i_2\}$, then either $j \in \{i'_1, i'_2\}$ or $j \in \{i''_1, i''_2\}$.

a) Let us first consider the case that $j \notin \{i'_1, i'_2\}$ (Fig. 4.15b shows this case). Then $z''_i w''_i \in M''$ for all $i \in \{0, \dots, m'' - 1\}$ and there is exactly

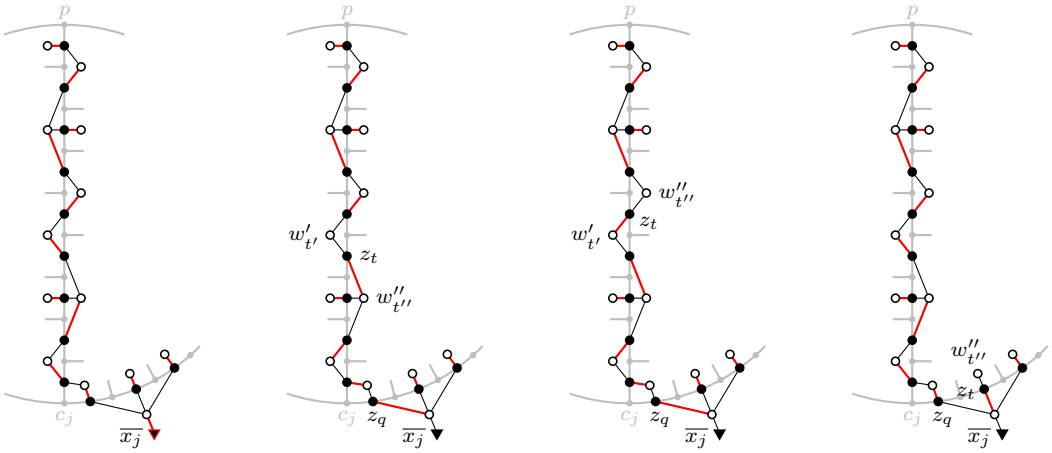

(a) $j \in \{i_1, i_2\}$ (b) $j \notin \{i_1, i_2\}$, $j \in \{i''_1, i''_2\}$ (c) $j \notin \{i_1, i_2\}$, $j \in \{i'_1, i'_2\}$, $t < q$ (d) $j \notin \{i_1, i_2\}$, $j \in \{i'_1, i'_2\}$, $t \geq q$

Figure 4.15: Construction of the matching M from the matchings M' and M'' in the different cases distinguished in the proof of Lemma 4.22.

one $t' \in \{0, \dots, m' - 1\}$ such that $z'_{t'}w'_{t'} \notin M'$. Let t be maximal such that $w'_{t'}z_t$ is an edge of $\widetilde{H}$ and choose t'' such that $w''_{t''}z_t$ is an edge of $\widetilde{H}$. Then, for $i = 0, \dots, t' - 1$, we add the edge $w'_i z_r$ to M with r chosen maximal such that there is an edge $w'_i z_r$ in $\widetilde{H}$ and, for $i = t' + 1, \dots, m' - 1$, we add the edge $w'_i z_r$ to M with r chosen minimal such that $w'_i z_r$ is an edge of $\widetilde{H}$. Further, for $i = 0, \dots, t'' - 1$, we add the edge $w''_i z_s$ to M with s maximal such that there is an edge $w''_i z_s$ in $\widetilde{H}$ and, for $i = t'', \dots, m'' - 1$, we add the edge $w''_i z_s$ to M with s chosen minimal such that there is an edge $w''_i z_s$ in $\widetilde{H}$. Note that z_q is the only edge-variable-vertex that is still unmatched. Therefore, we add the edge $z_q u_j$ to M to make M an $\{\overline{x_{i_1}}, \overline{x_{i_2}}\}$-perfect matching of $\widetilde{H}$.

b) Now let us consider the case that $j \in \{i'_1, i'_2\}$. Then $z'_i w'_i \in M'$ for all $i \in \{0, \dots, m' - 1\}$ and there is exactly one $t'' \in \{0, \dots, m'' - 1\}$ such that $z''_{t''}w''_{t''} \notin M''$. Let t be maximal such that $w''_{t''}z_t$ is an edge of $\widetilde{H}$. We distinguish two cases.

A) If $t < q$ (Fig. 4.15c shows this case), we choose t' such that $w''_{t'}z_t$ is an edge of $\widetilde{H}$. Then, for $i = 0, \dots, t' - 1$, we add the edge $w'_i z_r$ to M with r chosen maximal such that there is an edge $w'_i z_r$ in $\widetilde{H}$ and, for $i = t', \dots, m' - 1$, we add the edge $w'_i z_r$ to M with r chosen minimal such that $w'_i z_r$ is an edge of $\widetilde{H}$. Further, for $i = 0, \dots, t'' - 1$, we add the edge $w''_i z_s$ to M with s maximal such that there is an edge $w''_i z_s$ in $\widetilde{H}$ and, for $i = t'' + 1, \dots, m'' - 1$, we add the edge $w''_i z_s$ to M with s chosen minimal such that there is an edge $w''_i z_s$ in $\widetilde{H}$. Then z_q is the only edge-variable-vertex that is still unmatched and we make M an $\{\overline{x_{i_1}}, \overline{x_{i_2}}\}$-perfect matching of $\widetilde{H}$ by adding the edge $z_q u_j$ to it.

B) If $t \geq q$ (Fig. 4.15d shows this case), for $i = 0, \ldots, m' - 1$, we add the edge $w'_i z_r$ to M with r chosen maximal such that there is an edge $w'_i z_r$ in $\widetilde{H}$ and, for $i = 0, \ldots, q'' - 1, q'' + 1, \ldots, m'' - 1$, we add the edge $w''_i z_s$ to M with s chosen maximal such that there is an edge $w''_i z_r$ in $\widetilde{H}$. Then z_t is the only edge-variable-vertex that is still unmatched and we make M an $\{\overline{x_{i_1}}, \overline{x_{i_2}}\}$-perfect matching of $\widetilde{H}$ by adding the edge $z_t u_j$ to it.

Hence, in each case there exists an $\{\overline{x_{i_1}}, \overline{x_{i_2}}\}$-perfect matching of $\widetilde{H}$. □

4.4 Equations for similarly-aligned odd K-gon contact representations

In this section, let $K \geq 3$ be an odd integer, let G be an inner triangulation of the K-cycle $a_0, \ldots, a_{K-1}$ (in clockwise order), let S be a K-contact structure of G, and let $G^\star_+ := G^\star_+(S)$. Further, for each inner vertex v of G, let P_v be a convex K-gon and let Q be a convex K-gon with sides $q_0, \ldots, q_{K-1}$ in clockwise order such that the P_v and Q are similarly-aligned odd K-gons. We call P_v the *prototype* of v and q_i the prototype of the outer vertex a_i. We will propose a system of linear equations that allows us to compute a similarly-aligned odd K-gon contact representation of G in which each inner vertex v is represented by a homothetic copy of its prototype P_v and the outer face is represented by a K-gon whose sides have the same slopes as the sides of Q and which induces the K-contact structure S. If such a contact representation does not exist, the solution of the system will have negative variables.

Description of the system of equations. We start by describing how to obtain the *skeleton graph* of the contact representation. See Fig. 4.16 for an example of the following construction. The skeleton graph G_{skel} is a subgraph of the medial graph of $G^\star_+$. It contains exactly those edges of the medial graph that correspond to an angle of a normal vertex in an inner face of $G^\star_+$. We orient the edges of G_{skel} in clockwise order around each normal vertex of $G^\star_+$ and assign a slope to each of these oriented edges (if we assign the slope s to the edge (v, w), we also assign the slope $-s$ to the edge (w, v)). If the edge corresponds to an angle of an inner normal vertex v and this angle lies between the outgoing edges of colors i and $i+1$ in clockwise order in the K-proper coloring of $G^\star_+$ (we denote the set of these edges by $E_{i+\frac{K+1}{2}}(v)$), then we assign the slope of $\text{side}_{i+\frac{K+1}{2}}(P_v)$ to this edge. If the edge corresponds to an angle of the outer normal vertex a_j, then we assign the negation of the slope of the side q_j of Q to this edge. Note that the wanted contact representation of G is a straight-line drawing of G_{skel} in which each edge has the slope that has been assigned to it. Further, note that an inner face of G_{skel} either corresponds to an inner vertex of G or to an inner face of G.

The purpose of the system of linear equations is to find edge lengths for the edges of G_{skel} in such a drawing with the additional property that the faces of G_{skel} corresponding to the inner vertices of G are homothets of the given prototypes. We

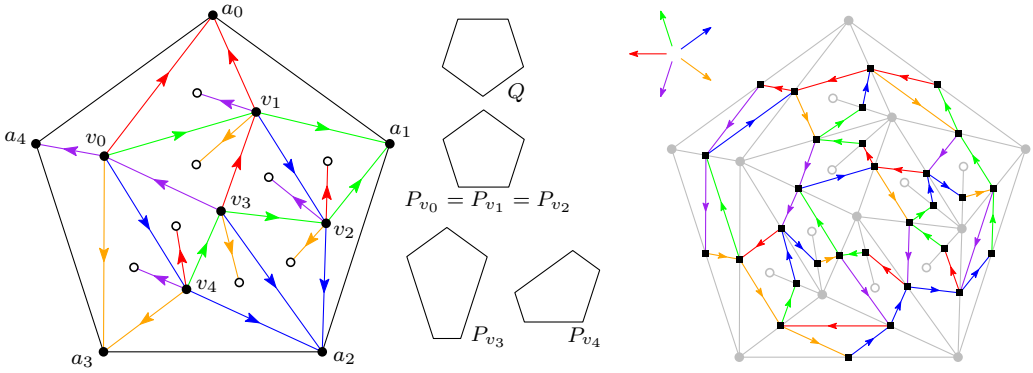

Figure 4.16: Left: the graph $G^\star_+$ with its 5-proper coloring. Middle: equiangular prototypes for this graph. Right: the skeleton graph G_{skel} of the contact representation corresponding to $G^\star_+$ with colors representing the slopes assigned to the edges (since the prototypes are equiangular, there are only 5 different slopes in total). The contact representation in Fig. 3.13 is a drawing of G_{skel} using these slopes.

have a variable x_e for each edge e of G_{skel} representing its length and a variable x_v for each inner vertex v of G representing the scaling factor of its prototype P_v. We have equations which ensure that the scaling factor x_v of each normal vertex v fits together with the edge lengths x_e of the face of G_{skel} corresponding to v. For $i = 0, \dots, K-1$, let $\ell_i(P_v)$ be the length of $\text{side}_i(P_v)$. Then the sum of the lengths of the edges in $E_i(v)$ has to be equal to $x_v \ell_i(P_v)$, the scaled side length of the prototype:

$$\sum_{e \in E_i(v)} x_e - \ell_i(P_v) x_v = 0 \ . \tag{4.5}$$

Further, we have two equations for each inner face f of G ensuring that the edges of the face of G_{skel} corresponding to f form a closed curve (these are the pseudotriangles). Let $e_0, \dots, e_{k-1}$ be the edges of this face of G_{skel} and, for $i = 0, \dots, k-1$, let s_i be the slope assigned to e_i. Then

$$\sum_{i=0}^{k-1} x_i s_i = 0 \ . \tag{4.6}$$

Finally, we add one more equation to our system stating that the perimeter of the outer K-gon of the contact representation is one. With E_{out} denoting the set of edges of the outer face of G_{skel}, this last equation is

$$\sum_{e \in E_{\text{out}}} x_e = 1 \ . \tag{4.7}$$

This equation is the only inhomogeneous equation and will ensure that the solution of the system is unique and not degenerate. We denote the entire system by $A_S \mathbf{x} = \mathbf{e_1}$ where A_S is a matrix depending on the K-contact structure S and $\mathbf{e_1} = (1, 0, 0, \dots, 0)$.

For the analysis of the system $A_S \mathbf{x} = \mathbf{e_1}$ we want to make use of the theory developed in the last section and replace the equations of the type (4.6) by equivalent equations as shown in Lemma 4.21. Therefore, we have to show that the polygons corresponding to the faces of G are pseudotriangles.

Lemma 4.23. *Let $e_0, \dots, e_{k-1}$ be the edges of a face f of G_{skel} corresponding to an inner face of G in clockwise order. Further, for $i = 0, \dots, k-1$, let s_i be the slope assigned to e_i (in the direction of the clockwise traversal of the face). Then $s_0, \dots, s_{k-1}$ is a slope sequence of a pseudotriangle.*

Proof. For all i, let v_i be the common incident vertex of e_i and e_{i+1}. By the construction of G_{skel}, exactly three vertices v_A, v_B, v_C incident to f are of degree four and the vertices v_i with $i \notin \{A, B, C\}$ are of degree two. Since the prototypes are similarly-aligned odd K-gons, for $i \in \{A, B, C\}$, the right angle α_i between a side of slope s_i and a side of slope s_{i+1} is in the range $0 \leq \beta < \pi$. Since the prototypes are convex polygons, for $i \notin \{A, B, C\}$, the right angle α_i between a side of slope s_i and a side of slope s_{i+1} is in the range $\pi \leq \alpha_i < 2\pi$.

These ranges of the angles α_i immediately imply $\sum \alpha_i \geq (k-3)\pi$. If the angle between sides of slopes s and s' is π, then $s = s'$ and, if the angle is 0, then $s = -s'$. Therefore, it is not possible that $\alpha_i = 0$ for all $i \in \{A, B, C\}$ and $\alpha_i = \pi$ for all $i \notin \{A, B, C\}$. Hence, we have $\sum \alpha_i > (k-3)\pi$ and thus $\sum \alpha_i \geq (k-2)\pi$.

The slopes assigned to the edges of G_{skel} define a value for each angle between two consecutive incident edges of a vertex of G_{skel}. For the vertices of degree two, it is clear that the sum of the values of the two incident angles is 2π. For a vertex v of degree four, let $r_0, \dots, r_3$ be the slopes assigned to the incident edges of v (in outgoing orientation for v) in clockwise order. Then the sum of the values of the four incident angles of v is 2π if and only if the slopes $r_0, \dots, r_3$ are sorted in clockwise direction in this order (otherwise the sum is 4π or 6π). Since the prototypes are similarly-aligned, this is the case for all vertices v of degree four. Therefore, for all vertices of G_{skel}, the sum of the values of the two incident angles is 2π.

The values of the outer angles of the outer face f_{o} of G_{skel} are equal to the outer angles of a subdivision of Q. Since Q is a simple polygon, the sum of the values of the outer angles of f_{o} is $(\deg(f_{\text{o}}) + 2)\pi$. For an inner face f' of G_{skel} corresponding to an inner vertex v of G, the values of the inner angles of f' are equal to the inner angles of a subdivision of the prototype P_v. Thus, since P_v is a simple polygon, the sum of the values of the inner angles of f' is $(\deg(f') - 2)\pi$. For the inner faces f of G_{skel} corresponding to an inner face of G, we have shown above that the sum of the values of the inner angles of f' is at least $(\deg(f') - 2)\pi$. Let V, E, F be the sets of vertices, edges, and faces of G_{skel}. Then, by double counting the sum of the values of all these angles, we obtain

$$|V| \cdot 2\pi \geq \sum_{f' \in F \setminus \{f_{\text{o}}\}} (\deg(f') - 2)\pi + (\deg(f_{\text{o}}) + 2)\pi = (2|E| - 2|F| + 4)\pi = 2|V|\pi \ ,$$

where the last equality is due to Euler's formula. Therefore, the first inequality has to be fulfilled with equality. In particular, coming back to the face f, this implies $\sum \alpha_i = (k-2)\pi$. Hence, $s_0, \dots, s_{k-1}$ is a slope sequence of a pseudotriangle. □

We denote the system of equations obtained from $A_S\mathbf{x} = \mathbf{e_1}$ by replacing each equation of the type (4.6) according to Lemma 4.21 by $A'_S\mathbf{x} = \mathbf{e_1}$.

Unique solvability. Now we will prove that the system of equations $A_S\mathbf{x} = \mathbf{e_1}$ is uniquely solvable. For this purpose we need a technical lemma about perfect matchings in plane bipartite graphs. The lemma is well known from the context of Pfaffian orientations, see, e.g., [Tho06]. We include a proof for completeness. Let H be a bipartite graph with vertex classes $\{v_1, \dots, v_k\}$ and $\{w_1, \dots, w_k\}$. Then a perfect matching of H induces a permutation $\sigma \in \mathcal{S}_k$ via $\sigma(i) = j :\Leftrightarrow \{v_i, w_j\} \in M$. We define the *sign* $\operatorname{sgn}(M)$ of a perfect matching M of H as the sign of the corresponding permutation. Note that the sign $\operatorname{sgn}(M)$ of a perfect matching M depends on the labeling of the vertices of H, but the product $\operatorname{sgn}(M)\operatorname{sgn}(M')$ of the signs of two perfect matchings M, M' does not depend on it.

Lemma 4.24. *Let H be a bipartite graph and let M, M' be two perfect matchings of H. Then the symmetric difference of M and M' is the disjoint union of a set $\mathcal{C}$ of simple cycles. For $r = 0, 2$, let $\mathcal{C}_r = \{\, C \in \mathcal{C} \colon \ell(C) \equiv r \pmod 4 \,\}$ where $\ell(C)$ is the length of C. Then $\operatorname{sgn}(M) = \operatorname{sgn}(M')$ if and only if $|\mathcal{C}_0|$ is even.*

Proof. Let $\mathcal{C}_0 = \{C_1, \dots, C_k\}$ and $\mathcal{C}_2 = \{C'_1, \dots, C'_m\}$. Further, for $i = 1, \dots, k$, let $\ell(C_i) = 4n_i$ and, for $j = 1, \dots, m$, let $\ell(C'_j) = 4n'_j + 2$. For each $C \in \mathcal{C}$, on the vertices of C, the permutations σ and σ' corresponding to M and M', respectively, differ in a cyclic permutation τ_C of length $\frac{\ell(C)}{2}$, see Fig. 4.17. Hence, we have $\sigma' = \sigma \circ \tau_{C_1} \circ \cdots \circ \tau_{C_k} \circ \tau_{C'_1} \circ \cdots \circ \tau_{C'_m}$ and therefore

$$\begin{aligned}
\operatorname{sgn}(\sigma') &= \operatorname{sgn}(\sigma) \cdot \operatorname{sgn}(\tau_{C_1}) \cdots \operatorname{sgn}(\tau_{C_k}) \cdot \operatorname{sgn}(\tau_{C'_1}) \cdots \operatorname{sgn}(\tau_{C'_m}) \\
&= \operatorname{sgn}(\sigma) \cdot (-1)^{2n_1 - 1} \cdots (-1)^{2n_k - 1} \cdot (-1)^{2n'_1} \cdots (-1)^{2n'_m} \\
&= \operatorname{sgn}(\sigma) \cdot (-1)^k \ ,
\end{aligned}$$

which implies the statement. □

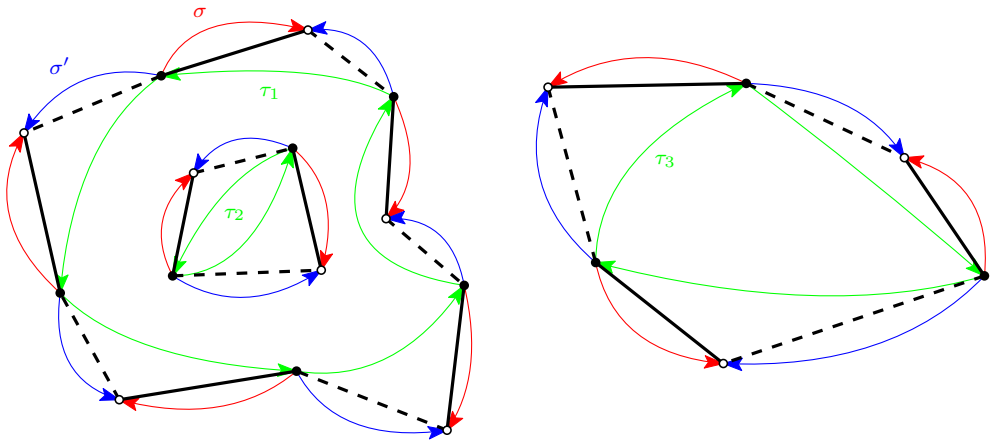

Figure 4.17: Two perfect matchings (solid and dashed) of the same bipartite graph and the corresponding permutations σ and σ' in red and blue, respectively. With the cyclic permutations τ_i we have $\sigma' = \sigma \circ \tau_1 \circ \tau_2 \circ \tau_3$.

Lemma 4.25. *If H is a plane graph such that every inner face f of H is bounded by a simple cycle of length $\ell_f \equiv 2 \pmod 4$, then any two perfect matchings M, M' of H fulfill $\operatorname{sgn}(M) = \operatorname{sgn}(M')$.*

Proof. We will first show a relation between the length of a simple cycle and the number of vertices enclosed by it.

Claim 1. *Let C be a simple cycle of length ℓ in H with k vertices in its interior. Then $\ell + 2k \equiv 2 \pmod 4$.*

Proof. The proof is by induction on the number of faces enclosed by C. If C is a facial cycle, then $k = 0$ and $\ell \equiv 2 \pmod 4$ by the conditions of this lemma. Otherwise, let P be a simple chordal path of C that intersects C exactly at its two endpoints. Further, let ℓ_P be the length of P. The path P splits C into two simple cycles C' and C''. Let ℓ' and ℓ'' be the lengths of C' and C'', respectively, and let k' and k'' be the numbers of vertices in the interiors of C' and C'', respectively. Then $\ell' + \ell'' = \ell + 2\ell_P$ and $k = k' + k'' + \ell_P - 1$. Together, this gives $\ell + 2k = (\ell' + 2k') + (\ell'' + 2k'') - 2$. Since, by induction, we have $\ell' + 2k' \equiv 2 \pmod 4$ and $\ell'' + 2k'' \equiv 2 \pmod 4$, this implies $\ell + 2k \equiv 2 \pmod 4$. △

The symmetric difference of M and M' is the disjoint union of simple cycles $C_1, \ldots, C_m$ each of which contains an even number of vertices in its interior. Therefore, due to Claim 1, $\ell_i \equiv 2 \pmod 4$ for $i = 1, \ldots, m$ and the statement of the lemma follows from Lemma 4.24. □

Now we have everything together that we need to prove the unique solvability of the system $A_S\mathbf{x} = \mathbf{e_1}$.

Theorem 4.26. *The system $A_S\mathbf{x} = \mathbf{e_1}$ is uniquely solvable.*

Proof. Due to Lemma 4.21 it suffices to show that the system $A'_S\mathbf{x} = \mathbf{e_1}$ is uniquely solvable. The matrix A'_S is a square matrix as we will implicitly show later in Claim 1. Therefore, we can prove the unique solvability by showing that $\det(A'_S) \neq 0$. Note that all entries of A'_S are non-negative.

Let H be the incidence graph of the system $A'_S\mathbf{x} = \mathbf{e_1}$. Then we have

$$\det(A'_S) = \sum_{\sigma} \operatorname{sgn}(\sigma) \prod_i (A'_S)_{i,\sigma(i)} = \sum_M \operatorname{sgn}(M) p_M \ ,$$

where the second sum goes over all perfect matchings M of H and where $p_M > 0$ is a product of positive entries of A'_S for all perfect matchings M.

Next we will define a crossing-free embedding of H into the plane. We start with a crossing-free drawing of $G^\star_+$, in which single edges are straight lines and multiple edges are allowed to have one bend. Then we put pairwise disjoint disks around all normal vertices. We put a second, smaller circle around the inner normal vertices. The smaller circle around a normal vertex u is cut at the outgoing edges of u into K arcs. These K arcs are the drawings of the K equation-vertices incident to u. The larger circle around u is cut into arcs at all incident edges of u. These arcs are the

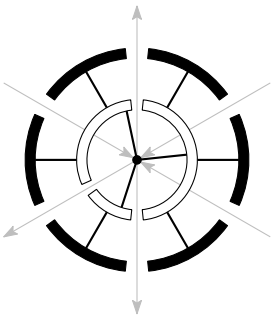

Figure 4.18: Gadget for embedding the incidence graph H of $A'_S\mathbf{x} = \mathbf{e_1}$ into the plane. In the center we have an inner normal vertex. Its incident edges of $G^\star_+$ are drawn in gray. The gadget itself is drawn in black with white equation-vertices and black variable-vertices.

drawings of edge-variable-vertices. Then we add edges between u and all arcs on the smaller circle around u, and we add edges between an arc on the smaller and an arc on the larger circle around u if there is a straight line crossing u and both arcs. See Fig. 4.18 for an illustration.

Each inner face f of the induced drawing of G contains the drawings of the edge-variable-vertices corresponding to exactly those edges of G_{skel} that are part of the boundary of the corresponding pseudotriangle P_f. The remaining variables and equations corresponding to P_f can then be embedded inside this face according to Lemma 4.20.

We want to mention that, except for Fig. 4.18, we will not draw vertices as arcs in figures. The arcs only serve as a tool to define the embedding.

Claim 1. *The graph H has a perfect matching.*

Proof. We describe an explicit construction of a perfect matching of H. We look at the unique K-proper coloring of $G^\star_+$. The K equation-vertices adjacent to an inner

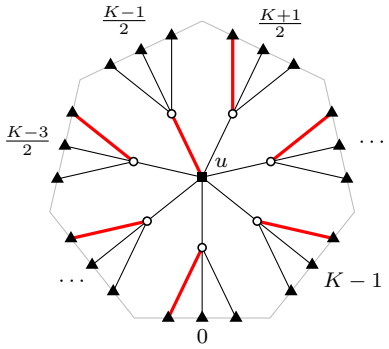

Figure 4.19: Illustration of the matching rule for the K equation-vertices corresponding to an inner vertex of G. In the center there is a vertex-variable-vertex u. The white vertices are its adjacent equation-vertices corresponding to the colors $0, \ldots, K-1$. The outer black vertices are their adjacent edge-variable-vertices.

normal vertex u of $G^\star_+$ are corresponding to the K colors: an equation-vertex has color c if it is opposite to the outgoing edge of color c. We always match the vertex u with the equation-vertex of color $\frac{K-1}{2}$. The equation-vertices of colors $0, \dots, \frac{K-3}{2}$ are matched with the adjacent edge-variable-vertex that precedes u in the clockwise order of adjacent vertices and the equation-vertices of colors $\frac{K+1}{2}, \dots, K-1$ are matched with the adjacent edge-variable-vertex that succeeds u in the clockwise order of adjacent vertices. See Fig. 4.19 for an illustration.

Now we will show that exactly two edge-variable-vertices of every stack vertex f remain unmatched. Let $v_0^{(0)}, \dots, v_{k_0-1}^{(0)}$, $v_0^{(1)}, \dots, v_{k_1-1}^{(1)}$, and $v_0^{(2)}, \dots, v_{k_2-1}^{(2)}$ be the edge-variable-vertices of the three concave arcs of P_f in counterclockwise order (see Fig. 4.20), and let $c_i^{(j)}$ be the color of $v_i^{(j)}$. Further, for $j = 0, 1, 2$, let v_j be the vertex-variable-vertex corresponding to the vertices $v_i^{(j)}$ (we also denote the corresponding normal vertex of $G^\star$ by v_j). Note that $c_{k_j-1}^{(j)} = c_0^{(j+1)} + \frac{K-1}{2}$ for $j = 0, 1, 2$ and upper indices taken modulo 3.

We will now take a closer look which of the vertices $v_i^{(j)}$ are already matched. Let $j \in \{0, 1, 2\}$. If $i \notin \{0, k_j - 1\}$, then $v_i^{(j)}$ and v_j are the only neighbors of their common adjacent equation-vertex. Since v_j is matched with its adjacent equation-vertex of color $\frac{K-1}{2}$, this leads to the following observation.

Fact 1. *Let $i \in \{1, \dots, k_j - 2\}$. Then the vertex $v_i^{(j)}$ is already matched if and only if $c_i^{(j)} \neq \frac{K-1}{2}$.*

If the edge $v_j v_{j+1}$ is oriented from v_j to v_{j+1} in $G^\star_+$, then $v_{k_j-1}^{(j)}$ precedes v_j in the clockwise order of adjacent vertices of its adjacent equation-vertex and v_0^{j+1} does not succeed v_{j+1} in the clockwise order of adjacent vertices of its adjacent equation-vertex. Therefore, if $c_{k_j-1}^{(j)} \in \{0, \dots, \frac{K-3}{2}\}$ (and thus $c_0^{(j+1)} \in \{\frac{K+1}{2}, \dots, K-1\}$), the vertex $v_{k_j-1}^{(j)}$ is already matched and $v_0^{(j+1)}$ is not matched yet. Similarly, it follows

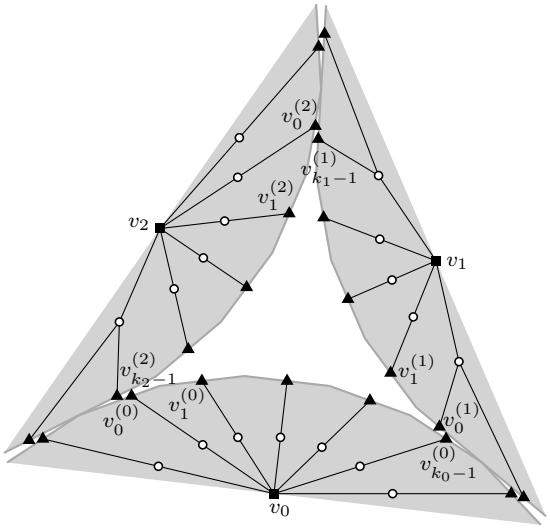

Figure 4.20: The edge-variable-vertices corresponding to stack vertex.

that if the edge v_jv_{j+1} is oriented from v_{j+1} to v_j in $G^\star_+$ and the colors $c^{(j)}_{k_j}$ and $c^{(j+1)}_0$ are in the same ranges as before, then $v^{(j+1)}_0$ is already matched, but $v^{(j)}_{k_j}$ is not matched yet. This leads to the following observation.

Fact 2. *If $c^{(j)}_{k_j-1} \in \{0,\dots,\frac{K-3}{2}\}$ (or equivalently $c^{(j+1)}_0 \in \{\frac{K+1}{2},\dots,K-1\}$), then exactly one of $v^{(j)}_{k_j-1}$ and $v^{(j+1)}_0$ is already matched.*

Now we distinguish two cases. See Fig. 4.21 for examples of these two cases.

i) First, we assume that there is an edge-variable-vertex of color $\frac{K-1}{2}$. After possibly relabeling the three concave arcs, we can assume that $c^{(0)}_{i^*} = \frac{K-1}{2}$ for some i^*. Then $v^{(0)}_{i^*}$ is not matched yet. Since the colors $c^{(j)}_i$ are pairwise different, it follows from Fact 1 that, for all j and i with $i \notin \{0, k_j-1\}$ and $(j,i) \neq (0,i^*)$, the vertex $v^{(j)}_i$ is already matched. We will now consider the cases where $i \in \{0, k_j-1\}$. If $i^* \neq 0$, then $c^{(0)}_0 \in \{1,\dots,\frac{K-3}{2}\}$ and, since $k_0 \neq 1$, the vertex $v^{(0)}_0$ precedes v_0 in the clockwise order of adjacent vertices of their common adjacent equation-vertex. Hence, $v^{(0)}_0$ is already matched in this case. Analogously, it follows that $v^{(0)}_{k_0-1}$ is already matched if $i^* \neq k_0-1$. If $k_1 = 1$, then $v^{(1)}_0 = v^{(1)}_{k_1-1}$ and will be considered when we consider $v^{(1)}_{k_1-1}$. Otherwise, if $k_1 \neq 1$, then $c^{(1)}_0 \in \{0,\dots,\frac{K-3}{2}\}$ and $v^{(1)}_0$ precedes v_1 in the clockwise order of adjacent vertices of their common adjacent equation-vertex. Hence, $v^{(1)}_0$ is already matched in this case. Analogously, it follows that $v^{(2)}_{k_2-1}$ is already matched if $k_2 \neq 1$. Finally, since $c^{(1)}_{k_1-1}\{0,\dots,\frac{K-3}{2}\}$, it follows from Fact 2 that exactly one of $v^{(1)}_{k_1-1}$ and $v^{(2)}_0$ is already matched.

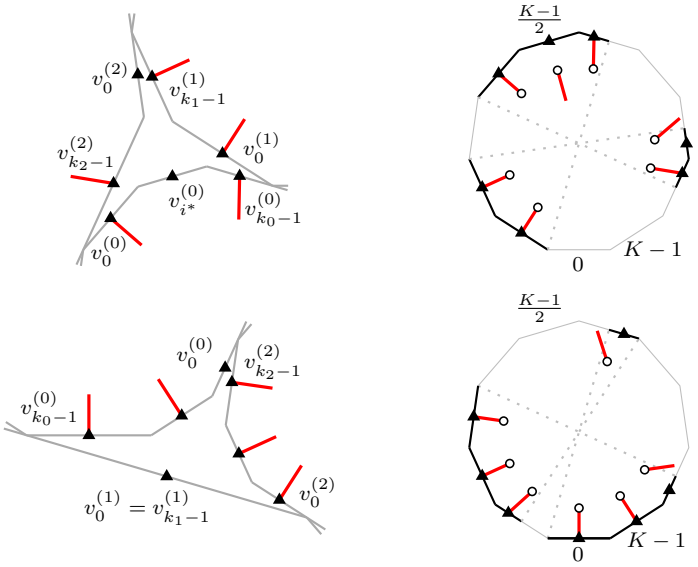

Figure 4.21: Left: examples of the two cases in the proof of Claim 1. In each case exactly two of the edge-variable-vertices are not matched. Right: visualizations of the three arcs of each of the two pseudotriangles explaining the matching edges.

ii) Now we assume that there is no edge-variable-vertex of color $\frac{K-1}{2}$. Then, for $j = 0, 1, 2$, exactly one of $c^{(j)}_{k_j-1}$ and $c^{(j+1)}_0$ is contained in $\{0, \dots, \frac{K-3}{2}\}$ and the other one in $\{\frac{K+1}{2}, \dots, K-1\}$. Therefore, exactly three of the $c^{(j)}_0$ and $c^{(j)}_{k_j-1}$ are contained in each of these two parts. Thus, after possibly relabeling the three concave arcs, we can assume that $c^{(0)}_{k_0-1}, c^{(2)}_0, c^{(2)}_{k_2-1} \in \{0, \dots, \frac{K-3}{2}\}$ and $c^{(1)}_0, c^{(1)}_{k_1-1}, c^{(0)}_0 \in \{\frac{K+1}{2}, \dots, K-1\}$. Then, by Fact 2, exactly one of $v^{(0)}_0$ and $v^{(2)}_{k_2-1}$ and exactly one of $v^{(0)}_{k_0-1}$ and $v^{(1)}_0$ are already matched. Further, if $k_1 \neq 1$, then $v^{(1)}_{k_1-1}$ succeeds v_1 in the clockwise order of adjacent vertices of their common adjacent equation-vertex and, hence, $v^{(1)}_{k_1-1}$ is already matched in this case. Analogously, it follows that $v^{(2)}_0$ is already matched if $k_2 \neq 1$. The remaining edge-variable-vertices we have not considered yet are already matched due to Fact 1.

Since in both cases exactly two of the edge-variables-vertices are unmatched, we can apply Lemma 4.22 in each inner face of G to extend the matching to a perfect matching of H. △

Claim 2. *Let M_1, M_2 be perfect matchings of H. Then* $\operatorname{sgn}(M_1) = \operatorname{sgn}(M_2)$.

Proof. Due to Lemma 4.25, it suffices to show that each inner face f of H is bounded by a simple cycle of length $\ell_f \equiv 2 \pmod 4$. This can be verified by distinguishing all different types of inner faces of H, see Fig. 4.22:

i) The inner faces of the pseudotriangle gadgets have length $10 \equiv 2 \pmod 4$ by Lemma 4.20.

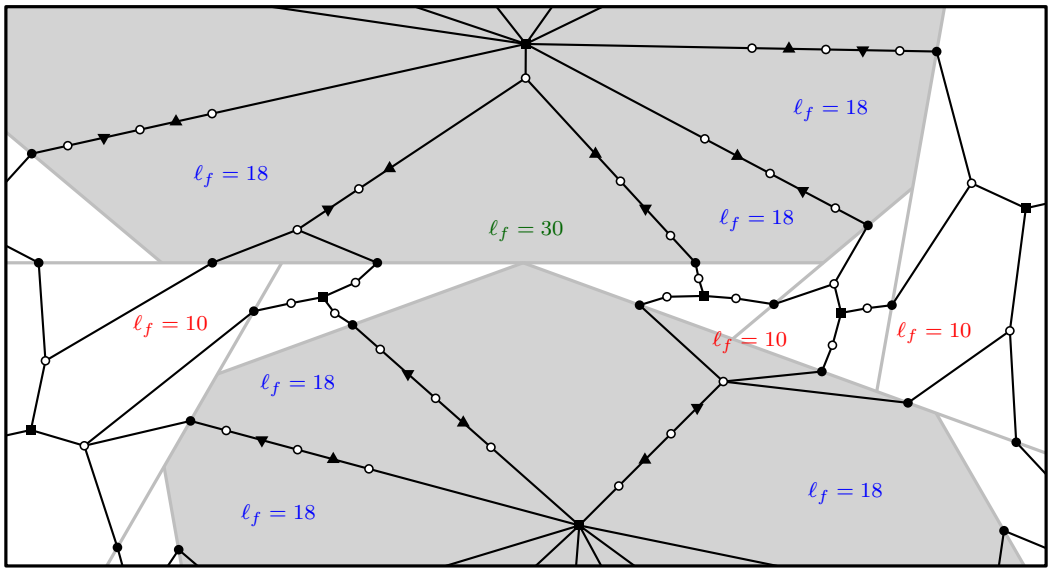

Figure 4.22: A part of the incidence graph of the system $A'_S\mathbf{x} = \mathbf{e_1}$ showing the different lengths of its faces.

ii) The inner faces corresponding to a polygon corner which is not touching another polygon have length $4 + 14 \equiv 2 \pmod 4$ where the 4 comes from the part inside the polygon (a path consisting of an edge-variable-vertex, an equation-vertex, a vertex-variable-vertex, another equation-vertex, and another edge-variable-vertex) and the 14 comes from the part inside the pseudotriangle due to Lemma 4.20.

iii) The inner faces corresponding to a corner of a polygon P_1 which is touching the side of another polygon P_2 have length $4 + 2 + 2 \cdot 12 \equiv 2 \pmod 4$ where the 4 comes from the part inside P_1 as in the previous case, the 2 comes from the part inside P_2 (a path consisting of an edge-variable-vertex, an equation-vertex, and another edge-variable-vertex), and the two 12's come from the parts inside the two pseudotriangles due to Lemma 4.20.

Since these are all types of inner faces of H, this finishes the proof. △

Finally, from Claims 1 and 2 we immediately obtain

$$\det(A'_S) = \sum_M \operatorname{sgn}(M) p_M \neq 0 \ . \qquad \square$$

We want to remark that, in the proof of Theorem 4.26, we only considered the signs of the entries of A'_S to show that $\det(A'_S) \neq 0$. Matrices with this property are known as *sign non-singular matrices*. See, e.g., [BS95] for more information on this topic.

From the solution to a drawing. Next we will show that the system of equations $A_S\mathbf{x} = \mathbf{e_1}$ is appropriate for computing similarly-aligned odd K-gon contact representations.

Theorem 4.27. *The unique solution of the system $A_S\mathbf{x} = \mathbf{e_1}$ is non-negative if and only if the K-contact structure S is induced by a similarly-aligned odd K-gon contact representation of G in which each vertex is represented by a homothetic copy of its prototype.*

Proof. Assume that there is a contact representation $\mathcal{S}$ of G with the given prototypes that induces the K-contact-structure S. Then the edge lengths and prototype scaling factors given by $\mathcal{S}$ define a non-negative solution of $A_S\mathbf{x} = \mathbf{e_1}$.

For the opposite direction, assume that the solution of $A_S\mathbf{x} = \mathbf{e_1}$ is non-negative. Let f be an inner face of G. Further, let $x_0, \ldots, x_{k-1}$ be the edge-variables of the corresponding face of G_{skel} in clockwise order and, for $i = 0, \ldots, k-1$, let s_i be the slope assigned to the edge of G_{skel} corresponding to x_i. Then, due to Lemma 4.18, there exists a pseudotriangle P_f with slopes $s_0, \ldots, s_{k-1}$ and side lengths $x_0, \ldots, x_{k-1}$ in clockwise order. Thus the existence of the wanted contact representation of G follows from Lemma 4.13 by assigning to each inner face of G_{skel} which corresponds to a face f of G the pseudotriangle P_f and to each face of G_{skel} which corresponds to a vertex v of G the prototype P_v scaled by the factor x_v. $\square$

4.5 Equations for parallel-sided even K-gon contact representations

In this section let $K \geq 6$ be an even integer, let G be an inner triangulation of the K-cycle $a_0, \ldots, a_{K-1}$ (in clockwise order), let S be a K-contact structure of G, and let $2G^\star_+ := 2G^\star_+(S)$. Further, for each inner vertex v of G, let P_v be a convex K-gon and let Q be a convex K-gon with sides $q_0, \ldots, q_{K-1}$ in clockwise order such that the P_v and Q are parallel-sided even K-gons. We call P_v the *prototype* of v and q_i the prototype of the outer vertex a_i. We will propose a system of linear equations that allows us to compute a parallel-sided even K-gon contact representation of G in which each inner vertex v is represented by a homothetic copy of its prototype P_v and the outer face is represented by a K-gon whose sides have the same slopes as the sides of Q and which induces the K-contact structure S. If such a contact representation does not exist, the solution of the system will have negative variables.

Description of the system of equations. The skeleton graph G_{skel} of the wanted contact representation can be constructed in a similar way as in the last section. See Fig. 4.23 for an example of the following construction. The skeleton graph G_{skel} is a subgraph of the medial graph of $2G^\star_+$. It contains exactly those edges of the medial graph of $2G^\star_+$ that correspond to an angle of an inner normal vertex. In particular, it contains all vertices of the medial graph except those corresponding to the outer edges of $2G^\star_+$. As in the last section, we assign slopes to the orientations of the edges of G_{skel}. Here we have to be a bit more careful than in the last section. Since $2G^\star_+$ has faces of degree two, some edges of G_{skel} do not correspond to a unique angle of $2G^\star_+$.

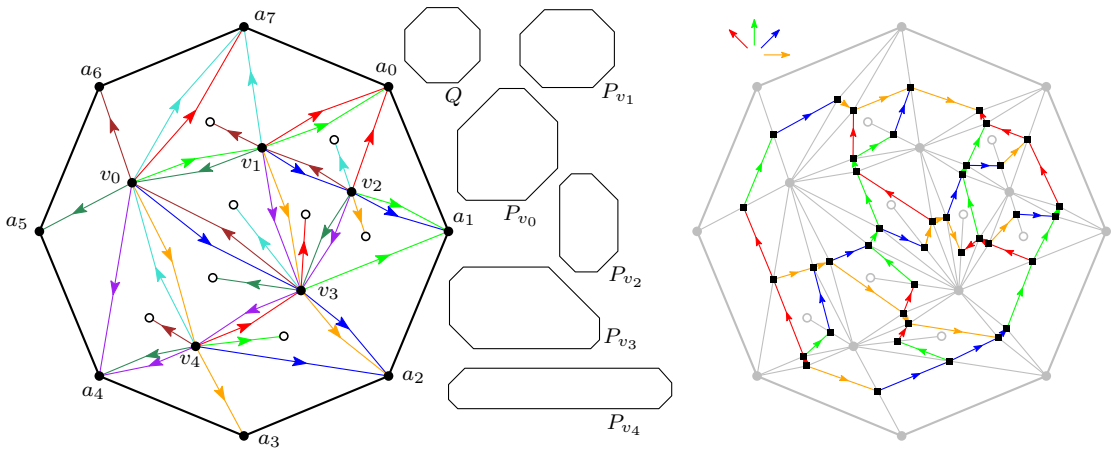

Figure 4.23: Left: the graph $2G^\star_+$ with its 8-proper coloring. Middle: equiangular prototypes for this graph. Right: the skeleton graph G_{skel} of the contact representation corresponding to $2G^\star_+$ with colors representing the slopes assigned to the edges (since the prototypes are parallel-sided even 8-gons, there are only 4 different slopes in total). The contact representation in Fig. 3.25 is a drawing of G_{skel} using these slopes.

Therefore, the slopes of these edges are multiply defined. Let e be such an edge and let v and w be the two normal vertices of $2G^\star_+$ to whose angles the edge e corresponds. If $e \in E_i(v)$, then by definition of the K-proper coloring, $e \in E_{i+\frac{K}{2}}(w)$. Therefore, we assign the slope $\text{slope}_i(P_v)$ to one orientation of e and the slope $\text{slope}_{i+\frac{K}{2}}(P_w)$ to the opposite orientation of e. Since P_v and P_w are parallel-sided even K-gons, we have $\text{slope}_i(P_v) = -\text{slope}_{i+\frac{K}{2}}(P_w)$. Hence, the assignment of the slopes to the edges of G_{skel} is well-defined. Note that, as in the last section, the wanted contact representation of G is a straight-line drawing of G_{skel} in which each edge has the slope that has been assigned to it.

The variables and equations are defined as in the last section. We have a vertex-variable x_v for each inner vertex v of G and an edge-variable x_e for each edge e of G_{skel} fulfilling equations (4.5)–(4.7). The entire system is denoted by $A_S\mathbf{x} = \mathbf{e_1}$. Analogously to Lemma 4.21 in the last section, it can be shown that the slopes assigned to the edges of a face of G_{skel} form a slope sequence of a pseudotriangle. Therefore, we can replace the equations of the type (4.6) according to Lemma 4.21. We denote the resulting system of equations by $A'_S\mathbf{x} = \mathbf{e_1}$.

Unique solvability. We will prove the unique solvability of $A_S\mathbf{x} = \mathbf{e_1}$ using the same technique as in the last section.

Theorem 4.28. *The system $A_S\mathbf{x} = \mathbf{e_1}$ is uniquely solvable.*

Proof. As in the proof of Theorem 4.26, it suffices to show that $\det(A'_S) \neq 0$. For this purpose, we will define a crossing-free embedding of the incidence graph H of the system $A'_S\mathbf{x} = \mathbf{e_1}$ into the plane. This embedding is defined as in the proof of Theorem 4.26 with the following difference: Let f be a face of $2G^\star_+$ with $\deg(f) = 2$. Then f intersects the larger circles around its two incident vertices. We merge the two corresponding edge-variable-vertices to a single edge-variable-vertex by connecting them inside f. Only the edge-variable-vertices inside an inner face of $2G^\star_+$ of degree at least 3 (these faces correspond to the inner faces of G) contribute to the boundary of a pseudotriangle.

Claim 1. *The graph H has a perfect matching.*

Proof. We describe an explicit construction of a perfect matching of H. We look at the unique K-proper coloring of $2G^\star_+$. The K equation-vertices adjacent to an inner normal vertex u of $2G^\star_+$ are corresponding to the K colors: an equation-vertex has color c if it is opposite to the outgoing edges of colors c and $c+1$. The equation-vertices of colors $0, \dots, \frac{K}{2} - 2$ are always matched with the adjacent edge-variable-vertex that precedes u in the clockwise order of adjacent vertices. The equation-vertices of colors $\frac{K}{2} + 1, \dots, K - 1$ are always matched with the adjacent edge-variable-vertex that succeeds u in the clockwise order of adjacent vertices. For the remaining two equation-vertices, we distinguish three cases concerning the outgoing edge e of color 0 in $2G^\star_+$, see Fig. 4.24 for an illustration.

i) If e is a stack edge, we can choose either of the constructions for the two remaining cases.

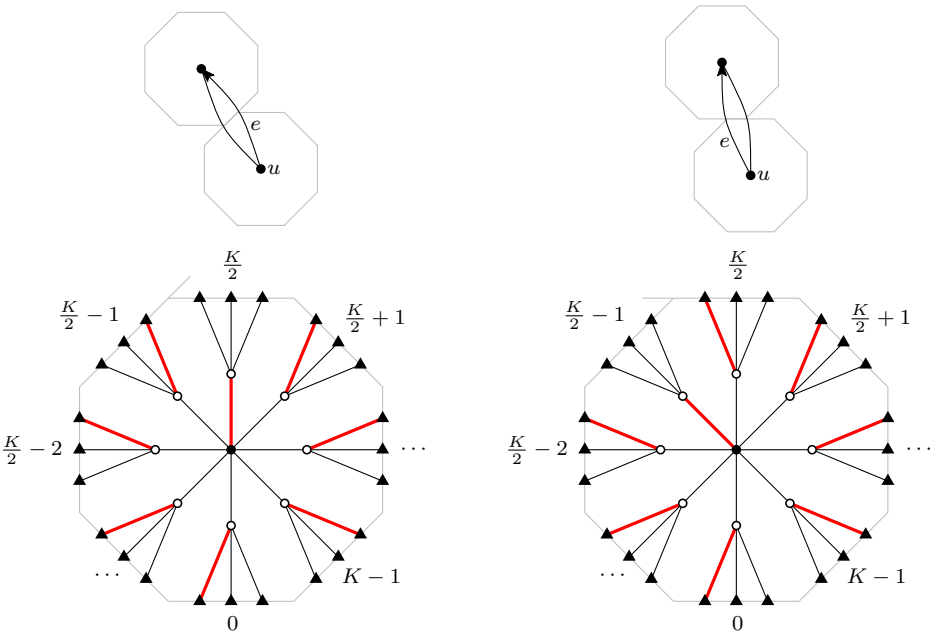

Figure 4.24: Illustration of the matching rule for the K equation-vertices corresponding to an inner vertex of G, compare Fig. 4.19. Two cases are distinguished concerning the segment ending in the upper left corner.

ii) If e is a normal edge and the parallel edge of e is the predecessor of e in the clockwise order of the incident edges of u, then u is matched with the equation-vertex of color $\frac{K}{2}$ and the equation-vertex of color $\frac{K}{2}-1$ with the adjacent edge-variable-vertex that precedes u in the clockwise order of adjacent vertices.

iii) If e is a normal edge and the parallel edge of e is the successor of e in the clockwise order of the incident edges of u, then u is matched with the equation-vertex of color $\frac{K}{2}-1$ and the equation-vertex of color $\frac{K}{2}$ with the adjacent edge-variable-vertex that succeeds u in the clockwise order of adjacent vertices.

It is clear that all vertex-variable-vertices and their adjacent equation-vertices are incident to exactly one matching edge. Now we will show that also the edge-variable-vertices corresponding to a face of $2G^\star_+$ of degree two are incident to exactly one matching edge. Let u be such an edge-variable-vertex. Then u is adjacent to two equation-vertices v and v' corresponding to colors i and $i+\frac{K}{2}$, respectively, for some i. By possibly exchanging the names of v and v', we can assume that $i \in \{0,\dots,\frac{K}{2}-1\}$. Let w and w' be the vertex-variable-vertices adjacent to v and v', respectively. Note that u precedes w in the clockwise order of adjacent vertices of v if and only if u does not succeed w' in the clockwise order of adjacent vertices of v'. Therefore, if $i \neq \frac{K}{2}-1$, then u is matched with v if and only if it is not matched with v'. The same holds if $i = \frac{K}{2}-1$ and w is not matched with v. If w is matched with v, then we are in case **iii)** of the above case distinction, see Fig. 4.24 (right). Thus u is not the vertex preceding w in the clockwise order of adjacent vertices of v since that vertex does not correspond to a face of $2G^\star_+$ of degree two. Hence, in this last case, u is matched with v' and not with v.

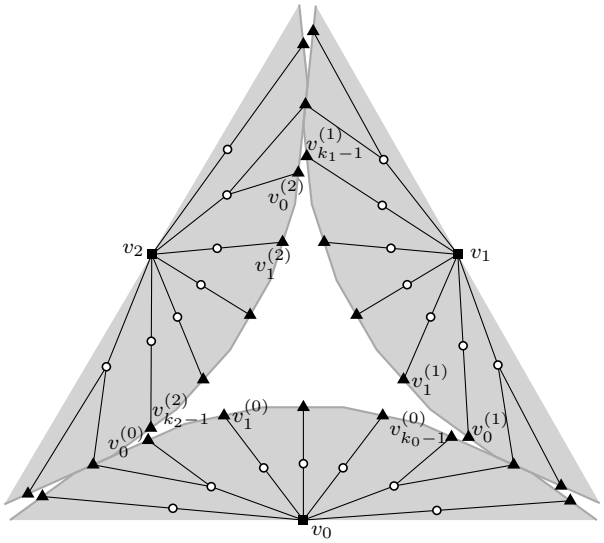

Figure 4.25: The edge-variable-vertices corresponding to stack vertex.

Next we will show that exactly two edge-variable-vertices of every stack vertex f remain unmatched. Let $v_0^{(0)}, \dots, v_{k_0-1}^{(0)}$, $v_0^{(1)}, \dots, v_{k_1-1}^{(1)}$, and $v_0^{(2)}, \dots, v_{k_2-1}^{(2)}$ be the edge-variable-vertices of the three concave arcs of P_f in counterclockwise order (see Fig. 4.25), and let $c_i^{(j)}$ be the color of $v_i^{(j)}$. Further, for $j = 0, 1, 2$, let v_j be the vertex-variable-vertex corresponding to the vertices $v_i^{(j)}$ (we also denote the corresponding normal vertex of $2G^\star$ by v_j). Note that $c_{k_j-1}^{(j)} = c_0^{(j+1)} + \frac{K}{2} - 1$ for $j = 0, 1, 2$ and upper indices taken modulo 3.

We will now take a closer look which of the vertices $v_i^{(j)}$ are already matched. Let $j \in \{0, 1, 2\}$. If $i \notin \{0, k_j - 1\}$, then $v_i^{(j)}$ and v_j are the only neighbors of their common adjacent equation-vertex. This leads to the following observation.

Fact 1. *Let $i \in \{1, \dots, k_j - 2\}$ and let $c \in \{\frac{K}{2} - 1, \frac{K}{2}\}$ be the color of the equation-vertex that v_j is matched with. Then the vertex $v_i^{(j)}$ is already matched if and only if $c_i^{(j)} \neq c$.*

Let e be the first one of the two edges between v_j and v_{j+1} in the clockwise order of incident edges of v_j. If e is oriented from v_j to v_{j+1} in $2G_+^\star$, then $v_{k_j-1}^{(j)}$ precedes v_j in the clockwise order of adjacent vertices of its adjacent equation-vertex and v_0^{j+1} does not succeed v_{j+1} in the clockwise order of adjacent vertices of its adjacent equation-vertex. Therefore, if $c_{k_j-1}^{(j)} \in \{0, \dots, \frac{K}{2} - 2\}$ (and thus $c_0^{(j+1)} \in \{\frac{K}{2} + 1, \dots, K - 1\}$), the vertex $v_{k_j-1}^{(j)}$ is already matched and $v_0^{(j+1)}$ is not matched yet. Similarly, it follows that if e is oriented from v_{j+1} to v_j in $2G_+^\star$ and the colors $c_{k_j}^{(j)}$ and $c_0^{(j+1)}$ are in the same ranges as before, then $v_0^{(j+1)}$ is already matched, but $v_{k_j}^{(j)}$ is not matched yet. This leads to the following observation.

Fact 2. *If $c_{k_j-1}^{(j)} \in \{0, \dots, \frac{K}{2} - 2\}$ (or equivalently $c_0^{(j+1)} \in \{\frac{K}{2} + 1, \dots, K - 1\}$), then exactly one of $v_{k_j-1}^{(j)}$ and $v_0^{(j+1)}$ is already matched.*

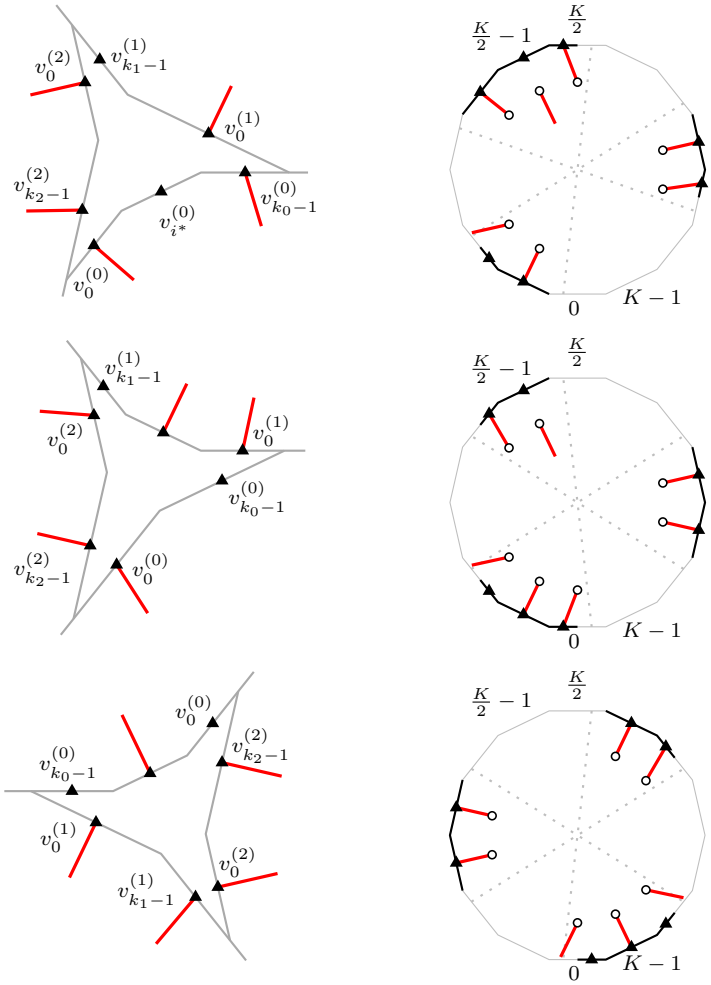

Figure 4.26: Left: examples of the three cases in the proof of Claim 1. In each case exactly two of the edge-variable-vertices are not matched. Right: visualizations of the three arcs of each of the three pseudotriangles explaining the matching edges.

Now we distinguish three cases. See Fig. 4.26 for examples of these three cases.

i) First, we assume that there are edge-variable-vertices of colors $\frac{K}{2}-1$ and $\frac{K}{2}$. After possibly relabeling the three concave arcs, we can assume that $c_{i^*}^{(0)} = \frac{K}{2}-1$ and $c_{i^*+1}^{(0)} = \frac{K}{2}$ for some i^*. Then, exactly one of $v_{i^*}^{(0)}$ and $v_{i^*+1}^{(0)}$ is already matched. Since the colors $c_i^{(j)}$ are pairwise different, it follows from Fact 1 that, for all j and i with $i \notin \{0, k_j - 1\}$ and $(j,i) \neq (0,i^*)$, the vertex $v_i^{(j)}$ is already matched. We will now consider the cases where $i \in \{0, k_j - 1\}$. If $i^* \neq 0$, then $c_0^{(0)} \in \{3, \dots, \frac{K}{2}-2\}$ and, since $k_0 \neq 1$, the vertex $v_0^{(0)}$ precedes v_0 in the clockwise order of adjacent vertices of their common adjacent equation-vertex. Hence, $v_0^{(0)}$ is already matched in this case. Analogously, it follows that $v_{k_0-1}^{(0)}$ is already matched if $i^* \neq k_0 - 1$. If $k_1 = 1$, then $v_0^{(1)} = v_{k_1-1}^{(1)}$ and will be considered when we consider $v_{k_1-1}^{(1)}$. Otherwise, if $k_1 \neq 1$, then

$c_0^{(1)} \in \{1, \dots, \frac{K}{2} - 3\}$ and $v_0^{(1)}$ precedes v_1 in the clockwise order of adjacent vertices of their common adjacent equation-vertex. Hence, $v_0^{(1)}$ is already matched in this case. Analogously, it follows that $v_{k_2-1}^{(2)}$ is already matched if $k_2 \neq 1$. Finally, since $c_{k_1-1}^{(1)} \in \{1, \dots \frac{K}{2} - 3\}$, it follows from Fact 2 that exactly one of $v_{k_1-1}^{(1)}$ and $v_0^{(2)}$ is already matched.

ii) Now we assume that there is an edge-variable-vertex of color $\frac{K}{2} - 1$ but none of color $\frac{K}{2}$ (the case that there is an edge-variable-vertex of color $\frac{K}{2}$ but none of color $\frac{K}{2} - 1$ is symmetric). After possibly relabeling the three concave arcs, we can assume that $c_{k_0-1}^{(0)} = \frac{K}{2} - 1$. If $v_{k_0-1}^{(0)}$ precedes v_0 in the clockwise order of adjacent vertices of their common adjacent equation vertex, then v_0 is matched with this equation-vertex and $v_{k_0-1}^{(0)}$ is not matched yet. Otherwise, $v_{k_0-1}^{(0)}$ is not matched yet anyways. Analogously to case **i)**, it follows that exactly one of $v_{k_1-1}^{(1)}$ and $v_0^{(2)}$ is already matched and the remaining edge-variable-vertices are already matched.

iii) Finally, we assume that there are no edge-variable-vertices of colors $\frac{K}{2} - 1$ and $\frac{K}{2}$. Then, for $j = 0, 1, 2$, exactly one of $c_{k_j-1}^{(j)}$ and $c_0^{(j+1)}$ is contained in the set $\{0, \dots, \frac{K}{2} - 2\}$ and the other one in $\{\frac{K}{2} + 1, \dots, K - 1\}$. Therefore, exactly three of the $c_0^{(j)}$ and $c_{k_j-1}^{(j)}$ are contained in each of these two parts. Thus, after possibly relabeling the three concave arcs, we can assume that $c_{k_0-1}^{(0)}, c_0^{(2)}, c_{k_2-1}^{(2)} \in \{0, \dots, \frac{K}{2} - 2\}$ and $c_0^{(1)}, c_{k_1-1}^{(1)}, c_0^{(0)} \in \{\frac{K}{2} + 1, \dots, K - 1\}$. Then, by Fact 2, exactly one of $v_0^{(0)}$ and $v_{k_2-1}^{(2)}$ and exactly one of $v_{k_0-1}^{(0)}$ and $v_0^{(1)}$ are already matched. Further, if $k_1 \neq 1$, then $v_{k_1-1}^{(1)}$ succeeds v_1 in the clockwise order of adjacent vertices of their common adjacent equation-vertex and, hence, $v_{k_1-1}^{(1)}$ is already matched in this case. Analogously, it follows that $v_0^{(2)}$ is already matched if $k_2 \neq 1$. The remaining edge-variable-vertices we have not considered yet are already matched due to Fact 1.

Since in all three cases exactly two of the edge-variables-vertices are not matched yet, we can apply Lemma 4.22 to extend the matching to a perfect matching of H. △

Claim 2. *Let M_1, M_2 be perfect matchings. Then* $\operatorname{sgn}(M_1) = \operatorname{sgn}(M_2)$.

Proof. Due to Lemma 4.25, it suffices to show that each inner face f of H is bounded by a simple cycle of length $\ell_f \equiv 2 \pmod 4$. This can be verified by distinguishing all different types of inner faces of H, see Fig. 4.27:

i) The inner faces of the pseudotriangle gadgets have length $10 \equiv 2 \pmod 4$ by Lemma 4.20.

ii) The inner faces corresponding to a polygon corner which is not touching another polygon have length $4 + 14 \equiv 2 \pmod 4$ where the 4 comes from the part inside the polygon (a path consisting of an edge-variable-vertex, an equation-vertex, a vertex-variable-vertex, another equation-vertex, and another edge-variable-vertex) and the 14 comes from the part inside the pseudotriangle due to Lemma 4.20.

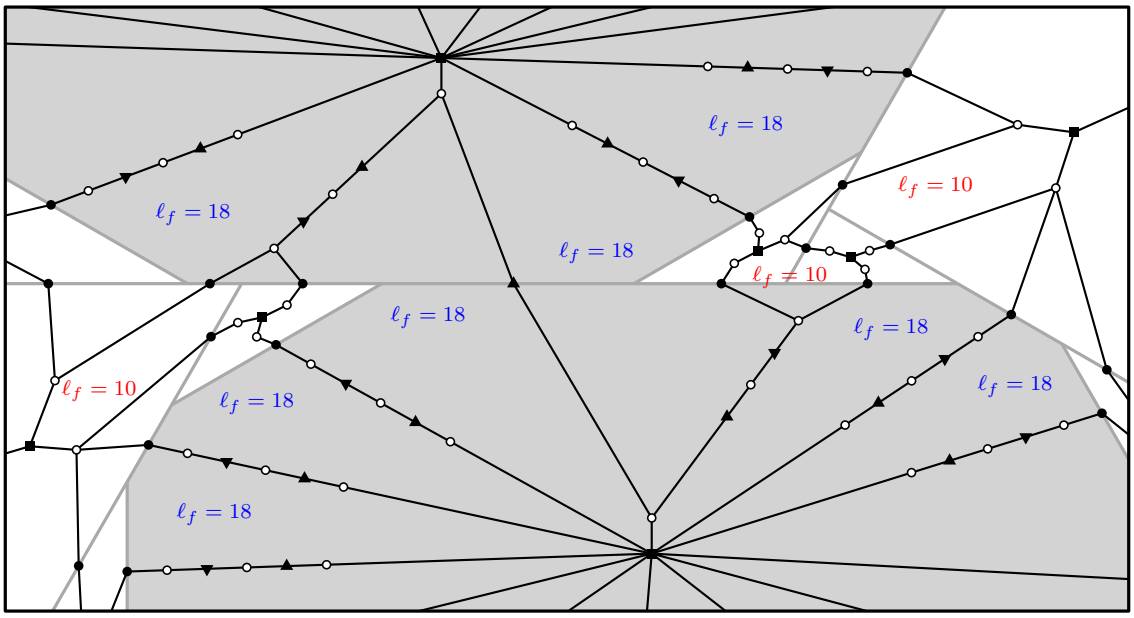

Figure 4.27: A part of the incidence graph of the system $A'_S\mathbf{x} = \mathbf{e_1}$ showing the different lengths of its faces.

iii) The inner faces corresponding to a corner of a polygon P_1 which is touching the side of another polygon P_2 have length $4+2+12 \equiv 2 \pmod 4$ where the 4 comes from the part inside P_1 as in the previous case, the 2 comes from the part inside P_2 (a path consisting of an edge-variable-vertex, an equation-vertex, and another edge-variable-vertex), and the 12 comes from the part inside the pseudotriangle due to Lemma 4.20.

Since these are all types of inner faces of H, this finishes the proof. △

From Claims 1 and 2 we immediately obtain

$$\det(A'_S) = \sum_M \operatorname{sgn}(M) P_M \neq 0 \ ,$$

which closes the proof. □

From the solution to a drawing. Analogously to the similarly-aligned odd K-gon contact representations in the last section, it can be shown that the system of equations $A_S\mathbf{x} = \mathbf{e_1}$ is appropriate for computing parallel-sided even K-gon contact representations.

Theorem 4.29. *The unique solution of the system $A_S\mathbf{x} = \mathbf{e_1}$ is non-negative if and only if the K-contact structure S is induced by a parallel-sided even K-gon contact representation of G in which each vertex is represented by a homothetic copy of its prototype.* □

4.6 Properties of the solutions

It turns out that the signs of the variables in the solution of the system $A_S\mathbf{x} = \mathbf{e_1}$ have some special properties. These properties play a central role in the following chapters. We will first prove these properties for the general case where the solution contains negative variables and then prove similar properties for the case that the solution is non-negative.

4.6.1 Solutions with negative variables

In this section we consider solutions of the system $A_S\mathbf{x} = \mathbf{e_1}$ that may contain negative variables. First, we study in detail the case that K is odd. Afterwards, we briefly consider the case that K is even.

Equations for odd K. We will introduce a notion of edges of $G^\star$ that separate edges of G_{skel} whose corresponding edge-variable-vertices have different signs in the solution of $A_S\mathbf{x} = \mathbf{e_1}$, considering the canonical simultaneous embedding of $G^\star_+$ and G_{skel} (remember that G_{skel} is a subgraph of the medial graph of $G^\star_+$ and see Figs. 2.1 and 4.16). In the following, if we refer to the value of a variable x, we always refer to the value of x in the unique solution of $A_S\mathbf{x} = \mathbf{e_1}$. Further, we set $\text{sign}(x) := +1$, if $x \geq 0$, and $\text{sign}(x) := -1$ otherwise. If $\text{sign}(x) = +1$, we say that x is *non-negative* and, if $\text{sign}(x) = -1$, we say that x is *negative*. We also translate this notion to the edges e of G_{skel} by setting $\text{sign}(e) := \text{sign}(x_e)$.

Now we will define a multiset $E_{+,-}$ of orientations of edges of $G^\star$ and call it the set of *sign-separating edges*. The definition we give here is not exactly the definition given in [FSS18a]. It is simpler and also allows simpler proofs. We distinguish different types of vertices z of G_{skel} and the signs of their incident edges, see Fig. 4.28.

i) If $\deg(z) = 2$, its two incident faces correspond to a normal vertex v and a stack vertex w of $G^\star$. If the two incident edges of z have different signs, i.e., one of them is non-negative and the other one is negative, we add the edge (v, w) to $E_{+,-}$ and say that it is a *sign-separating edge of type (I)*.

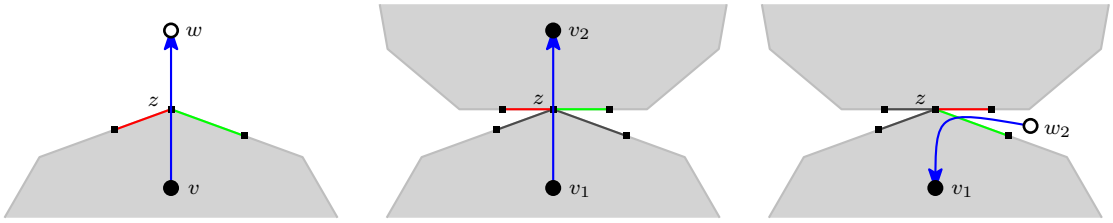

(a) Type (I). (b) Type (II). (c) Type (III).

Figure 4.28: Definition of the set $E_{+,-}$ of sign-separating edges. The edges of G_{skel} are drawn in green, if they are non-negative, in red, if they are negative, and in gray if the sign does not matter. The sign-separating edges are drawn in blue.

ii) If $\deg(z) = 4$, its incident faces correspond in clockwise order to a normal vertex v_1, a stack vertex w_1, a normal vertex v_2, and a stack vertex w_2 of $G^\star$. We denote these faces by f_{v_1}, f_{w_1}, f_{v_2}, and f_{w_2}, respectively. We assume that in S the edge v_1v_2 is oriented from v_1 to v_2. If the two common incident edges of z and f_{v_2} have different signs, then we add the edge (v_1, v_2) to $E_{+,-}$ and say that it is a *sign-separating edge of type (II)*.

iii) If $\deg(z) = 4$ and if the two common incident edges of z and f_{w_i} for an $i \in \{1, 2\}$ have different signs, we add the edge (w_i, v_1) to $E_{+,-}$ and say that it is a *sign-separating edge of type (III)*.

Next we will study the sign-separating edges incident to a fixed stack vertex w of $G^\star$. Let f be the face of G_{skel} corresponding to w and let $e_0, \dots, e_{k-1}$ be the clockwise traversal of the corresponding facial cycle. For $i = 0, \dots, k-1$, let s_i be the slope assigned to e_i. Further, let $A, B, C \in \{0, \dots, k-1\}$ be the three indices such that s_i and s_{i+1} induce a convex corner between the drawings of e_i and e_{i+1} in the pseudotriangle corresponding to f, compare Section 4.3. If, for some i, one of the edges e_i and e_{i+1} is non-negative and the other one is negative, we call this a *sign change* at the common incident vertex of e_i and e_{i+1}. If $i \in \{A, B, C\}$, we call this sign change a *convex sign change* and otherwise a *concave sign change*. The following lemma shows that in $E_{+,-}$ there are at least as many incoming as outgoing edges for w.

Lemma 4.30. *In the facial cycle of a face f of G_{skel} corresponding to a stack vertex of $G^\star$, there are at least as many concave sign changes as convex sign changes.*

Proof. Let P_f be the pseudotriangle corresponding to the face f. We will prove that the statement of the lemma is not only true for P_f itself but also for any subpseudotriangle P of P_f in an arbitrary cutting of P_f into triangles. The proof is by induction on the number of concave corners of P. If there is no concave corner, i.e., P is a triangle, then the equations for this pseudotriangle ensure that all three edge-variables have the same sign as the triangle-variable corresponding to the unique triangle of the trivial cutting of P into triangles. Therefore, there is no sign change and the statement of the lemma holds.

Now we consider the case that P has at least one concave corner. The following claim allows us to apply the induction hypothesis to P.

Claim 1. *If P has a convex sign change at the corner c_j and one of the corners c_{j-1} and c_{j+1} is a concave corner without a sign change, then we can cut P into two subpseudotriangles such that one of these two subpseudotriangles has the same number of convex and concave sign changes as P.*

Proof. This proof is illustrated in Fig. 4.29 (first row). Because of symmetry we can assume that c_{j+1} is a concave corner without a sign change. We cut P along a line from the corner c_{j+1} to a point p on the side between the corners c_{j-1} and c_j into two subpseudotriangles. Let P' be the resulting subpseudotriangle that has c_j as one of its corners and let P'' be the other resulting subpseudotriangle. Then P' is in fact a triangle and thus all three sides of P' have the same sign. In the following, we denote

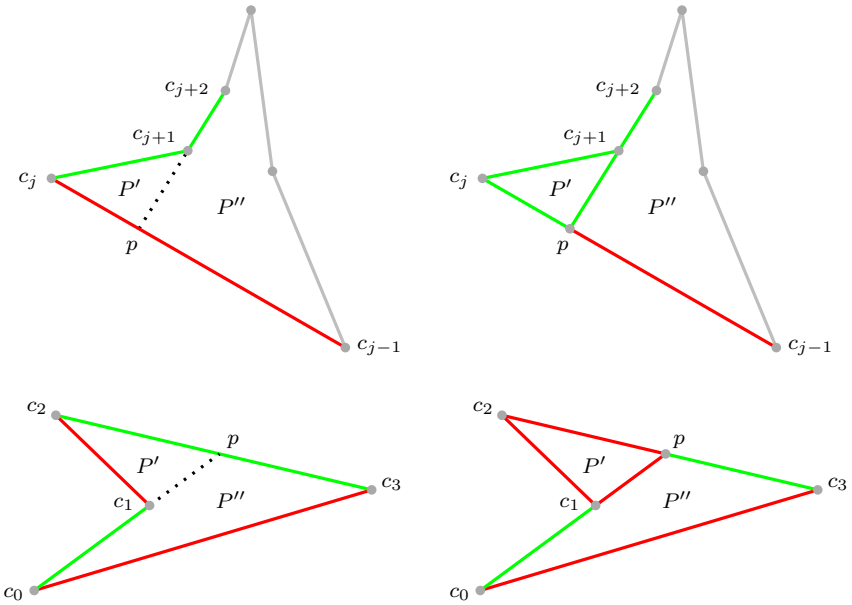

Figure 4.29: On the left, two pseudotriangles with some sides marked as negative (red) or non-negative (green) and a cutting into two subpseudotriangles P' and P'' are shown. On the right, the resulting signs of the edges of the skeleton of the respective cut pseudotriangle are shown.

the edge-variable corresponding to the edge vw of the skeleton graph by $x_{v,w}$. Then the fact, that P' is a triangle, implies that $\operatorname{sign}(x_{p,c_{j+1}}) = \operatorname{sign}(x_{c_j,c_{j+1}}) = \operatorname{sign}(x_{c_{j+1},c_{j+2}})$ and, therefore, $\operatorname{sign}(x_{p,c_{j+2}}) = \operatorname{sign}(x_{p,c_{j+1}})$. Further, it implies that $\operatorname{sign}(x_{p,c_j}) = \operatorname{sign}(x_{p,c_{j+1}}) = \operatorname{sign}(x_{p,c_{j+2}})$. Together with $x_{c_{j-1},c_j} = x_{c_{j-1},p} + x_{p,c_j}$ and $\operatorname{sign}(x_{c_{j-1},c_j}) \neq \operatorname{sign}(x_{c_j,c_{j+1}})$, it follows that $\operatorname{sign}(x_{c_{j-1},p}) = \operatorname{sign}(x_{c_{j-1},c_j}) \neq \operatorname{sign}(x_{p,c_{j+2}})$. Hence, P'' has a convex sign change at p and it has sign changes at c_{j-1} and c_{j+2} if and only if P has sign changes at c_{j-1} and c_{j+2}, respectively. Therefore, P'' has the same number of convex and concave sign changes as P. △

Since a pseudotriangle has only three convex corners, there are at most three convex sign changes. Further, the total number of sign changes is even. We distinguish four cases concerning the number of convex sign changes of P.

i) If there is no convex sign change, the statement of the lemma trivially holds.

ii) If there is exactly one convex sign change, there is at least one concave sign change since the total number of sign changes is even. Thus the statement of the lemma also holds in this case.

iii) If there are exactly two convex sign changes, there is either no concave sign change or there are at least two concave sign changes. Since in the latter case the statement of the lemma holds, we assume the former case. One of the two convex corners with a sign change has a neighboring concave corner. Since P has no concave sign changes, we can apply Claim 1 to P. Therefore, there is a proper subpseudotriangle of P that also has two convex but no concave sign changes, in contradiction to the induction hypothesis.

iv) If there are three convex sign changes, there is either exactly one concave sign change or there are at least three concave sign changes. Since in the latter case the statement of the lemma holds, we assume the former case. If P has at least two concave corners, there are also at least two concave corners that have a neighboring convex corner. Then there exists a concave corner without a sign change that has a neighboring convex corner. Since there are sign changes at all convex corners, we can apply Claim 1 to P in this case and obtain a proper subpseudotriangle of P that also has three convex sign changes and only one concave sign change, in contradiction to the induction hypothesis.

It remains to consider the case that P has only one concave corner. See Fig. 4.29 (second row) for an illustration of this situation. We denote the corners of P by $c_0, \dots, c_3$ in clockwise order. By relabeling the corners, we can assume that c_1 is the unique concave corner. Note that there is a sign change at each of the four corners. We cut P along a line from c_1 to a point p on the side between c_2 and c_3 into two subpseudotriangles. Let P' be the resulting subpseudotriangle that has c_2 as one of its corners and let P'' be the other resulting subpseudotriangle. Then P' and P'' are in fact triangles. Since P' is a triangle, we have $\operatorname{sign}(x_{c_2,p}) = \operatorname{sign}(x_{c_1,c_2})$. Because of $\operatorname{sign}(x_{c_2,c_3}) \neq \operatorname{sign}(x_{c_1,c_2})$ and $x_{c_2,c_3} = x_{c_2,p} + x_{p,c_3}$, this implies $\operatorname{sign}(x_{p,c_3}) = \operatorname{sign}(x_{c_2,c_3})$. Then, because of $\operatorname{sign}(x_{c_2,c_3}) \neq \operatorname{sign}(x_{c_3,c_1})$, the triangle P'' has a sign change at c_3. This contradicts the fact that there are no sign changes in a triangle.

Hence, in all four cases the statement of the lemma holds. □

In the following lemmas we prove some basic properties of the set $E_{+,-}$.

Lemma 4.31. *If the solution of $A_S\mathbf{x} = \mathbf{e_1}$ is not non-negative, then $E_{+,-} \neq \emptyset$.*

Proof. We distinguish two cases concerning the existence of a sign change in a face of G_{skel} corresponding to a stack vertex of $G^\star$.

i) Assume that there exists such a sign change. Since each concave sign change induces a sign-separating edge of type (I) and each convex sign change induces a sign-separating edge of type (III), we have $E_{+,-} \neq \emptyset$ in this case.

ii) Assume that there is no such sign change. Since each edge of G_{skel} is incident to a face corresponding to a stack vertex of $G^\star$, there exists such a face with only negative edges and another one with only non-negative edges in this case. Therefore, since G_{skel} is connected, there is a vertex of G_{skel} that is incident to such a face with only negative edges and such a face with only non-negative edges, implying the existence of a sign separating edge of type (II). Therefore, also in this case, we have $E_{+,-} \neq \emptyset$.

Hence, in both cases the statement of the lemma is true. □

Lemma 4.32. *In $E_{+,-}$ every vertex appears the same number of times as the start vertex and as the end vertex of an edge.*

Proof. The strategy of the proof is the following: We assign to each edge $e \in E_{+,-}$ a predecessor $\operatorname{pred}(e) \in E_{+,-}$. This assignment will be injective and fulfill the property

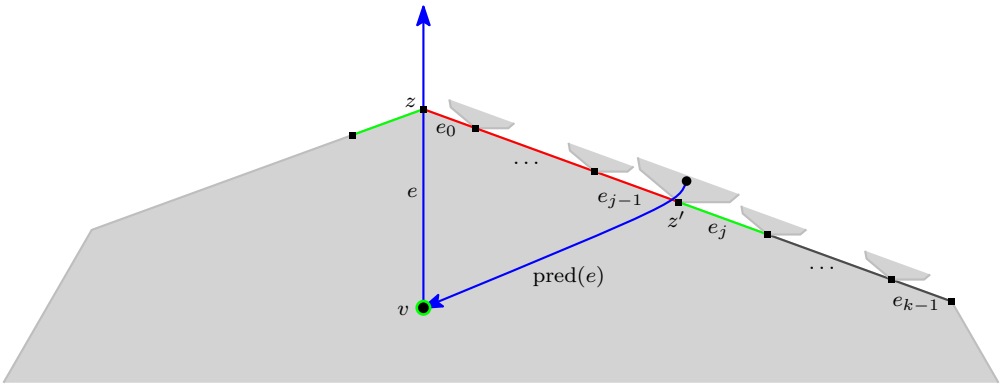

Figure 4.30: Construction of the predecessor edge of a sign-separating edge e of type (I). Normal vertices of $G^\star$ are drawn as disks. A green ring indicates that the corresponding variable is non-negative. The vertices of G_{skel} are drawn as squares. The edges of G_{skel} are drawn in green, if they are non-negative, in red, if they are negative, and in gray, if their sign does not matter.

that, for each edge $e \in E_{+,-}$, the endpoint of $\text{pred}(e)$ is the starting point of e. Since this assignment is a function from the finite set $E_{+,-}$ to the same set $E_{+,-}$, it has to be bijective. Finally, this implies the statement of the lemma.

First, let $e = (v, w)$ be a sign-separating edge of type (I). The following construction is illustrated in Fig. 4.30. Let z be the vertex of G_{skel} the edge e corresponds to. Assume that $\text{sign}(x_v) = +1$ (the case that $\text{sign}(x_v) = -1$ is analogous). Let $e_0, e_1, \dots, e_{k-1}$ be the edges of the cyclic traversal of the facial cycle of G_{skel} corresponding to v, starting at z with its negative incident edge (the other incident edge of z in this facial cycle is non-negative since e is a sign-separating edge of type (I)) and ending at the next vertex of G_{skel} that corresponds to an outgoing edge of v in $G^\star_+$, i.e., all intermediate vertices correspond to incoming edges of v in $G^\star_+$. Then $A_S\mathbf{x} = \mathbf{e_1}$ contains the equation $x_v = \sum_{i=0}^{k-1} x_{e_i}$. Since $x_v \geq 0$ and $x_{e_0} < 0$, there is a $j \in \{1, \dots, k-1\}$ with $x_{e_j} \geq 0$. We choose the minimal j with this property. Let z' be the start vertex of e_j in the oriented path $e_0, e_1, \dots, e_{k-1}$. Then z' is a vertex of degree four and we have $\text{sign}(e_{j-1}) = -1$ and $\text{sign}(e_j) = +1$. Therefore, z' corresponds to a sign-separating edge e' of type (II) that is incoming for v and we set $\text{pred}(e) = e'$.

Now let $e = (v_1, v_2)$ be a sign-separating edge of type (II). Let z be the vertex of G_{skel} the edge e corresponds to. Further, let f_{v_1} and f_{v_2} be the faces of G_{skel} corresponding to v_1 and v_2, respectively. If the two common incident edges of z and f_{v_1} have different signs, we define $\text{pred}(e)$ as in the case that e is a sign-separating edge of type (I), see Fig. 4.31a. Thus let us assume that these two edges have the same sign. The following construction is illustrated in Fig. 4.31b. Since e is a sign-separating edge of type (II), the two common incident edges of z and f_{v_2} have different signs. Let w_1 and w_2 be the stack vertices of $G^\star$ corresponding to the two remaining incident faces of z. We denote these faces by f_{w_1} and f_{w_2}, respectively. Then there is exactly one $i \in \{1, 2\}$ such that the two common incident edges of z

(a) First case: two edges incident to z are non-negative and two are negative.

(b) Second case: three edges incident to z are non-negative and one is negative, or vice versa.

Figure 4.31: Construction of the predecessor edge of a sign-separating edge e of type (II). Stack vertices are drawn as circles. See Fig. 4.30 for an explanation of the remaining vertex shapes and the edge colors used in this figure.

and f_{w_i} have different signs. Therefore, there is a sign-separating edge $e' = (w_i, v_1)$ of type (III) corresponding to z and we set $\text{pred}(e) = e'$.

Finally, let $e = (w, v)$ be a sign-separating edge of type (III). Let f_w be the face of G_{skel} corresponding to w. Each sign-separating edge of type (III) that is starting at w corresponds to a convex sign change in the facial cycle of f_w. Further, each concave sign change in this facial cycle corresponds to a sign-separating edge of type (I) that is ending at w. Due to Lemma 4.30 this facial cycle has at least as many concave sign changes as convex sign changes. Therefore, we can find an injective assignment from the sign-separating edges of type (III) starting at w to the sign-separating edges of type (I) ending at w. This assignment defines $\text{pred}(e)$.

It remains to prove the injectivity of the predecessor assignment. A sign-separating edge $e = (w, v)$ of type (I) can only be the predecessor of a sign-separating edge of type (III) starting at w. Since the assignment of the predecessor edges of the sign-separating edges of type (III) starting at w is injective by definition, there is at most one edge e' with $\text{pred}(e') = e$.

Now let $e = (v_1, v_2)$ be a sign-separating edge of type (II). Let f_{v_2} be the face of G_{skel} corresponding to v_2. Then e corresponds to a sign change in the facial cycle of f_{v_2}. Let z be the vertex of G_{skel} at which this sign change happens. If $x_{v_2} \geq 0$, a sign-separating edge e' with $\text{pred}(e') = e$ has to be a sign-separating of type (I) or (II) corresponding to the first vertex z' in the traversal of the facial cycle of f_{v_2} that corresponds to an edge of $G^\star_+$ that is outgoing for v_2 in S when starting at z and going in the direction of the negative incident edge of z. Analogously, if $x_w < 0$, the edge e' has to correspond to the first vertex z' in this traversal that corresponds to an edge of $G^\star_+$ that is outgoing for v_2 in S when going from z in the direction of the non-negative incident edge of z. If $\deg(z') = 2$, there is at most one sign-separating edge of type (I) corresponding to it and none of type (II) and, if $\deg(z') = 4$, there is at most one sign-separating edge of type (II) corresponding to it and none of type (I). Therefore, there is at most one edge e' with $\text{pred}(e') = e$.

Finally, let $e = (w, v)$ be a sign-separating edge of type (III). Then e corresponds to a sign change at a vertex z in the facial cycle of the face of G_{skel} corresponding to w. Further, a sign-separating edge e' with $\text{pred}(e') = e$ has to be a sign-separating

edge of type (I) or (II) that is outgoing for v and corresponds to the vertex z. As in the previous case, this edge is unique and, therefore, there is at most one edge e' with $\text{pred}(e') = e$. Hence, the predecessor assignment is injective. □

This immediately implies the following for the solution values of the variables corresponding to the edges of the outer face of G_{skel}.

Lemma 4.33. *The solution values of all variables corresponding to edges of the outer face of G_{skel} are non-negative.*

Proof. Since there are no sign-separating edges that are outgoing edges of outer normal vertices of $G^\star$, Lemma 4.32 implies that there are no sign-separating edges incident to outer normal vertices of $G^\star$. Therefore, either all variables corresponding to the edge of the outer face of G_{skel} are non-negative or all of them are negative. But since their sum is 1 (this is one of the equations), the latter is not possible and, hence, all of them are non-negative. □

The fact that the predecessor assignment in the proof of Lemma 4.32 is a bijection has implications for the signs of the edges of G_{skel}. For sign-separating edges e and e' with $\text{pred}(e) = e'$, we call e the *successor* of e'.

Lemma 4.34. *In a facial cycle of G_{skel} corresponding to a stack vertex w of $G^\star$, there are exactly as many concave sign changes as convex sign changes.*

Proof. The concave sign changes in this facial cycle correspond to the sign-separating edges of type (I) ending at w and the convex sign changes of this facial cycle correspond to the sign-separating edges of type (III) starting at w. Since the predecessor assignment induces a bijection between these two kinds of sign-separating edges, the numbers of concave and convex sign changes have to be equal. □

Lemma 4.35. *Let z be a vertex of G_{skel} corresponding to the normal edge (v_1, v_2) of $G^\star_+$. Let $e_1, \dots, e_4$ be the incident edges of z in clockwise order, starting with the two edges incident to the face of G_{skel} corresponding to v_1. Then $\text{sign}(e_1) = \text{sign}(e_4)$ or $\text{sign}(e_2) = \text{sign}(e_3)$. Further, if $\text{sign}(e_3) = \text{sign}(e_4)$, then $\text{sign}(e_1) = \text{sign}(e_2) = \text{sign}(e_3) = \text{sign}(e_4)$, see Fig. 4.32.*

Proof. Let w_1 and w_2 be the stack vertices of $G^\star$ such that e_2, e_3 are incident edges of the face of G_{skel} corresponding to w_1 and e_1, e_4 are incident edges of the face of G_{skel} corresponding to w_2. If $\text{sign}(e_1) \neq \text{sign}(e_4)$, then (w_2, v_1) is a sign-separating edge and its successor is (v_1, v_2). If $\text{sign}(e_2) \neq \text{sign}(e_3)$, then (w_1, v_1) is a sign-separating edge and its successor is also (v_1, v_2). Since (v_1, v_2) is contained at most once in $E_{+,-}$, this proves the first part of the statement of the lemma.

If $\text{sign}(e_1) \neq \text{sign}(e_4)$ or $\text{sign}(e_2) \neq \text{sign}(e_3)$, then, as we showed above, (v_1, v_2) is a sign-separating edge and, therefore, $\text{sign}(e_3) \neq \text{sign}(e_4)$. This proves the second part of the statement of the lemma. □

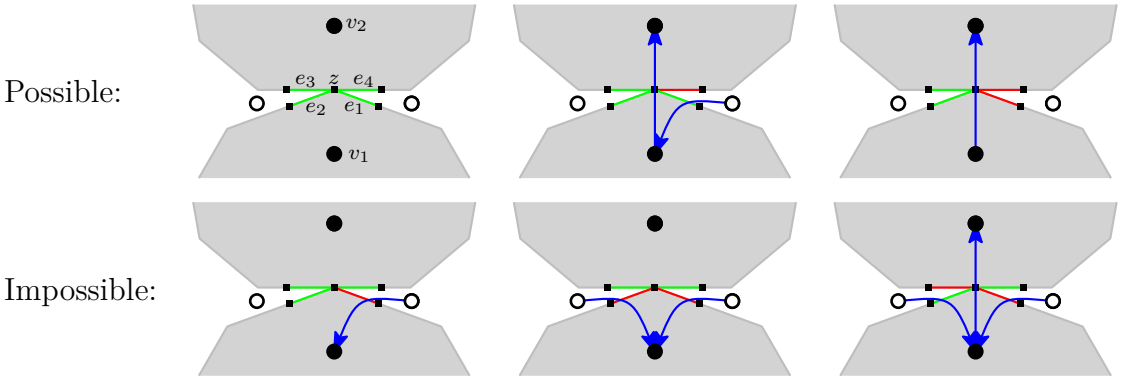

Figure 4.32: All possible (first row) and impossible (second row) combinations of signs of the incident edges of a vertex z of G_{skel} of degree four (in the case that K is odd), up to symmetry and the exchange of non-negative and negative edges. The sign-separating edges corresponding to sign changes at z are shown in blue.

Equations for even K. If K is even, we can define the set $E_{+,-}$ of sign-separating edges similar as in the case that K is odd. Again, we distinguish different types of vertices z of G_{skel} and the signs of their incident edges, see Fig. 4.33.

i) If $\deg(z) = 2$, its two incident faces correspond to a normal vertex v and a stack vertex w of $2G^\star$. If the two incident edges of z have different signs, i.e., one of them is non-negative and the other one is negative, we add the edge (v, w) to $E_{+,-}$ and say that it is a *sign-separating edge of type (I)*.

ii) If $\deg(z) = 3$, its incident faces correspond to two normal vertices v_1 and v_2 and a stack vertex w. We denote these faces by f_{v_1}, f_{v_2}, and f_w, respectively. We assume that in S the edge v_1v_2 is oriented from v_1 to v_2. If the two common incident edges of z and f_{v_2} have different signs, then we add the edge (v_1, v_2) to $E_{+,-}$ and say that it is a *sign-separating edge of type (II)*.

iii) If $\deg(z) = 3$ and if the two common incident edges of z and f_w have different signs, we add the edge (w, v_1) to $E_{+,-}$ and say that it is a *sign-separating edge of type (III)*.

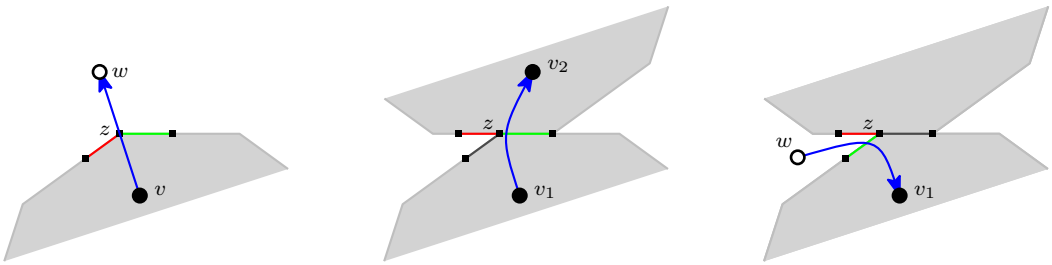

(a) Type (I). (b) Type (II). (c) Type (III).

Figure 4.33: Definition of the set $E_{+,-}$ of sign-separating edges for even K. The edges of G_{skel} are drawn in green, if they are non-negative, in red, if they are negative, and in gray if the sign does not matter. The sign-separating edges are drawn in blue.

In the following we will prove results for even K similar to those we have proven for odd K.

Lemma 4.36. *In the facial cycle of a face f of G_{skel} corresponding to a stack vertex of $G^\star$, there are at least as many concave sign changes as convex sign changes.*

In the proof of Lemma 4.30 we do not make use of the fact that K is odd. Therefore, we can prove Lemma 4.36 in exactly the same way.

Lemma 4.37. *If the solution of $A_S\mathbf{x} = \mathbf{e_1}$ is not non-negative, then $E_{+,-} \neq \emptyset$.*

Proof. We distinguish two cases concerning the existence of a sign change in a face of G_{skel} corresponding to a stack vertex of $2G^\star$.

i) If there exists such a sign change, it follows as in the proof for odd K (Lemma 4.31) that there exists a sign-separating edge.

ii) Assume that there is no such sign change. Let G'_{skel} be the graph obtained from G_{skel} by contracting all edges that are incident to two faces corresponding to normal vertices. Then in G'_{skel} each edge is incident to a face corresponding to a stack vertex. Now it follows as in the proof for odd K (Lemma 4.31) that in G'_{skel} there exists a vertex z that is incident to such a face f_1 with only negative edges and such a face f_2 with only non-negative edges. In G_{skel}, the vertex z corresponds to an edge $e = z_1z_2$ that is incident to two faces corresponding to normal vertices of $2G^\star$. For $i = 1, 2$, let z_i be the endpoint of e incident to f_i. If $\operatorname{sign}(e) = +1$, then there exists a sign-separating edge of type (II) corresponding to a sign change at z_1 and, if $\operatorname{sign}(e) = +1$, then there exists a sign-separating edge of type (II) corresponding to a sign change at z_2.

Hence, in each case we have $E_{+,-} \neq \emptyset$. □

Lemma 4.38. *In $E_{+,-}$ every vertex appears the same number of times as the start vertex and as the end vertex of an edge.*

Proof. As in the proof for odd K (Lemma 4.32), we assign to each edge $e \in E_{+,-}$ a predecessor $\operatorname{pred}(e) \in E_{+,-}$ that ends at the starting point of e and show that this assignment is injective.

For sign-separating edges of types (I) and (III), the predecessor is defined exactly as in the case that K is odd. So let e be a sign separating edge of type (II). Let z be the vertex of G_{skel} the edge e corresponds to. Further, let f_{v_1} and f_{v_2} be the faces of G_{skel} corresponding to v_1 and v_2, respectively. Let f_w be the third face of G_{skel} incident to z and let w be the stack vertex it corresponds to. If the two common incident edges of z and f_{v_1} have different signs, we define $\operatorname{pred}(e)$ as in the case that e is a sign-separating edge of type (I). Otherwise, the two common incident edges of z and f_w have different signs whence there exists a sign-separating edge $e' = (w, v_1)$ of type (III) corresponding to the sign change of the facial cycle of f_w at z. Then we set $\operatorname{pred}(e) = e'$.

It follows analogously to the proof for odd K that this predecessor assignment is injective. □

As for odd K, this has an immediate implication for the solution values of the variables corresponding to the edges of the outer face of G_{skel}.

Lemma 4.39. *The solution values of all variables corresponding to edges of the outer face of G_{skel} are non-negative.* □

Lemma 4.40. *In a facial cycle of G_{skel} corresponding to a stack vertex w of $2G^\star$, there are exactly as many concave sign changes as convex sign changes.*

Since the definition of the predecessor of a sign-separating edge of type (III) is the same for odd and for even K, the proof of Lemma 4.34 also proves Lemma 4.40.

For Lemma 4.35 we can formulate the following analogous lemma for the case that K is even.

Lemma 4.41. *Let z be a vertex of G_{skel} corresponding to the normal edge (v_1, v_2) of $2G^\star_+$. Let e_1, e_2, e_3 be the incident edges of z where e_1 and e_2 are the two edges incident to the face of G_{skel} corresponding to v_1. Then, if $\operatorname{sign}(e_1) = \operatorname{sign}(e_2)$, we have $\operatorname{sign}(e_1) = \operatorname{sign}(e_2) = \operatorname{sign}(e_3)$, see Fig. 4.34.*

Proof. Let w be the stack vertex corresponding to one of the incident faces of z. If $\operatorname{sign}(e_1) = \operatorname{sign}(e_2) \neq \operatorname{sign}(e_3)$, then (w, v_1) is a sign-separating edge of type (III). Thus (v_1, v_2) is its successor and, in particular, a sign-separating edge of type (II), in contradiction to $\operatorname{sign}(e_1) = \operatorname{sign}(e_2)$. □

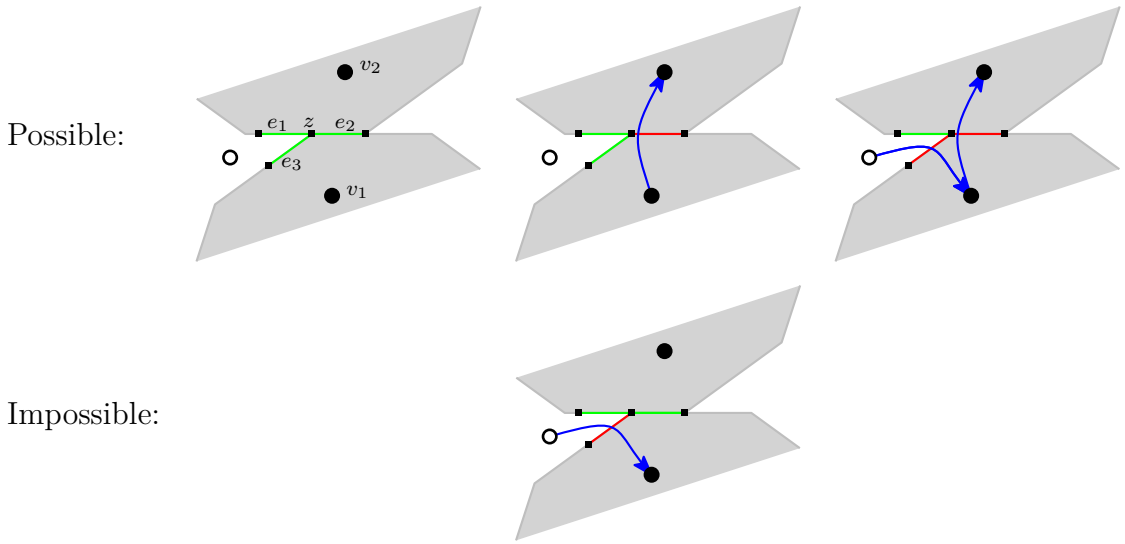

Figure 4.34: All possible (first row) and impossible (second row) combinations of signs of the incident edges of a vertex z of G_{skel} of degree three (in the case that K is even), up to symmetry and the exchange of non-negative and negative edges. The sign-separating edges corresponding to sign changes at z are shown in blue.

4.6.2 Solutions without negative variables

In this section we consider non-negative solutions of the system $A_S\mathbf{x} = \mathbf{e_1}$, i.e., solutions that do not contain negative variables. As in the previous section, we first study the case that K is odd in detail and afterwards briefly consider the case that K is even.

Equations for odd K. We will introduce a notion of edges of $G^\star$ similar to the sign-separating edges in the case that the solution is not non-negative. Since there are no negative edges, we aim at separating the edges of G_{skel} whose corresponding edge-variables have a positive value in the solution of $A_S\mathbf{x} = \mathbf{e_1}$ from those whose corresponding edge-variables have value zero in this solution. As before, if we refer to the value of a variable x, we always refer to the value of x in the unique solution of $A_S\mathbf{x} = \mathbf{e_1}$. We set $\text{sign}_+(x) := +1$, if $x > 0$, and $\text{sign}_+(x) := 0$ otherwise. If $\text{sign}_+(x) = +1$, we say that x is *positive* and, if $\text{sign}_+(x) = 0$, we say that x is *degenerate*. Again, we also translate this notion to the edges e of G_{skel} by setting $\text{sign}_+(e) := \text{sign}_+(x_e)$.

We define the multiset $E_{+,0}$ of *weak sign-separating edges* analogously to the set $E_{+,-}$ of sign-separating edges, just considering $\text{sign}_+(x)$ instead of $\text{sign}(x)$ for the variables x. In particular, there are weak sign-separating edges of types (I), (II), and (III). Further, if in a facial cycle of G_{skel} there are consecutive edges one of which is positive and the other one degenerate, we call this a *weak sign change*.

All properties of sign-separating edges proven in the last paragraph are also true for weak sign-separating edges and can be proven in the same way.

Lemma 4.42. *In a facial cycle of G_{skel} corresponding to a stack vertex w of $G^\star$, there are exactly as many concave weak sign changes as convex weak sign changes.* □

Lemma 4.43. *If the solution of $A_S\mathbf{x} = \mathbf{e_1}$ is not positive, then $E_{+,0} \neq \emptyset$.* □

Lemma 4.44. *In $E_{+,0}$ every vertex appears the same number of times as the start vertex and as the end vertex of an edge.* □

Lemma 4.45. *If the solution of $A_S\mathbf{x} = \mathbf{e_1}$ is non-negative, then the solution values of all variables corresponding to edges of the outer face of G_{skel} are positive.* □

In the following, we prove additional properties of weak sign-separating edges.

Lemma 4.46. *If the solution of $A_S\mathbf{x} = \mathbf{e_1}$ is non-negative, in the facial cycle of a face f of G_{skel} corresponding to a stack vertex of $G^\star$, either all edges are degenerate or in each concave arc there is at least one positive edge.*

Proof. Let P_f be the pseudotriangle corresponding to f. We will prove the following strengthening of the statement of the lemma: For any subpseudotriangle P of P_f in an arbitrary cutting of P_f into triangles, if P has only non-negative sides (note that a subpseudotriangle of P_f can have negative sides), it either has only degenerate sides or it has at least one positive side in each concave arc. The proof is by induction

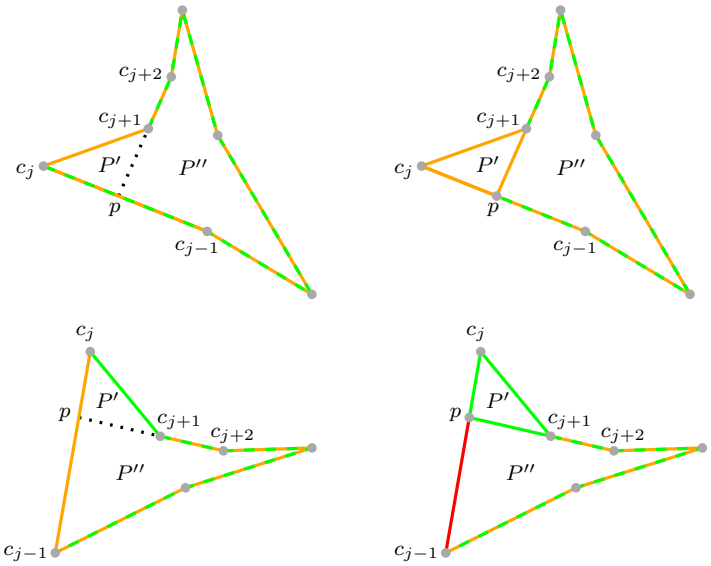

Figure 4.35: On the left: two pseudotriangles with some sides marked as positive (green), zero (orange), negative (red), or non-negative (green-orange) and a cutting into two subpseudotriangles P' and P''. On the right: the resulting signs of the edges of the skeleton of the respective cut pseudotriangle.

on the number of concave corners of P. If there is no concave corner, there is also no concave weak sign change. Then it follows from Lemma 4.42 that there is also no convex weak sign change. Therefore, either all three side-variables of P are degenerate or all of them are positive.

Now we consider the case that P has at least one concave corner. If P has only positive sides or only degenerate sides, the statement is fulfilled. Therefore, we assume that there are positive and degenerate sides. We distinguish two cases concerning the existence of a degenerate side with incident corners of special types (see the first and the second row of Fig. 4.35 for illustrations of these two cases).

i) If P has a degenerate side that is incident to a convex and a concave corner of P, we can assume, because of symmetry, that this side lies between the convex corner c_j and the concave corner c_{j+1}. Then we cut P along a line from the corner c_{j+1} to a point p on the side between the corners c_{j-1} and c_j into two subpseudotriangles. Let P' be the resulting pseudotriangle that has c_j as one of its corners and let P'' be the other resulting subpseudotriangle. Then P' is in fact a triangle and thus all three sides of P' have the same sign, i.e., $x_{p,c_j} = x_{p,c_{j+1}} = x_{c_j,c_{j+1}} = 0$. Therefore, we have $x_{c_{j-1},p} = x_{c_{j-1},c_j} - x_{p,c_j} = x_{c_{j-1},c_j}$ and $x_{p,c_{j+2}} = x_{p,c_{j+1}} + x_{c_{j+1},c_{j+2}} = x_{c_{j+1},c_{j+2}}$. Hence, all sides of P'' are non-negative with at least one being positive. Thus, by induction, in each concave arc of P'' there is at least one positive side. Each side of P'' except the sides between c_{j-1} and p and between p and c_{j+2} are also sides of P. If $x_{c_{j-1},p} > 0$, we have $x_{c_{j-1},c_j} = x_{c_{j-1},p} + x_{p,c_j} = x_{c_{j-1},p} > 0$ and, if $x_{p,c_{j+2}} > 0$, we have $x_{c_{j+1},c_{j+2}} = x_{p,c_{j+2}} - x_{p,c_{j+1}} = x_{p,c_{j+2}} > 0$. Hence, also P has a positive side in each concave arc.

ii) Since P has positive and degenerate sides, it follows from Lemma 4.42 that there is a convex weak sign change in P. Therefore, if there is no degenerate side that is incident to a convex and a concave corner, there is a degenerate side that is incident to two convex corners. We denote these corners by c_{j-1} and c_j. Because of symmetry, we can assume that c_{j+1} is a concave corner. Then $x_{c_j,c_{j+1}} > 0$ since otherwise we would be in the previous case. We cut P along a line from the corner c_{j+1} to a point p on the side between the corners c_{j-1} and c_j into two subpseudotriangles. Let P' be the resulting pseudotriangle that has c_j as one of its corners and let P'' be the other resulting subpseudotriangle. Then P' is in fact a triangle and thus all three sides of P' have the same sign. Since $x_{c_j,c_{j+1}} > 0$, this implies $x_{p,c_j}, x_{p,c_{j+1}} > 0$. Because of $x_{c_{j-1},p} + x_{p,c_j} = x_{c_{j-1},c_j} = 0$, this implies $x_{c_{j-1},p} < 0$. Further, we have $x_{p,c_{j+2}} = x_{p,c_{j+1}} + x_{c_{j+1},c_{j+2}} > 0$. Therefore, since all sides of P'' except the sides between c_{j-1} and p and between p and c_{j+2} are also sides of P, the side between c_{j-1} and p is the only negative side of P''. As c_{j-1} and p are convex corners of P'', this contradicts Lemma 4.30 and the assumption that P has no degenerate side that is incident to a convex and a concave corner is wrong.

Hence, the first case is the only one that is possible and the claimed statement is fulfilled. □

If all edges incident to a face f of G_{skel} are degenerate, we call the face f and the vertex of $G^\star$ corresponding to f *degenerate*. Note that a normal vertex v of $G^\star$ is degenerate if and only if $x_v = 0$. The following lemma shows that vertices of $G^\star$ can only be degenerate if $K = 3$.

Lemma 4.47. *If $K \geq 5$, the graph $G^\star$ has no degenerate vertices.*

Proof. Let H be a maximal connected component of the subgraph of $G^\star$ induced by the degenerate vertices. From the following claims we obtain some structural properties of H.

Claim 1. *All stack vertices adjacent to a degenerate normal vertex are degenerate.*

Proof. Let w be a stack vertex that is adjacent to the degenerate normal vertex v. Let f_w and f_v be the faces of G_{skel} corresponding to w and v, respectively. Then all common incident edges of f_w and f_v are degenerate. Since these edges form one of the three concave arcs of the facial cycle of f_w, it follows from Lemma 4.46 that all edges incident to f_w are degenerate. Hence, w is degenerate. △

Claim 2. *No stack vertices adjacent to an outer normal vertex a_i is degenerate.*

Proof. Let w be a stack vertex of $G^\star$ incident to an outer normal vertex. Let f_w be the face of G_{skel} corresponding to w. Then f_w is adjacent to the outer face of G_{skel}. By Lemma 4.45, the outer edges of G_{skel} are positive. Since the common incident edges of f_w and the outer face are the only edges of their concave arcs of the facial cycle of f_w, it follows with Lemma 4.46 that f_w and therefore also w are not degenerate. △

Claims 1 and 2 together also imply that normal vertices that are adjacent to an outer normal vertex are not degenerate. Hence, in $G^\star$ the subgraph H is surrounded by a cycle C of positive inner normal vertices.

Consider the orientations of the edges of C in S. Let v be a vertex on C and let f_v be the corresponding face of G_{skel}. If both incident edges of v on C are outgoing for v, at least one entire side of the facial cycle of f_v consists only of degenerate edges. Then v is degenerate, in contradiction to the fact that v is a vertex of C. Therefore, each vertex of C has an incoming and an outgoing incident edge on C, i.e., C is an oriented cycle. In particular, each vertex of C has an outgoing edge in C. Therefore, if there is an outgoing edge of v going into the interior of C, again at least one entire side of the facial cycle of f_v consists only of degenerate edges whence v is degenerate, in contradiction to the fact that v is a vertex of C. Hence, C is a cycle in $G^\star_+$, consisting only of normal vertices and without edges pointing from C into the interior of C. Therefore, due to Lemma 3.22 we have $\frac{K-1}{2}\ell - K = 0$ where ℓ is the length of C. Then we have $\ell = \frac{2K}{K-1}$ which implies $K = 3$ and $\ell = 3$. □

We can translate Lemma 4.35 to the case that the solution of $A_S\mathbf{x} = \mathbf{e_1}$ is non-negative by just considering $\text{sign}_+(x)$ instead of $\text{sign}(x)$ for all variables x. If $K \geq 5$, we can strengthen this in the following way.

Lemma 4.48. *Let $K \geq 5$ and let z be a vertex of G_{skel} corresponding to the normal edge (v_1, v_2) of $G^\star_+$. Let $e_1, \dots, e_4$ be the incident edges of z in clockwise order, starting with the two edges incident to the face of G_{skel} corresponding to v_1. Then we have $\text{sign}_+(e_1) = \text{sign}_+(e_2) = +1$ and further $\text{sign}_+(e_3) = +1$ or $\text{sign}_+(e_4) = +1$, see Fig. 4.36.*

Proof. Assume that $\text{sign}_+(e_1) = 0$. Let f_{v_1} be the face of G_{skel} corresponding to v_1 and let $f_w \neq f_{v_1}$ be the other incident face of e_1. Then e_1 is an entire side of the facial cycle of f_{v_1} (see Fig. 4.37a) or it is the only edge of its concave arc of the facial cycle of f_w (see Fig. 4.37b). The former implies that f_{v_1} is degenerate and by Lemma 4.46 the latter implies that f_w is degenerate, both in contradiction to Lemma 4.47. Therefore, the assumption was wrong and we have $\text{sign}_+(e_1) = +1$. Analogously, we can show that $\text{sign}_+(e_2) = +1$.

Now it follows as in the proof of Lemma 4.35 that $\text{sign}_+(e_3) = \text{sign}_+(e_2) = +1$ or $\text{sign}_+(e_4) = \text{sign}_+(e_1) = +1$. □

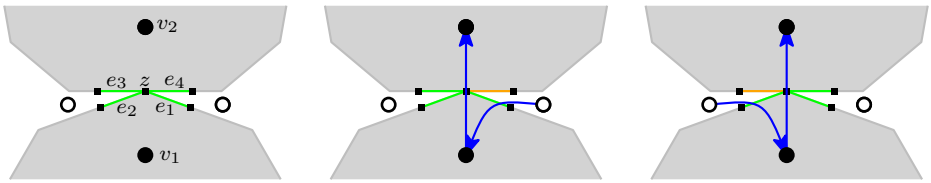

Figure 4.36: All possible combinations of signs of the incident edges of a vertex z of G_{skel} of degree four (in the case that K is odd) if the solution of $A_S\mathbf{x} = \mathbf{e_1}$ is non-negative. The weak sign-separating edges corresponding to weak sign changes at z are shown in blue.

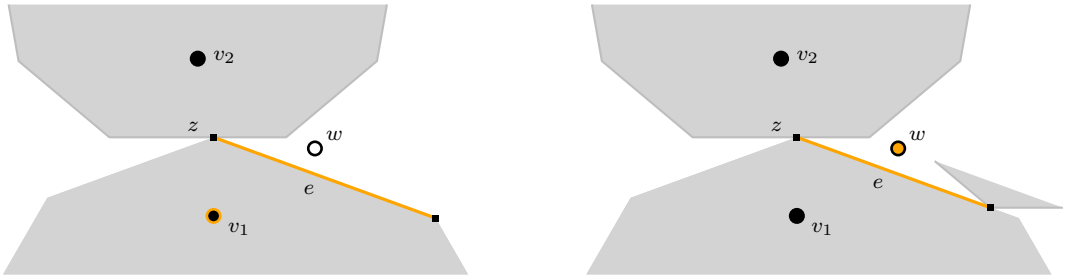

(a) First case: v_1 is degenerate. (b) Second case: w is degenerate.

Figure 4.37: A degenerate edge e incident to a vertex z of G_{skel} with $\deg(z) = 4$. The two subfigures show the two possibilities for the endpoint of e other than z.

Next we prove a strengthening of Lemma 4.32 for weak sign-separating edges.

Lemma 4.49. *The set $E_{+,0}$ is an edge-disjoint union of oriented essential cycles.*

Proof. Let us first consider the case that $K = 3$. Then there are no (weak) sign-separating edges of types (I) and (III) and as a consequence of the proof of Lemma 4.47 the weak sign-separating edges of type (II) can be partitioned into oriented cycles of length $\ell = 3$. Due to Theorem 3.29 these are essential cycles.

Now let $K \geq 5$. The predecessor assignment in the proof of Lemma 4.32 defines a partition of $E_{+,0}$ into oriented cycles. Since in this proof the predecessors of the sign-separating edges of type (III) are not explicitly defined, we will first make this predecessor assignment explicit. Afterwards we will show that the oriented cycles are essential cycles of $G^\star$.

Let $e = (w, v)$ be a weak sign-separating edge of type (III) corresponding to the vertex z of G_{skel}. Let e_1 be the common incident edge of z and the faces f_v and f_w of G_{skel} corresponding to v and to w, respectively. Let $e_2 \neq e_1$ be the other common incident edge of z and f_w. Then we have $\operatorname{sign}_+(e_1) \neq \operatorname{sign}_+(e_2)$ and, therefore, due to Lemma 4.48 we have $\operatorname{sign}_+(e_1) = +1$ and $\operatorname{sign}_+(e_2) = 0$. Then, due to Lemma 4.46 there is a concave weak sign change on the concave arc of the facial cycle of f_w containing e_2. In particular, the normal vertex v' corresponding to this concave arc is positive. Let $z' \neq z$ be the second endpoint of e_2 and let $e_3 \neq e_2$ be the second common incident edge of z' and f_w. If e_2 and e_3 are the only two sides of their concave arc, there has to be a concave weak sign change at z'. If they are not the only sides of their concave arc, then e_3 is an entire side of the facial cycle corresponding to v' and, therefore, e_3 is positive. Hence, also in this case there is a concave weak sign change at z'. Let e' be the sign-separating edge of type (I) corresponding to the weak sign change at z'. Then we set $\operatorname{pred}(e) = e'$.

We have to show that this predecessor assignment is injective. Let $e' = (v', w)$ be a weak-sign-separating edge of type (I) corresponding to a concave weak sign change at the vertex z' of G_{skel}. Then $\deg(z') = 2$ and z is incident to a degenerate edge e_2 and a positive edge e_3. Let $z \neq z'$ be the second endpoint of e_2. Then, if there is an edge e with $\operatorname{pred}(e) = e'$, this edge e is a weak sign-separating edge of type (III)

starting at w that corresponds to a convex weak sign change at z. Since this edge e is unique, the predecessor assignment is injective.

By Lemma 4.48 we can associate a unique degenerate edge of G_{skel} with each weak sign-separating edge of type (II). With weak sign-separating edges of types (I) and (III) we can also associate a unique degenerate edge of G_{skel} in a canonical way. Then each degenerate edge e of G_{skel} is associated with exactly one weak sign-separating edge e_1 of type (I), exactly one weak sign-separating edge e_2 of type (II), and exactly one sign-separating edge e_3 of type (III). Further, these edges fulfill $\text{pred}(e_1) = e_2$, $\text{pred}(e_2) = e_3$, and $\text{pred}(e_3) = e_1$. Hence, the edges of $E_{+,0}$ can be partitioned into oriented triangles associated with the degenerate edges of G_{skel}. Due to Theorem 3.29 these triangles are essential cycles. □

Equations for even K. If K is even, we define the set $E_{+,0}$ of weak sign-separating edges as in the case that K is odd, by considering $\text{sign}_+(x)$ instead of $\text{sign}(x)$ for the variables x. Then, again, the following lemmas can be derived immediately from the analogous results for solutions with negative variables.

Lemma 4.50. *In a facial cycle of G_{skel} corresponding to a stack vertex w of $2G^\star$, there are exactly as many concave weak sign changes as convex weak sign changes.* □

Lemma 4.51. *If the solution of $A_S\mathbf{x} = \mathbf{e_1}$ is not positive, then $E_{+,0} \neq \emptyset$.* □

Lemma 4.52. *In $E_{+,0}$ every vertex appears the same number of times as the start vertex and as the end vertex of an edge.* □

Lemma 4.53. *If the solution of $A_S\mathbf{x} = \mathbf{e_1}$ is non-negative, then the solution values of all variables corresponding to edges of the outer face of G_{skel} are positive.* □

The next lemma can be proven in exactly the same way as Lemma 4.46 since we do not make use of the fact that K is odd in this proof.

Lemma 4.54. *If the solution of $A_S\mathbf{x} = \mathbf{e_1}$ is non-negative, in the facial cycle of a face f of G_{skel} corresponding to a stack vertex of $2G^\star$, either all edges are degenerate or in each concave arc there is at least one positive edge.* □

We continue with an analogous result of Lemma 4.47 for even K.

Lemma 4.55. *If $K \geq 8$, the graph $2G^\star$ has no degenerate vertices.*

Proof. Let H be a maximal connected component of the subgraph of $2G^\star$ induced by the degenerate vertices. As in the proof of Lemma 4.47, it follows that H is surrounded by a cycle C of positive inner normal vertices that, viewed as a cycle in $2G^\star_+$ without edges in its interior that are parallel to edges of C, has no edges pointing from C into the interior of C. Therefore, Lemma 3.37 implies that we have $\frac{K-2}{2}\ell - K = 0$ where ℓ is the length of C. Then we have $\ell = \frac{2K}{K-2}$ which implies $K = 6$ and $\ell = 3$. □

The following lemma is an analogous result of Lemma 4.48.

Lemma 4.56. *Let $K \geq 8$ and let z be a vertex of G_{skel} corresponding to the normal edge (v_1, v_2) of $2G_+^\star$. Let e_1, e_2, e_3 be the incident edges of z where e_1, e_2 are the two edges incident to the face of G_{skel} corresponding to v_1 and e_2, e_3 are the two edges incident to the face of G_{skel} corresponding to v_2. Then $\operatorname{sign}_+(e_1) = +1$ and further $\operatorname{sign}_+(e_2) = +1$ or $\operatorname{sign}_+(e_3) = +1$.*

Proof. Let w be the stack vertex corresponding to one of the three faces incident to z. Analogously to the proof of Lemma 4.48, $\operatorname{sign}_+(e_1) = 0$ would imply that v_1 or w is degenerate, in contradiction to Lemma 4.55. Therefore, we have $\operatorname{sign}_+(e_1) = +1$.

Now it follows as in the proof of Lemma 4.41 that $\operatorname{sign}_+(e_2) = \operatorname{sign}_+(e_1) = +1$ or $\operatorname{sign}_+(e_3) = \operatorname{sign}_+(e_1) = +1$. □

Finally, we prove an analogous result of Lemma 4.49 for the case that K is even.

Lemma 4.57. *The set $E_{+,0}$ is an edge-disjoint union of oriented essential cycles.*

Proof. Let us first consider the case that $K = 6$. Then there are no (weak) sign-separating edges of types (I) and (III) and as a consequence of the proof of Lemma 4.55 the weak sign-separating edges of type (II) can be partitioned into oriented cycles of length $\ell = 3$. Due to Theorem 3.56 these are essential cycles.

Now let $K \geq 8$. Then the predecessors of sign-separating edges of types (I) and (II) are explicitly given by the proof of Lemma 4.38 and we can make the predecessors of sign-separating edges of type (III) explicit in exactly the same way as in the proof for odd K (Lemma 4.49).

Then by Lemma 4.56 we can associate a unique degenerate edge of G_{skel} with each weak sign-separating edge of type (II). With weak sign-separating edges of types (I) and (III) we can also associate a unique degenerate edge of G_{skel} in a canonical way. Let e be a degenerate edge of G_{skel}. We distinguish two cases concerning the endpoints of e.

- **i)** If e has two endpoints of degree three, then e is associated with two weak sign-separating edges e_1, e_2 of type (II). These edges fulfill $\operatorname{pred}(e_1) = e_2$ and $\operatorname{pred}(e_2) = e_1$. Further, due to Theorem 3.56 the cycle consisting of e_1 and e_2 is an essential cycle.
- **ii)** If e has an endpoint of degree three and an endpoint of degree two, then e is associated with exactly one weak sign-separating edge e_1 of type (I), exactly one weak sign-separating edge e_2 of type (II), and exactly one sign-separating edge e_3 of type (III). These edges fulfill $\operatorname{pred}(e_1) = e_2$, $\operatorname{pred}(e_2) = e_3$, and $\operatorname{pred}(e_3) = e_1$. Further, due to Theorem 3.56 the cycle consisting of e_1, e_2, and e_3 is an essential cycle.

Hence, the edges of $E_{+,0}$ can be partitioned into oriented cycles which are essential cycles. □

4.6.3 How flipping the K-contact structure changes the solution

We have always considered the system of equations corresponding to a fixed K-contact structure S. In this section we will study how the solution of the system of equations changes if we change the underlying K-contact structure in the smallest possible way, i.e., by applying a flip to S and thereby going to a K-contact structure S' covering S in the distributive lattice of K-contact structures.

We call two K-contact structures S and S' *neighboring* if S covers S' in the distributive lattice of K-contact structures or vice versa. In the following we will show that, in the solutions of the systems of equations corresponding to such a pair of neighboring K-contact structures S and S', some of the variables change their signs. More precisely, these are the variables corresponding to the parts of the K-contact structures that are different in S and S'. The proofs of these statements will be based on the following variant of Lemma 4.25.

Lemma 4.58. *Let H be a plane graph and e an edge of H such that every inner face f of $H \setminus e$ is bounded by a simple cycle of length $\ell_f \equiv 2 \pmod 4$ and e is incident to two inner faces f_1, f_2 of H that are bounded by simple cycles of length $\ell_{f_i} \equiv 0 \pmod 4$, $i = 1, 2$. Further, let M and M' be perfect matchings of H with $e \in M$ and $e \notin M'$. Then $\operatorname{sgn}(M) \neq \operatorname{sgn}(M')$.*

Proof. The symmetric difference of M and M' is the disjoint union of simple cycles $C_1, \dots, C_m$, where $e \in C_1$ and $e \notin C_i$ for $i = 2, \dots, m$. For $i = 1, \dots, m$, let ℓ_i be the length of C_i. Since $C_2, \dots, C_m$ are cycles in $H \setminus e$, it follows as in Lemma 4.25 that $\ell_i \equiv 2 \pmod 4$ for $i = 2, \dots, m$.

Now let H' be the graph obtained from H by subdividing e into three edges. Then in H' every inner face f is bounded by a simple cycle of length $\ell_f \equiv 2 \pmod 4$. Let C_1' be the cycle in H' obtained from C_1 by replacing e by its three subdivision edges. Then, again, it follows as in Lemma 4.25 that $\ell(C_1') \equiv 2 \pmod 4$ where $\ell(C_1')$ is the length of C_1'. Therefore, $\ell_1 = \ell(C_1') - 2 \equiv 0 \pmod 4$.

Hence, we have $\operatorname{sgn}(M) \neq \operatorname{sgn}(M')$ by Lemma 4.24. □

In the following, let S and S' always be neighboring K-contact structures. Further, let $A_S\mathbf{x} = \mathbf{e_1}$ and $A_{S'}\mathbf{x}' = \mathbf{e_1}$ be the systems of linear equations corresponding to S and S', respectively, (or, more precisely, these systems with equations of the type (4.6) replaced according to Lemma 4.21) and x_i and x_i', respectively, denote the value of a variable in the unique solution of this system. The incidence graphs of the two systems of equations with their canonical crossing-free drawing are denoted by H and H', respectively. We will now distinguish four different cases concerning the value of K and the type of the flip. For completeness, we will also consider the case $K = 3$ which is well-known, see Theorem 4.6 in the beginning of this chapter.

Flips for $\mathbf{K = 3}$. In this case, according to Theorem 3.29, S' can be obtained from S by changing the orientation of an oriented triangle in S. We only consider the special case that this triangle is the boundary of a face f of G. In a similarly-aligned

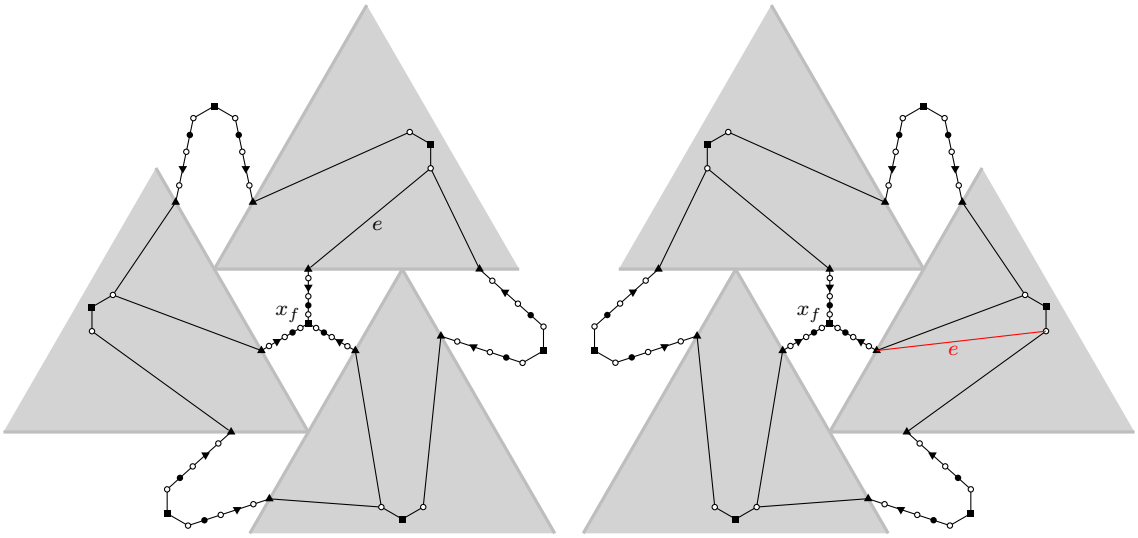

Figure 4.38: The cycle C in the incidence graphs H (left) and H' (right) of the systems of equations $A_S\mathbf{x} = \mathbf{e_1}$ and $A_{S'}\mathbf{x} = \mathbf{e_1}$, respectively. The only differences of H and H' are the edges between vertices on C and vertices inside C. The edge e is an edge of H but not of H'. The graph H' extended by e (see the red edge) is the planar graph $\widetilde{H}$.

triangle contact representation of G, the pseudotriangles corresponding to the faces of G are triangles. Hence, the cutting of such a pseudotriangle into triangles consists of one single triangle and we associate the variable corresponding to this triangle with the corresponding face of G. In the case of f, we denote this variable by x_f.

Theorem 4.59. *Let S and S' be neighboring 3-contact structures which are related by the reorientation of the facial cycle of a face f. Then $x_f x'_f < 0$ or $x_f = x'_f = 0$.*

Proof. Note that there is a canonical bijection between the vertices of H and H'. Therefore, we will not distinguish the vertices of H and H'. The face f corresponds to a cycle C of length 48 in H and H', see Fig. 4.38. We say that a variable or equation lies inside C, on C, or outside C if the corresponding vertex lies inside C, on C, or outside C. Note that H and H' only differ in the edges connecting vertices inside C with vertices on C.

Claim 1. $\det(A_S)\det(A_{S'}) < 0$.

Proof. Remember from the proof of Theorem 4.26 that $\det(A_S), \det(A_{S'}) \neq 0$ and that all perfect matchings of H and H', respectively, have the same sign. Therefore, it suffices to show that there are perfect matchings M and M' of H and H', respectively, with $\operatorname{sgn}(M) \neq \operatorname{sgn}(M')$.

Let M and M' be arbitrary perfect matchings of H and H', respectively. In both graphs, there is exactly one more variable-vertex inside C than equation-vertices and the neighbors of all equations-vertices inside C are also inside C. Therefore, there is exactly one edge e in M connecting a vertex inside C with a vertex on C. Then e is the only edge of M that is not an edge of H'.

Let $\widetilde{H}$ be the graph obtained from H' by adding the edge e. Then $\widetilde{H}$ is still a planar graph (see Fig. 4.38) and the edge e splits an inner face of H' of length $30 \equiv 2 \pmod 4$ into two faces of lengths $4, 28 \equiv 0 \pmod 4$. Remember from Theorem 4.26 that all inner faces of H' have length $\ell \equiv 2 \pmod 4$. Since both M and M' are perfect matchings of $\widetilde{H}$ and $e \in M$ but $e \notin M'$, it then follows from Lemma 4.58 that $\operatorname{sgn}(M) \neq \operatorname{sgn}(M')$. △

Claim 2. *Let $A_S^{(f)}$ and $A_{S'}^{(f)}$ be the matrices A_S and $A_{S'}$, respectively, with the column corresponding to x_f replaced by $\mathbf{e_1}$. Then $\det\left(A_S^{(f)}\right) = \det\left(A_{S'}^{(f)}\right)$.*

Proof. As we have seen in the proof of Claim 1, in H and H' there is exactly one more variable-vertex inside C than equation-vertices and the neighbors of all equation-vertices inside C are also inside C. The incidence graphs $H^{(f)}$ and $H'^{(f)}$ of $A_S^{(f)}$ and $A_{S'}^{(f)}$ are obtained from H and H', respectively, by deleting all incident edges of the variable-vertex x_f and connecting it to the equation-vertex w corresponding to the first row of the respective matrix instead. Therefore, in a perfect matching of $H^{(f)}$ or $H'^{(f)}$ the vertex x_f is matched with w and the remaining vertices inside C are matched with other vertices inside C. Since $H^{(f)}$ and $H'^{(f)}$ only differ in edges connecting vertices inside C with vertices on C, this implies that each edge of a perfect matching of $H^{(f)}$ is also an edge of $H'^{(f)}$ and vice versa. Thus $H^{(f)}$ and $H'^{(f)}$ have the same perfect matchings.

We want to apply the Leibniz formula to prove $\det\left(A_S^{(f)}\right) = \det\left(A_{S'}^{(f)}\right)$. Therefore, it remains to show that each perfect matching of $H^{(f)}$ and $H'^{(f)}$ has the same weight in $H^{(f)}$ and $H'^{(f)}$. But this is clear since the weights of the edges on C and outside C are the same in H and H' and the only edges inside C that used to have weights $\neq 1$ are the edges incident to x_f which are no edges of $H^{(f)}$ and $H'^{(f)}$. △

Because of Claims 1 and 2 we obtain by applying Cramer's rule

$$x_e x'_e = \frac{\det\left(A_S^{(f)}\right)}{\det(A_S)} \frac{\det\left(A_{S'}^{(f)}\right)}{\det(A_{S'})} = \frac{\det\left(A_S^{(f)}\right)^2}{\det(A_S)\det(A_{S'})} \leq 0 \ ,$$

where the value 0 is attained if and only if $\det\left(A_S^{(f)}\right) = 0$ and thus $x_f = x'_f = 0$. □

Flips for odd $\mathbf{K \geq 5}$. We assume that S' is obtained from S by a flip. Then, according to Theorem 3.29, S' can be obtained from S by changing the orientation of a normal edge (v_1, v_2) in S, decreasing the weight of $v_2 w$ by one, and increasing the weight of $v_1 w$ by one, where w is the stack vertex corresponding to the face to the left of (v_1, v_2), see Fig. 4.39. Let G_{skel} and G'_{skel} be the skeleton graphs corresponding to S and S', respectively. Let Q_1 and Q_2 be the faces (K-gons) of G_{skel} and G'_{skel} corresponding to v_1 and v_2 and let P_w be the face (pseudotriangle) corresponding to w. Further, let p be the vertex of G_{skel} and G'_{skel} that is incident to Q_1 and Q_2 (the contact point of the two K-gons). Then let e be the edge of G_{skel} that is incident to Q_2, P_w, and p. Similarly, let e' be the edge of G'_{skel} that is incident to Q_1, P_w

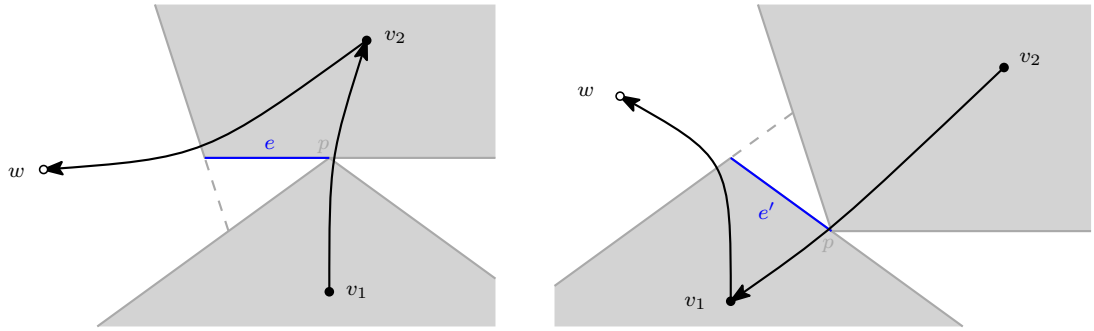

Figure 4.39: Two neighboring K-contact structures S (left) and S' (right) for an odd $K \geq 5$. In the background it is shown what the difference of S and S' means for a similarly-aligned odd K-gon contact representation inducing S and S', respectively. Two edges e and e' of the corresponding skeleton graphs are highlighted. Further, in both cases one cutting edge of a cutting of the pseudotriangle P_w corresponding to w into triangles is drawn as a dashed line.

and p. See Fig. 4.39 for a visualization of the edges e and e'. We denote the variables corresponding to e and e' by x_e and $x'_{e'}$.

Theorem 4.60. *Let S and S' be neighboring K-contact structures with odd $K \geq 5$. Further, let the edges e and e' be defined as above. Then $x_e x'_{e'} < 0$ or $x_e = x'_{e'} = 0$.*

Proof. We will fix a cutting of the pseudotriangles corresponding to the inner faces of G into triangles and consider the systems of equations corresponding to these cuttings. For G_{skel} we fix that there is a cutting edge from the endpoint of e that is not p to the edge incident to Q_1, P_w, and p and that there is no cutting edge ending at this cutting edge. Similarly, for G'_{skel} we fix that there is a cutting edge from the endpoint of e' that is not p to the edge incident to Q_2, P_w, and p and that there is no cutting edge ending at this cutting edge. Apart from that, the remaining cutting edges can be chosen arbitrarily. The incidence graphs H and H' of the resulting systems of equations are shown at the top of Fig. 4.40.

In G_{skel} and G'_{skel} let f be the triangle of the cutting of P_w that is incident to p. Further, let x_f be the variable corresponding to f. Then $x_f = x_e$ and $x'_f = x'_{e'}$. Now we will slightly modify the two systems of equations. The incidence graphs of the modified systems are shown at the bottom of Fig. 4.40. Let x_e and $x_{\tilde{e}}$ be the vertices with distance 2 to x_f in H corresponding to the edge e and to an edge incident to Q_1, respectively. Then x_e has distance 5 to a neighbor y of x_{v_2}. We delete the connecting path and all intermediate vertices and instead connect x_e directly with an edge of weight 1 to y. Further, $x_{\tilde{e}}$ has distance 5 to a neighbor $\tilde{y}$ of x_{v_1}. Let x_j be the last vertex before $\tilde{y}$ on the connecting path. Then we delete the path of length 4 between $x_{\tilde{e}}$ and x_j with all intermediate vertices and instead connect $x_{\tilde{e}}$ directly with an edge of weight 1 to $\tilde{y}$. Note that this modification of the system $A_S\mathbf{x} = \mathbf{e_1}$ is still uniquely solvable and that x_j is the only variable whose solution value changes (to the former value of $x_j - x_{\tilde{e}}$). In particular, the value of x_f does not change. We change the other system of equations analogously with the vertices defined as follows: x_e

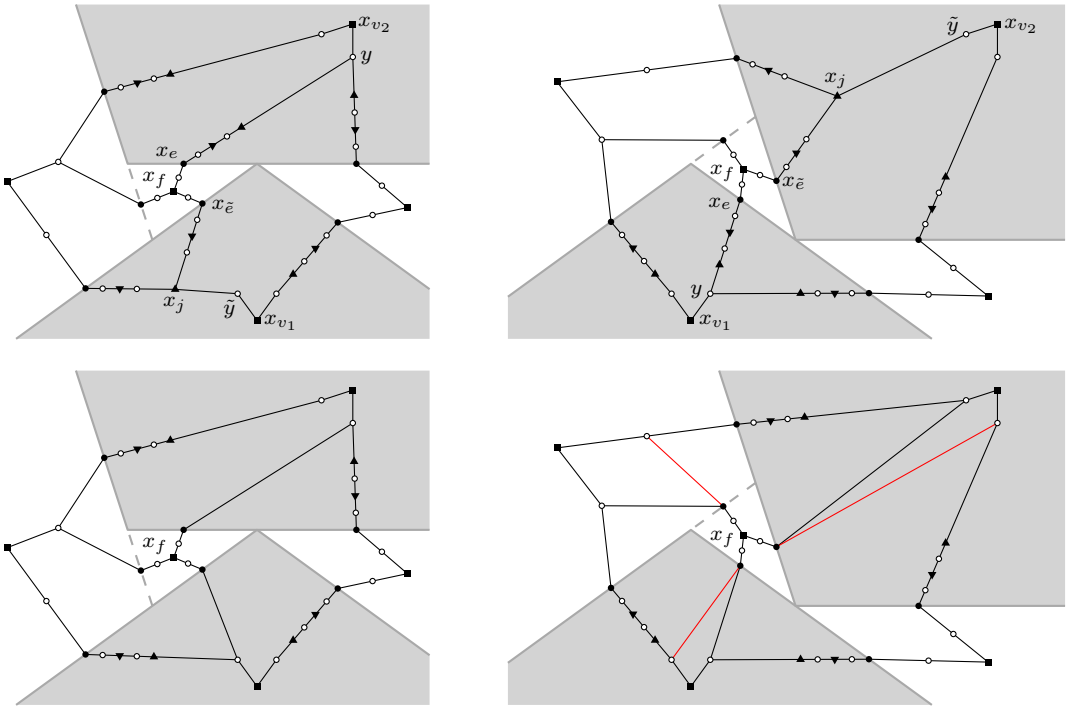

Figure 4.40: Top: the incidence graphs H and H' for odd $K \geq 5$. Bottom: the incidence graphs of the modified systems of equations. The edges of the modified graph H that are no edges of the modified graph H' are added in red to the drawing of the latter one.

and $x_{\tilde{e}}$ are the vertices with distance 2 to x_f in H' corresponding to the edge e and to an edge incident to Q_2, respectively; y is the neighbor of x_{v_1} that has distance 5 to x_e; $\tilde{y}$ is the neighbor of x_{v_2} that has distance 5 to $x_{\tilde{e}}$; and x_j is the neighbor of $\tilde{y}$ with distance 4 to $x_{\tilde{e}}$. Then also the modification of the system $A_{S'}\mathbf{x} = \mathbf{e_1}$ is still uniquely solvable and the value of x_f does not change.

From now on we only consider the modified systems of equations. Then the graphs H and H' only differ inside a cycle C of length 32. In both cases, inside C there is exactly one more variable-vertex than equation-vertices and all neighbors of the equation-vertices inside C are also inside C. Further, all edges of H connecting a vertex inside C and a vertex on C can be added to H' without producing a crossing and by splitting a face of length $\ell \equiv 2 \pmod 4$ into two faces of lengths $4, \ell - 2 \equiv 0 \pmod 4$. Therefore, it follows as in the proof of Theorem 4.59 that $x_f x'_f < 0$ or $x_f = x'_f = 0$. □

Digon flips for even $K \geq 6$. For even K, there are two different types of flips, digon flips and triangle flips, see Theorem 3.56. We first consider the case of digon flips. Note that in this case the skeleton graphs corresponding to S and S' are equal and only the prescribed slope of one edge e of the skeleton graph changes.

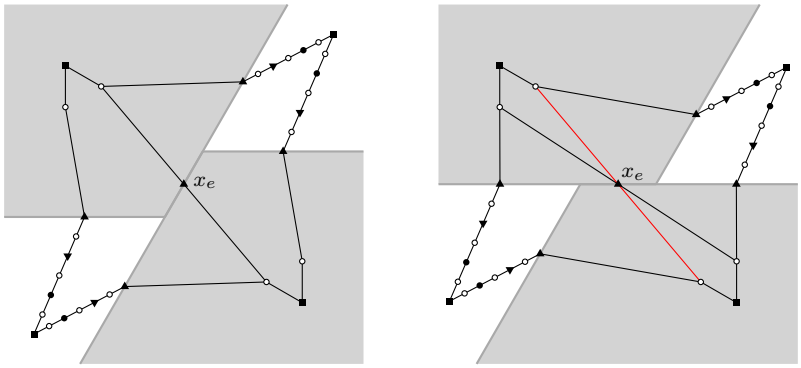

Figure 4.41: The incidence graphs H and H' in the case of a digon flip for even $K \geq 6$. The edges of H that are no edges of H' are added in red to the drawing of H'.

Theorem 4.61. *Let S and S' be neighboring K-contact structures with even $K \geq 6$ which are related by a digon flip corresponding to the edge e of the skeleton graph. Then $x_e x'_{e'} < 0$ or $x_e = x'_{e'} = 0$.*

Proof. The incidence graphs H and H' only differ in the edges connecting the unique vertex x_e inside a cycle C of length 32 to the vertices on C, see Fig. 4.41. Each edge of H that is inside C can be added to H' without producing a crossing and by splitting an inner face of length $18 \equiv 2 \pmod 4$ into two faces of lengths $4, 16 \equiv 0 \pmod 4$. Therefore, it follows as in the proof of Theorem 4.59 that $x_e x'_e < 0$ or $x_e = x'_e = 0$. □

Triangle flips for even K ≥ 6. The case of triangle flips for $K = 6$ is analogous to the case of flips for $K = 3$. So, also in this case we only consider flips corresponding to the reorientation of a triangle in G that is the boundary of a face f. See Fig. 4.42 for an illustration of the incidence graphs H and H' in this case. We denote the variable corresponding to f by x_f.

Theorem 4.62. *Let S and S' be neighboring 6-contact structures which are related by the reorientation of the facial cycle of a face f. Then $x_f x'_f < 0$ or $x_f = x'_f = 0$.* □

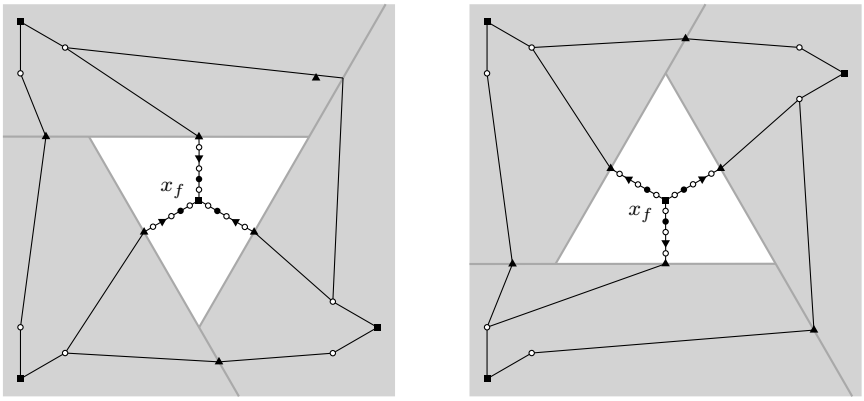

Figure 4.42: The incidence graphs H and H' in the case of a triangle flip for $K = 6$.

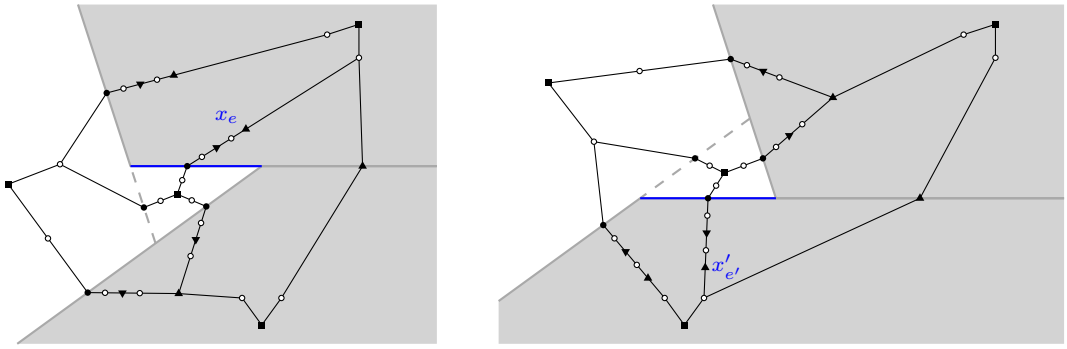

Figure 4.43: The incidence graphs H and H' in the case of a triangle flip for even $K \geq 8$.

The remaining case of triangle flips for even $K \geq 8$ is analogous to the case of flips for odd $K \geq 5$. See Fig. 4.43 for an illustration of the incidence graphs H and H' in this case. Also read off the definition of the variables x_e and $x'_{e'}$ from this figure.

Theorem 4.63. *Let S and S' be neighboring K-contact structures with even $K \geq 8$ which are related by a triangle flip. Further, let the edges e and e' be defined as mentioned above. Then $x_e x'_{e'} < 0$ or $x_e = x'_{e'} = 0$.* □

4.7 Drawings from solutions with negative variables

Remember that, if the solution of $A_S\mathbf{x} = \mathbf{e_1}$ is non-negative, then the wanted contact representation of G is obtained as a drawing of G_{skel} with each edge e being drawn with the slope s_e that has been assigned to it and with the length given by the value of the corresponding edge-variable x_e in the solution of $A_S\mathbf{x} = \mathbf{e_1}$. This drawing can also be defined for solutions with negative variables: If an edge-variable x_e is negative, then the corresponding edge e is drawn with slope $-s_e$ and length $|x_e|$. Figure 4.44 shows an example of such a drawing of G_{skel} induced by a solution of $A_S\mathbf{x} = \mathbf{e_1}$ with negative variables.

Surprisingly, in this drawing the drawings of the faces are pairwise non-overlapping. In particular, the drawings of the edges do not cross in the sense that their intersection is not a single point that is in the relative interior of the drawings of both edges.

Theorem 4.64. *In the drawing of G_{skel} defined by the solution of $A_S\mathbf{x} = \mathbf{e_1}$, each inner face is drawn as a weakly simple polygon, the drawings of the inner faces are pairwise interiorly disjoint, the drawing of a face of G_{skel} corresponding to an inner vertex v of G is a (possibly negative) homothetic copy of the prototype P_v, the drawing of the outer face is a K-gon whose sides have the same slopes as the sides of Q, and the entire drawing of G_{skel} is inside the drawing of the outer face.*

Proof. The strategy of the proof is as follows: We will first extend the skeleton graph G_{skel} and then apply Lemma 4.14 to this extension G'_{skel}. Since we choose the drawings of the faces of G'_{skel} in such a way that the drawings of the edges of G_{skel} are as defined by the solution of $A_S\mathbf{x} = \mathbf{e_1}$, the subdrawing of G_{skel} will fulfill the properties listed in the lemma.

The extension G'_{skel} is obtained from G_{skel} as follows: For each inner face of G_{skel} corresponding to an inner vertex v of G, we insert K edges into this face connecting the K vertices corresponding to the corners of the corresponding K-gon in a cyclic way. Each of these edges corresponds to a side $\text{side}_i(P_v)$ of this K-gon and we assign to it the slope of this side and the value $x_v\ell_i(P_v)$.

To be able to apply Lemma 4.14 to G'_{skel} and the given edge drawings, we have to show that the drawing of each inner face of G'_{skel} is a weakly simple polygon. We distinguish three types of inner faces of G'_{skel}.

i) Let f be an inner face of G'_{skel} corresponding to an inner normal vertex v of G. Then the drawing of f is a homothetic copy of the simple polygon P_v and, therefore, a weakly simple polygon.

ii) Let f be an inner face of G'_{skel} corresponding to a side of a polygon P_v. Then the drawings of the edges incident to f are pairwise homothetic, i.e., they are pairwise parallel or antiparallel. Therefore, the drawing of f is a weakly simple polygon.

iii) Let f be an inner face of G'_{skel} corresponding to an inner face of G and let $s_0, \dots, s_{k-1}$ be the slopes assigned to the edges of f in clockwise order. Then $s_0, \dots, s_{k-1}$ is a slope sequence of a pseudotriangle. Let A, B, C be the indices of the convex corners of this slope sequence as in Section 4.3. Further, for $i = 0, \dots, k-1$, let x_i be the solution value of the edge-variable corresponding to the edge with assigned slope s_i.

If $x_i \geq 0$ for $i = 0, \dots, k-1$, it follows from Lemma 4.18 that the drawing of f is a weakly simple polygon. If $x_i < 0$ for $i = 0, \dots, k-1$, it also follows from Lemma 4.18 that the drawing of f is a weakly simple polygon since, due to Lemma 4.15, $-s_0, \dots, -s_{k-1}$ is also a slope sequence of a pseudotriangle. It remains to consider the case that there are sign changes along the boundary of f. We will argue this case by induction on the number of sign changes.

We first consider the case that there is a convex and a concave sign change without another sign change or convex corner in-between. We assume that $\text{sign}(x_A) \neq \text{sign}(x_{A+1}) = \text{sign}(x_{A+2}) = \cdots = \text{sign}(x_j) \neq \text{sign}(x_{j+1})$ with $j+1 \leq B$. Due to multiple application of Lemma 4.17, $s_0, \dots, s_A, -s_{A+1}, -s_{A+2}, \dots, -s_j, s_{j+1}, \dots, s_{k-1}$ is also a slope sequence of a pseudotriangle. Therefore, we can apply the induction hypothesis to this new slope sequence and solution values $x_0, \dots, x_A, -x_{A+1}, -x_{A+2}, \dots, -x_j, x_{j+1}, \dots, x_{k-1}$.

Because of Lemmas 4.34 and 4.40 the only remaining case we have to consider is the case that there is exactly one convex and exactly one concave sign change and these two sign changes do not happen at the same concave arc. We assume that $\text{sign}(x_A) \neq \text{sign}(x_{A+1}) = \text{sign}(x_{A+2}) = \cdots = \text{sign}(x_j) \neq \text{sign}(x_{j+1})$ with $B < j < C$. Then, due to multiple application of Lemma 4.17,

$s_0, \dots, s_A, -s_{A+1}, -s_{A+2}, \dots, -s_j, s_{j+1}, \dots, s_{k-1}$ is also a slope sequence of a pseudotriangle. Therefore, we can apply the induction hypothesis to this new slope sequence and solution values $x_0, \dots, x_A, -x_{A+1}, -x_{A+2}, \dots, -x_j$, $x_{j+1}, \dots, x_{k-1}$.

Due to Lemmas 4.33 and 4.39 we have $x_e \geq 0$ for each edge e of the outer face of G'_{skel}. Therefore, the drawing of the outer face of G_{skel} is a K-gon whose sides have the same slopes as the sides of Q. Further, due to Lemma 4.14, the entire drawing of G'_{skel} is inside the drawing of the outer face. □

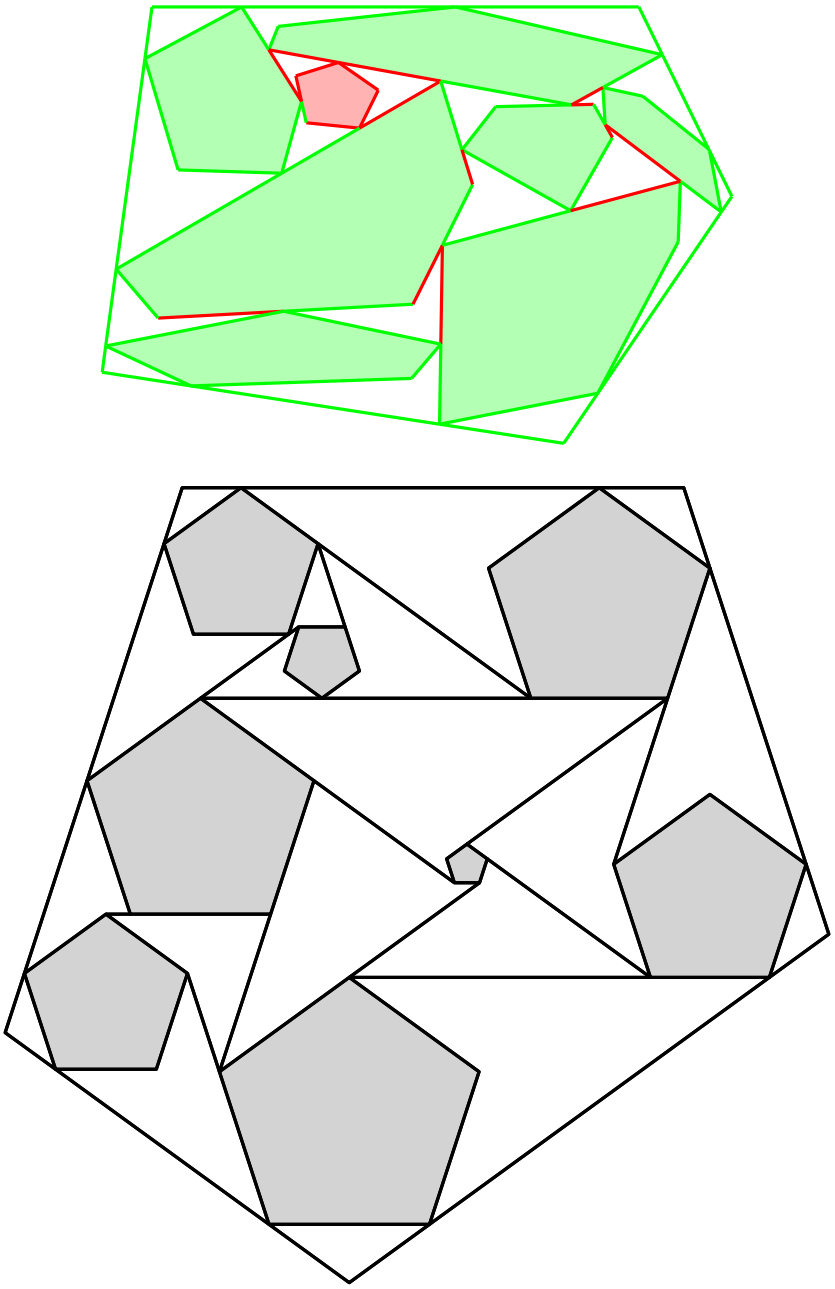

Figure 4.44: The drawing obtained from a solution of $A_S\mathbf{x} = \mathbf{e_1}$ that contains negative variables. At the top, the 5-contact structure S is shown via a general pentagon contact representation inducing S (in this contact representation, the corners of each pentagon can be labeled with $0, \ldots, 4$ in clockwise order such that corners with label i only touch the relative interiors of sides opposite to corners of label i and, hence, it induces a unique 5-contact structure). Regular pentagons with a horizontal base are assumed as prototypes for all pentagons. The signs of the variables in the solution are indicated via the colors of the edges and the pentagons: Green corresponds to non-negative variables and red corresponds to negative variables. At the bottom, the drawing obtained from the solution is shown.

Chapter 5

Existence of convex contact representations

In this chapter, we will reprove the existence of contact representations of plane graphs with given convex prototypes for each vertex. It is a well-known result that such contact representations exist. We will recall the corresponding literature in Section 5.1. Then, in Section 5.2, we will give a new, more elementary and constructive proof for the existence of similarly-aligned odd K-gon and parallel-sided even K-gon contact representations that is based on the systems of equations that we developed in Chapter 4. Finally, in Section 5.3, we will deduce the existence of contact representations for arbitrary given convex prototypes from this result.

5.1 Overview of known results

The following beautiful theorem by Schramm widely settles the question of the existence of contact representations of planar graphs with individual convex prototypes for the vertices of the graph. Without further mentioning, in the following all convex prototypes are assumed to be compact.

Theorem 5.1 (Convex Packing Theorem [Sch07])**.** *Let G be an inner triangulation of the 3-cycle a_0, a_1, a_2. Further, let C be a simple closed curve in the plane, partitioned into three arcs C_0, C_1, C_2, and, for each inner vertex v of G, let P_v be a convex prototype for v, i.e., a convex set in the plane containing more than one point. Then there exists a contact representation of a supergraph of G (on the same vertex set but possibly with more edges) where each inner vertex v is represented by a single point or a positive homothetic copy of its prototype P_v and each outer vertex a_i by the arc C_i.*

The proof of Theorem 5.1 is based on the Monster Packing Theorem [Sch07] which in turn makes use of Brouwer's Fixed Point Theorem. Since the computation of Brouwer fixed points is hard in general [HPV89], it is unlikely that an efficient algorithm can be derived from this proof. Thus, while Theorem 5.1 settles the question of the existence of convex contact representations, it leaves open two central

related questions: Can these contact representations be computed efficiently? Are they unique?

There are three results for special cases of Theorem 5.1 which at least answer the latter question. The first one is the classical Koebe-Andreev-Thursten Theorem.

Theorem 5.2 (Circle Packing Theorem [Koe36; Thu79b]). *Let G be a plane triangulation. Then G has a contact representation with disks. Further, this contact representation is unique up to Möbius transformations.*

In particular, the circle packing is unique if the outer vertices of the graph G are not represented by circles but by the sides of a given triangle in the plane. This has been generalized by Schramm to arbitrary convex shapes as prototypes.

Theorem 5.3 (Smooth Convex Packing Theorem [Sch91]). *Let G be an inner triangulation of the 3-cycle a_0, a_1, a_2. Further, let T be a triangle in the plane with sides C_0, C_1, C_2, and, for each inner vertex v of G, let P_v be a convex prototype for v with a smooth boundary. Then there exists a unique contact representation of G in which each inner vertex v is represented by a positive homothetic copy of its prototype P_v and each outer vertex a_i by the line segment C_i.*

The third theorem is about contact representations with axis-aligned rectangles, also by Schramm.

Theorem 5.4 (Schramm [Sch93]). *Let G be an inner triangulation of the 4-cycle a_0, a_1, a_2, a_3 without separating triangles. For each inner vertex v of G, let P_v be a prototype that is an axis-aligned rectangle. Then there exists a contact representation of a supergraph of G (on the same vertex set but possibly with more edges) where each inner vertex v is represented by a single point or a positive homothetic copy of its prototype P_v and the outer vertices a_0, a_1, a_2, a_3 are represented by the upper, right, lower, and left side of an axis-aligned rectangle in this order. Further, this contact representation is unique up to scaling.*

Although Schramm is the author of Theorems 5.1, 5.3 and 5.4, their proofs are completely independent.

5.2 New proof for K-gon contact representations

In this section, we will prove the existence of similarly-aligned odd K-gon and parallel-sided even K-gon contact representations based on the systems of linear equations developed in Chapter 4. Let G be an inner triangulation of a K-cycle with $K \geq 3$ and $K \neq 4$. In the following, when we say *K-gon contact representation*, we mean a similarly-aligned odd K-gon contact representation, if K is odd, and a parallel-sided even K-gon contact representation if K is even. The system of linear equations from Chapter 4 for the computation of a K-gon contact representation of G depends on a K-contact structure S of G, the slopes of the sides of the given prototypes for the vertices of G, and the side lengths of

the prototypes for the inner vertices of G. Let $v_0, \dots, v_{n-1}$ be the inner vertices of G and let r_{ij} be the length of $\text{side}_j(P_i)$ where P_i is the prototype for v_i. We set $\mathbf{r} := (r_{0,0}, \dots, r_{0,K-1}, r_{1,0}, \dots, r_{1,K-1}, \dots, r_{n-1,0}, \dots, r_{n-1,K-1})$. In the following, we assume that the slopes of the prototypes are fixed and consider the system of linear equations in dependence of the K-contact structure S and the side length vector $\mathbf{r}$. We denote this system of linear equations by $\mathcal{A}_{S,\mathbf{r}}$.

The approach we will take in this section has already been taken in [Sch16; Sch17] for triangle and rectangle contact representations. Nevertheless, the proof that we will give here is simpler than those given in [Sch16; Sch17]. This simplification is obtained by means of the following observation: The proofs in Chapter 4 (except for those of Theorems 4.27, 4.29 and 4.64) do not rely on the fact that the r_{ij} are actually the side lengths of polygons with the slopes used for constructing the systems of equations, but only rely on the fact that $r_{ij} > 0$ for all i, j. So the crucial idea will be that we consider the system $\mathcal{A}_{S,\mathbf{r}}$ for all K-contact structures S and all $\mathbf{r} \in \mathbb{R}^{nK}_{>0}$. With this purely algebraic point of view on these systems of linear equations we are able to skip the geometric parts of the proofs given in [Sch16; Sch17].

Let $\mathbf{x}^{(S,\mathbf{r})}$ be the unique solution of $\mathcal{A}_{S,\mathbf{r}}$. For a K-contact structure S, we set $R_S := \{\, \mathbf{r} \in \mathbb{R}^{nK}_{>0} : \mathbf{x}^{(S,\mathbf{r})} > 0 \,\}$ and $\overline{R_S} := \{\, \mathbf{r} \in \mathbb{R}^{nK}_{>0} : \mathbf{x}^{(S,\mathbf{r})} \geq 0 \,\}$. Our goal is to prove that $\bigcup_S \overline{R_S} = \mathbb{R}^{nK}_{>0}$. Then, in particular for each $\mathbf{r} \in \mathbb{R}^{nK}_{>0}$ which is the vector of side lengths of actual polygons with the fixed slopes, there exists a K-contact structure S such that the solution of $\mathcal{A}_{S,\mathbf{r}}$ is non-negative. And, due to Theorems 4.27 and 4.29, this non-negative solution implies the existence of a K-gon contact representation of G in which the inner vertices of G are represented by homothetic copies (which might degenerate to points if $K = 3$ or $K = 6$) of the prototypes given by this side length vector $\mathbf{r}$.

Reduction to graphs without separating triangles in the cases $\mathbf{K = 3}$ and $\mathbf{K = 6}$. Since the existence proof will be based on Theorems 4.59 to 4.63 which make statements about all flips in K-contact structures except for non-facial flips in the cases $K = 3$ and $K = 6$, we first want to show that in these two cases we can reduce the problem to the case that G has no separating triangles. Then all flips in K-contact structures of G are facial flips.

Let $\mathbf{r} \in \mathbb{R}^{nK}_{>0}$ be an arbitrary side length vector for G. Let $T = v_0, v_1, v_2$ be a separating triangle of G, let G_{out} be the graph G without the vertices inside T, and let G_{in} be the graph G without the vertices outside T (with v_0, v_1, v_2 as outer vertices). Further, let $\mathbf{r}_{\text{out}}$ and $\mathbf{r}_{\text{in}}$ be the restrictions of $\mathbf{r}$ to the inner vertices of G_{out} and G_{in}, respectively.

Let us first consider the case $K = 3$. See Fig. 5.1 for an illustration of the decomposition process described in the following. Assume that there exists a 3-contact structure (Schnyder wood) S_{out} of G_{out} such that $\mathbf{r}_{\text{out}} \in \overline{R_{S_{\text{out}}}}$. Let $G^{\text{out}}_{\text{skel}}$ be the corresponding skeleton graph. Then T corresponds to an inner face of $G^{\text{out}}_{\text{skel}}$ with its three edges e_0, e_1, and e_2 corresponding to the vertices v_0, v_1, and v_2, respectively. The 3-contact structure S_{out} assigns sides of the prototypes of v_0, v_1, and v_2 to these three edges which we denote by $\text{side}_{i_0}(P_{v_0})$, $\text{side}_{i_1}(P_{v_1})$, and $\text{side}_{i_2}(P_{v_2})$, re-

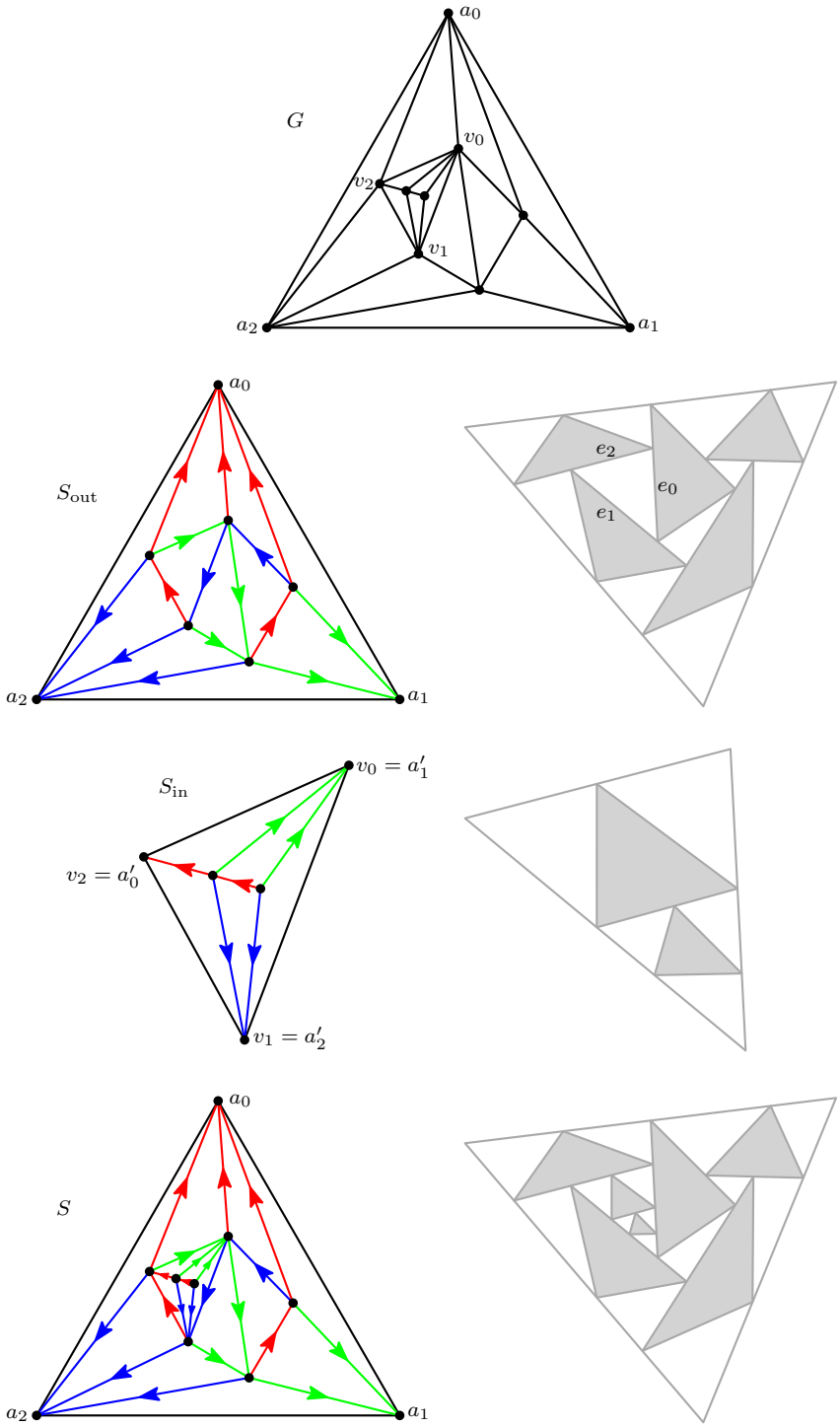

Figure 5.1: Decomposition of a triangulation at a separating triangle for the computation of a similarly-aligned triangle contact representation.

spectively. Now we can interpret v_0, v_1, and v_2 as outer vertices a'_{i_0}, a'_{i_1}, and a'_{i_2}, respectively, of G_{in} and set the slopes of the prototypes of these three outer vertices to $\text{slope}_{i_0}(P_{v_0})$, $\text{slope}_{i_1}(P_{v_1})$, and $\text{slope}_{i_2}(P_{v_2})$. Assume that in this setting there exists a 3-contact structure S_{in} of G_{in} such that $\mathbf{r}_{\text{in}} \in \overline{R_{S_{\text{in}}}}$. Let S be the 3-contact structure of G obtained by plugging S_{in} into S_{out}. Then $\mathbf{r} \in \overline{R_S}$ since the non-negative solution of $\mathcal{A}_{S_{\text{in}},\mathbf{r}_{\text{in}}}$ scaled with the non-negative factor $x_{e_0} + x_{e_1} + x_{e_2}$ and combined with the non-negative solution of $\mathcal{A}_{S_{\text{out}},\mathbf{r}_{\text{out}}}$ gives a non-negative solution of $\mathcal{A}_{S,\mathbf{r}}$.

Let us now consider the case $K = 6$. This case is illustrated in Fig. 5.2. As in the previous case, assume that there exists a 6-contact structure S_{out} of G_{out} such that $\mathbf{r}_{\text{out}} \in \overline{R_{S_{\text{out}}}}$ and let $G^{\text{out}}_{\text{skel}}$ be the corresponding skeleton graph. Then, again, T corresponds to an inner face of $G^{\text{out}}_{\text{skel}}$ with its three edges e_0, e_1, and e_2 corresponding to the vertices v_0, v_1, and v_2. The 6-contact structure S_{out} assigns sides of the prototypes of v_0, v_1, and v_2 to these three edges which we denote by $\text{side}_{i_0}(P_{v_0})$, $\text{side}_{i_1}(P_{v_1})$, and $\text{side}_{i_2}(P_{v_2})$, respectively. Note that $\{i_0, i_1, i_2\} \in \{\{0, 2, 4\}, \{1, 3, 5\}\}$. Now we modify G_{in} as follows: We subdivide the three outer edges and then connect each of the three subdivision vertices to the unique common neighbor of its two neighbors. Then G_{in} is an inner triangulation of a 6-cycle. Now we can interpret v_0, v_1, and v_2 as outer vertices a'_{i_0}, a'_{i_1}, and a'_{i_2}, respectively, of G_{in} and the other three outer vertices accordingly as a'_i for $i \in \{0, \dots, 5\} \setminus \{i_0, i_1, i_2\}$. Assume that in this setting there exists a 6-contact structure S_{in} of G_{in} such that $\mathbf{r}_{\text{in}} \in \overline{R_{S_{\text{in}}}}$. Let S be the 6-contact structure of G obtained by first contracting the edges $a'_{i_j} a'_{i_j+1}$, $j = 0, 1, 2$, in S_{in} and then plugging this modification of S_{in} into S_{out}. Then $\mathbf{r} \in \overline{R_S}$ since the non-negative solution of $\mathcal{A}_{S_{\text{in}},\mathbf{r}_{\text{in}}}$ scaled with a proper non-negative factor and combined with the non-negative solution of $\mathcal{A}_{S_{\text{out}},\mathbf{r}_{\text{out}}}$ gives a non-negative solution of $\mathcal{A}_{S,\mathbf{r}}$.

These observations show that in the cases $K = 3$ and $K = 6$, if $\bigcup_S \overline{R_S} = \mathbb{R}^{nK}_{>0}$ holds for all inner triangulations G of a K-cycle without separating triangles, then it also holds for all remaining triangulations G of a K-cycle (with separating triangles). Hence, for the rest of this section, we can assume that G has no separating triangles if $K = 3$ or $K = 6$.

The idea. The idea of the proof is to start with a side length vector $\mathbf{r_0}$ for that we know a K-contact structure S_0 with $\mathbf{r_0} \in \overline{R_{S_0}}$ and from there proceed along a straight line segment in $\mathbb{R}^{nK}$ to the desired side length vector $\tilde{\mathbf{r}}$, maintaining the invariant that for the current side length vector $\mathbf{r}$ there exists a K-contact structure S with $\mathbf{r} \in \overline{R_S}$.

For now, let S be a fixed K-contact structure. As a first step towards this goal, the following lemma gives a characterization of the sets R_S and $\overline{R_S}$ in terms of polynomials of bounded degree.

Lemma 5.5. *There are polynomials $p_0, \dots, p_{m-1}$ in nK variables with $\deg p_k \le m$ for all k where $m = O(nK)$ such that*

$$R_S = \{\, \mathbf{r} \in \mathbb{R}^{nK}_{>0} : p_k(\mathbf{r}) > 0 \text{ for all } k \,\} \ ,$$
$$\overline{R_S} = \{\, \mathbf{r} \in \mathbb{R}^{nK}_{>0} : p_k(\mathbf{r}) \ge 0 \text{ for all } k \,\} \ .$$

In particular, R_S is an open set and $\overline{R_S}$ its closure.

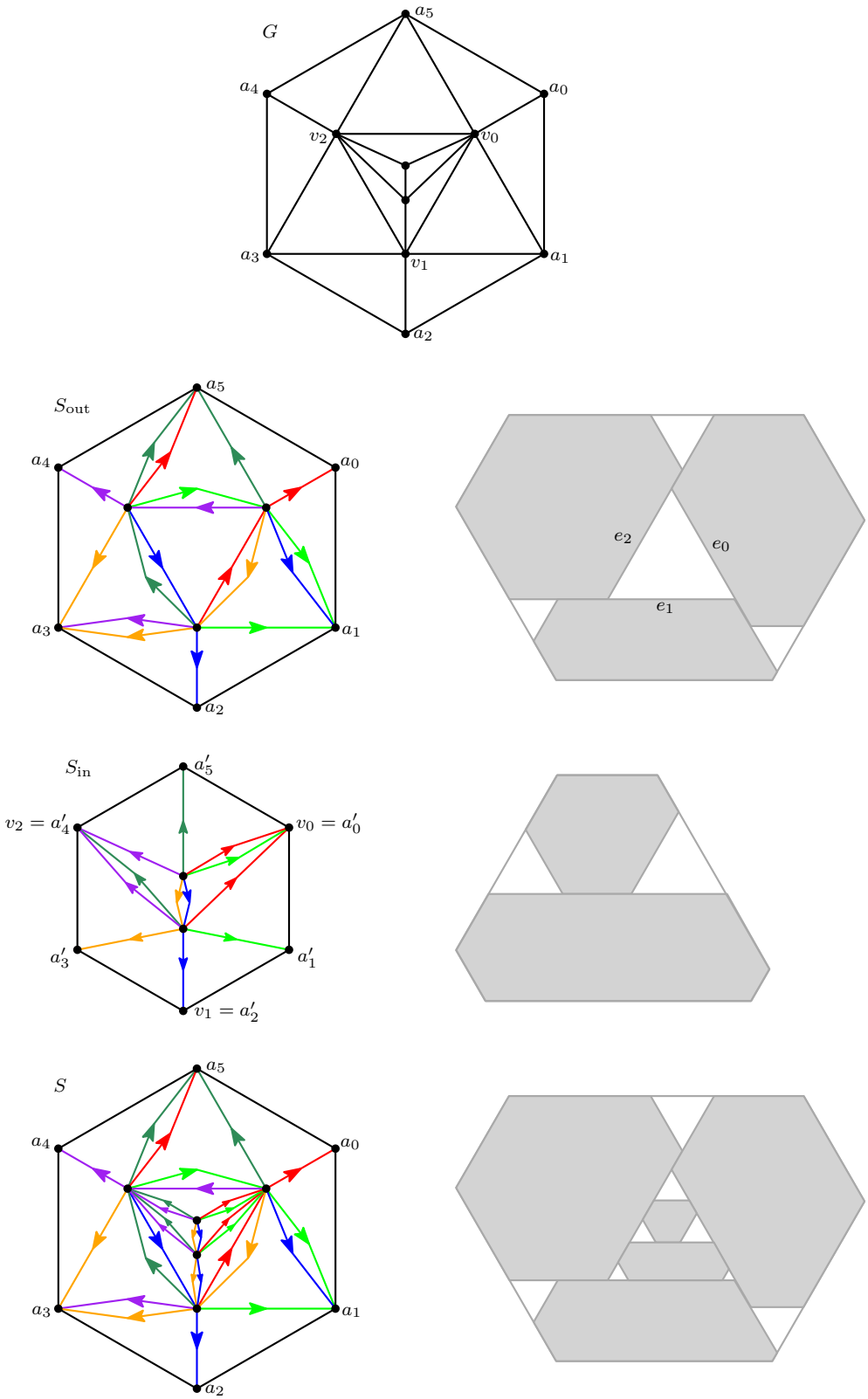

Figure 5.2: Decomposition of an inner triangulation of a 6-cycle at a separating triangle for the computation of a parallel-sided hexagon contact representation.

Proof. Let m be the number of variables of $\mathcal{A}_{S,\mathbf{r}}$ which is also the number of equations of $\mathcal{A}_{S,\mathbf{r}}$. Then $m = O(nK)$. For $k = 0, \dots, m-1$, let $A^{(k)}_{S,\mathbf{r}}$ be the matrix obtained from $A_{S,\mathbf{r}}$ by replacing the kth column with $\mathbf{e_1}$. Then, for $k = 0, \dots, m-1$, we have $x_k^{(S,\mathbf{r})} = \frac{\det A^{(k)}_{S,\mathbf{r}}}{\det A_{S,\mathbf{r}}}$ by Cramer's rule. Further, each entry of $A_{S,\mathbf{r}}$ and thus also each entry of $A^{(k)}_{S,\mathbf{r}}$ is a polynomial in the variables r_{ij} of degree at most 1. Therefore, $\det A^{(k)}_{S,\mathbf{r}}$ is a polynomial in the variables r_{ij} of degree at most m. Hence, to obtain the wanted representations of R_S and $\overline{R_S}$, we can set $p_k := \operatorname{sgn}(\det A_{S,\mathbf{r}}) \det A^{(k)}_{S,\mathbf{r}}$ for $k = 0, \dots, m-1$. Note that $\operatorname{sgn}(\det A_{S,\mathbf{r}})$ is constant, since $\det A_{S,\mathbf{r}}$ is a continuous function in the parameter $\mathbf{r}$ and $\det A_{S,\mathbf{r}} \neq 0$ for all $\mathbf{r} \in \mathbb{R}^{nK}_{>0}$ by Theorems 4.26 and 4.28, and therefore p_k as required. □

Now we want to study what Lemma 5.5 means for the complexity of the intersection of R_S or $\overline{R_S}$ with a straight line in $\mathbb{R}^{nK}$.

Lemma 5.6. *Let $\mathbf{r_0}, \mathbf{r_1} \in \mathbb{R}^{nK}_{>0}$ be different side length vectors and, for each $t \in [0,1]$, let $\mathbf{r_t} := (1-t)\mathbf{r_0} + t\mathbf{r_1}$. Then there are open intervals $I_0, \dots, I_{k-1}$ with $k \leq c(n,K) = O((nK)^2)$ such that*

$$I_0 \cup \dots \cup I_{k-1} = \{\, t \in [0,1] \colon \mathbf{r_t} \in R_S \,\} \ ,$$
$$\overline{I_0} \cup \dots \cup \overline{I_{k-1}} = \{\, t \in [0,1] \colon \mathbf{r_t} \in \overline{R_S} \,\} \ .$$

Proof. By Lemma 5.5, there are polynomials $p_0, \dots, p_{m-1}$ with $m = O(nK)$ and with $\deg p_i \leq m$ for all i such that $\mathbf{r_t} \in R_S$ if and only if $p_i(\mathbf{r_t}) > 0$ for all i, and $\mathbf{r_t} \in \overline{R_S}$ if and only if $p_i(\mathbf{r_t}) \geq 0$ for all i. There, $p_i(\mathbf{r_t})$ can be viewed as a polynomial in the variable t with $\deg_t p_i(\mathbf{r_t}) \leq m$.

Then, for each i, there are open intervals $I^{(i)}_0, \dots, I^{(i)}_{k_i-1}$ with $k_i \leq \frac{m}{2} + 1$ such that $p_i(\mathbf{r_t}) > 0$ if and only if $t \in \bigcup_j I^{(i)}_j$, and $p_i(\mathbf{r_t}) \geq 0$ if and only if $t \in \bigcup_j \overline{I^{(i)}_j}$. We can assume that, for each i, the intervals $I^{(i)}_0, \dots, I^{(i)}_{k_i-1}$ are pairwise disjoint.

Now let $J := \bigcap_{i=0,\dots,m-1} \bigcup_{j=0,\dots,k_i-1} I^{(i)}_j$. Then J is also the disjoint union of open intervals $I_0, \dots, I_{k-1}$. Since each endpoint of each of these intervals is also an endpoint of one of the intervals $I^{(i)}_j$, we have $k \leq \sum_i k_i \leq m^2 = O((nK)^2)$. Since $\mathbf{r_t} \in R_S$ if and only if $t \in J$, and $\mathbf{r_t} \in \overline{R_S}$ if and only if $t \in \overline{I_0} \cup \dots \cup \overline{I_{k-1}}$, this completes the proof. □

Lemma 5.6 shows that, if $\mathbf{r_t} \in R_S$, then for $\varepsilon > 0$ small enough also $\mathbf{r_{t+\varepsilon}} \in R_S$. So the main problem is to find a way to proceed towards $\mathbf{r_1}$ if $\mathbf{r_t} \in \overline{R_S} \setminus R_S$.

Due to Lemmas 4.49 and 4.57, if $\mathbf{r} \in \overline{R_S} \setminus R_S$, then the weak sign-separating edges of the corresponding solution of $\mathcal{A}_{S,\mathbf{r}}$ are a non-empty disjoint union of essential cycles. In the following, we pretend that each of these essential cycles corresponds to exactly one variable x_e that is zero although in the case $K = 3$ this essential cycle always corresponds to exactly three edge-variables that are zero and in the case $K = 6$ it can correspond to one or three edge-variables that are zero. In those cases, all statements that we make about this variable x_e are true for all three variables.

The following lemma is just a reformulation of Theorems 4.59 to 4.63. Note that in the cases $K = 3$ and $K = 6$ this is only true because we only consider graphs G without separating triangles in these cases.

Lemma 5.7. *Let S and S' be neighboring K-contact structures related by a flip corresponding to the variable x_e. Then $x_e^{(S,\mathbf{r})} > 0$ if and only if $x_e^{(S',\mathbf{r})} < 0$. In particular, if $\mathbf{r} \in R_S$, then $\mathbf{r} \notin \overline{R_{S'}}$.* □

The next lemma shows that, if we reach the boundary of $\overline{R_S}$, i.e., $\mathbf{r} \in \overline{R_S} \setminus R_S$, and in the corresponding solution of $\mathcal{A}_{S,\mathbf{r}}$ exactly one edge-variable x_e is zero, then we can proceed with the neighboring K-contact structure of S obtained by flipping the essential cycle corresponding to x_e.

Lemma 5.8. *Let $\{\, \mathbf{r_t} = (1-t)\mathbf{r_0} + t\mathbf{r_1} : t \in [0,1] \,\}$ be a line segment of side length vectors. Let $t_0 \in (0,1)$ such that $\mathbf{r_{t_0}} \in \overline{R_S} \setminus R_S$, in the corresponding solution of $\mathcal{A}_{S,\mathbf{r_0}}$ only one variable x_e is zero, and there is an $\varepsilon > 0$ such that, for each $t \in (t_0, t_0+\varepsilon]$, we have $\mathbf{r_t} \notin \overline{R_S}$. Let S' be the neighboring K-contact structure of S obtained by flipping the essential cycle corresponding to e. Then there exists an $\varepsilon' > 0$ such that $\mathbf{r_t} \in R_{S'}$ for all $t \in (t_0, t_0+\varepsilon']$.*

Proof. Note that $\mathbf{x}^{(S,\mathbf{r_{t_0}})} = \mathbf{x}^{(S',\mathbf{r_{t_0}})}$. Therefore, $\mathbf{x}_i^{(S,\mathbf{r_{t_0}})}, \mathbf{x}_i^{(S',\mathbf{r_{t_0}})} > 0$ for all $i \neq e$ and thus, because of continuity, there is an $\varepsilon'' > 0$ with $\mathbf{x}_j^{(S,\mathbf{r_t})}, \mathbf{x}_j^{(S',\mathbf{r_t})} > 0$ for all $j \neq i$ and $t \in [t_0, t_0+\varepsilon'']$. Let $\varepsilon' := \min\{\varepsilon, \varepsilon''\}$. Then, since $\mathbf{r_t} \notin \overline{R_S}$ for all $t \in (t_0, t_0+\varepsilon]$, we have $x_e^{(S,\mathbf{r_t})} < 0$ for all $t \in (t_0, t_0+\varepsilon']$. Therefore, Lemma 5.7 implies that $x_e^{(S',\mathbf{r_t})} > 0$ and, hence, $\mathbf{r_t} \in R_{S'}$ for all $t \in (t_0, t_0+\varepsilon']$. □

Lemma 5.8 can only be applied when we run into a situation where only one single variable is zero. In the following we prove a more general lemma that can also be applied when we run into a situation where more than one variable is zero. By $B(\mathbf{r},\delta) = \{\, \mathbf{r}' : \|\mathbf{r}'-\mathbf{r}\| < \delta \,\}$ and $\overline{B}(\mathbf{r},\delta) = \{\, \mathbf{r}' : \|\mathbf{r}'-\mathbf{r}\| \leq \delta \,\}$, where $\|\cdot\|$ denotes the maximum norm, we denote the open and closed ball, respectively, with center $\mathbf{r}$ and radius δ.

Lemma 5.9. *Let $\mathbf{r} \in \overline{R_S} \setminus R_S$. Then, for each $\varepsilon > 0$, there exists an $\mathbf{r}' \in B(\mathbf{r},\varepsilon)$ and a neighboring K-contact structure S' of S such that $\mathbf{r}' \in R_{S'}$.*

Proof. Let G_{skel} be the skeleton graph corresponding to S and let e be an edge of G_{skel} with $x_e^{(S,\mathbf{r})} = 0$. Further, let S' be the neighboring K-contact structure of S obtained by the flip corresponding to e. Then we have $\mathbf{x}^{(S,\mathbf{r})} = \mathbf{x}^{(S',\mathbf{r})}$. Let G'_{skel} be the skeleton graph corresponding to S'. We set $\mathbf{x} := \mathbf{x}^{(S',\mathbf{r})}$ and we will construct a perturbation $\mathbf{x}'$ of $\mathbf{x}$ such that $\mathbf{x}' > 0$ and $\mathbf{x}' = \mathbf{x}^{(S',\mathbf{r}')}$ for a vector $\mathbf{r}' \in B(\mathbf{r},\varepsilon)$.

Since $x_{v_i} > 0$ for all inner vertices v_i of G, we have $\varepsilon' := \min_i x_{v_i} \cdot \varepsilon > 0$. Let e' be an edge of G'_{skel} with $x_{e'} = 0$. Then, in $\mathcal{A}_{S',\mathbf{r}}$, the variable $x_{e'}$ is contained in at most one equation of the type (4.6).

i) If $x_{e'}$ is not contained in an equation of the type (4.6), we set $x_{e'}$ to an arbitrary value in the interval $(0, \frac{\varepsilon'}{n_0})$ where n_0 denotes the the number of zeros of $\mathbf{x}$.

ii) If $x_{e'}$ is not contained in an equation of the type (4.6), let e'' and e''' be edges of the other two concave arcs of the pseudotriangle corresponding to this equation. Then, due to Lemmas 4.16 and 4.19, there are $\tilde{x}_{e'}, \tilde{x}_{e''}, \tilde{x}_{e'''} > 0$ such that, for each $\delta > 0$, after increasing $x_{e'}$, $x_{e''}$, and $x_{e'''}$ by $\delta\tilde{x}_{e'}$, $\delta\tilde{x}_{e''}$, and $\delta\tilde{x}_{e'''}$, respectively, all equations of the type (4.6) are still fulfilled. We choose δ small enough such that $\delta\tilde{x}_{e'}, \delta\tilde{x}_{e''}, \delta\tilde{x}_{e'''} < \frac{\varepsilon'}{n_0}$ where n_0 is defined as in the previous case.

We repeat this iteratively for all edges e' of G'_{skel} with $x_{e'} = 0$ and denote the resulting vector by $\mathbf{x}'$. Then, clearly $\mathbf{x}' > 0$ and $\mathbf{x}'$ fulfills all equations of $\mathcal{A}_{S',\mathbf{r}}$ that are of the type (4.6). The remaining equations of $\mathcal{A}_{S',\mathbf{r}}$ might not be fulfilled anymore.

Now we will construct a side length vector $\mathbf{r}'$ such that $\mathbf{x}'$ also fulfills the equations of $\mathcal{A}_{S',\mathbf{r}'}$ of the type (4.5). Since the equations of the type (4.6) are independent of the side length vector, these equations will still be fulfilled. Let v_i be an inner vertex of G and let $j \in \{0, \dots, K-1\}$. Then the corresponding equation of $\mathcal{A}_{S',\mathbf{r}}$ of type (4.5) implies that $r_{ij} = \frac{\sum_{e \in E_j(v_i)} x_e}{x_{v_i}}$. If we set $x'_{v_i} := x_{v_i}$ and $r'_{ij} := \frac{\sum_{e \in E_j(v_i)} x'_e}{x'_{v_i}}$, then also $\mathbf{x}'$ fulfills the corresponding equation of $\mathcal{A}_{S',\mathbf{r}'}$ of type (4.5). In each increasing step of $\mathbf{x}$ in the last paragraph, at most one of the edges of $E_j(v_i)$ was involved. Therefore, $0 \leq \sum_{e \in E_j(v_i)} x'_e - \sum_{e \in E_j(v_i)} x_e < \varepsilon'$ and, hence, $0 \leq r'_{ij} - r_{ij} < \frac{\varepsilon'}{x_{v_i}} \leq \varepsilon$. We repeat this for all inner vertices v_i of G and all $j \in \{0, \dots, K-1\}$. Then $\mathbf{r}' \in B(\mathbf{r}, \varepsilon)$ and $\mathbf{x}'$ fulfills all equations equations of $\mathcal{A}_{S',\mathbf{r}'}$ except for the equation (4.7). By scaling the entire vector $\mathbf{x}'$ with a positive factor, also this last equation can be fulfilled. Hence, $\mathbf{r}' \in R_{S'}$. □

Theorem 5.10. *Let $\tilde{\mathbf{r}} \in \mathbb{R}^{nK}_{>0}$. Then there exists a K-contact structure S such that $\tilde{\mathbf{r}} \in \overline{R_S}$.*

Proof. Assume that there is no K-contact structure S with $\tilde{\mathbf{r}} \in \overline{R_S}$. The idea of the proof is to construct – under this assumption – a line segment contradicting Lemma 5.6. We will construct a sequence $(S_i)_{i \in \mathbb{N}}$ of K-contact structures, two sequences $(\mathbf{r_i})_{i \in \mathbb{N}}$ and $(\mathbf{r'_i})_{i \in \mathbb{N}}$ of side length vectors, and two sequences $(\varepsilon_i)_{i \in \mathbb{N}}$ and $(\varepsilon'_i)_{i \in \mathbb{N}}$ of positive real numbers fulfilling the following invariants:

(I1) $\overline{B}(\mathbf{r_i}, \varepsilon_i) \subset R_{S_i}$.

(I2) For each $\mathbf{r}' \in \overline{B}(\mathbf{r'_i}, \varepsilon'_i)$, the line segment $\{\, (1-t)\mathbf{r}' + t\tilde{\mathbf{r}} \colon t \in [0,1] \,\}$ intersects the balls $\overline{B}(\mathbf{r_0}, \varepsilon_0), \dots, \overline{B}(\mathbf{r_i}, \varepsilon_i)$ in this order (with increasing t).

(I3) Either $\mathbf{r_i} = \mathbf{r'_i}$ or the point $\mathbf{r_i}$ is in the relative interior of the line segment connecting the points $\mathbf{r'_i}$ and $\tilde{\mathbf{r}}$. In particular, these three points are collinear.

(I4) The K-contact structures S_i and S_{i+1} are neighboring.

It remains to show how these sequences can be constructed and why their existence contradicts Lemma 5.6.

To construct the sequences, we start with an arbitrary K-contact structure S_0 of G that exists due to Theorems 3.14 and 3.39.

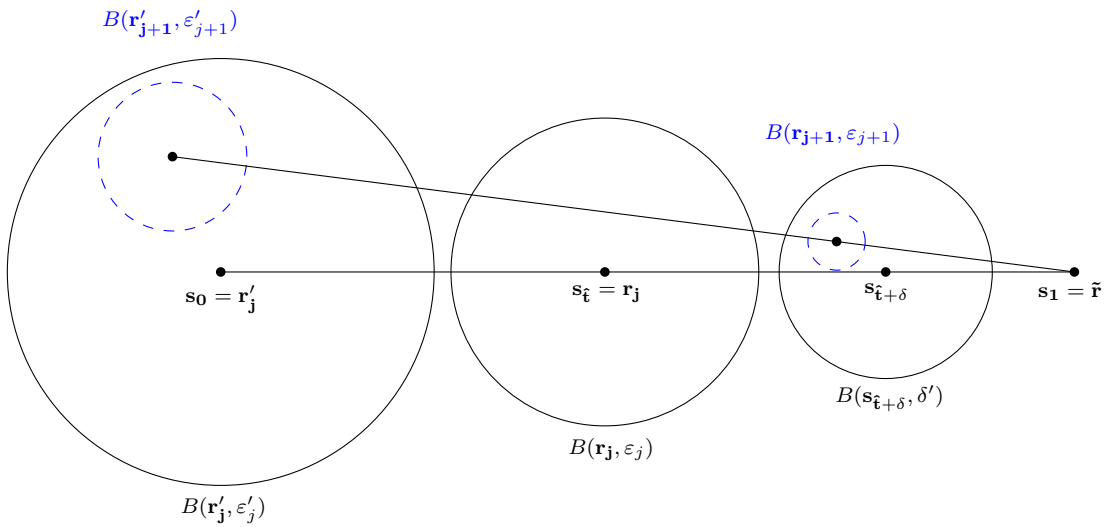

Figure 5.3: Illustration of the construction of the sequences in the proof of Theorem 5.10.

Claim 1. *For each K-contact structure S, we have $R_S \neq \emptyset$.*

Proof. Each edge-variable x_e of the system of equations $\mathcal{A}_S$ is contained in exactly one equation of the type (4.6). Therefore, Lemma 4.19 implies that we can find positive values for all edge-variables such that all equations of this type are fulfilled. Then, after scaling all these values with a unique positive factor, also equation (4.7) can be fulfilled. Further, we set $x_{v_i} := 1$ for all inner vertices v_i of G. Then also equation (4.5) is fulfilled if we set $r_{ij} := \sum_{e \in E_j(v_i)} x_e > 0$. Hence, $\mathbf{r} := (r_{ij}) \in R_S$. $\triangle$

Because of Claim 1, there exists a side length vector $\mathbf{r_0}$ with $\mathbf{r_0} \in R_{S_0}$. Then, due to Lemma 5.5, there exists an $\varepsilon_0 \in (0,1)$ such that $\overline{B}(\mathbf{r_0}, \varepsilon_0) \subset R_{S_0}$. Further, we set $\mathbf{r'_0} := \mathbf{r_0}$ and $\varepsilon'_0 := \varepsilon_0$. Then these initial values fulfill each of the four invariants.

Now we describe how to construct the $(j+1)$th sequence members from the jth ones. This construction is illustrated in Fig. 5.3. We set $\mathbf{s_t} := (1-t)\mathbf{r'_j} + t\tilde{\mathbf{r}}$ for all $t \in [0,1]$. Then, because of (I3), there is a $\hat{t} \in [0,1)$ with $\mathbf{s_{\hat{t}}} = \mathbf{r_j}$ and therefore, because of (I1), we have $\mathbf{s_{\hat{t}}} \in R_{S_j}$. Thus Lemma 5.6 gives us a $\delta > 0$ such that $\mathbf{s_t} \in R_{S_j}$ for all $t \in [\hat{t}, \hat{t}+\delta)$ and $\mathbf{s_{\hat{t}+\delta}} \in \overline{R_{S_j}} \setminus R_{S_j}$. Because of our assumption we have $\hat{t}+\delta < 1$ and because of $\mathbf{s_{\hat{t}+\delta}} \notin \overline{B}(\mathbf{r_j}, \varepsilon_j) \subset R_{S_j}$ we have $\|\mathbf{r_j} - \mathbf{s_{\hat{t}+\delta}}\| > \varepsilon_j$. Now we set

$$\delta' := \min\left\{\left(1-(\hat{t}+\delta)\right)\varepsilon'_j,\ \|\mathbf{r_j} - \mathbf{s_{\hat{t}+\delta}}\| - \varepsilon_j\right\} > 0\ .$$

Then Lemma 5.9 gives us an $\mathbf{r_{j+1}} \in B(\mathbf{s_{\hat{t}+\delta}}, \delta') \cap R_{S_{j+1}}$ for a neighboring K-contact structure S_{j+1} of S_j. Now we set $\mathbf{r'_{j+1}} := \mathbf{r'_j} + \frac{1}{1-(\hat{t}+\delta)}(\mathbf{r_{j+1}} - \mathbf{s_{\hat{t}+\delta}})$. Then

$$\|\mathbf{r'_{j+1}} - \mathbf{r'_j}\| = \frac{1}{1-(\hat{t}+\delta)}\|\mathbf{r_{j+1}} - \mathbf{s_{\hat{t}+\delta}}\| < \frac{1}{1-(\hat{t}+\delta)}\delta' \leq \varepsilon'_j$$

and therefore $\mathbf{r'_{j+1}} \in B(\mathbf{r'_j}, \varepsilon'_j)$. Moreover, Lemma 5.5 implies that there is an $\varepsilon_{j+1} \in (0, \delta' - \|\mathbf{r_{j+1}} - \mathbf{s_{\hat{t}+\delta}}\|)$ such that $\overline{B}(\mathbf{r_{j+1}}, \varepsilon_{j+1}) \subset R_{S_{j+1}}$. Finally, we set $\varepsilon'_{j+1} := \frac{1}{1-(\hat{t}+\delta)}\varepsilon_{j+1}$.

Clearly, the invariants (I1), (I3), and (I4) are fulfilled for the $(j+1)$th sequence members. Since $\overline{B}(\mathbf{r'_{j+1}}, \varepsilon'_{j+1}) \subseteq \overline{B}(\mathbf{r'_j}, \varepsilon'_j)$, for each $\mathbf{r'} \in \overline{B}(\mathbf{r'_{j+1}}, \varepsilon'_{j+1})$, the line segment $\{\,(1-t)\mathbf{r'} + t\tilde{\mathbf{r}} \colon t \in [0,1]\,\}$ intersects the balls $\overline{B}(\mathbf{r_0}, \varepsilon_0), \ldots, \overline{B}(\mathbf{r_j}, \varepsilon_j)$ in the right order. It immediately follows from the construction that the ball $\overline{B}(\mathbf{r_{j+1}}, \varepsilon_{j+1})$ is also intersected by this line segment. Moreover, because of $\delta' \leq \|\mathbf{r_j} - \mathbf{s_{\hat{t}+\delta}}\| - \varepsilon_j$ and $\overline{B}(\mathbf{r_{j+1}}, \varepsilon_{j+1}) \subseteq B(\mathbf{s_{\hat{t}+\delta}}, \delta')$, the intersection with $\overline{B}(\mathbf{r_{j+1}}, \varepsilon_{j+1})$ is closer to $\tilde{\mathbf{r}}$ than the intersection with $\overline{B}(\mathbf{r_j}, \varepsilon_j)$. Therefore, also the invariant (I2) is fulfilled for the $(j+1)$th sequence members.

Now we will show that the sequences constructed above contradict Lemma 5.6. Let L be the number of K-contact structures of G and let $c := c(n, K)$ be the value of the function from Lemma 5.6. We set $M := Lc + 1$. Then it follows from the pigeonhole principle that there is a K-contact structure S such that there are indices $0 \leq i_0 < \cdots < i_c \leq M$ with $S = S_{i_0} = \cdots = S_{i_c}$. For $l = 0, \ldots, c$, let $\hat{\mathbf{r}}_\mathbf{l}$ be an intersection point of the line segment $\{\,(1-t)\mathbf{r'_M} + t\tilde{\mathbf{r}} \colon t \in [0,1]\,\}$ and the ball $\overline{B}(\mathbf{r_{i_l}}, \varepsilon_{i_l})$. Thus $\hat{\mathbf{r}}_\mathbf{l} \in R_S$ for $l = 0, \ldots, c$. From Lemma 5.6 it follows that the intersection of $\{\,(1-t)\mathbf{r'_M} + t\tilde{\mathbf{r}} \colon t \in [0,1]\,\}$ and R_S is a disjoint union of at most c open intervals. Therefore, there is an l such that $\hat{\mathbf{r}}_\mathbf{l}$ and $\hat{\mathbf{r}}_\mathbf{l+1}$ belong to the same interval. In particular, for each $\tau \in [0,1]$, we have $(1-\tau)\hat{\mathbf{r}}_\mathbf{l} + \tau\hat{\mathbf{r}}_\mathbf{l+1} \in R_S$. Because of (I4), the K-contact structure $S' := S_{i_l+1}$ and S are neighboring. Moreover, because of (I2), there is a $\tau' \in [0,1]$ with $(1-\tau')\hat{\mathbf{r}}_\mathbf{l} + \tau'\hat{\mathbf{r}}_\mathbf{l+1} \in \overline{B}(\mathbf{r_{i_l+1}}, \varepsilon_{i_l+1})$. But then, because of (I1), we also have $(1-\tau')\hat{\mathbf{r}}_\mathbf{l} + \tau'\hat{\mathbf{r}}_\mathbf{l+1} \in R_{S'}$, contradicting Lemma 5.7.

Hence, our assumption that there is no K-contact structure S with $\tilde{\mathbf{r}} \in \overline{R_S}$ was wrong. □

5.3 Derived proof for general convex shapes

In this section, we will show that we can derive a slightly weaker version of the Convex Packing Theorem (Theorem 5.1) from Theorem 5.10. Before that, we will discuss the case that the prototypes are arbitrary convex polygons.

Arbitrary polygons as prototypes. Let G be an inner triangulation of the 3-cycle a_0, a_1, a_2. Let C be a triangle in the plane with sides C_0, C_1, C_2 in clockwise order. Further, for each inner vertex v of G, let P_v be a prototype that is a convex polygon. The task is to find a contact representation of G in which, for $i = 0, 1, 2$, the outer vertex a_i is represented by C_i and each inner vertex v is represented by a homothetic copy of its prototype P_v. We will now describe how this setting can be interpreted as the setting for the computation of a similarly-aligned odd K-gon or a parallel-sided even K-gon contact representation by adding sides of length zero to the prototypes.

We start with describing the interpretation as a parallel-sided even K-gon contact representation. Let $s_0, \ldots, s_{K-1}$ be the set of all slopes arising as a slope of C or

of P_v for an inner vertex v of G and all their opposite oriented slopes, in sorted order. Then each of the prototypes P_v can be interpreted as a K-gon whose sides have these slopes and positive or zero length. Further, let Q be an arbitrary K-gon with sides of slopes $s_0, \dots, s_{K-1}$. We subdivide the outer edges of G multiple times such that the outer face becomes a K-cycle and we can assign the slopes $s_0, \dots, s_{K-1}$ in clockwise order to the outer vertices in such a way that the slopes assigned to the former outer vertex a_i is the slope of C_i for $i = 0, 1, 2$. Afterwards we retriangulate this graph without producing chords. Then we are exactly in the setting of computing a parallel-sided even K-gon contact representation of G. Let $\mathcal{C}$ be the contact representation obtained by this approach. If we extend the sides of the outer K-gon of $\mathcal{C}$ that have the slopes of C_0, C_1, and C_2 to a triangle, we actually end up with the wanted contact representation of G.

Starting with this interpretation as a parallel-sided even K-gon contact representation, we can obtain an interpretation as a similarly-aligned odd K-gon contact representation in the following way: We just add one more arbitrarily chosen additional slope to the set of slopes $s_0, \dots, s_{K-1}$, compare Fig. 3.15 on Page 24.

We conjecture that the system of linear equations $\mathcal{A}_{S,\mathbf{r}}$ is also uniquely solvable for $\mathbf{r} \in \mathbb{R}^{nK}_{\geq 0}$, i.e., for side length vectors with some of the side lengths being zero, as long as for each prototype the side lengths of at least three sides whose slopes are the slopes of a triangle are positive.

Conjecture 5.11. *If $\mathbf{r} \in \mathbb{R}^{nK}_{\geq 0}$ and, for each i, there are indices j_0, j_1, j_2 such that not all three of them are contained in any of the sets $\{j', j'+1, \dots, j'+\lfloor \frac{K}{2} \rfloor\}$, $j' = 0, \dots, K-1$, and $r_{ij} \neq 0$ for $j = j_0, j_1, j_2$, then the system of linear equations $\mathcal{A}_{S,\mathbf{r}}$ is uniquely solvable.*

If Conjecture 5.11 is true, then also all results from Section 4.6 hold in this case and therefore also the proof of Theorem 5.10. Hence, Conjecture 5.11 would imply the existence of contact representations with arbitrary convex polygons as prototypes for the vertices of the graph. Since convex polygons are a special case of the general convex shapes considered in the following, we can actually prove the existence of these contact representations by the approach presented in the following.

Arbitrary convex shapes as prototypes. Now we will give a new proof for the existence of contact representations with arbitrary convex shapes as prototypes for the inner vertices of G. The idea is to obtain the wanted contact representation as a limit of contact representation obtained by Theorem 5.10.

Theorem 5.12. *Let G be an inner triangulation of the 3-cycle a_0, a_1, a_2. Further, let C be a triangle in the plane with sides C_0, C_1, C_2 and, for each inner vertex v of G, let P_v be a convex prototype for v, i.e., a convex set in the plane containing more than one point. Then there exists a contact representation of a supergraph of G (on the same vertex set but possibly with more edges) where each inner vertex v is represented by a single point or a positive homothetic copy of its prototype P_v and each outer vertex a_i by the line segment C_i.*

Proof. As a first step, we approximate the prototypes P_v with arbitrary polygons. For each $k \in \mathbb{N}$, let $Q_v^{(k)}$ be a polygon with $P_v \subset Q_v^{(k)}$ and $d(P_v, Q_v^{(k)}) \leq \frac{1}{2k}$ where d denotes the Hausdorff metric. Now we want to interpret these prototypes as parallel-sided even K-gons, as described in the beginning of this section. But instead of adding sides of length zero to the polygons $Q_v^{(k)}$, we add short sides of positive length (and maybe also extend the original sides of $Q_v^{(k)}$ a bit) such that the obtained polygons $P_v^{(k)}$ fulfill $Q_v^{(k)} \subset P_v^{(k)}$ and $d(Q_v^{(k)}, P_v^{(k)}) \leq \frac{1}{2k}$ and, therefore, $P_v \subset P_v^{(k)}$ and $d(P_v, P_v^{(k)}) \leq \frac{1}{k}$.

Now, for each $k \in \mathbb{N}$, the existence of a parallel-sided even K-gon contact representation of G with the prototypes $P_v^{(k)}$ follows from Theorem 5.10. As described in the beginning of this section, we can interpret this contact representation as a contact representation of G in which the outer vertices a_0, a_1, and a_2 are represented by C_0, C_1, and C_2, respectively. Let $\lambda_v^{(k)}$ be the scaling factor of the homothetic copy $\tilde{P}_v^{(k)}$ of $P_v^{(k)}$ in this representation and let $p_v^{(k)}$ be the centroid of $\tilde{P}_v^{(k)}$. Since $p_v^{(k)}$ is inside the triangle C and the homothetic copy of $P_v^{(k)} \supset P_v$ has to fit inside C, both sequences $(p_v^{(k)})_{k\in\mathbb{N}}$ and $(\lambda_v^{(k)})_{k\in\mathbb{N}}$ are bounded. Hence, they have cluster points p_v^* and λ_v^*, respectively. By considering appropriate subsequences, we can assume that p_v^* and λ_v^* are limit points.

Now we place, for each inner vertex v of G, a homothetic copy $\tilde{P}_v$ of P_v, scaled with the factor λ_v^*, with its centroid on the point p_v^* inside C. Then, clearly, for each inner vertex v of G, the sequence $(\tilde{P}_v^{(k)})_{k\in\mathbb{N}}$ converges to $\tilde{P}_v$ in the Hausdorff metric. For the outer vertices a_i, $i = 0, 1, 2$, of G, we set $\tilde{P}_{a_i}^{(k)} = \tilde{P}_{a_i} = C_i$ for all $k \in \mathbb{N}$. Let v and w be two neighboring vertices of G. If $\tilde{P}_v$ and $\tilde{P}_w$ would be disjoint, this would be a contradiction to the fact that $\tilde{P}_v^{(k)}$ and $\tilde{P}_w^{(k)}$ intersect for all $k \in \mathbb{N}$. Now let v and w be arbitrary different vertices of G. If $\tilde{P}_v$ and $\tilde{P}_w$ would overlap, this would be a contradiction to the fact that $\tilde{P}_v^{(k)}$ and $\tilde{P}_w^{(k)}$ do not overlap for all $k \in \mathbb{N}$. Hence, the collection of the $\tilde{P}_v$ is a contact representation of a supergraph of G. □

Chapter 6

Algorithms

In this chapter, we will study two different algorithms for the computation of the different types of convex polygon contact representations we studied in the last chapters. The core of these algorithms are the systems of equations we studied in Chapter 4. In Section 6.1, we will present the first of these two algorithms that turns out to perform well in practice. Then, in Section 6.2, we will present the second algorithm which is inspired by the proof of Theorem 5.10. But, as the first algorithm, it lacks a proof of termination in general.

6.1 A fast heuristic

To be able to describe the algorithm in a generic way, we will now fix a generic setting for the computation of contact representations with convex polygons. We are given a plane graph G that is an inner triangulation of a cycle and search for a contact representation of G from a given class of contact representations. The combinatorial structure of such a contact representation of G can be described by an (ω, c_l, c_u)-flow of a fixed graph D. Further, for each ω-flow S, there is a system $\mathcal{A}_S$ of linear equations that is uniquely solvable. The solution of $\mathcal{A}_S$ is non-negative if and only if there exists a contact representation of G inducing the combinatorial structure S. If the solution is non-negative, the contact representation can be constructed from this solution. If the solution has negative variables, the signs of the variables define a non-empty set of sign-separating edges in D that are a disjoint union of simple directed cycles in the residual graph of S and thus can be reverted to obtain a new combinatorial structure S'.

A simple approach to find a contact structure S such that the solution of $\mathcal{A}_S$ is non-negative would be to solve the system of equations for all ω-flows S. Since the number of ω-flows is in general exponential in the size of the given graph G (e.g., there are plane triangulations with $\Omega(2.37^n)$ Schnyder woods (3-contact structures) [FZ08]), this approach does not lead to an efficient algorithm. Therefore, we have to find a more sophisticated way to find a contact structure S such that the solution of $\mathcal{A}_S$ is non-negative. The following algorithm is an attempt to do so.

Algorithm 1: Generic heuristic for the computation of contact representations.

$S \leftarrow$ arbitrary contact structure
$\mathbf{x} \leftarrow$ solution of $\mathcal{A}_S$
while $\mathbf{x} \not\geq 0$ **do**
  $E_{\text{sep}} \leftarrow$ sign-separating edges induced by $\mathbf{x}$
  change the orientations of the edges of E_{sep} in S
  $\mathbf{x} \leftarrow$ solution of $\mathcal{A}_S$
end
compute the contact representation from $\mathbf{x}$

There are two possible scenarios: Either Algorithm 1 finds a contact structure S such that the solution of $\mathcal{A}_S$ is non-negative or at some point it visits a contact structure that has already been visited before and then begins to loop through the same sequence of contact structures again and again and never terminates.

6.1.1 Implementations

Algorithm 1 has been implemented for the following settings: for the computation of homothetic triangle contact representations [Ruc11], for the computation of axis-aligned square contact representation [Pic11], and for the computation of homothetic regular pentagon contact representations [Raa17]. During the work on this thesis, Scheucher and Schrezenmaier have extended this set of implementations with an implementation for the computation of equiangular odd K-gon contact representations for arbitrary odd $K \geq 3$ with individually prescribed prototypes for the inner vertices of G in SageMath [Sage]. See [SS21] for animations of the search process of Algorithm 1 generated with this implementation. Experiments with all of the implementations led to similar observations that we will discuss in the following.

Termination. The main observation was that Algorithm 1 always terminated and never started to cycle, for any contact structure to start with. The only case in which Algorithm 1 is known to terminate is the case of the computation of a squaring whose induced segment contact graph is a given maximal planar bipartite graph, see Pages 2 and 3 for a sketch of this approach. Felsner [Fel13] showed that in this case the algorithm terminates after at most one change of the contact structure which is a separating decomposition in this case. In all other cases, there has been a lot of effort to find a proof for the termination, e.g., by finding an invariant that improves with every iteration of the algorithm, but without any success.

Conjecture 6.1. *Algorithm 1 terminates for every contact structure S to start with.*

Unique contact representation. Another observation was that, if Algorithm 1 was started with different contact structures, it always returned the same contact representation in the end. We can confirm this observation for our new implementation. The only case in which we know that the contact representation is unique is the

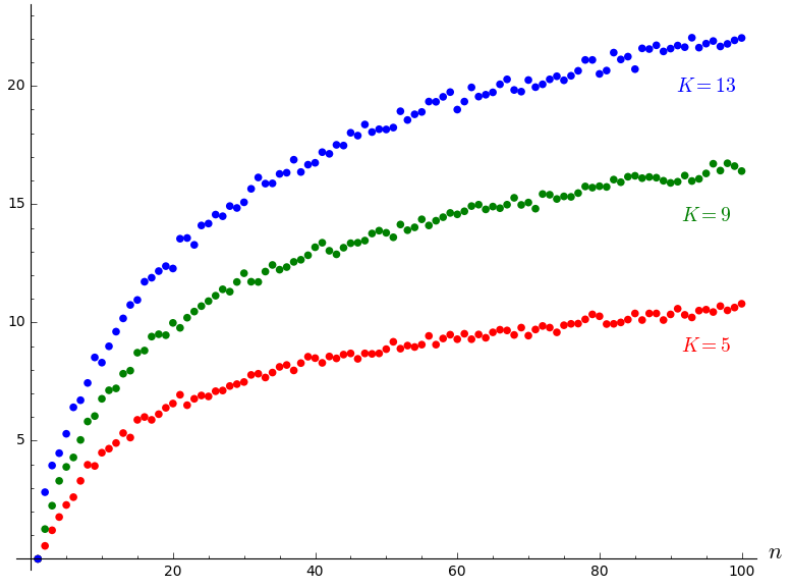

Figure 6.1: The average number of iterations Algorithm 1 took for the computation of regular K-gon contact representations of 100 random graphs with $n = 1, \ldots, 100$ inner vertices when starting with the minimal K-contact structure.

case of an axis-aligned rectangle contact representations of an inner triangulation G of a 4-cycle without separating triangles with given prototypes for the inner vertices of G [Sch93]. Because of Lemmas 4.49 and 4.57, if in a non-negative solution of $\mathcal{A}_S$ there are some variables zero, then there are more contact structure S' (obtained by reverting a subset of the essential cycles in S formed by the weak sign-separating edges) for which the solution of $\mathcal{A}_{S'}$ is the same non-negative solution as the solution of $\mathcal{A}_S$. And because of Lemma 5.7, if for two neighboring contact structures S and S' the solutions of $\mathcal{A}_S$ and $\mathcal{A}_{S'}$ are both non-negative, then these solutions have to be equal. Hence, the conjecture of the uniqueness of the contact representation can be formulated in terms of contact structures in the following way.

Conjecture 6.2. *The set of contact structures S for which the solution of $\mathcal{A}_S$ is non-negative, forms a sublattice of the distributive lattice of all contact structures of G.*

Number of iterations. When running Algorithm 1 for random triangulations of size n, the observed numbers of iterations the algorithm needed in the experiments until it terminated always led to the conjecture that the expected number of iterations is $o(n)$. With our new implementation, we ran experiments for the computation of regular K-gon contact representations for $K = 5, 9, 13$. For each $n \in \{1, \ldots, 100\}$, we generated 100 random inner triangulations of a K-cycle with n inner vertices using the algorithm from [PS06].[1] The algorithm was always started with the minimal

[1] The implementation of this algorithm has been integrated to SageMath by the author during the work on this thesis and is available from SageMath version 8.9, see [Sch19].

contact structure. Figure 6.1 shows the average number of iterations Algorithm 1 needed during these experiments until it terminated, in dependence of the size of the input graph. Since the implementation uses floating-point arithmetic to solve the systems of linear equations, it could not decide the signs of the variables for roughly every 500th input graph which might have led to inaccurate data. Further, the size of the experiments is not large enough to make an educated guess on the actual asymptotic behavior of the average number of iterations. But still the experiments confirm the observations made with the older implementations.

Conjecture 6.3. *When running Algorithm 1 for a random graph of size n, the expected number of iterations is $o(n)$.*

6.1.2 Bounding the worst case number of iterations

As mentioned in Section 6.1.1, the experiments with implementations of Algorithm 1 give rise to the conjecture that the average number of iterations of the heuristic is $o(n)$. In the following, we will show that this is not true for the worst case number of iterations. Indeed, the worst case number of iterations of Algorithm 1 used for the computation of similarly-aligned odd K-gon contact representations is $\Omega(n)$. We will prove this for the case $K = 3$ and refer to animations of example graphs in [SS21] for $K \geq 5$.

Theorem 6.4. *There is a family $(G_n)_{n=1,2,\dots}$ of plane triangulations G_n with $n+3$ inner vertices and a family $(S_n)_{n=1,2,\dots}$ of 3-contact structures (Schnyder woods) S_n of G_n such that Algorithm 1 applied to the computation of an equilateral triangle contact representation of G_n with initial 3-contact structure S_n takes $\Omega(n)$ iterations.*

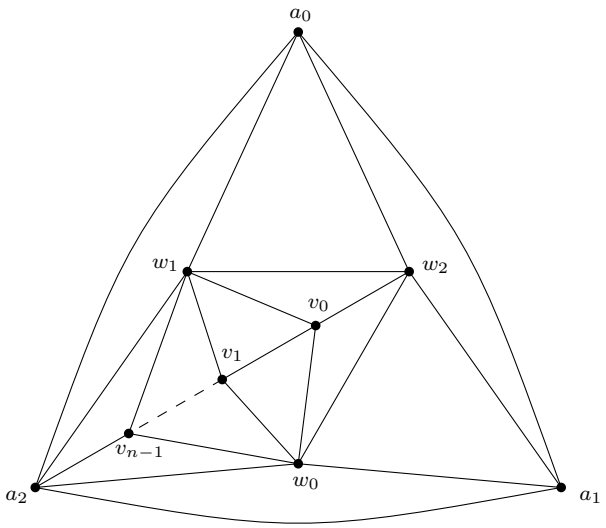

Figure 6.2: A class of triangulations G_n with $n+3$ inner vertices on which Algorithm 1 takes $\Theta(n)$ iterations when starting with the minimal 3-contact structure (Schnyder wood).

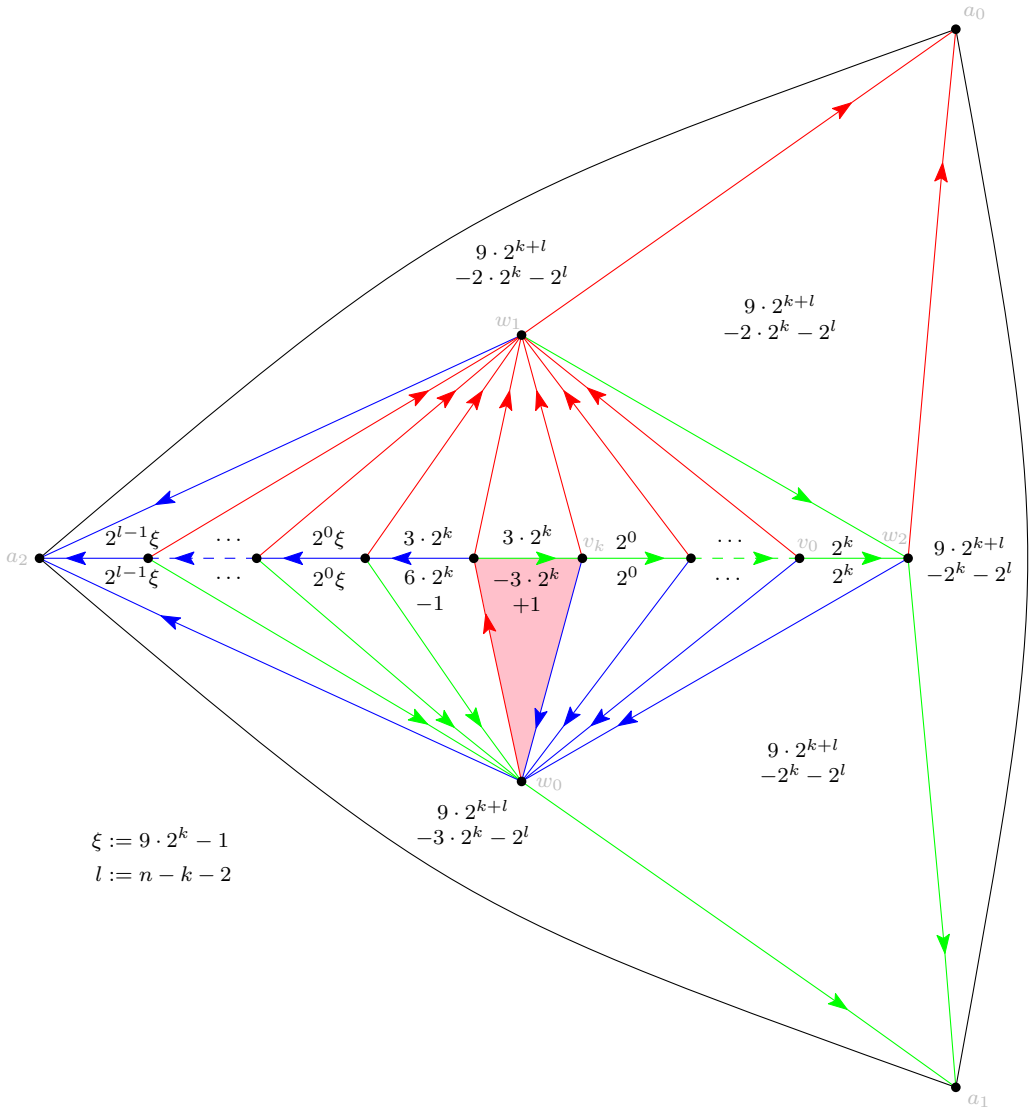

Figure 6.3: A class $S_k^{(n)}$, $k = 0, \ldots, n-2$, of Schnyder woods of G_n. The values of the face-variables in the solution of the corresponding system of linear equations are written into the faces. It can easily be verified that these values fulfill all equations except equation (4.7). By multiplying all values with a constant positive factor, we could obtain the solution of the normalized system. Note that the highlighted face $v_{k+1}v_kw_0$ is the only face whose variable has a negative value in this solution. Further, for $k = 1, \ldots, n-1$, the Schnyder wood $S_{k-1}^{(n)}$ is obtained from $S_k^{(n)}$ by flipping this face.

Proof. Let $n \in \{1, 2, \dots\}$. Figure 6.2 illustrates the graph G_n and Fig. 6.3 shows Schnyder woods $S_k^{(n)}$, $k = 0, \dots, n-2$, of G_n. Further, in Fig. 6.3 the values of the face-variables in the solution of the system of linear equations $\mathcal{A}_{S_k^{(n)}}$ are shown. It can easily be verified that these values fulfill all equations. There is exactly one negative face-variable and the corresponding flip transforms $S_k^{(n)}$ into $S_{k-1}^{(n)}$. Hence, when starting with $S_n := S_{n-2}^{(n)}$, Algorithm 1 takes at least $n - 2 = \Omega(n)$ iterations. □

In fact, it can even be shown that the distributive lattice of the 3-contact structures of G_n is a chain of length $\Theta(n)$ and that Algorithm 1, when started with the minimal or maximal 3-contact structure, follows this chain step by step to the unique 3-contact structure S for which the solution of $\mathcal{A}_S$ is non-negative. Hence, also the average number of iterations when starting Algorithm 1 with an arbitrary 3-contact structure of G_n is $\Theta(n)$.

6.2 A slow heuristic

We will conclude this chapter with another heuristic for the computation of similarly-aligned odd K-gon and parallel-sided even K-gon contact representations that is inspired by the proof of Theorem 5.10. In this proof, we start with a side length vector $\mathbf{r_0}$ and a contact structure S such that $\mathbf{r_0} \in R_S$, i.e., the solution of $\mathcal{A}_{S,\mathbf{r_0}}$ is positive. Then we consider the line segment $\{\, \mathbf{r_t} = (1-t)\mathbf{r_0} + t\mathbf{r} \colon t \in [0,1] \,\}$ of side length vectors where $\mathbf{r}$ is the vector we search a contact representation for. We want to move along this line segment, maintaining the invariant that the current vector $\mathbf{r_t}$ fulfills $\mathbf{r_t} \in R_S$. To achieve this, we have to change the contact structure S from time to time. When we reach a vector $\mathbf{r_t}$ such that $\mathbf{r_t} \in \overline{R_S} \setminus R_S$ and in the corresponding solution of $\mathcal{A}_{S,\mathbf{r_t}}$ only one edge-variable x_e is zero, there are two possibilities. Either there is an $\varepsilon' > 0$ such that $\mathbf{r_{t+\varepsilon}} \in R_S$ for all $\varepsilon \in (0, \varepsilon')$ or, due to Lemma 5.8, there is an $\varepsilon' > 0$ such that $\mathbf{r_{t+\varepsilon}} \in R_{S'}$ for all $\varepsilon \in (0, \varepsilon')$ where S' is the neighboring contact structure of S obtained by the flip corresponding to x_e. In particular, S' is obtained by solving the system of linear equations $\mathcal{A}_{S,\mathbf{r_{t+\varepsilon}}}$ for an $\varepsilon \in (0, \varepsilon')$ and then reverting all sign-separating edges. This idea can be generalized in the following way. If $\mathbf{r} \notin \overline{R_S}$, we search for a side length vector $\mathbf{r_t}$ such that $\mathbf{r_t} \notin \overline{R_S}$ and reverting the sign-separating edges induced by the solution of $\mathcal{A}_{S,\mathbf{r_t}}$ in S leads to a contact structure S' with $\mathbf{r_t} \in R_{S'}$. Realizing this search as a binary search yields Algorithm 2.

If, for no contact structure S and no $\mathbf{r_t}$ on the line segment between $\mathbf{r_0}$ and $\mathbf{r}$, the solution of $\mathcal{A}_{S,\mathbf{r_t}}$ is non-negative with more than one edge-variable x_e being zero and if Conjecture 6.2 is true, then Theorem 5.10 implies that Algorithm 2 terminates. But even if a variant of this algorithm provably computes the wanted contact representation, it is unlikely that it has polynomial running time or even only a much better running time than solving $\mathcal{A}_{S,\mathbf{r}}$ for all contact structures S. Therefore, we have not further investigated this approach.

Algorithm 2: Heuristic for the computation of K-contact representations.

$S \leftarrow$ arbitrary contact structure
$\mathbf{r_0} \leftarrow$ arbitrary side length vector with $\mathbf{r_0} \in R_S$
while $\mathbf{x}^{(S,\mathbf{r})} \not\geqslant 0$ **do**
  $\mathbf{r_1} \leftarrow \mathbf{r}$
  loop
    $\mathbf{r_m} \leftarrow \frac{\mathbf{r_0}+\mathbf{r_1}}{2}$
    $E_{\text{sep}} \leftarrow$ sign-separating edges induced by $\mathbf{x}^{(S,\mathbf{r_m})}$
    $S' \leftarrow$ contact structure obtained from S by reverting edges of E_{sep}
    if $S' = S$ **then**
      $\mathbf{r_0} \leftarrow \mathbf{r_m}$
    else if $\mathbf{x}^{(S',\mathbf{r_m})} \not\geqslant 0$ **then**
      $\mathbf{r_1} \leftarrow \mathbf{r_m}$
    else
      break loop
    end
  end
  $S \leftarrow S'$
  $\mathbf{r_0} \leftarrow \mathbf{r_m}$
end
compute the contact representation from $\mathbf{x}^{(S,\mathbf{r})}$

Chapter 7

Conclusion

We will conclude this thesis with a summary of the results in this thesis and a discussion of open problems and possible future directions of research.

Existence of convex contact representations. It was already known before the work on this thesis that contact representation of plane triangulations exist in which the inner vertices are represented by non-negative homothetic copies of arbitrary individually prescribed convex prototypes and the outer vertices are represented by curves in the plane that together form a simple closed curve. This is the Convex Packing Theorem by Schramm [Sch07]. The proof of this general form of the theorem is based on the Monster Packing Theorem [Sch07]. For the case that the prototypes for the inner vertices have smooth boundaries and the curves representing the outer vertices are the sides of a triangle, Schramm [Sch91] also gives a more elementary proof that is based on a proof of the uniqueness of the contact representation. In this thesis, we reproved the existence for arbitrary convex prototypes if the outer vertices are represented by the sides of triangle. Our proof is also more elementary than the Monster Packing Theorem and, since it does not require the uniqueness of the contact representation, it also holds for the cases we do not know the uniqueness for (see the next paragraph).

Uniqueness of convex contact representations. It is a well-known result that contact representations of plane triangulations with disks are unique up to Möbius transformations [Koe36; Thu79b]. In particular, the contact representation is unique if the outer vertices are represented by the sides of a fixed triangle in the plane. Schramm [Sch91] generalized this result by proving that the contact representation is also unique if we allow arbitrary convex prototypes with a smooth boundary curve for the inner vertices of the triangulation. The reason why Schramm's result cannot be applied to polygonal convex prototypes is that the prototypes are required to be *blunt*, i.e., for each boundary point p of the prototype there has to be a smooth convex body that is a subset of the prototype and contains the point p. On the other hand, Schramm says that the motivation for this requirement is that in a contact representation with these prototypes no three polygons can share a point. This

property is also fulfilled for equiangular K-gons with a horizontal side at the bottom for a fixed $K \geq 5$, $K \neq 6$, as prototypes. Therefore, the proof in [Sch91] might also hold for these classes of prototypes, but for this Schramm's proof needs to be checked in detail. Further, our experiments suggest that for all similarly-aligned odd K-gons for a fixed odd $K \geq 3$ as prototypes the contact representation is unique. Therefore, we conjecture the following.

Conjecture 7.1. *Let G be an inner triangulation of the 3-cycle a_0, a_1, a_2. Further, let C be a triangle in the plane with sides C_0, C_1, C_2 and, for each inner vertex v of G, let P_v be a convex prototype for v, i.e., a compact, convex set in the plane containing more than one point. Then there exists a* unique *contact representation of a supergraph of G (on the same vertex set but possibly with more edges) where each inner vertex v is represented by a single point or a positive homothetic copy of its prototype P_v and each outer vertex a_i by the line segment C_i.*

Realizability of K-contact structures. In Chapter 3, we have shown that the combinatorial structure of each similarly-aligned odd K-gon or parallel-sided even K-gon contact representation can be described as a K-contact structure. What we have not shown is that each such K-contact structure indeed is the combinatorial structure of a contact representation from these classes. For 3-contact structures (Schnyder woods) it is known that each Schnyder wood describes the combinatorial structure of a triangle contact representation [FOR94]. The triangles can even be required to have a horizontal basis and to be isosceles or to have a right angle at the lower left or lower right corner. For 5-contact structures it was shown in [Ste16] that for each such contact structure there is a contact representation with arbitrary convex pentagons (compare Fig. 4.44 (top)) that induces this contact structure. The technique used in this proof is the following: The 5-contact structure defines a contact system of pseudosegments such that, if all these pseudosegments were drawn as straight line segments, the resulting contact system of line segments is the wanted contact representation of pentagons. Then a general result [FO07; AF17] about the stretchability of such contact systems of arcs is applied. This technique was first used by Gonçalves et al. [GLP12] to prove that each generalized Schnyder wood is induced by a primal-dual triangle contact representation (remember Section 3.1.3). We believe that this technique can also be used to prove that each K-contact structure is induced by a contact representation of arbitrary convex K-gons.

Conjecture 7.2. *For each K-contact structure S, there exists a contact representation with arbitrary convex K-gons inducing S.*

Computation of minimal/maximal K-contact structures. Schnyder [Sch90a] already showed that a 3-contact structure (Schnyder wood) of a given plane triangulation can be found in linear time. Even the minimal or maximal element of the distributive lattice of 3-contact structures can be computed in linear time [Bre00; Fus07]. Remember that K-contact structures can be described as ω_K-flows, i.e., integral flows of one of the graphs $G^\star$ and $2G^\star$ (see Pages 33 and 60). Such an

ω_K-flow can be found in $O(nK)$ time using the Ford-Fulkerson algorithm since $G^\star$ and $2G^\star$ have $O(n)$ edges and the maximum flow on an edge is $O(K)$. It would be interesting to know whether this can be improved and whether the minimal and maximal K-contact structures can also be computed in linear time if K is fixed.

Computation of convex contact representations. Although there are various proofs for the existence of contact representations of plane graphs with convex prototypes, none of these proofs leads to an efficient algorithm for the computation of these contact representations. Still, Algorithm 1 seems to be a good candidate for an algorithm for the computation of contact representation with convex polygons as prototypes in polynomial time. Let L be the total number of sides of the given prototypes (including the three sides of the triangle representing the outer vertices). If Conjecture 5.11 holds, we can, using the approach from Section 5.2, interpret the prototypes as parallel-sided even K-gons for a fixed $K \leq 2L$, which is polynomial in the input size, and apply Algorithm 1 to this setting. The initial K-contact structure in Algorithm 1 can be found in polynomial time (see the last paragraph). Further, the systems of equations that are solved in Algorithm 1 have polynomial size and thus can be solved in polynomial time if the K slopes of the prototypes are given as direction vectors with Euclidean coordinates and the prototypes are given by their side lengths.

Approach with Ys for homothetic triangle contact representations. Remember the setting for the computation of square contact representations from Section 3.1.2. We are given an inner triangulation G of the 4-cycle v_N, v_E, v_S, v_W without separating 3-cycles and want to represent the inner vertices by squares and the outer vertices by the sides of a rectangle. Assume that the width of the final contact representation is 1. Then, obviously, for each path P in G from a neighbor of v_W to a neighbor of v_E, we have $\sum_{v\in P} x_v \geq 1$ where x_v denotes the side length of the square representing v in the wanted contact representation. Schramm [Sch93] proved that minimizing $\sum_{v\in V_{\text{inner}}} x_v^2$ under these constraints leads to values x_v that are indeed the side lengths of the squares in the wanted contact representation. This way, he proves the existence as well as the uniqueness of this contact representation.

It would be interesting to know whether a similar approach can be applied to homothetic equilateral triangle contact representations. So let G be an inner triangulation of the 3-cycle a_0, a_1, a_2. Assume that the altitude of the final contact representation is 1. Let w be an inner vertex of G and let Y be the union of paths from a neighbor of w to a neighbor of a_i for $i = 0, 1, 2$. Viviani's Theorem states that in an equilateral triangle the sum of the distances from an interior point to the three sides is equal to the altitude of the triangle. Thus, by Viviani's Theorem, $2x_w + \sum_{v\in Y} x_v \geq 1$ where x_v denotes the altitude of the equilateral triangle representing v, see Fig. 7.1 (left). So the question is whether there is an objective function such that minimizing this function under these constraints leads to values x_v that are indeed the altitudes of the triangles in the wanted contact representation. Figure 7.1 shows two more alternative ways to define these Y-structures.

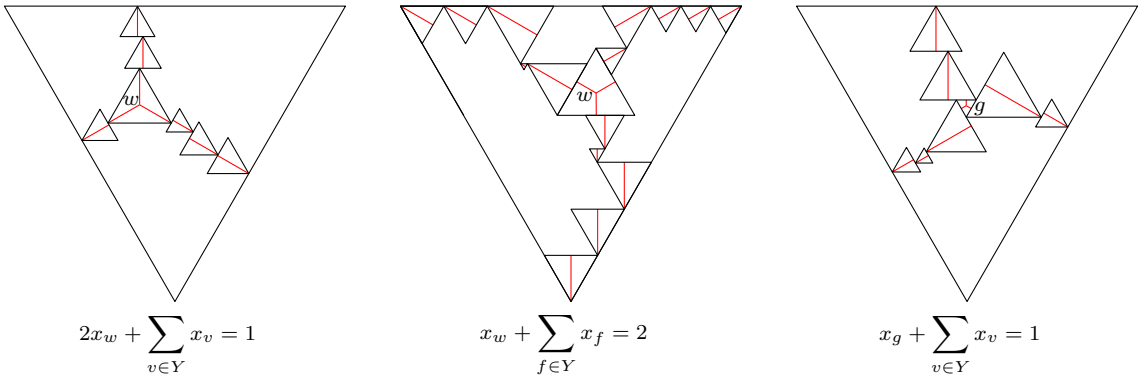

Figure 7.1: Different ways to define Y-structures for homothetic equilateral triangle contact representations. The altitude of the outer triangle is 1. For each inner vertex v of G, the variable x_v denotes the altitude of the primal triangle representing v and, for each inner face f of G, the variable x_f denotes the altitude of the dual triangle representing f. The displayed equations are fulfilled by Viviani's Theorem.

Non-degenerate contact representations. We conjectured (Conjecture 7.1) that the contact representation of a plane triangulation is unique if each inner vertex has to be represented by a non-negative homothetic copy of a prescribed convex prototype and the outer vertices by the sides of a given triangle. In particular, if this conjecture is true and if in the contact representation some vertices are represented by a single point, i.e., the contact representation is degenerate, then this cannot be avoided. So it might be interesting to consider cases in which not all conditions of the conjecture are fulfilled and to ask for non-degenerate contact representations. One such conjecture by Gonçalves et al. [GLP12] is that every 3-connected plane graph has a non-degenerate primal-dual triangle contact representation in which each primal vertex is represented by a triangle with a horizontal basis and a right angle at the bottom-left corner and each dual vertex is represented by a right triangle with a horizontal top and a right angle at the top-right corner. Another such question is whether each plane quadrangulation has a contact representation with non-degenerate squares. Since in such a contact representation the squares representing the four vertices of an inner face of the quadrangulation enclose a rectangle, we can also interpret it as a rectangle contact representation of the triangulation obtained by stacking a vertex into each inner face of the quadrangulation. We can prescribe squares as prototypes for the original vertices and choose arbitrary rectangles as prototypes for the stacked vertices. Then we know that for each such choice of prototypes there exists a contact representation that might be degenerate. It would be interesting to see whether in such a degenerate case we can always perturb the prototypes in such a way that the new contact representation is non-degenerate. An approach to this problem could be a deeper analysis of the system of equations whose solution leads to the degenerate contact representation. A similar problem of characterizing partial 2-trees (without a fixed embedding to the plane) that allow a non-degenerate contact representation with squares was studied in [DDEJ17].

Contact representations in higher dimensions. In this thesis, we have only considered contact representations of plane graphs in the plane. A natural generalization of homothetic equilateral triangle contact representations of a plane triangulation to dimension $d \geq 3$ are homothetic regular d-dimensional simplex contact representations of a topological triangulation of a d-simplex. In contrast to the results about contact representations in 3-space mentioned in Section 1.1, we do not only prescribe the graph but also its topological embedding induced by the contact representation. By describing the coordinates of the simplices representing the inner vertices of the triangulation as barycentric coordinates in relation to the simplex representing the outer vertices, it should be possible to come up with a system of linear equations for computing the wanted contact representation if we fix a combinatorial description of this contact representation. Therefore, an interesting question is how we can describe the combinatorial structure of such a contact representation and whether the set of all possible combinatorial structures has properties similar to those in the case $d = 2$ like forming a distributive lattice and allowing to interpret the solution of the system of equations as an indicator how to change the combinatorial structure. Then it might be possible to apply the apparatus of this thesis also to this kind of contact representations.

Bibliography

[AF17] Nieke Aerts and Stefan Felsner. "Straight Line Triangle Representations". In: *Discrete Comput. Geom.* 57.2 (2017), pp. 257–280. DOI: 10.1007/s00454-016-9850-y.

[AEK+15] Muhammad J. Alam, William Evans, Stephen G. Kobourov, Sergey Pupyrev, Jackson Toeniskoetter, and Torsten Ueckerdt. "Contact Representations of Graphs in 3D". In: *Proc. WADS*. 2015, pp. 14–27. DOI: 10.1007/978-3-319-21840-3_2.

[AKK16] Muhammad J. Alam, Michael Kaufmann, and Stephen G. Kobourov. "On Contact Graphs with Cubes and Proportional Boxes". In: *Proc. SOFSEM*. 2016, pp. 107–120. DOI: 10.1007/978-3-662-49192-8_9.

[And70a] Eugene M. Andreev. "On convex polyhedra in Lobačevskiĭ space". In: *Math. USSR Sb.* 10.3 (1970), pp. 413–440. DOI: 10.1070/SM1970v010n03ABEH001677.

[And70b] Eugene M. Andreev. "On convex polyhedra of finite volume in Lobačevskiĭ space". In: *Math. USSR Sb.* 12.2 (1970), pp. 255–259. DOI: 10.1070/SM1970v012n02ABEH000920.

[BNZ91] Irith Ben-Arroyo Hartman, Ilan Newman, and Ran Ziv. "On grid intersection graphs". In: *Discrete Math.* 87.1 (1991), pp. 41–52. DOI: 10.1016/0012-365X(91)90069-E.

[Bre00] Enno Brehm. "3-orientations and Schnyder 3-tree-decompositions". Diplomarbeit (diploma thesis). Freie Universität Berlin, 2000. URL: https://page.math.tu-berlin.de/~felsner/Diplomarbeiten/brehm.ps.gz.

[BEF+12] David Bremner, William Evans, Fabrizio Frati, Laurie Heyer, Stephen G. Kobourov, William J. Lenhart, Giuseppe Liotta, David Rappaport, and Sue H. Whitesides. "On Representing Graphs by Touching Cuboids". In: *Proc. Graph Drawing*. 2012, pp. 187–198. DOI: 10.1007/978-3-642-36763-2_17.

[BS93] Graham R. Brightwell and Edward R. Scheinerman. "Representations of planar graphs". In: *SIAM J. Discrete Math.* 6.2 (1993), pp. 214–229. DOI: 10.1137/0406017.

[BSST40] Rowland L. Brooks, Cedric A. B. Smith, Arthur H. Stone, and William T. Tutte. "The dissection of rectangles into squares". In: *Duke Math. J.* 7.1 (1940), pp. 312–340. DOI: 10.1215/S0012-7094-40-00718-9.

[BS95] Richard A. Brualdi and Bryan L. Shader. *Matrices of Sign-Solvable Linear Systems*. Cambridge Tracts in Mathematics. Cambridge University Press, 1995. DOI: 10.1017/CBO9780511574733.

[CCD+02] Natalia de Castro, Francisco J. Cobos, Juan C. Dana, Alberto Marquez, and Marc Noy. "Triangle-Free Planar Graphs and Segment Intersection Graphs". In: *J. Graph Algorithms Appl.* 6.1 (2002), pp. 7–26. DOI: 10.7155/jgaa.00043.

[DDEJ17] Giordano Da Lozzo, William E. Devanny, David Eppstein, and Timothy Johnson. "Square-Contact Representations of Partial 2-Trees and Triconnected Simply-Nested Graphs". In: *Proc. ISAAC*. 2017, 24:1–24:14. DOI: 10.4230/LIPIcs.ISAAC.2017.24.

[Die17] Reinhard Diestel. *Graph Theory*. 5th ed. Graduate Texts in Mathematics 173. Springer, 2017. DOI: 10.1007/978-3-662-53622-3.

[ERS+19] William Evans, Paweł Rzążewski, Noushin Saeedi, Chan-Su Shin, and Alexander Wolff. "Representing Graphs and Hypergraphs by Touching Polygons in 3D". In: *Proc. GD*. 2019, pp. 18–32. DOI: 10.1007/978-3-030-35802-0_2.

[Fel01] Stefan Felsner. "Convex Drawings of Planar Graphs and the Order Dimension of 3-Polytopes". In: *Order* 18.1 (2001), pp. 19–37. DOI: 10.1023/A:1010604726900.

[Fel03] Stefan Felsner. "Geodesic Embeddings and Planar Graphs". In: *Order* 20.2 (2003), pp. 135–150. DOI: 10.1023/B:ORDE.0000009251.68514.8b.

[Fel04] Stefan Felsner. "Lattice structures from planar graphs". In: *Electron. J. Comb.* 11.1 (2004), R15. DOI: 10.37236/1768.

[Fel09] Stefan Felsner. "Triangle contact representations". In: *Midsummer Combinatorial Workshop, Praha*. 2009. URL: https://page.math.tu-berlin.de/~felsner/Paper/prag-report.pdf.

[Fel13] Stefan Felsner. "Rectangle and Square Representations of Planar Graphs". In: *Thirty Essays on Geometric Graph Theory*. Springer, 2013, pp. 213–248. DOI: 10.1007/978-1-4614-0110-0_12.

[FF11] Stefan Felsner and Mathew C. Francis. "Contact Representations of Planar Graphs with Cubes". In: *Proc. SoCG*. 2011, pp. 315–320. DOI: 10.1145/1998196.1998250.

[FK09] Stefan Felsner and Kolja B. Knauer. "ULD-lattices and Δ-bonds". In: *Comb. Probab. Comput.* 18.5 (2009), pp. 707–724. DOI: 10.1017/S0963548309010001.

[FKU20] Stefan Felsner, Kolja B. Knauer, and Torsten Ueckerdt. "Plattenbauten: Touching Rectangles in Space". In: *Proc. WG*. 2020, pp. 161–173. DOI: 10.1007/978-3-030-60440-0_13.

[FR19] Stefan Felsner and Günter Rote. "On Primal-Dual Circle Representations". In: *Proc. SOSA*. 2019, 8:1–8:18. DOI: 10.4230/OASIcs.SOSA.2019.8.

[FSS17] Stefan Felsner, Hendrik Schrezenmaier, and Raphael Steiner. "Pentagon Contact Representations". In: *Proc. Eurocomb*. 2017, pp. 421–427. DOI: 10.1016/j.endm.2017.06.069.

[FSS18a] Stefan Felsner, Hendrik Schrezenmaier, and Raphael Steiner. "Equiangular Polygon Contact Representations". In: *Proc. WG*. 2018, pp. 203–215. DOI: 10.1007/978-3-030-00256-5_17.

[FSS18b] Stefan Felsner, Hendrik Schrezenmaier, and Raphael Steiner. "Pentagon Contact Representations". In: *Electron. J. Comb.* 25.3 (2018), P3.39. DOI: 10.37236/7216.

[FZ08] Stefan Felsner and Florian Zickfeld. "On the Number of Planar Orientations with Prescribed Degrees". In: *Electron. J. Comb.* 15.1 (2008), R77. DOI: 10.37236/801.

[FO01] Hubert de Fraysseix and Patrice Ossona de Mendez. "On topological aspects of orientations". In: *Discrete Math.* 229.1–3 (2001), pp. 57–72. DOI: 10.1016/S0012-365X(00)00201-6.

[FO07] Hubert de Fraysseix and Patrice Ossona de Mendez. "Barycentric systems and stretchability". In: *Discrete Appl. Math.* 155.9 (2007), pp. 1079–1095. DOI: 10.1016/j.dam.2005.12.009.

[FOP94] Hubert de Fraysseix, Patrice Ossona de Mendez, and János Pach. "Representation of planar graphs by segments". In: *Coll. Math. Soc. János Bolyai*. Vol. 63. Intuitive Geometry, Szeged, 1991. 1994, pp. 109–117.

[FOR94] Hubert de Fraysseix, Patrice Ossona de Mendez, and Pierre Rosenstiehl. "On Triangle Contact Graphs". In: *Comb. Probab. Comput.* 3.2 (1994), pp. 233–246. DOI: 10.1017/S0963548300001139.

[Fus07] Éric Fusy. "Combinatoire des cartes planaireset applications algorithmiques". PhD thesis. École Polytechnique, Paris, 2007. URL: https://www.lix.polytechnique.fr/Labo/Eric.Fusy/Theses/these_eric_fusy.pdf.

[Fus09] Éric Fusy. "Transversal structures on triangulations: A combinatorial study and straight-line drawings". In: *Discrete Math.* 309.7 (2009), pp. 1870–1894. DOI: 10.1016/j.disc.2007.12.093.

[Gon19] Daniel Gonçalves. "3-Colorable Planar Graphs Have an Intersection Segment Representation Using 3 Slopes". In: *Proc. WG*. 2019, pp. 351–363. DOI: 10.1007/978-3-030-30786-8_27.

[GIP18] Daniel Gonçalves, Lucas Isenmann, and Claire Pennarum. "Planar Graphs as L-intersection or L-contact graphs". In: *Proc. SODA*. 2018, pp. 172–184. DOI: 10.1137/1.9781611975031.12.

[GLP12] Daniel Gonçalves, Benjamin Lévêque, and Alexandre Pinlou. "Triangle Contact Representations and Duality". In: *Discrete Comput. Geom.* 48.1 (2012), pp. 239–254. DOI: 10.1007/s00454-012-9400-1.

[He93] Xin He. "On Finding the Rectangular Duals of Planar Triangular Graphs". In: *SIAM J. Comput.* 22.6 (1993), pp. 1218–1226. DOI: 10.1137/0222072.

[HPV89] Michael D. Hirsch, Christos H. Papadimitriou, and Stephen A. Vavasis. "Exponential lower bounds for finding Brouwer fix points". In: *J. Complex.* 5.4 (1989), pp. 379–416. DOI: 10.1016/0885-064X(89)90017-4.

[Koe36] Paul Koebe. "Kontaktprobleme der konformen Abbildung". In: *Ber. Sächs. Akad. Wiss. Leipzig, Math.-phys. Kl.* 88 (1936), pp. 141–164.

[KK85] Krzysztof Koźmiński and Edwin Kinnen. "Rectangular duals of planar graphs". In: *Networks* 15.2 (1985), pp. 145–157. DOI: 10.1002/net.3230150202.

[Lov19] László Lovász. *Graphs and Geometry*. Colloquium Publications 65. American Mathematical Society, 2019.

[Oss94] Patrice Ossona de Mendez. "Orientations bipolaires". PhD thesis. École des Hautes Études en Sciences Sociales, Paris, 1994.

[Pic11] Thomas Picchetti. "Finding a square dual of a graph". 2011. URL: https://page.math.tu-berlin.de/~felsner/Diplomarbeiten/rapport_picchetti.pdf.

[PS06] Dominique Poulalhon and Gilles Schaeffer. "Optimal Coding and Sampling of Triangulations". In: *Algorithmica* 46.3–4 (2006), pp. 505–527. DOI: 10.1007/s00453-006-0114-8.

[Raa17] Nadine Raasch. "Kontaktdarstellungen planarer Graphen mit Fünfecken". Masterarbeit (master thesis). Technische Universität Berlin, 2017. URL: https://page.math.tu-berlin.de/~felsner/Diplomarbeiten/Masterarbeit_Nadine-Raasch.pdf.

[Ruc11] Julia Rucker. "Kontaktdarstellungen von planaren Graphen". Diplomarbeit (diploma thesis). Technische Universität Berlin, 2011. URL: https://page.math.tu-berlin.de/~felsner/Diplomarbeiten/dipl-Rucker.pdf.

[Sage] The Sage Developers. *SageMath, the Sage Mathematics Software System (Version 8.0)*. 2017. URL: https://www.sagemath.org.

[SS21] Manfred Scheucher and Hendrik Schrezenmaier. *K-Contact Representations*. 2021. URL: https://www3.math.tu-berlin.de/diskremath/research/kgon-representations/index.html.

[Sch90a] Walter Schnyder. "Embedding planar graphs on the grid". In: *Proc. SODA*. 1990, pp. 138–148.

[Sch90b] Oded Schramm. "Packing two-dimensional bodies with prescribed combinatorics and applications to the construction of conformal and quasiconformal mappings". PhD thesis. Princeton University, 1990.

[Sch91] Oded Schramm. "Existence and uniqueness of packings with specified combinatorics". In: *Isr. J. Math.* 73.3 (1991), pp. 321–341. DOI: 10.1007/BF02773845.

[Sch93] Oded Schramm. "Square tilings with prescribed combinatorics". In: *Isr. J. Math.* 84.1–2 (1993), pp. 97–118.

[Sch07] Oded Schramm. *Combinatorically prescribed packings and applications to conformal and quasiconformal maps*. Modified version of [Sch90b]. 2007. arXiv: 0709.0710 [math-cv].

[Sch16] Hendrik Schrezenmaier. "Zur Berechnung von Kontaktdarstellungen". Masterarbeit (master thesis). Technische Universität Berlin, 2016. URL: https://page.math.tu-berlin.de/~schrezen/Papers/Masterarbeit.pdf.

[Sch17] Hendrik Schrezenmaier. "Homothetic Triangle Contact Representations". In: *Proc. WG*. 2017, pp. 425–437. DOI: 10.1007/978-3-319-68705-6_32.

[Sch19] Hendrik Schrezenmaier. *RandomTriangulation method in SageMath*. 2019. URL: https://doc.sagemath.org/html/en/reference/graphs/sage/graphs/generators/random.html#sage.graphs.generators.random.RandomTriangulation.

[Sei15] Felix Seibert. "Representing planar graphs with contacts of homothetic objects". Masterarbeit (master thesis). Technische Universität Berlin, 2015.

[Ste16] Raphael Steiner. "Existenz und Konstruktion von Dreieckszerlegungen triangulierter Graphen und Schnyder woods". Bachelorarbeit (bachelor thesis). FernUniversität in Hagen, 2016. URL: https://www.fernuni-hagen.de/mathematik/DMO/pubs/Bachelorarbeit_Raphael_Steiner.pdf.

[Tho06] Robin Thomas. "A survey of Pfaffian orientations of graphs". In: *Proc. ICM*. 2006, pp. 963–984. DOI: 10.4171/022-3/47.

[Tho86] Carsten Thomassen. "Interval representations of planar graphs". In: *J. Comb. Theory Ser. B* 40.1 (1986), pp. 9–20. DOI: 10.1016/0095-8956(86)90061-4.

[Thu79a] William P. Thurston. *The geometry and topology of three-manifolds*. Unpublished lecture notes, Princeton University. 1979. URL: https://archive.org/details/ThurstonTheGeometryAndTopologyOfThreeManifolds/page/n1.

[Thu79b] William P. Thurston. *The geometry and topology of three-manifolds*. Electronic edition of [Thu79a]. 2002. URL: http://library.msri.org/books/gt3m/.

[Ung53] Peter Ungar. "On Diagrams Representing Maps". In: *J. London Math. Soc. (1)* 28.3 (1953), pp. 336–342. DOI: 10.1112/jlms/s1-28.3.336.

Appendix A

Overview of structures associated with contact representations

In this appendix, there is an overview of the graphs and structures associated with contact representations that are defined in this thesis. First, in Fig. A.1, there is an example of a similarly-aligned odd K-gon contact representation with all of its associated structures and then, in Fig. A.2, there is an example of a parallel-sided even K-gon contact representation with all of its associated structures. The purpose of this overview is to have an easy to find place to look up these structures when reading the thesis.

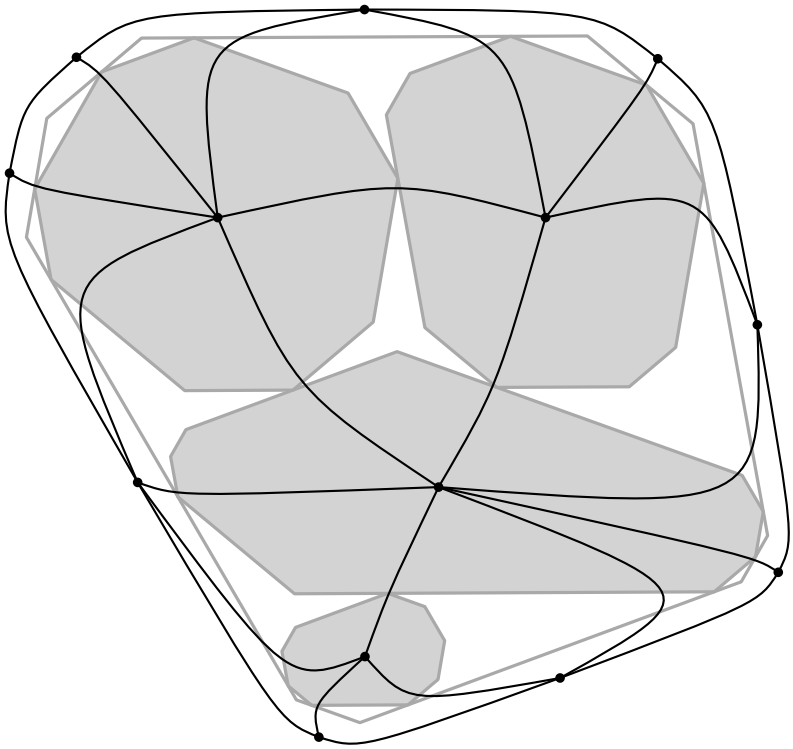

(a) The contact graph G.

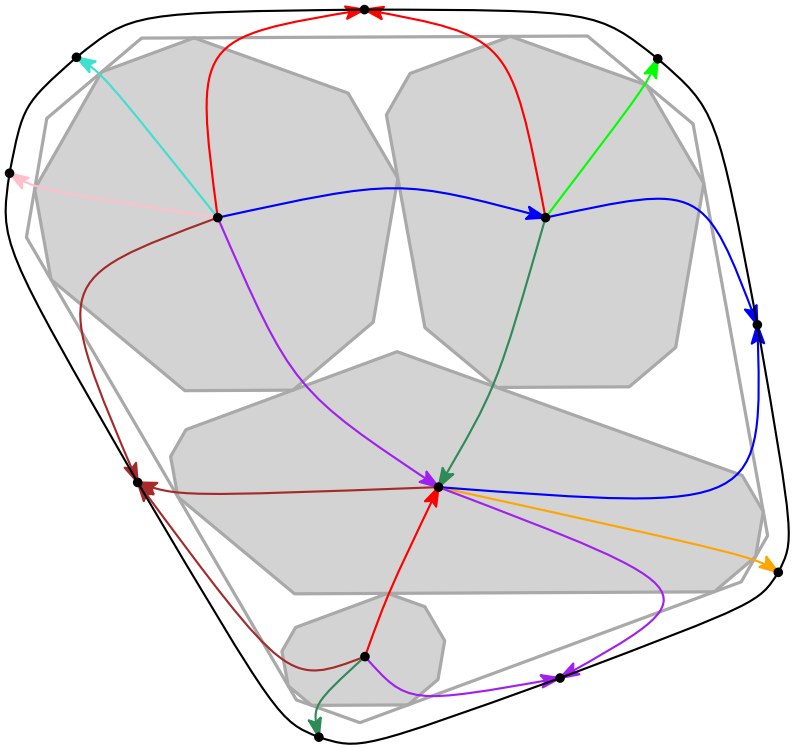

(b) The K-color forest.

Figure A.1: Overview of the graphs associated with a similarly-aligned odd K-gon contact representation.

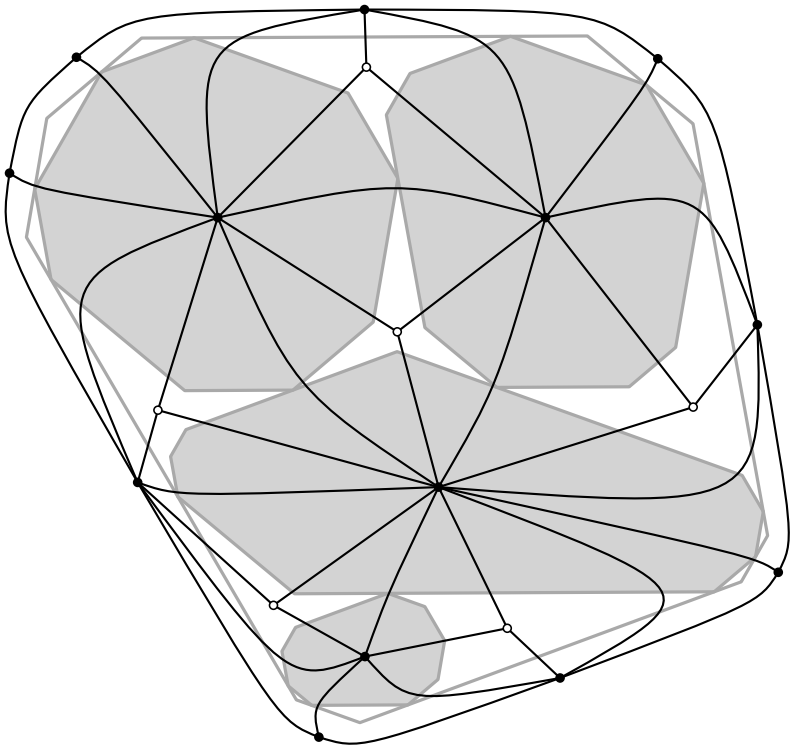

(c) The stack extension $G^\star$.

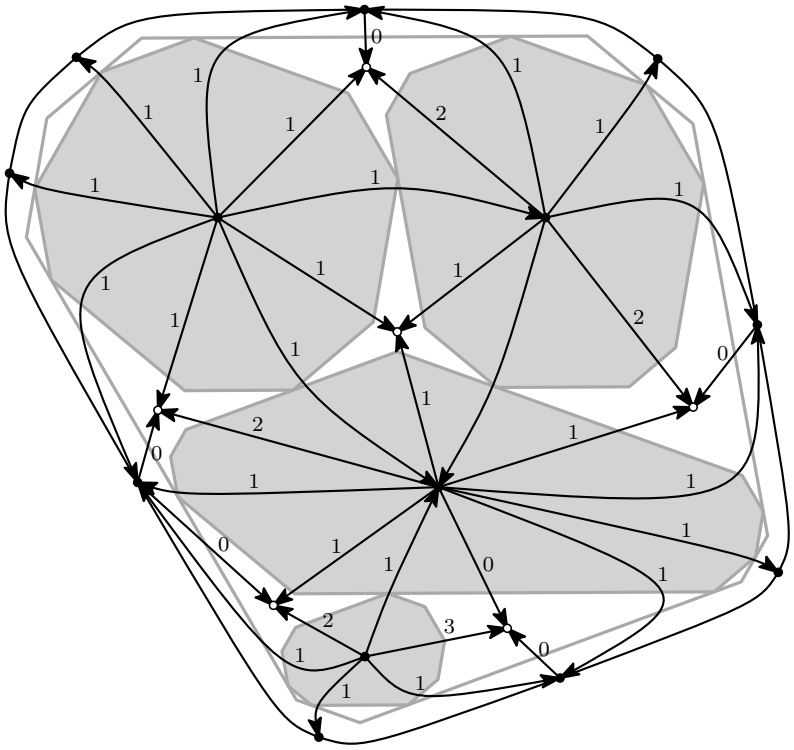

(d) The K-contact structure.

Figure A.1: Overview of the graphs associated with a similarly-aligned odd K-gon contact representation (cont.).

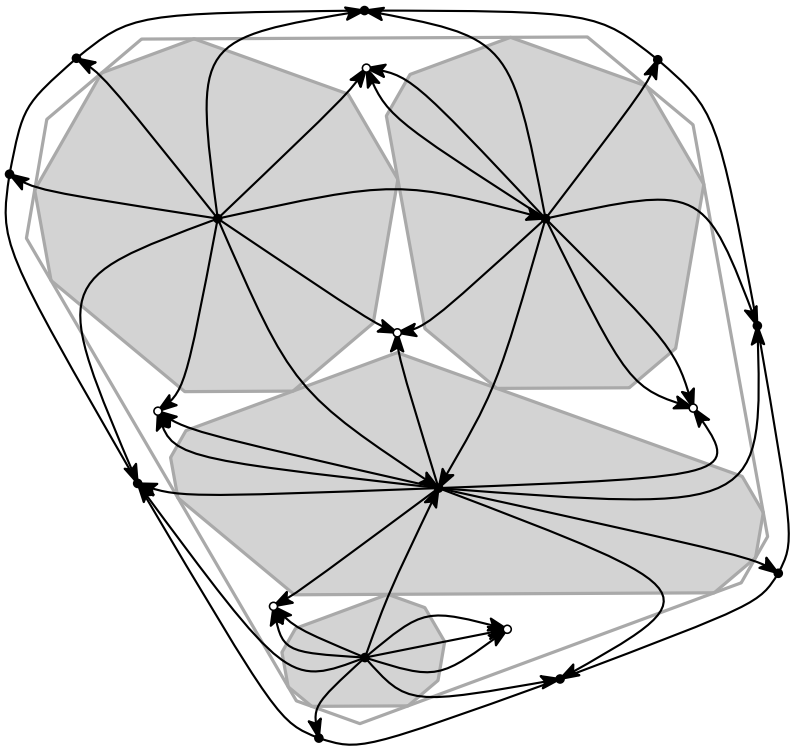

(e) The graph $G^{\star}_{+}$.

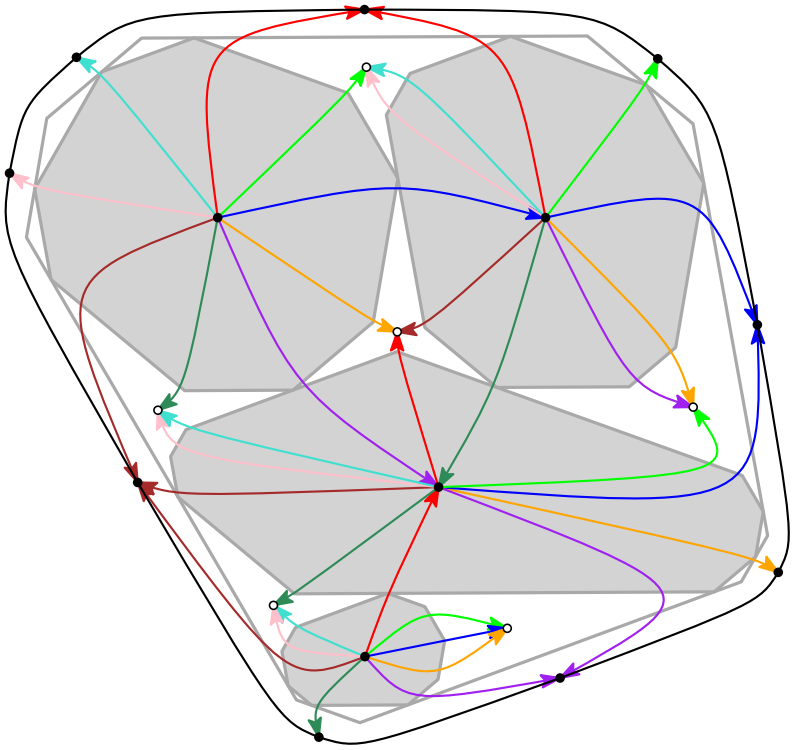

(f) The K-proper coloring of $G^{\star}_{+}$.

Figure A.1: Overview of the graphs associated with a similarly-aligned odd K-gon contact representation (cont.).

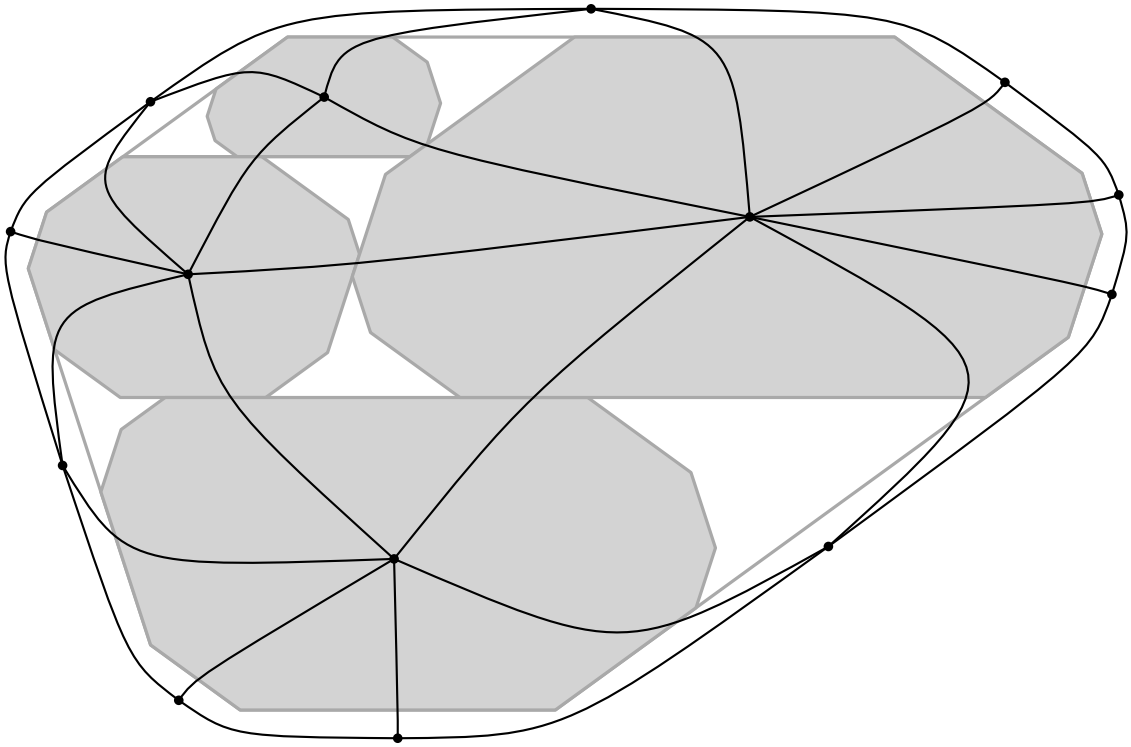

(a) The contact graph G.

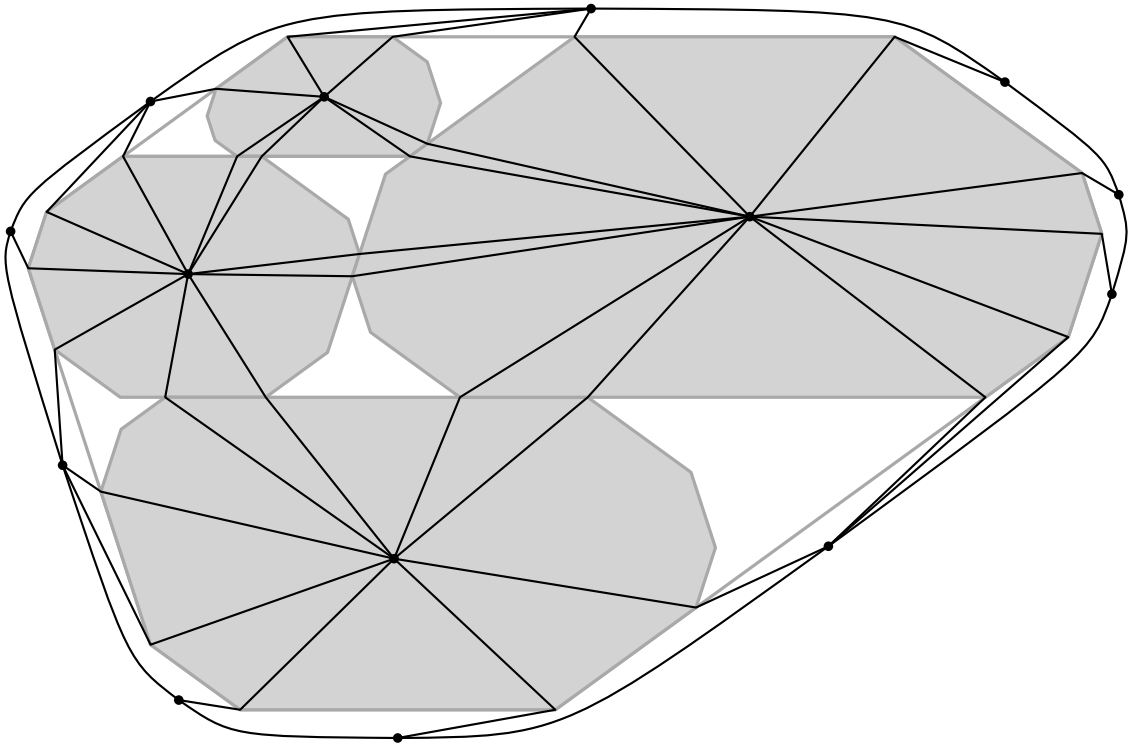

(b) The graph $2G$.

Figure A.2: Overview of the graphs associated with a parallel-sided even K-gon contact representation.

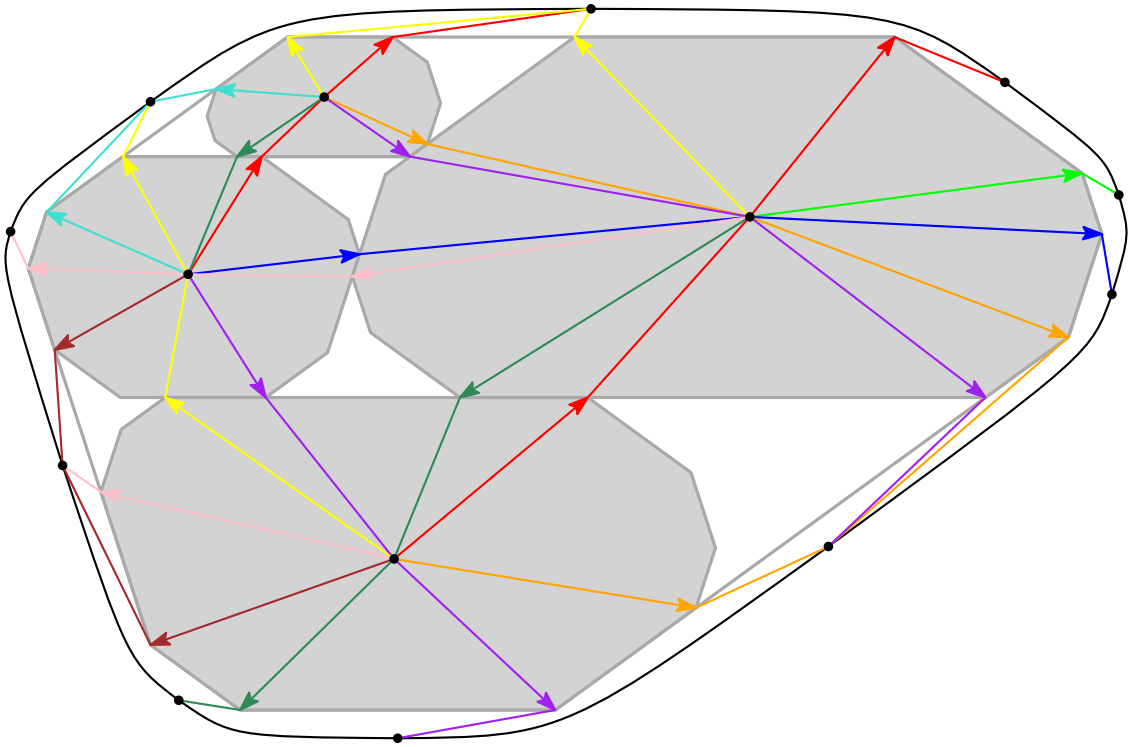

(c) The K-color forest.

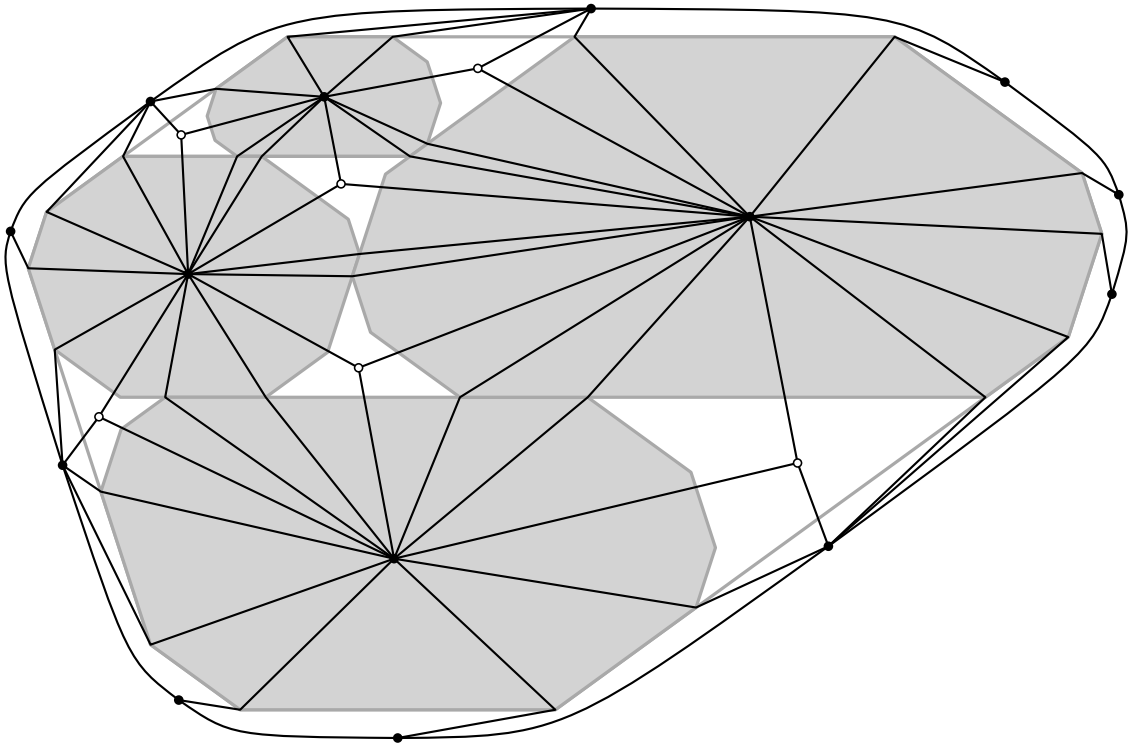

(d) The stack extension $2G^{\star}$.

Figure A.2: Overview of the graphs associated with a parallel-sided even K-gon contact representation (cont.).

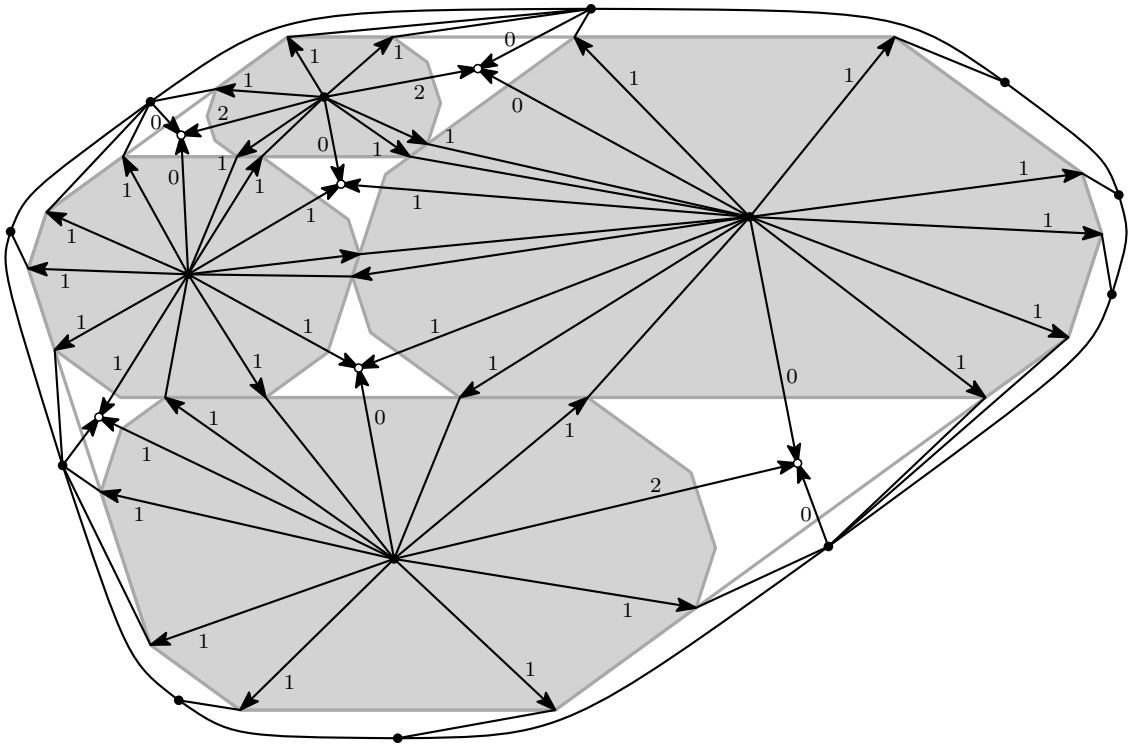

(e) The K-contact structure.

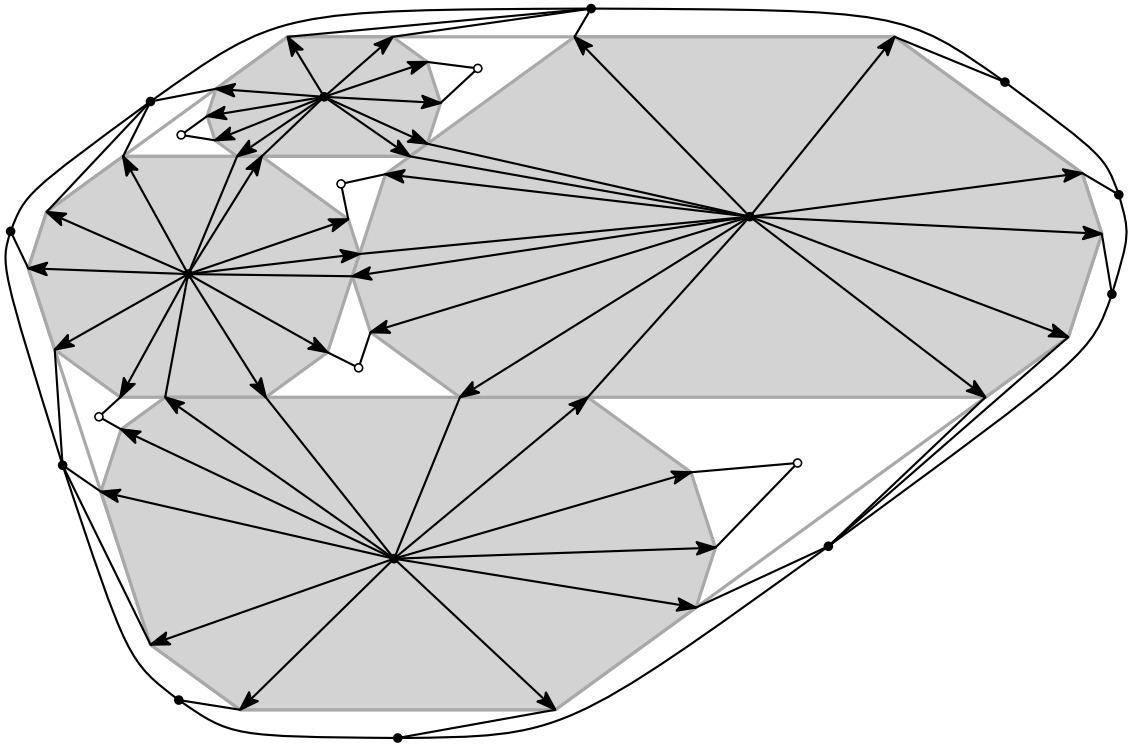

(f) The graph $2G^{\star}_{+}$.

Figure A.2: Overview of the graphs associated with a parallel-sided even K-gon contact representation (cont.).

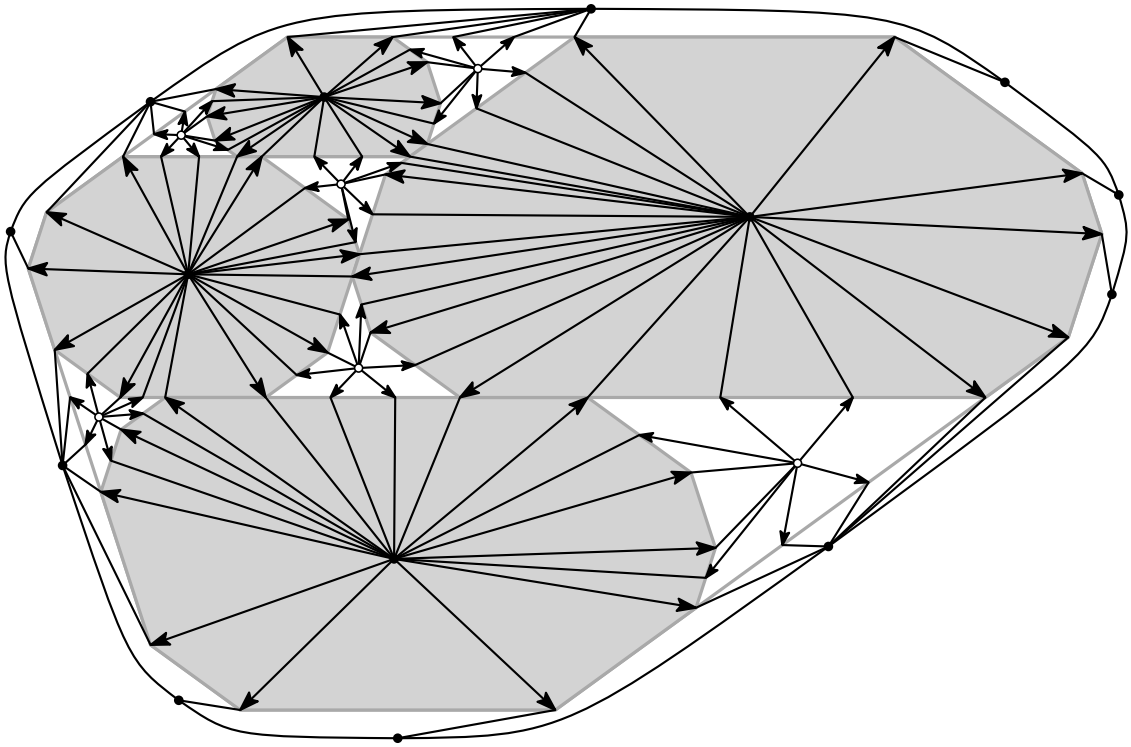

(g) The graph $2G^{\star}_{++}$.

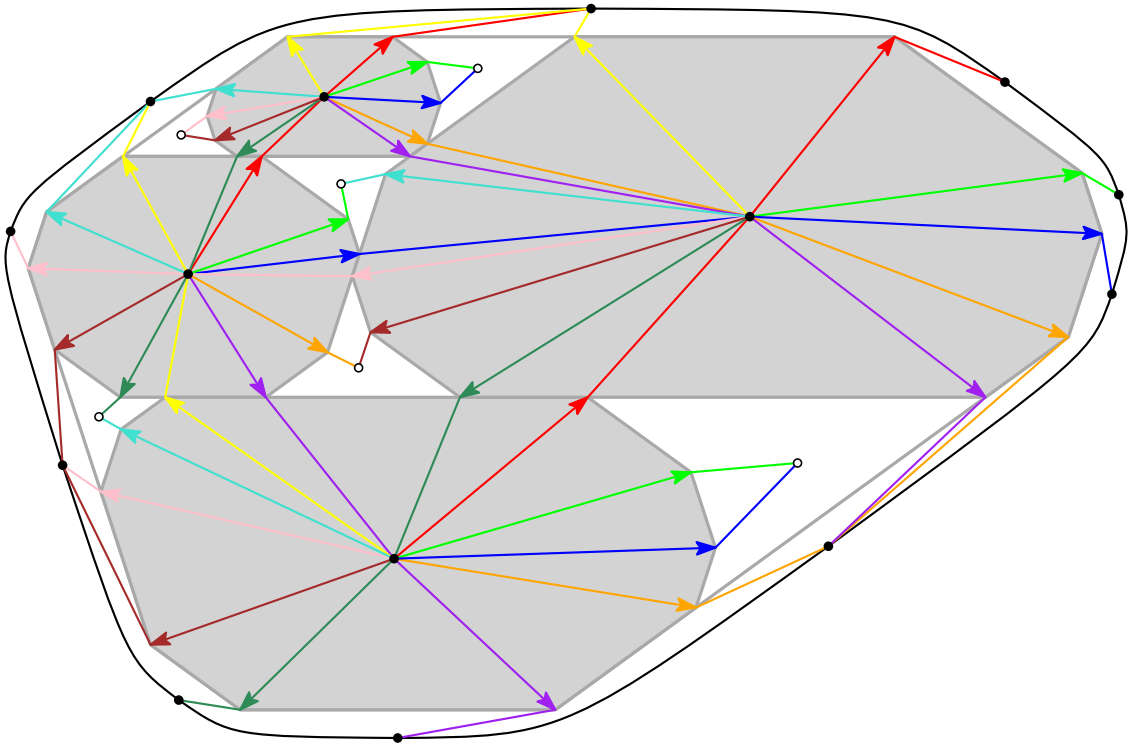

(h) The K-proper coloring of $2G^{\star}_{+}$.

Figure A.2: Overview of the graphs associated with a parallel-sided even K-gon contact representation (cont.).

Appendix B

Visualizations of the heuristic

In this appendix, we will show visualizations of the iterations of Algorithm 1 for some arbitrarily chosen examples. As we showed in Theorem 4.64, also solutions of the system of linear equations that are not non-negative can be used to produce a drawing. In the following we will show these drawings coming from the solutions of the systems of linear equations $\mathcal{A}_{S_i}$, $i = 0, 1, \ldots, k-1$, where $(S_i)_{i=0,1,\ldots,k-1}$ is the sequence of K-contact structures visited by Algorithm 1. Figures B.1 to B.3 show examples with regular polygons as prototypes, Figs. B.4 and B.5 show examples with non-regular polygons as prototypes. Although we do not know any invariant that improves with the iterations of the algorithm, it can be seen in these examples that the polygons representing the vertices of the given graph move closer from iteration to iteration, in some sense that we cannot quantify. For an interactive animation of more examples see [SS21].

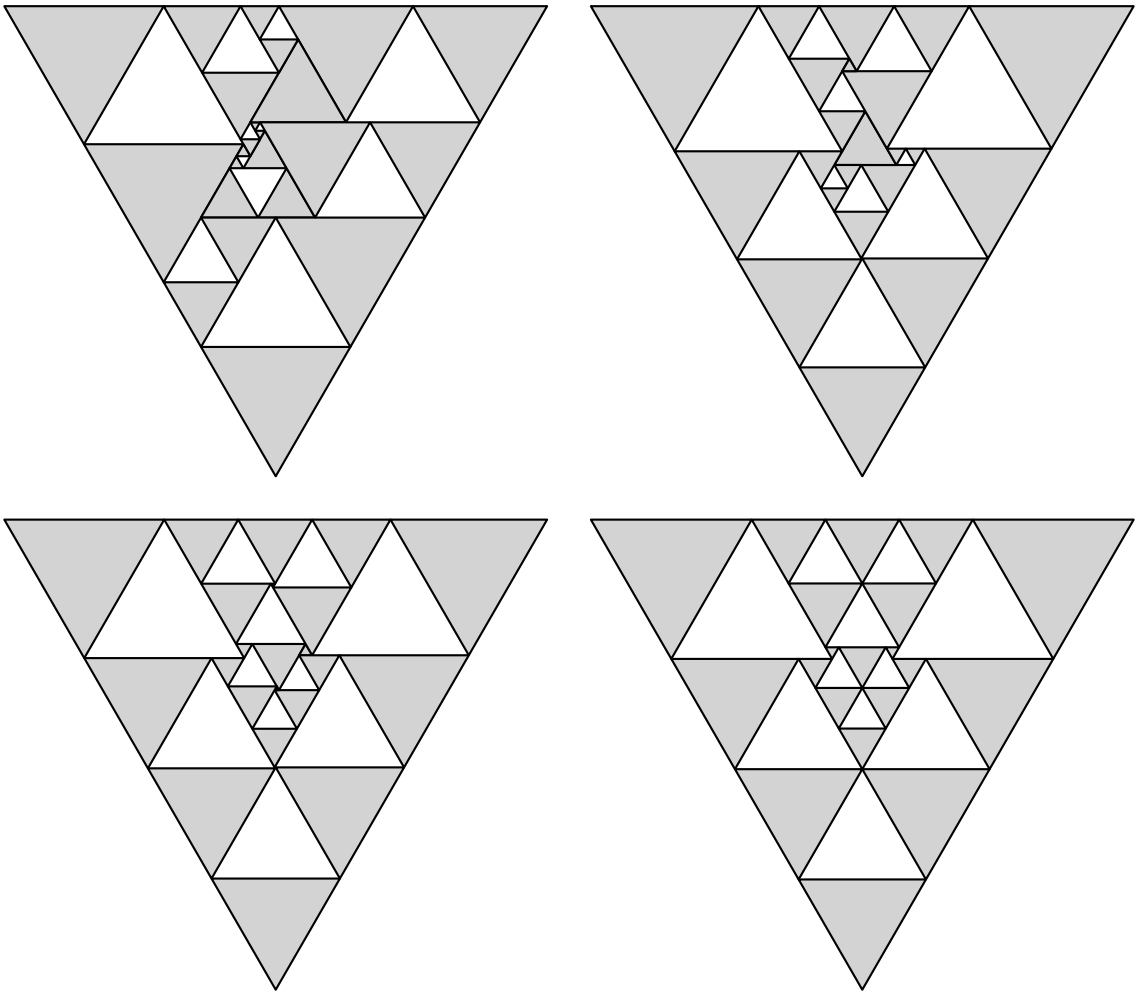

Figure B.1: Computation of a homothetic equilateral triangle contact representation of a triangulation with 11 inner vertices.

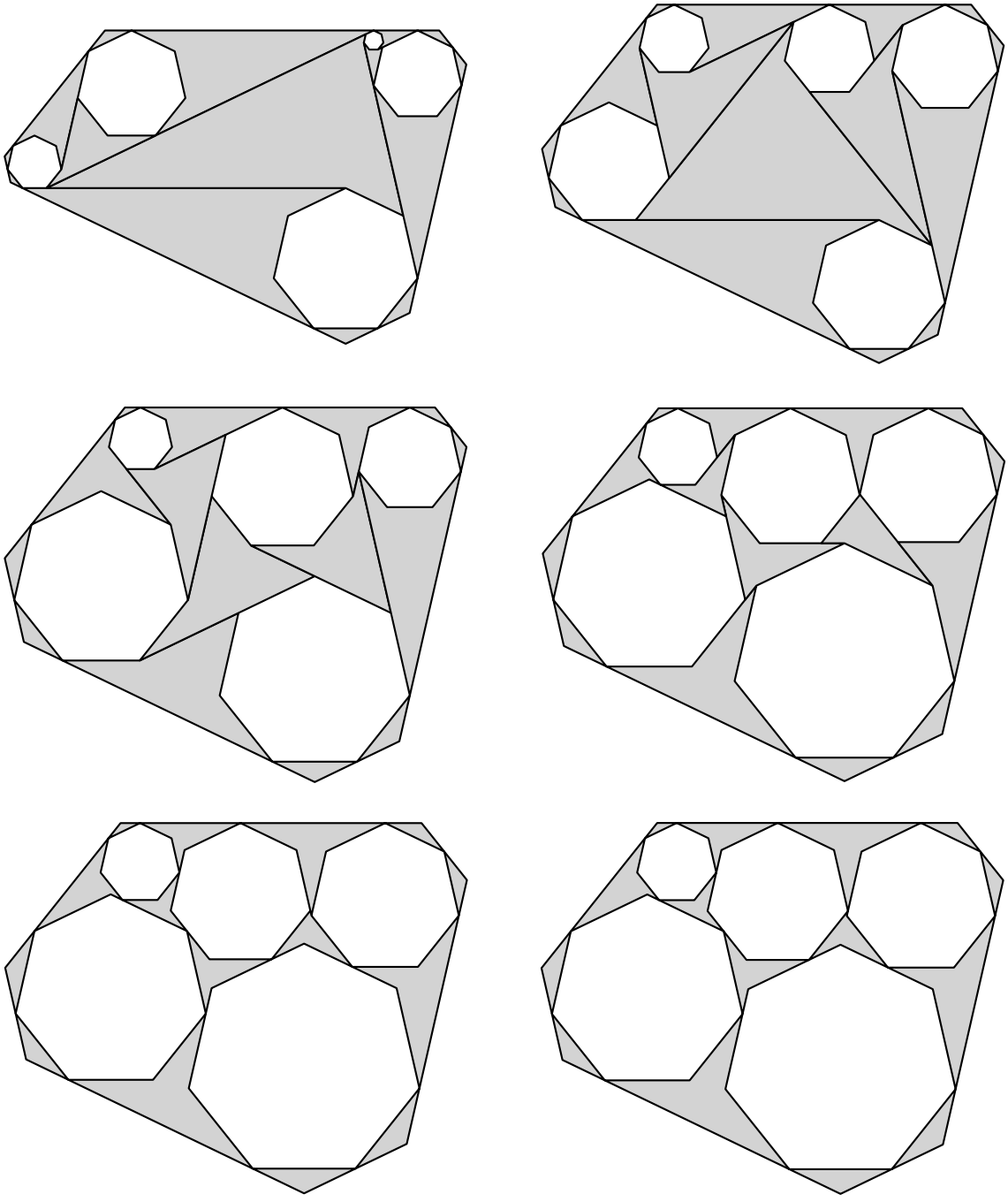

Figure B.2: Computation of a homothetic regular heptagon contact representation of an inner triangulation of a 7-cycle with 5 inner vertices.

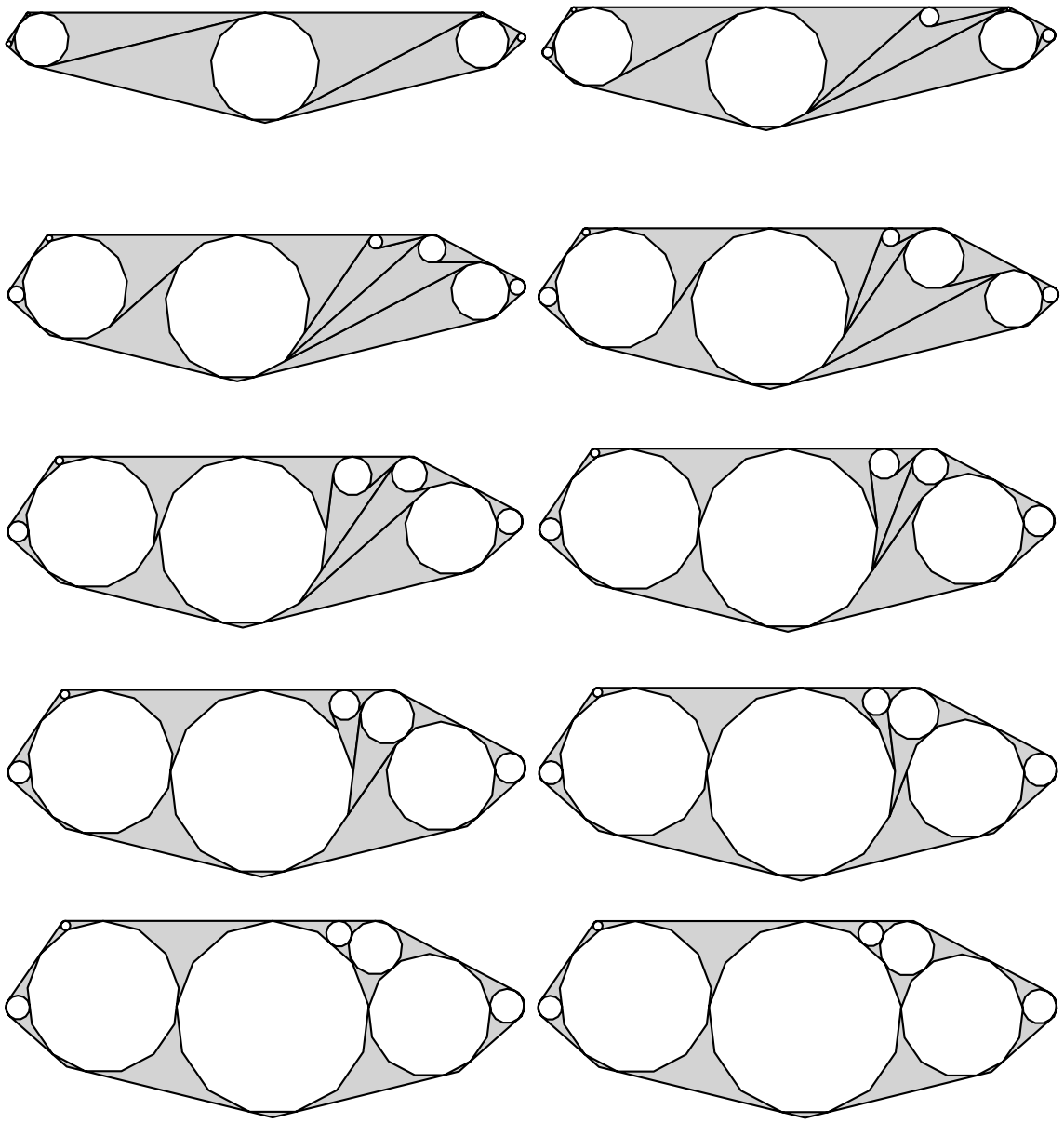

Figure B.3: Computation of a homothetic regular 13-gon contact representation of an inner triangulation of a 13-cycle with 10 inner vertices.

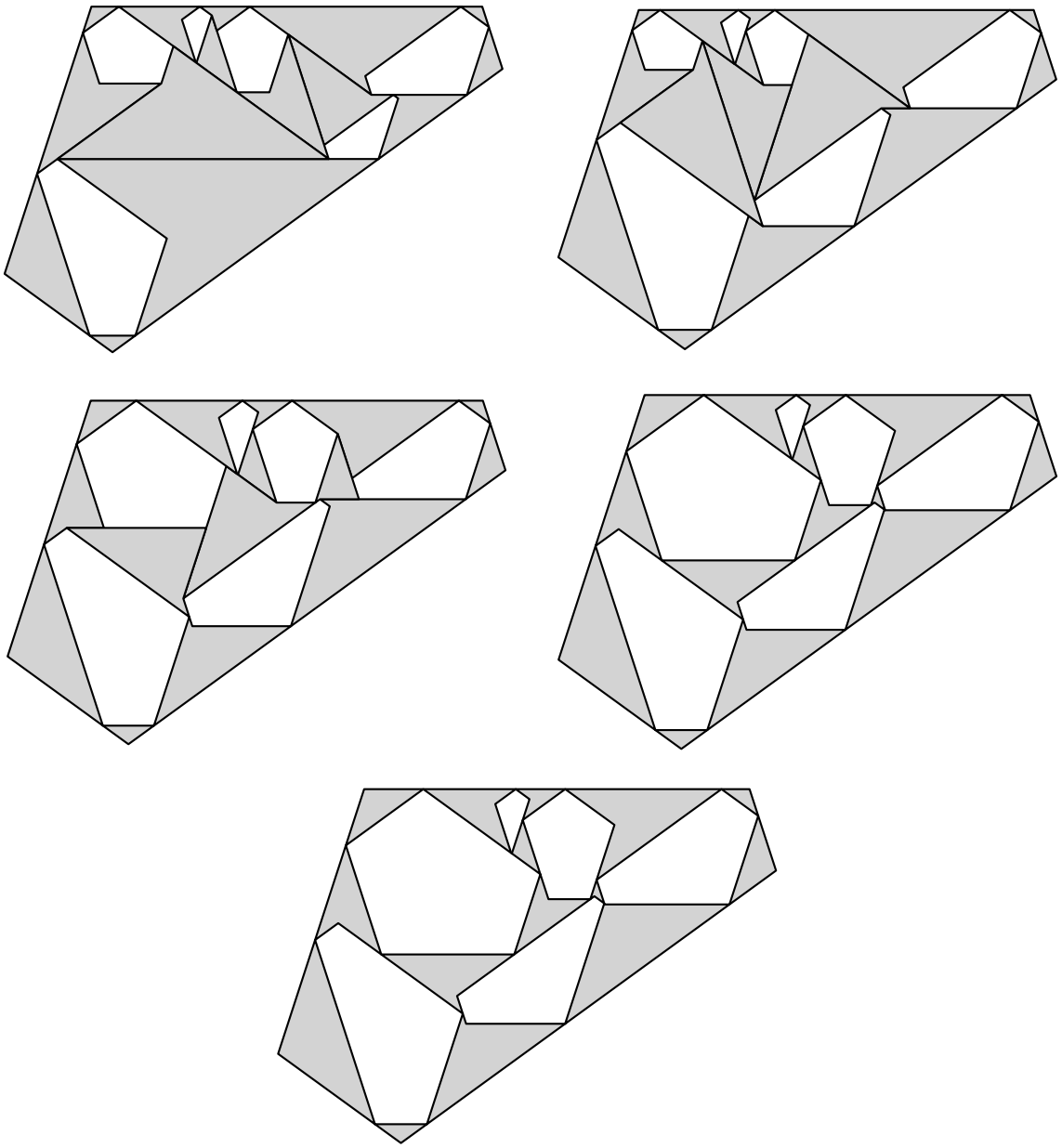

Figure B.4: Computation of a pentagon contact representation of an inner triangulation of a 5-cycle with 6 inner vertices with individual equiangular pentagons as prototypes.

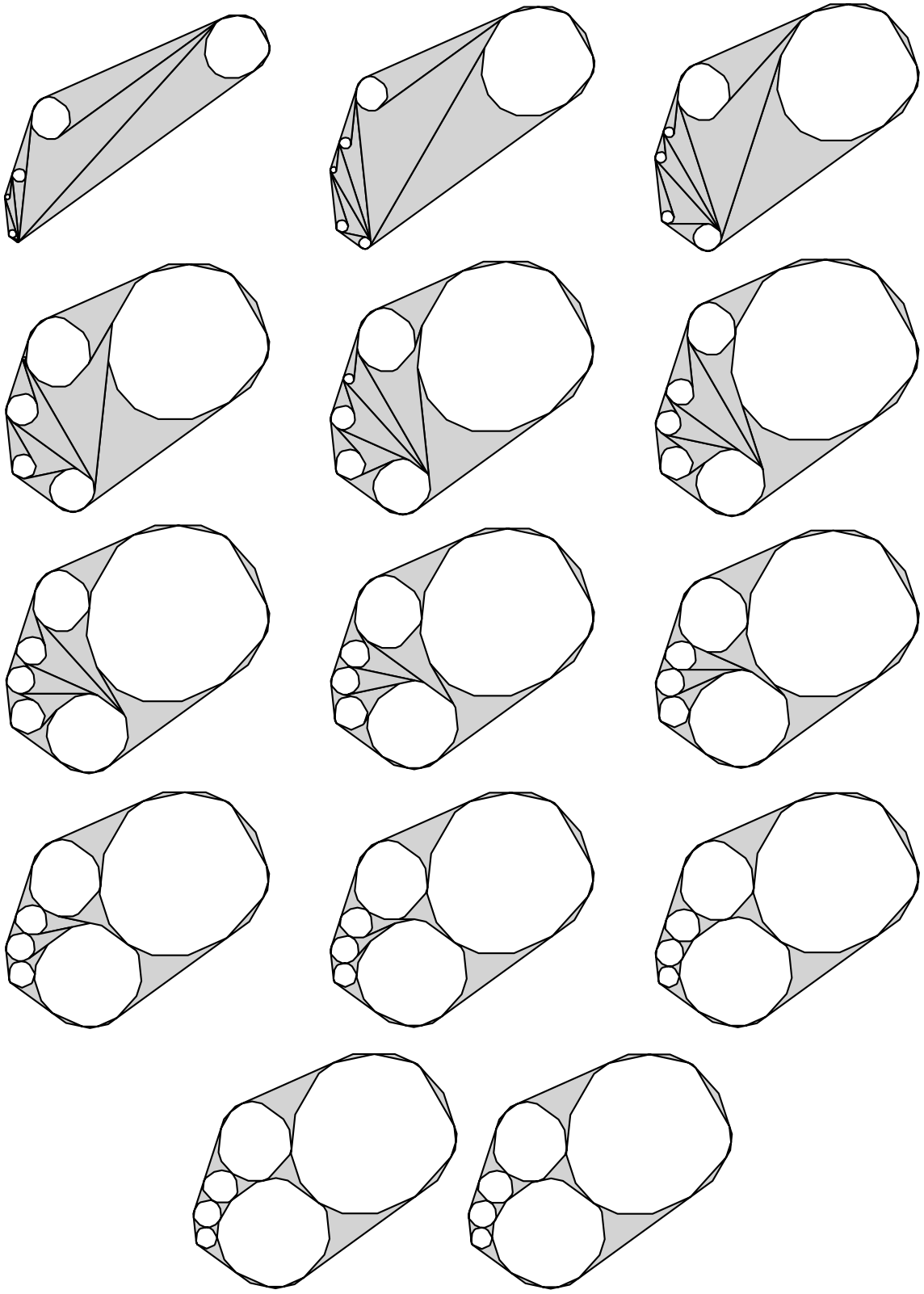

Figure B.5: Computation of a 15-gon contact representation of an inner triangulation of a 15-cycle with 6 inner vertices with individual equiangular 15-gons as prototypes.